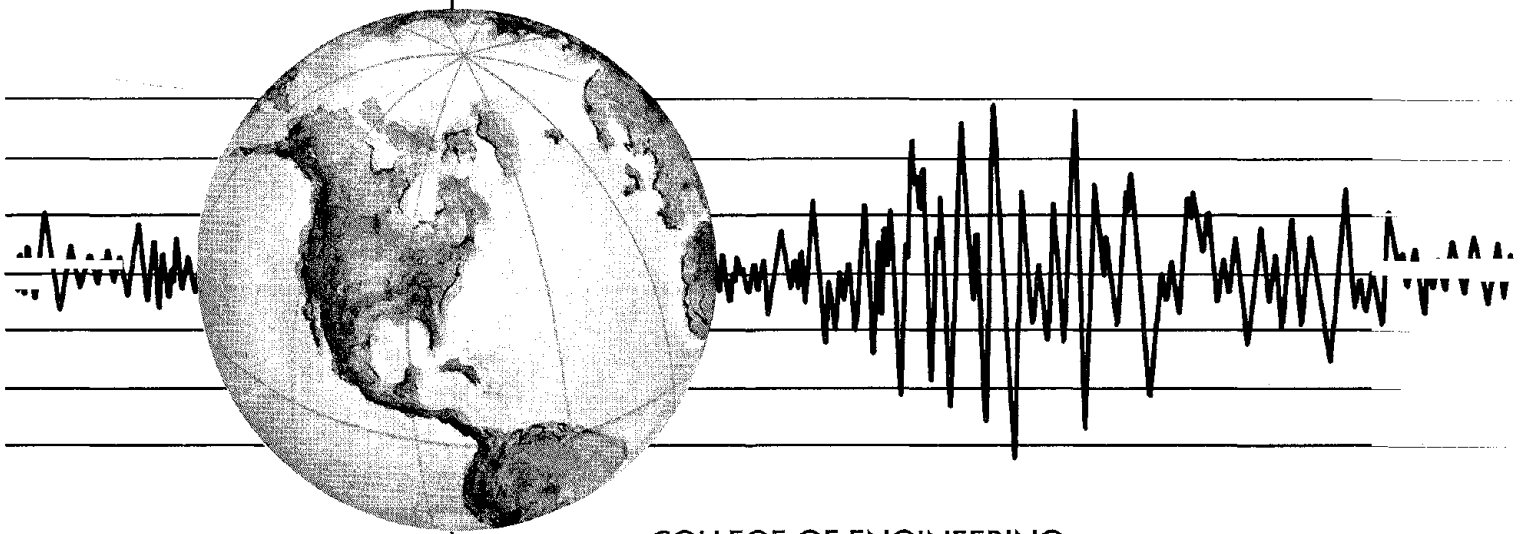


REPORT NO.  
UCB/EERC-80/37  
SEPTEMBER 1980

EARTHQUAKE ENGINEERING RESEARCH CENTER

# EARTHQUAKE ENGINEERING RESEARCH AT BERKELEY - 1980

Papers presented by faculty participants and research personnel associated with the Earthquake Engineering Research Center at the Seventh World Conference on Earthquake Engineering, Istanbul, Turkey, September 1980.



COLLEGE OF ENGINEERING

UNIVERSITY OF CALIFORNIA • Berkeley, California

PRODUCT OF:  
NATIONAL TECHNICAL  
INFORMATION SERVICE  
U.S. DEPARTMENT OF COMMERCE  
SPRINGFIELD, VA. 22161

For sale by the National Technical Information Service, U.S. Department of Commerce, Springfield, Virginia 22161.

See back of report for up to date listing of EERC reports.

**DISCLAIMER**

Any opinions, findings, and conclusions or recommendations expressed in this publication are those of the authors and do not necessarily reflect the views of the Sponsors or the Earthquake Engineering Research Center, University of California, Berkeley

<b>REPORT DOCUMENTATION PAGE</b>	<b>1. REPORT NO.</b> NSF/RA-800405	<b>2.</b>	<b>3. Recipient's Accession No.</b> <b>PBM 20587 4</b>	
<b>4. Title and Subtitle</b> EARTHQUAKE ENGINEERING RESEARCH AT BERKELEY - 1980			<b>5. Report Date</b> September 1980	
<b>7. Author(s)</b>			<b>6.</b>	
<b>9. Performing Organization Name and Address</b> Earthquake Engineering Research Center University of California, Berkeley 47th Street and Hoffman Blvd. Richmond, California 94804			<b>8. Performing Organization Rept. No.</b> UCB/EERC-80/37	
<b>12. Sponsoring Organization Name and Address</b> National Science Foundation 1800 G Street, N.W. Washington, D.C. 20550			<b>10. Project/Task/Work Unit No.</b>	
<b>15. Supplementary Notes</b>			<b>11. Contract(C) or Grant(G) No.</b> (C) (G) PFR-77-20667	
<b>16. Abstract (Limit: 200 words)</b>  At the Seventh World Conference on Earthquake Engineering held in Istanbul, Turkey, September 8-13, 1980, twenty one papers were presented by faculty participants and research personnel associated with the Earthquake Engineering Research Center, University of California, Berkeley. The papers have been compiled in this report to illustrate some of the research work in earthquake engineering being conducted at the University of California, Berkeley. The research work described in the papers has been sponsored by the following agencies: National Science Foundation; Department of Energy; Masonry Institute of America; Western States Clay Products Association; Concrete Masonry Association of California and Nevada; Department of Housing and Urban Development; American Iron and Steel Institute.			<b>13. Type of Report &amp; Period Covered</b>	
<b>14.</b>			<b>14.</b>	
<b>17. Document Analysis</b> <b>a. Descriptors</b>          <b>b. Identifiers/Open-Ended Terms</b>          <b>c. COSATI Field/Group</b>				
<b>18. Availability Statement:</b>  Release Unlimited			<b>19. Security Class (This Report)</b>	<b>21. No. of Pages</b> 183
			<b>20. Security Class (This Page)</b>	<b>22. Price</b>



EARTHQUAKE ENGINEERING RESEARCH CENTER

EARTHQUAKE ENGINEERING RESEARCH  
AT BERKELEY - 1980

Papers presented by faculty participants and  
research personnel associated with the  
Earthquake Engineering Research Center at the  
Seventh World Conference on Earthquake Engineering  
Istanbul, Turkey  
September 1980

Report No. UCB/EERC-80/37  
College of Engineering  
University of California  
Berkeley, California

September 1980

*1. a*



## FOREWORD

At the Seventh World Conference on Earthquake Engineering held in Istanbul, Turkey, September 8-13, 1980, twenty one papers were presented by faculty participants and research personnel associated with the Earthquake Engineering Research Center, University of California, Berkeley. The papers have been compiled in this report to illustrate some of the research work in earthquake engineering being conducted at the University of California, Berkeley. The research work described in the papers has been sponsored by the following agencies: National Science Foundation; Department of Energy; Masonry Institute of America; Western States Clay Products Association; Concrete Masonry Association of California and Nevada; Department of Housing and Urban Development; American Iron and Steel Institute.

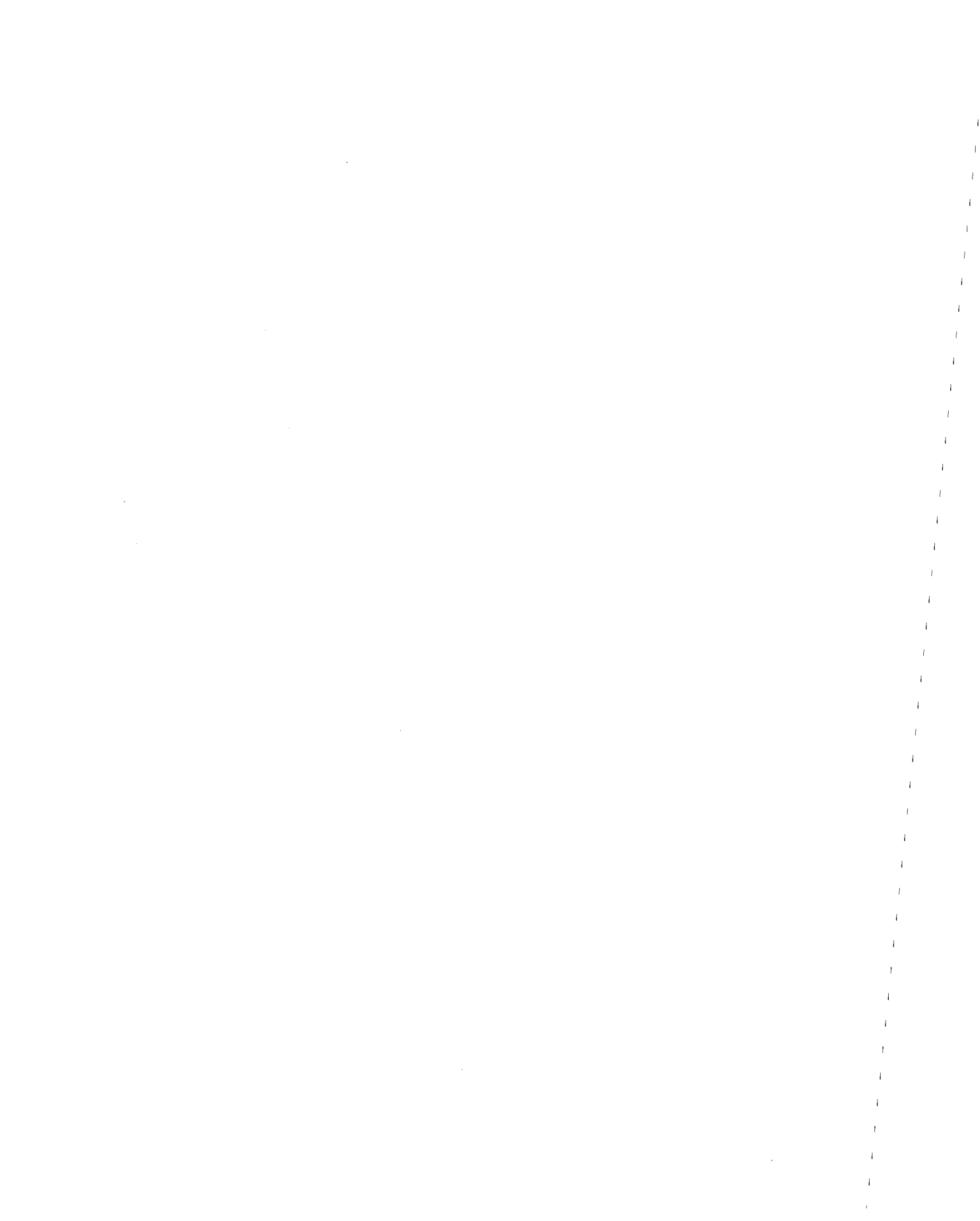




TABLE OF CONTENTS

Paper No.		Page No.
1.	"Report on the Activities of Earthquake Engineering Research Center, University of California, Berkeley" by J. Penzien . . . . .	1
2.	"Ground Motion Intensity Based on Earthquake Effects on Historical Monuments" by C-S. Yim, J. Penzien and A.K. Chopra . . . . .	17
3.	"Dynamic Properties of Prefabricated Apartment Buildings" by J.G. Bouwkamp and R.M. Stephen . . . . .	25
4.	"Modeling the Stiffness Contribution of Infill Panels to Framed Structures by a Constraint Approach" by J.W. Axley . . . . .	33
5.	"Lessons from Structural Damages Observed in Recent Earthquakes" by V.V. Bertero, S.A. Mahin and J.W. Axley . . . . .	37
6.	"A Lifetime Cost Approach to Automated Earthquake Resistant Design" by N.D. Walker Jr. and K.S. Pister . . . . .	45
7.	"Earthquake Analysis of Coupled Shear Wall Buildings" by T. Srichatrapimuk and A.K. Chopra . . . . .	53
8.	"Effects of Duration and Aftershocks on Inelastic Design Earthquakes" by S.A. Mahin . . . . .	61
9.	Address to State-of-the-Art Panel No. 6 "System Identification in Earthquake Engineering" by H.D. McNiven . . . . .	65
10.	"Evaluation of Nonlinear Structural Response to Seismic Excitations by System Identification" by B.S. Yanev . . . . .	73
11.	"Linear Mathematical Models to Predict the Seismic Response of a Three-Story Steel Frame" by H.D. McNiven and I. Kaya . . . . .	81
12.	"Seismic Behavior of R/C Wall Structural Systems" by V.V. Bertero . . . . .	89
13.	"Seismic Behavior of Reinforced Concrete Moment-Resisting Frames" by E.P. Popov . . . . .	97
14.	"Probabilistic Modal Combination for Earthquake Loading" by A. Der Kiureghian . . . . .	105



TABLE OF CONTENTS (CONT'D)

Paper No.		Page No.
15.	"Biaxial Shaking Table Study of a R/C Frame" by M.G. Oliva and R.W. Clough . . . . .	113
16.	"Sloshing of Liquids in Rigid Annular Cylindrical and Torus Tanks Due to Seismic Ground Motions" by M. Aslam, W.G. Godden and D.T. Scalise . . . . .	121
17.	"Seismic Behavior of Masonry Buildings" by P.A. Hidalgo, R.L. Mayes and H.D. McNiven . . . . .	129
18.	"An Investigation of the Seismic Behavior and Reinforcement Requirements for Single-Story Masonry Houses" by R.W. Clough, P. Gülkan and R.L. Mayes . .	137
19.	"Eccentric Seismic Bracing of Steel Frames" by E.P. Popov . . . . .	145
20.	"Seismic Isolation of an Electron Microscope" by W.G. Godden, M. Aslam and D.T. Scalise . . . . .	151
21.	"Earthquake Insurance and Microzoned Geologic Hazards: United States Practice" by K.V. Steinbrugge, H.J. Lagorio and S.T. Algermissen. . . . .	159
	List of EERC Reports . . . . .	167



REPORT ON THE ACTIVITIES OF  
EARTHQUAKE ENGINEERING RESEARCH CENTER  
UNIVERSITY OF CALIFORNIA, BERKELEY

by Joseph Penzien<sup>I</sup>

I. SUMMARY

Presented is an overview of the activities of the Earthquake Engineering Research Center (EERC), University of California, Berkeley. Section II provides background information on the Center, Section III lists the available research facilities, Section IV summarizes the current research programs under the classifications, Structural Engineering, Geotechnical Engineering, Hydraulic Engineering, Engineering Seismology, Interdisciplinary, and International Cooperation, Section V describes the National Information Service in Earthquake Engineering (NISEE) public service program containing three components, namely, computer program dissemination, abstract journal, and information exchange, Sections VI and VII provide information on the Center's publications and personnel, respectively, and Sections VIII and IX contain a closing statement and acknowledgments, respectively.

II. INTRODUCTION

The Earthquake Engineering Research Center, University of California, Berkeley, was established as an organized research unit on November 30, 1967, to coordinate earthquake engineering research within the College of Engineering on the Berkeley campus. Its research and public service programs, which have as their ultimate goal the mitigation of the earthquake hazard, may be classified according to their objectives as follows: (1) determining the characteristics and intensities of strong ground motions, (2) developing mathematical models and analytical procedures for estimating potential damage effects, (3) improving design methods and code requirements, and (4) collecting and disseminating information on earthquake engineering.

In the past, the activities of EERC have concentrated primarily on the technical fields with greatest effort involving researchers in various disciplines of civil engineering, i.e., structural engineering and structural mechanics, soil mechanics, foundation engineering, and fluid mechanics. Recently, the activities have expanded into other technical areas requiring interdisciplinary efforts of researchers in materials, civil engineering, electrical engineering, operations research, and engineering seismology. Future expansion is expected to include the development of activities in the general area of public policy which is important to the implementation of technical research results into engineering practice. This expansion will require the coordinated effort of researchers in economics, social science, political science, law, engineering, and engineering seismology. The overall trend in the expanding activities of EERC is consistent with

---

<sup>I</sup> Director, Earthquake Engineering Research Center, and Professor of Structural Engineering, University of California, Berkeley, Calif., USA.

the United States national effort and needs and is consistent with the broad interpretation of earthquake engineering research by the Division of Problem-Focused Research, Directorate of Engineering and Applied Science, National Science Foundation, which is the primary source of funding for earthquake engineering research in the United States.

### III. RESEARCH FACILITIES

Excellent research facilities are available for conducting earthquake engineering research at the University of California, Berkeley.

The experimental facilities include the Earthquake Simulator Laboratory, the Structural Research Laboratory, and the Soil Mechanics Laboratory located at the University's Richmond Field Station, which is five miles from the Berkeley campus, and the structural research laboratories located in Davis Hall on campus. The central feature of the Earthquake Simulator Laboratory is a modern hydraulically-powered electronically-controlled biaxial (vertical and horizontal) shaking table (20 x 20 ft.) capable of testing specimens weighing up to 120,000 lbs. under realistic seismic excitations of maximum credible intensity. This laboratory also has two portable 5000 lb. maximum force amplitude mechanical vibrators, each containing double rotating eccentric masses, which are used for dynamic testing of prototype structures. The Structural Research Laboratory provides a large tension (3,000,000 lbs.) - compression (4,000,000 lbs.) testing machine and a variety of fixtures capable of testing full-scale structural components and assemblages under force or displacement controlled quasi-static or dynamic loadings simulating realistic seismic conditions. Complementary testing fixtures of this same general type are also available in the Davis Hall laboratories. The Soil Mechanics Laboratory provides modern equipment for conducting experimental investigations on current seismic problems in the general area of soil mechanics and foundation engineering. Modern high speed data acquisition and processing systems are available in these laboratories.

To support the correlation studies of experimental results and the analytical research activities, the University provides modern computational facilities, including CDC-6400 and CDC-7600 computers. Also available to support the overall research program are extensive library facilities, including the Earthquake Engineering Library. This specialized library now has approximately 15,000 acquisitions providing access to current literature published throughout the world. It is an invaluable asset to the research activities of EERC.

### IV. RESEARCH PROGRAMS

#### A. STRUCTURAL ENGINEERING

##### 1. Shaking Table Tests

a. Three-story steel frame with diagonal bracing (R. W. Clough)\* - A half-scale three-story steel frame structure was used to study the performance of diagonal bracing installed across the weak axis of a frame. Three types of bracings were studied experimentally: half inch tie rods with

\* Name(s) in parenthesis indicate faculty participant(s) conducting investigation.

turnbuckles, 3/4 inch pipe sections welded at the end connections and central crossing, and double angle braces welded similarly. All tests have been completed and computer analyses have been correlated with the test results. Excellent correlation was achieved demonstrating the effectiveness of the mathematical models that were developed to represent the yielding and rupturing of the tie rods, and the yielding and buckling of the other bracing systems.

b. Three-story reinforced concrete frames (R. W. Clough) - A series of five two-story reinforced concrete frame structures have been tested. The first four specimens were tested with the horizontal excitation axis coinciding with a principal axis of the frame while the fifth specimen was tested with the horizontal excitation axis at 25° to the principal axis. This latter test was the first biaxial shaking table test of a concrete frame known to be carried out anywhere in the world. Correlation studies have been carried out between experimental results and analytical predictions of response. An objective of this investigation is the extrapolation of test behavior to expected field experience in real earthquakes.

c. Nine-story steel frame with uplift (R. W. Clough) - The uplifting behavior of building frames has been investigated using a one-third scale model of a nine-story, three-bay steel frame structure. In the most recent tests, the central bay of the structure was provided with K-bracings; thus, converting it effectively to a shear wall component. The tests were carried out to show how a shear wall frame behaves when subjected to seismic motions sufficient to cause uplift.

d. Single-story masonry houses (R. W. Clough) - Single-story masonry houses, consisting of typical wall panels assembled in a 16 ft. square with a typical timber truss roof structure bolted in place, have been tested to investigate their seismic performance and to develop improved design criteria.

e. Dam models (R. W. Clough) - As part of the University of California-National Taiwan University cooperative research program, shaking table tests have been conducted to investigate the seismic behavior of the Techí dam located in Taiwan. Experimental work has included development of a plaster-sand material with strength and stiffness properties adjusted for small-scale model similitude. Two types of models have been made with this material and tested on the shaking table: a segmented arch model to represent arch action of the prototype and a gravity section to represent the cantilever resistance of the prototype, each having a length scale factor 1:150. Three specimens of each type have been tested to failure. Analytical correlation studies are now being carried out.

f. Base isolation systems (J. M. Kelly) - Shaking table tests have been carried out to study the effectiveness of specially designed multi-layer natural rubber bearings in an isolation system designed to reduce seismic forces produced in building structures. The multi-layer design of the bearings provides a vertical stiffness several hundred times larger than the horizontal stiffness; thus, decoupling the building from the horizontal ground motion. A mechanical fuze in the form of a fracture sensitive shear pin is included in the system to provide restraint against wind loads. Theoretical correlation studies have been made in the investigation.

g. Equipment-structure interaction (J. M. Kelly) - A three-story steel frame, on which models of equipment are mounted, has been tested on the shaking table to study equipment-structure interaction effects during earthquakes.

Analyses have shown that light equipment having low damping can experience very large accelerations during earthquakes when mounted in large structures. The shaking table tests confirm the existence of these large accelerations under conditions which are often present in prototype structures. Design guidelines are being developed to cope with this problem.

h. Energy absorbing restrainers for nuclear power plant piping systems (W. G. Godden, J. M. Kelly) - Shaking table tests are being performed on small-size two-dimensional nuclear power plant piping systems using different types of support constraint. The main objective of the tests is to develop high energy absorbing support systems which will prevent large seismic forces from occurring in the pipes; thus, reducing construction and maintenance costs and providing enhanced safety. Correlation studies are being made using numerical analysis procedures and computer programs specifically developed for this purpose.

i. Oil storage tanks (R. W. Clough) - Over the past several years, a number of cylindrical tanks containing water have been tested on the shaking table to study both the sloshing and structural behavior of oil storage tanks during earthquakes. Both open and floating lid type tanks have been tested with both anchored and unanchored base conditions being used. Extensive analytical correlation studies have been conducted with the ultimate objective of developing improved design criteria for prototype tanks.

j. Frames and masonry walls (H.D. McNiven) - To provide basic response data for mathematical modelling using system identification procedures, a one-story steel frame and free-standing unreinforced masonry walls were tested on the shaking table using simulated seismic excitations. The steel frame was tested under a variety of conditions, i.e., with and without infill walls (masonry, prefabricated concrete, and timber). The masonry walls were constructed from miniature bricks for appropriate scaling. Accelerations and displacement response time-histories were recorded for each test.

## 2. Component Tests

a. Masonry structures (H.D. McNiven) - Numerous tests have been performed on full-scale single masonry piers using a test fixture which provides realistic boundary conditions, develops full dead load conditions, and generates cyclic shear loads simulating seismic conditions. Specimen parameters which have been varied include: type of masonry construction, height-to-width ratio, amount and arrangement of steel reinforcement, and type of grouting. The influence of varying the sequence of loading on strength and stiffness has been investigated and repair procedures have been studied. A mathematical model has been developed for predicting the elastic behavior of masonry piers and for predicting the beginning of cracking. Plans are now being made to extend this investigation to shaking table tests which will allow an even better assessment of the validity of the mathematical model.

b. Concentrically braced steel frames (E. P. Popov, J. G. Bouwkamp) - Experimental and analytical work on three half-scale models of three-story steel frames with K-braces subjected to severe quasi-static loading has been completed. Good agreement between the experimental and calculated results can be obtained by proper modelling of brace behavior.



c. Steel struts and eccentrically braced steel frames (E. P. Popov) - Many large-size steel struts having several kinds of boundary conditions have been subjected to severe tension-compression cyclic conditions and a number of eccentrically braced frames for buildings have been tested under simulated seismic conditions. Improved methods of analyses are being developed to predict their behavior.

d. Tubular frames (E. P. Popov, S. Mahin) - Experimental studies have been performed on X-braced tubular steel frames of the type used in offshore construction. Two one-sixth scale models of a complete frame of a typical four-leg production platform designed for 100-ft. water depth according to current wind and earthquake conditions applicable to Southern California have been tested under simulated seismic conditions. The primary variable in these tests is the diameter to wall thickness ratio of the bracing struts. Ratios of 33 and 48 have been considered. Other structural details are representative of current design practice. In addition to being useful in assessing the inelastic cyclic behavior of tubular steel offshore structures subjected to severe earthquake excitations, the experimental results obtained in this investigation can be employed to evaluate analytical models for predicting the seismic response of such structures.

e. Reinforced concrete beam-column sub-assemblages (V. V. Bertero, E. P. Popov) - Large-size reinforced concrete (ordinary and lightweight) beam-column sub-assemblages have been tested under large deformation cyclic loadings simulating severe earthquake conditions. Some specimens have been complete with floor slab and a cross beam loaded with gravity forces. Associated tests designed to investigate bond deterioration have also been made. Mathematical modelling and analysis procedures are being developed for predicting the seismic behavior of reinforced concrete moment-resisting frames subjected to seismic forces.

f. Coupled and uncoupled reinforced concrete shear walls (V. V. Bertero, E. P. Popov) - An extensive test program is being conducted to determine the large-deformation cyclic performance of coupled and uncoupled reinforced concrete shear walls under simulated seismic conditions. Improved detailing and criteria for the steel reinforcement are being developed to insure good seismic performance. Mathematical models and dynamic analysis procedures are also being developed.

g. Infilled frames (V. V. Bertero, E. P. Popov) - The main objective of integrated experimental and analytical research is to develop practical methods for seismic-resistant design, as well as the repair and retrofitting of structural systems based on the use of moment-resisting frames combined with masonry or concrete infills. Several experiments have been conducted on one-third scale model specimens of the three first stories of an eleven-story, three-bay, ductile moment-resisting frame. While some of these specimens were tested as a basic frame, others were tested using different types of infills and reinforcement. A new strut model and a new modeling technique based on a constraint approach have been formulated for studying the behavior of infilled frames. Establishment of guidelines regarding the strength and deformation capacities required of infills when subjected to different types of earthquake excitations based on parametric analytical studies of complete infilled frame systems is in progress.

### 3. Field Tests (J. Bouwkamp, R. W. Clough, R. M. Stephen, E. L. Wilson)

Field tests have been conducted to obtain information on the dynamic characteristics of buildings of unusual design or construction and to compare the results obtained with analytical predictions of performance. Both ambient and forced vibration excitations have been used in these tests. Recently, a 42-story pedestal base building and two prefabricated buildings (one nine stories high, the other twelve stories) have been tested. Field tests have also been performed on a 40-ft. high water tank and the Techí arch dam in Taiwan.

### 4. Analytical Studies

a. Certain aspects of building response (A. K. Chopra) - Five different aspects of the seismic response of buildings have been studied: Coupled lateral-torsional response, soil-structure interaction effects, evaluation of simulated ground motions for building response predictions, effects of gravity loads and vertical ground motion, and effects of foundation tipping.

b. Three-dimensional inelastic structural response (G. H. Powell) - To date, inelastic seismic analyses of buildings have been almost exclusively two-dimensional even though realistic conditions impose three-dimensional inelastic behavior; thus, an effort is being made to extend dynamic analysis capability to three-dimensional nonlinear systems. Nonlinear structural elements have been developed for the ANSR (Analysis of Nonlinear Structural Response) computer program to allow three-dimensional modelling of beams and columns in buildings. A new version of ANSR (ANSR-II) has recently been released which expands its three-dimensional nonlinear analysis capability.

c. Behavior of large precast panel buildings (G. H. Powell) - Buildings made by stacking large precast panels are being used increasingly in seismic zones. Because they have structural characteristics which are different from conventional buildings, there is concern over their ability to withstand earthquakes. Because of this concern, an analysis procedure and computer program suitable for calculating the response of large panel buildings has been developed. The procedure models the structure as an assemblage of elastic panels connected by elastic joints. Several different joint models have been considered and parameter studies are being carried out.

d. Behavior of reinforced concrete joints (G. H. Powell) - Because experimental studies are so expensive, accurate analysis procedures are needed to predict the behavior of reinforced concrete joints under severe seismic loads. The major difficulty in developing an analytical procedure is that concrete is an extremely complex material, especially under cyclic loading. A sophisticated mathematical model developed by Bazant is being implemented into the ANSR-II computer program to handle this joint problem. While it is complex and expensive to use, it has the potential to provide accurate predictions of joint behavior.

e. Pile foundation modelling (J. Penzien) - An important step in the dynamic analysis of pile-supported structures is to derive the dynamic stiffnesses of their pile foundations. A new method has recently been developed which involves the following four steps: (1) decomposition of the soil resistance function to pile movement obtained by numerical solution of a boundary value problem into the product of two orthogonal func-

tions yielding frequency-dependent subgrade stiffnesses, (2) computation of the dynamic stiffnesses of a single pile using the subgrade stiffnesses described above and the pile's inertia and damping properties, (3) determination of the pile group interaction factor using the soil resistance functions at adjacent piles when one pile in the group is excited, and (4) computation of the dynamic stiffnesses of a pile group from the results of steps (2) and (3) above. An independent check on this method is now being carried out using a finite element near field and a continuum model for the far field.

f. System identification (H. D. McNiven) - Methods of system identification are being used to develop linear and nonlinear mathematical models of structural systems. These methods have been used to develop models for a single-story steel frame structure, a three-story steel frame structure, and reinforced concrete beams. The models obtained accurately reflect both global and local behavior of these systems under realistic seismic conditions. Much has been learned in these investigations regarding the effectiveness (or ineffectiveness) of various response data in developing mathematical models through the use of system identification procedures.

g. Response of highway bridges (J. Penzien) - Over the past several years, analytical procedures and computer programs have been developed for predicting the nonlinear seismic response of highway bridges. Presently, parameter studies are being carried out with the objective of improving seismic design criteria and the previously developed analysis procedures, and computer programs are being documented for better use by the practicing engineer.

h. Response of dams (A. K. Chopra) - The basic purpose of this investigation has been the development of techniques for earthquake analysis of concrete dams, including effects of hydrodynamic and foundation interaction, and the development of an understanding of these effects on seismic response. Gravity and arch dams have been included in the study.

i. Response of rigid blocks (A. K. Chopra, W. G. Godden, J. Penzien) - A numerical procedure and a computer program have been developed to solve the nonlinear equations of motion governing the rocking of rigid blocks on a rigid base subjected to horizontal and vertical earthquake ground motions. Results obtained by this procedure and by shaking table tests show the response to be very sensitive to small changes in block size and slenderness ratio and to details of the ground motion; thus, it is concluded that realistic estimates of ground motion intensity based on observed effects on monuments, minarets, tombstones, and other similar objects can be made only in probabilistic form and then only when suitable data in sufficient quantity are available.

j. Computer-actuator-on-line control for seismic testing (S. A. Mahin) - Numerical computer simulations are being performed to assess the reliability of a relatively new experimental method for testing structural systems that are too large, massive or strong to be tested on existing shaking tables. A computer is used on-line to monitor and control a test specimen so that quasi-statically imposed displacements closely resemble those that would be developed if the specimen were tested dynamically. Experimental information regarding the nonlinear force-deformation characteristics of the test specimen are used during the test by the computer, along with numerically pre-

scribed information on the specimen's inertial and damping characteristics to determine the deformation that should be imposed for a numerical specified ground motion.

k. Post-earthquake damage analysis (V.V. Bertero, S.A. Mahin) - Various analytical and field investigations have been performed on structures damaged during recent major earthquakes. The objectives of these studies are (1) to identify the structural and/or construction causes of the observed damages, and thereby, assess the adequacy of current seismic resistant design, analysis, and construction methods, and (2) to suggest improvements in current seismic-resistant design practices. To accomplish those objectives, results of detailed analytical studies performed using elastic and inelastic dynamic analysis computer programs have been evaluated in terms of their ability to predict observed damages in selected buildings and in liquid storage tanks.

l. Safety evaluation of buildings exposed to earthquakes and other catastrophic environmental hazards (Bertero, Bresler, Axley) - Research efforts are devoted first, to refining both the methodology and the analytical models developed for evaluating structural response to normal and extreme environments; second, to applying the methodology and analytical models developed in a comprehensive analysis of an existing building; and third, to assessing the implications of the results obtained for practical application of the developed methodology by professional engineers, and suggesting practical guidelines for evaluating damageability of existing buildings by relatively simple means.

Damageability models for evaluating potential hazards to structures exposed to seismic or other extreme environments have been developed. In these models damage indices are associated with energy absorption capacity and with energy dissipation. The effects of two types of interaction between structural elements on damageability of the system are also investigated. A study of damage mechanisms in secondary structural elements (sometimes called nonstructural elements) has also been carried out. It focuses on panel-type elements, such as partitions, exterior finish panels, and windows.

m. Reliability analysis of structures (A. Der Kiureghian) - Probabilistic methods for reliability analysis and design of structures under multiple time varying loads have been developed with emphasis on the second-moment reliability technique. In addition, dynamic analyses of structures subjected to random earthquake type excitations have been carried out with special attention given to the responses of structures with closely spaced modes and to the response of tuned equipment in structures.

n. Development of automated seismic-resistant design procedures (V. V. Bertero, S. Mahin) - The main objective of this research is to develop automated seismic-design procedures that will satisfy three limit states simultaneously (serviceability, damageability, and safety against collapse). One such procedure has already been developed applying an optimization technique for the design of ductile reinforced concrete moment-resisting frame buildings. Reliability analyses of designs based on this procedure show significantly improved seismic response over standard designs based on present code provisions. A similar automated seismic-design procedure is being developed for reinforced concrete frame-coupled shear wall systems.

## B. GEOTECHNICAL ENGINEERING

### 1. Evaluation of Liquefaction Potential (H.B. Seed)

A detailed investigation is being made of the influence of sample disturbance on the cyclic load characteristics of specimens tested in the laboratory. The investigation includes tests on soil specimens obtained by block-sampling, undisturbed tube sampling, freezing techniques and tube sampling with freezing, and comparison of the results with those of the in-situ material from which the samples were extracted.

In addition a field study has been made of the conditions producing soil liquefaction at La Playa on the shore of Lake Amatitlan during the 1976 Guatemala earthquake. Liquefaction was shown to occur in a lightweight pumiceous sand, but the investigations indicated that the field behavior was consistent with standard approaches for investigating the liquefaction potential of soil deposits.

### 2. Influence of Soil Conditions on Ground Responses (H.B. Seed)

A study has been made to determine the influence of soil conditions on ground response during earthquakes, taking advantage of new data concerning site conditions at recording stations which has only recently been made available. Spectra have been normalized both with respect to peak acceleration and peak velocity and used to determine the influence of soil conditions on spectral shape.

### 3. Seismic Stability of Earth Dams (H.B. Seed)

The objective of this research is to contribute to the better understanding of the cyclic behavior of dense, granular materials in relation to the seismic stability of dams. Very few or no published results are available on the dynamic behavior of saturated coarse granular materials in the range of confining pressures and densities encountered in high earth-fill and rock-fill dams. Obtaining meaningful results from the dynamic analysis procedures for embankment dams developed in recent years requires the incorporation of representative dynamic soil properties.

A comprehensive cyclic triaxial test program was conducted on a modelled rock-fill material with the intent of simulating as closely as possible the field loading conditions developed during an earthquake. A modelled gradation with 2-inch maximum particle size was used for the 12-inch diameter specimen tested. Necessary design modifications were incorporated in the test facilities to accommodate a wide range of test pressures.

High pressure cyclic triaxial test equipment was designed and built, and samples of a modelled rock-fill material (gravel) with 1/2-inch maximum particle size were cyclically tested in a 2.8-inch diameter specimens after keeping them under sustained pressure for 10 weeks. The objective of these tests was to simulate the effect of aging of the dam on its cyclic response. The test results showed very significant increases in cyclic resistance in a relatively short period of 2-1/2 months when compared to data for normally consolidated samples tested immediately after compaction.

These results are now being used in the evaluation of the seismic stability of gravel-fill dams. In conjunction with these studies, procedures are being developed to evaluate the seismic response of dams taking into account their three-dimensional configuration when they are constructed in V-shaped valleys.

#### 4. Evaluation of Site Response Characteristics (J. Lysmer)

A study is being made to determine the seismic response of horizontally-layered sites to arbitrary seismic motions comprising different combinations of surface and body waves. The primary purpose of this project is to predict approximately the temporal and spatial variations of the seismic environments which may be expected at any given site and a computer program site has been developed for this purpose. The program is only applicable, however, for sites located at some distance from the earthquake source.

Studies conducted to date involve comparisons of the motions resulting from the propagation of Rayleigh waves and vertically propagating waves in different soil conditions. It is clear that Rayleigh wave motions generated in a layered system are completely different in characteristics from those generated in a half space and the layered system theory is therefore a necessary prerequisite to understanding the effects of Rayleigh waves at soil sites.

#### 5. Soil-Structure Interaction Analyses (J. Lysmer and H.B.Seed)

An analytical procedure is currently being developed which will permit the evaluation of soil-structure interaction effects, for three-dimensional embedded structures, and for wave fields of any arbitrary composition.

#### 6. Analysis of Pore-Pressure Dissipation Effects on Post-Earthquake Soil Behavior (H. B. Seed)

In a number of cases it has been noted that soil instability has developed some short time (several minutes to several hours) after the cessation of earthquake shaking. Studies are being made to investigate how the dissipation of pore pressures generated in the soils by earthquake shaking may be responsible for these post-earthquake failures.

#### 7. Interaction Between Shear and Compression Waves (W. N. Houston)

A study is being made of the soil properties involved in the simultaneous propagation of shear and compression waves in soils. Studies are being made using two types of apparatus. The first involves the use of resonant column techniques specially designed to simultaneously excite samples in both the longitudinal (compression) and torsional (shear) directions. The second involves the use of a new apparatus designed to excite a hollow cylindrical specimen simultaneously in the compressive and shear modes at strain amplitudes and frequencies approximately those experienced during earthquakes.

The resonant column phase, for which some preliminary data has been generated, will provide valuable information about the low-strain ("linear-elastic") interaction between shear wave excitation and compression wave excitation in a cohesionless material. This interaction will be studied as it relates to strain amplitude, density of material, and confining pressure.

The second phase, for which test data has just started to become available, will provide information about the complex interaction of these types of wave excitations in the higher-strain, non-linear range. The apparatus has been designed to provide some overlap in the strain range used for the resonant column testing. The hollow cylinder apparatus will also be used to study this interaction as it relates to strain amplitude, density of material, and confining pressure.

8. Influence of Site Characteristics on the Damage During the October 1974 Lima Earthquake (H. B. Seed, P. Repetto and I. Arango)

On October 3, 1974, a strong earthquake caused a total of 70 deaths in Lima, Peru, and in several villages to the south of the capital city. Property damage was estimated to be over \$200 million. Experience gained from previous earthquakes indicates that in the greater Lima area, the overall damage to buildings is slight except for several pockets of moderate to serious damage. However, the soil conditions in the areas of high damage intensity are now known.

The effect of local soil conditions on the damage pattern has been studied for a number of previous earthquakes throughout the world. The studies show that depth to rock or rock-like material, and the characteristics of the soils overlying it in many cases have had a strong influence on the observed damage to structures. This project will study the soil conditions in the heavy damage areas during the 1974 Lima earthquake, to compare them with those in the light damage areas and to determine if the site conditions could account for the major differences in earthquake damage and whether such differences might have been anticipated on the basis of previous studies of such effects. The overall project will consist of six major studies: (1) damage survey and preparation of damage distribution map of the greater Lima area, (2) survey of subsurface conditions of Lima area, (3) boring and further geophysical tests of selected tests of selected sites, (4) laboratory tests of subsurface materials, (5) development of subsurface profiles, and (6) analysis of data, soil response and cross comparison with results from previous earthquakes.

C. HYDRAULIC ENGINEERING

1. Analysis of Hydrodynamic Drag Forces on Offshore Structures (J. Penzien)

The dynamic analysis of offshore structures is made very complex by the fluid-structure interaction and the nonlinear form of the hydrodynamic drag forces. A special study has just been completed which compares the accuracy of results when drag is represented in three different ways: (a) in the original three-dimensional form represented by the well-known Morison equation, (b) in the so-called equivalent linearized form, and (c) in a modified nonlinear form suggested by Penzien and Tseng which is much more amenable to solution than using the nonlinear Morison form.

2. Hydrodynamic Forces on Submerged Structures (B.C. Gerwich, Jr., J. Penzien, R. L. Wiegel)

Analytical and experimental studies have been carried out to investigate the seismically induced hydrodynamic forces on underwater fixed structures. The experimental phase of the project has consisted of shaking table testing a submerged model of a storage tank and submerged vertical cylinders placed

sufficiently close together to produce hydrodynamic interaction. Hydrodynamic pressure distributions and their resultant forces were measured and they are now being correlated with analytical predictions. A general finite element analysis procedure has been developed for calculating the hydrodynamic pressure distributions produced on submerged axi-symmetrical bodies.

#### D. ENGINEERING SEISMOLOGY

##### 1. Earthquake Sources: Accelerometer Array (L. R. Johnson, T. V. McEvelly)

Investigation of earthquakes by examining the nature of sources through observations made in the near-field (less than 10 km) with wide-band (0.02 - 50 Hz) seismographs. Objective is to develop a model for the earthquake source, based on a propagating dislocation, which explains the wide-band near-field data. For an explosion, the source time history and the role of both near-surface motion and shear failure (s-wave radiation) are sought.

##### 2. In-Situ Seismic Wave Velocity Monitoring (T.V. McEvelly, H.F. Morrison)

Velocities of seismic P and S waves in rocks adjacent to the San Andreas fault in central California are being monitored for stability with a precision of better than 0.1% in a search for premonitory changes prior to moderate shocks in an earthquake prediction study. A "VIBROSEIS" programable source of repetitive seismic waves with known characteristics is being used to monitor velocities at selected sites as a function of time.

#### E. INTERDISCIPLINARY

##### 1. Design of Steel Energy Absorbing Restrainers and Their Incorporation into Nuclear Power Plants for Enhanced Safety (A. Chopra, I. Finnie, W. Godden, J. Kelly, E. Parker, J. Penzien, G. Powell, R. Steidel, E. Wilson, V. Zackay)

The objective of this program which started in August 1977 is to develop restrainer devices utilizing high energy-absorbing steels and to integrate such devices into the design of secondary nuclear power reactor systems, such as piping and equipment for the purpose of enhancing safety and reducing construction costs. Progress has been made in the following areas: (1) analysis of simple piping systems supported by high energy absorbing restrainers and subjected to seismic excitations; (2) development of general procedures for analyzing complex three-dimensional piping systems supported by high energy absorbing restrainers and subjected to seismic excitations, (3) study of steel behavior under high-strain cyclic conditions, and (4) preliminary investigation of the various designs of restrainer devices. An experimental phase will be carried out to investigate the dynamic response of three-dimensional piping systems to simulated seismic excitations using the shaking table.

##### 2. Analysis of Lifelines Subjected to Earthquakes (R.E. Barlow, K.S. Pister, A. Der Kiureghian)

The intent of this project is to develop methodologies for performing risk analyses of network systems such as gas, water, communication and electrical networks relative to earthquake hazards. One methodology found useful in this project is the fault tree analysis. A major computer program for analyzing fault trees called FTAP has been developed. This investigation is conducted jointly between the Operations Research Center and EERC.



3. Models for Identification and Simulation of Earthquake Ground Motions  
(R. M. Oliver, K. S. Pister)

A class of linear, discrete, autoregressive/moving average (ARMA) models has been used for analysis of accelerograms. Techniques for model identification and model parameter estimation have been developed and statistical comparisons of simulated and actual accelerograms conducted. This work is conducted jointly between the Operations Research Center and EERC.

4. Analytical Design (K. S. Pister, E. Polak)

In contrast to many analytical studies which are concerned with the performance of a specified structure when subjected to a given earthquake, this study has been directed toward the choice of a structural design which will provide optimum performance in a specified earthquake or class of earthquakes. A general purpose program, OPTDYN, for interactive optimal design of dynamically loaded structures has been developed in which dual, dynamic constraint levels are permissible.

5. Methods for Interactive Engineering Analysis, Synthesis and Optimal Design (K.S. Pister, E. Polak)

This project, conducted jointly between the Electronics Research Laboratory and EERC, is dedicated to research on interactive analysis and design using a mini-computer with peripheral equipment. A preliminary version of an interactive design algorithm has been implemented and is now in the process of being tested.

6. Influence of Rupture Characteristics on Seismic Ground Motions (B. Bolt, H. B. Seed)

The aims of this research are two-fold; firstly, to demonstrate the influence of rupture characteristics (i.e., the direction and speed of rupture propagation) on spatially recorded seismic ground motion parameters (i.e., accelerations, velocities, displacements, durations and spectral shapes) and secondly to develop some simple procedures for determining the influence of rupture propagation on ground motion parameters used for design purposes. A simple moving point source model has been developed to illustrate this phenomenon. The relative displacements, durations and spectral shapes obtained from this model for the most recent 1979 - Coyote Creek and 1979 - El Centro earthquakes have been found to correlate extremely well with those obtained from the spatial recordings from these events. Furthermore, studies are being made to evaluate the effects of this phenomenon (i.e., directivity) on near field acceleration recordings.

F. INTERNATIONAL COOPERATION

1. U.S.-Taiwan Cooperative Research

A number of cooperative research projects involving institutions from the U.S. and Taiwan are being carried out; the U.S. activities are under the sponsorship of the U.S. National Science Foundation. Current projects are as follows:

a. Ground motion studies (B.A. Bolt, Y.M. Hsiung, J. Penzien, T.B. Tsai)- In this investigation, characteristics of strong ground motions recorded from aftershocks of the Wufeng earthquake on seismographs at Tsengwen, Wanchui and Chiayi in Taiwan were studied in detail. A seismic hazard map for the entire island has been constructed using a probability law with memory to model the historical seismicity pattern and attenuation of intensity.

b. Soil-structure interaction(A.K. Chopra, T.W. Lin, J. Penzien, S.C. Yeh) - The objective of this investigation is to develop an improved method for treating soil-structure interaction. The method adopted makes use of a hybrid model which combines certain features of the finite element and impedance methods now commonly used in practice. By doing so, advantage can be taken of the good features of these latter methods while at the same time minimizing their undesirable features. This is accomplished by modelling the foundation near-field using three-dimensional axi-symmetric finite elements with the far-field modelled through continuous three-component impedance elements placed at the interface of the near- and far-fields. These impedance functions have been developed at the University of California using methods of system identification so that the resulting system will reproduce the known compliance functions for a rigid massless plate resting on an elastic half-space. At the National Taiwan University, certain impedance functions have been obtained using a more direct mathematical approach leading to closed form solutions.

c. Techi arch dam studies (R.W. Clough, S.T. Mau) - As described earlier in this report, field tests have been performed on the Techi arch dam in Taiwan and shaking table tests have been performed on two types of models representing the dam's arch and cantilever actions. In addition, a comprehensive finite element analysis of the Techi dam is being made to determine its response to strong motion earthquakes.

d. Taiwan large-scale, strong motion array (B.A. Bolt, J. Penzien) - This project will establish a large-scale strong ground motion array in Taiwan as part of a world-wide system of such arrays to study seismological and engineering aspects of strong earthquakes. The strong-motion digital accelerometers are provided by the United States (National Science Foundation) with the operation, maintenance, and data processing costs being covered by Taiwan (National Science Council). The seismological and engineering aspects of the array design and subsequent analyses of the recorded motions will be carried out on a cooperative basis by the investigators.

## 2. U.S.-Japan Cooperative Research

Planning for a U.S.-Japan Cooperative Research Program Utilizing Large-Scale Testing Facilities has been conducted over a two-year period with financial support on the U.S. side being provided by the National Science Foundation through a grant to UCB. The official planning group on the U.S. side consisted of B. Bresler, V. Bertero, S. Mahin and J. Penzien, UCB; G. Corley, Portland Cement Association; J. Jirsa, University of Texas; L. Lu, Lehigh University; E. Leyendecker, National Bureau of Standards; R. Hanson, University of Michigan; A. Mattock, University of Washington; and M. Sozen, University of Illinois. This group has made detailed plans and recommendations for an extended large-scale testing program to investigate the seismic response characteristics of prototype structural systems, including force-deformation relations, energy absorption capacities, and failure mechanisms.

### 3. U.S.-Yugoslavia Cooperative Research

Since 1972, EERC has participated in a cooperative earthquake engineering research program with a number of laboratories in Yugoslavia, under the financial support of the NSF International Programs Office. That program has been directed toward improving the earthquake engineering capabilities of selected research laboratories in the seismic areas of Yugoslavia. While the initial phase of this program has been essentially completed, it is continuing with studies on non-structural wall assemblies and masonry structures conducted cooperatively with institutions in Zagreb and Ljubljana, respectively. In addition, a program of cooperation between one of the Yugoslavia institutions, the Institute of Earthquake Engineering and Engineering Seismology of the University of Skopje, and EERC is continuing under the sponsorship of the U.S. National Academy of Sciences and the Yugoslavia Academy of Sciences. This research is concerned primarily with the seismic safety of high rise, large panel and poured-in-place reinforced concrete residential structures. A large number of UCB faculty are participating in this program.

#### V. NATIONAL INFORMATION SERVICE IN EARTHQUAKE ENGINEERING

The National Information Service in Earthquake Engineering (NISEE) is a public service program conducted jointly by EERC and the California Institute of Technology under separate grants from the National Science Foundation. The primary function of the service is to compile and disseminate information being generated around the world in earthquake engineering and its allied fields for use by professional engineers, researchers, educators, and representatives of business and government. The program contains three major components: (1) providing information on and the dissemination of computer programs, (2) publication of the Abstract Journal in Earthquake Engineering, and (3) information transfer from the Earthquake Engineering Library. Presently, forty nine different computer programs for solving complex problems in earthquake engineering are available along with documentary information. Over the past six years approximately 3,000 computer program decks and 11,000 documentation packages have been disseminated. The larger number of documentation packages in contrast with the smaller number of computer program decks is due to the fact that further dissemination of computer programs takes place outside the NISEE activity. Considerable effort is being made to convert computer programs to a form compatible with the new generation micro-computers. The Abstract Journal in Earthquake Engineering is published annually with the content of each volume covering literature on a world-wide basis over one calendar year. The number of abstracts in each recent volume has been well over 1,000, e.g., Volume 7 covering the literature for calendar year 1978 contains 1,390 abstracts. Information transfer from the Earthquake Engineering Library is an activity of NISEE that has expanded rapidly in recent years due to the library's excellent collection of current literature and the convenient service provided. Requests for and the transfer of information are made primarily by mail and telephone. More than 8,000 transactions of this type have taken place over the past two years.

#### VI. PUBLICATIONS

The EERC report series is the main source for detailed presentations of research results generated in the Center. Approximately 30 different reports are published each year which are widely distributed to earthquake engineering research organizations throughout the world. Because of cost considerations, limited copies are distributed by the Center to individuals. Copies can, however, be obtained from the National Technical Information Service, 5285 Port

Royal Road, Springfield, Virginia 22161, USA. A complete listing of these reports can be obtained directly from EERC, Building 451, University of California, Richmond Field Station, 47th Street and Hoffman Boulevard, Richmond, California 94804, USA.

The EERC News is a quarterly newsletter reporting on current EERC research. Each issue also provides its readers with up-to-date information on NISEE services, library acquisitions, new computer programs, and EERC reports. To receive a complimentary copy, write to EERC at the above address.

As previously mentioned, EERC publishes the Abstract Journal in Earthquake Engineering annually which is distributed on a subscription basis.

#### VII. PERSONNEL

Most of the research activities of EERC are carried out through the joint effort of faculty working directly with graduate students; thus, the Center provides major support for the educational programs. The number of faculty actively participating in the research programs is about 25 with the number of graduate students (master and doctorate levels) averaging about 65 each year. A limited number of undergraduate students also assist in the research activities.

Each year approximately 10 short-term (usually one year) post-doctoral researchers are employed to work with faculty. About the same number of scholars from the academic institutions throughout the world visit the Center. These scholars participate part-time in the Center's research without stipends with the remainder of their time spent in other academic endeavors, such as auditing courses, attending seminars, and individual study.

The number of full-time administrative, clerical, and technical support personnel employed by the Center is about 25. Some part-time employees also assist in these activities, as needed.

#### VIII. CLOSING STATEMENT

The overall program of the Earthquake Engineering Research Center, University of California, Berkeley, is continually in a transient state with new projects being initiated and others being phased out. Therefore, this report having been written in February 1980 provides an overview of its activities in the recent past through 1979. It is anticipated that the present level of effort will continue into the future for some time.

#### IX. ACKNOWLEDGMENTS

The author expresses his sincere thanks and appreciation to the investigators named herein for their contributions to this report. He also expresses thanks to the various sponsors of the research and public service activities reported, namely, U.S. National Science Foundation, sponsor of most of the programs, American Petroleum Institute, Malaysian Rubber Producers Research Association, U.S. Department of Energy, U.S. Department of Housing and Urban Development, American Iron and Steel Institute, California Department of Transportation, U.S. Sea Grant College Program, Esso Education Foundation, and Standard Oil Company of California.

GROUND MOTION INTENSITY BASED ON EARTHQUAKE  
EFFECTS ON HISTORICAL MONUMENTS

by Chik-Sing Yim<sup>I</sup>, Joseph Penzien<sup>II</sup>, Anil K. Chopra<sup>III</sup>

SUMMARY

A numerical procedure and computer program are developed to solve the nonlinear equations of motion governing the rocking of rigid blocks on a rigid base subjected to horizontal and vertical earthquake ground motions. The results obtained show this response to be very sensitive to small changes in block size and slenderness ratio and to details of the ground motion; thus, it is concluded that realistic estimates of ground motion intensity based on observed effects on monuments, minarets, tombstones, and other similar objects can be made only in probabilistic form and then only when suitable data in sufficient quantity are available.

INTRODUCTION

Toward the latter part of the 19th century and in the early part of this century, before instruments had been developed to record strong ground motions, procedures were proposed to estimate the intensity of ground shaking from its observed effects on tombstones and monumental columns, whether they overturned or remained standing [1-4]. A wealth of historical information from seismic areas of the world which were centers of the ancient Roman, Greek, Chinese, and Indian civilizations was available for this purpose. Some of the historical monuments in these areas were destroyed by earthquakes, while others withstood many destructive earthquakes. Such an approach was recently employed to estimate the accelerations in the epicentral region of the 1975, Ohita earthquake in Japan [5]. The proposed procedures idealized the free standing tombstone or column as a rigid block resting on a rigid base, and the ground motion was either idealized as an instantaneous impulse or its effects were represented by a static horizontal force acting on the block.

Motivated by the observations of damage to water tanks in the 1960 Chilean earthquakes, Housner was the first to systematically investigate the dynamics of a rigid block on a rigid horizontal base undergoing horizontal motion [6]. His work led to important results explaining the response of rigid blocks to rectangular and half-cycle sin-wave pulse type motions and to white noise excitation; however, due to its limited scope, there still remained unanswered questions with regard to the sensitivity of block parameters and ground motion properties on response. Later, concerned with the behavior of concrete blocks providing radiation shielding in particle accelerator laboratories, Godden investigated this problem by testing rigid blocks on the Berkeley shaking table [7]. These experiments demonstrated that the rocking response of a rigid block is very sensitive to its boundary conditions, the impact coefficient of restitution, and the ground

---

<sup>I</sup> Research Assistant, Univ. of Calif., Berkeley, Calif., U.S.A.  
<sup>II</sup> Professor of Structural Engr., Univ. of Calif., Berkeley, Calif., U.S.A.  
<sup>III</sup> Professor of Civil Engr., Univ. of Calif., Berkeley, Calif., U.S.A.

motion details.

In this paper, the results of an analytical investigation of the sensitivity of block parameters and ground motion properties on rocking response are presented. These results show, due to the high levels of response sensitivity present, that behavioral trends exist but only in a probabilistic sense. The implications of this finding on estimating the intensity of ground shaking from its observed effects on tombstones, monumental columns, and developing protective measures for historical monuments are presented.

### RIGID BLOCK EQUATIONS OF MOTION

A rigid block subjected to horizontal and vertical ground accelerations of a rigid base is shown in a rotated position in Fig. 1. The coefficient of friction is assumed to be sufficiently large so that there will be no sliding between the block and the base. Depending on the ground acceleration, the block may move rigidly with the ground or be set into rocking. In the latter case, it will oscillate about the centers of rotation  $O$  and  $O'$ . It is assumed that the block and base surfaces in contact are perfectly smooth so that the block will rotate only about edges  $O$  and  $O'$ .

When subjected to base accelerations  $a_g^x$  in the horizontal direction and  $a_g^y$  in the vertical direction, the block will be set into rocking when the overturning moment of the horizontal inertia force about one edge exceeds the restoring moment due to the weight of the block and vertical inertia force; i.e., when

$$\frac{W}{g} a_g^x \frac{H}{2} > \left( W + \frac{W}{g} a_g^y \right) \frac{B}{2} \quad (1)$$

where  $W$  is the weight of the block and  $g$  equals the acceleration of gravity. It is assumed here that the geometric and gravity centers of the block coincide.

The rigid block will oscillate about the centers of rotation  $O$  and  $O'$  when it is set into rocking. The equations of motion of the block, governing the angle from the vertical (Fig. 1), subjected to horizontal and vertical ground accelerations  $a_g^x(t)$  and  $a_g^y(t)$  are derived by considering the equilibrium of moments about the centers of rotation. These equations may be expressed as

$$I_O \ddot{\theta} + W \left( 1 + \frac{a_g^y(t)}{g} \right) R \sin(\theta_c - \theta) = - \frac{W}{g} R \cos(\theta_c - \theta) a_g^x(t) \quad (2)$$

when the block is rotating about  $O$ , and

$$I_O \ddot{\theta} - W \left( 1 + \frac{a_g^y(t)}{g} \right) R \sin(\theta_c + \theta) = - \frac{W}{g} R \cos(\theta_c + \theta) a_g^x(t) \quad (3)$$

when it is rotating about  $O'$ . In addition to the quantities defined earlier and in Fig. 1,  $I_O$  equals the mass moment of inertia of the block about  $O$  or  $O'$ ; and  $\theta_c = \cot^{-1}(H/B)$ . Because of the trigonometric functions of  $\theta$ , each of these equations is nonlinear. Another source of nonlinearity is the switching of equations back and forth between Eqs. 2 and 3 as the block rocks alternately about  $O$  and  $O'$ .

The relation between a static moment applied about  $O$  and  $O'$  and the resulting angle of rotation  $\theta$ , as identified from the linearized form of Eqs. 2 and 3, is shown in Fig. 2. Interpreting this relationship in terms of the

usual concepts of structural stiffness, the system has infinite stiffness until the magnitude of the applied moment reaches  $WR\theta_c$ ; thereafter, the stiffness is negative. When  $\theta$  exceeds  $\theta_c$ , the critical angle, the block will overturn under static moment; but, as will be seen later, not necessarily under dynamic conditions. Obviously, the properties of the rocking block are much different than those of a linear single-degree-of-freedom system where the stiffness is positive and constant. The former properties are reminiscent of a rigid plastic system except that, for the rocking block, the second slope is negative and the behavior is non-hysteretic.

As the rocking block instantaneously shifts its center of rotation from  $O$  to  $O'$  or from  $O'$  to  $O$ , a coefficient of restitution is applied to the impact as defined by

$$e \equiv \dot{\theta}_2 / \dot{\theta}_1 \quad (4)$$

where  $\dot{\theta}_1$  and  $\dot{\theta}_2$  are the angular velocities immediately before and after impact, respectively. If the impact is assumed to be such that there is no bouncing of the block and rotation continues smoothly through impact so that angular momentum about one point of rotation is conserved, then the coefficient of restitution will be given by the relation

$$e = 1 - \frac{3}{2} \sin^2 \theta_c \quad (5)$$

and the fraction of energy loss due to impact will be equal to  $(1-e^2)$ .

#### RESPONSE ANALYSIS

The rocking response of the rigid block to prescribed ground acceleration is determined by numerically solving Eqs. 2 and 3 with the condition for initiating rocking as defined by Eq. 1 and the condition of impact as defined by Eq. 4. The value of the coefficient of restitution,  $e$ , is specified either consistent with the conservation of angular momentum relation, Eq. 5, or with measured values found through experiments.

In this investigation, rocking response was obtained by this procedure using 20 sets of two simulated ground accelerations of 30 seconds duration modelled after four past earthquakes (El Centro, 1934; El Centro, 1940; Olympia, 1949; Taft, 1952); i.e., using [8,9]

$$\begin{aligned} a_g^x(t) &= I_x(t) a_x(t) \\ a_g^y(t) &= I_y(t) a_y(t) \end{aligned} \quad (6)$$

where  $I_x(t)$  and  $I_y(t)$  are deterministic intensity functions defined by

$$I_x(t) \equiv \begin{cases} \frac{t^2}{16} & 0 < t < 4 \text{ sec.} \\ 1 & 4 < t < 15 \\ \exp[-0.0992(t-15)] & 15 < t < 30 \end{cases} \quad (7)$$

and

$$I_y(t) = \begin{cases} 0.6 & 0 < t < 10 \text{ sec.} \\ \exp[-0.1010(t-10)] & 10 < t < 30 \end{cases} \quad (8)$$

respectively, and where  $a_x(t)$  and  $a_y(t)$  are stationary random processes having power spectral density functions of the form

$$S(\omega) = S_0 \frac{1 + 4 \xi_g^2 \left(\frac{\omega}{\omega_g}\right)^2}{\left\{ \left[1 - \left(\frac{\omega}{\omega_g}\right)^2\right]^2 + \xi_g^2 \left(\frac{\omega}{\omega_g}\right)^2 \right\}} \quad (9)$$

In this equation, the characteristic frequency  $\omega_g$  and the characteristic damping value  $\xi_g$  are assigned the numerical values  $5\pi$  rads/sec and 0.6, respectively, when generating sample values of  $a_x^x(t)$  and the numerical values  $7.5\pi$  and 0.6, respectively, when generating sample values of  $a_y^y(t)$ . Spectral density  $S_0$  was in each case assigned a numerical value consistent with a specified intensity level based on the average of the peak accelerations of members of the process, i.e., 1 g and 0.6 g for the mean peak values of  $a_x^x(t)$  and  $a_y^y(t)$ , respectively.

#### RESPONSE BEHAVIOR

Using the computer program mentioned earlier, the response of a number of rigid blocks to the same simulated motion was determined. The time-variation of the rotation of the block is presented in Fig. 3. In those cases where the rotation  $\theta$  continues to increase significantly beyond  $\theta_c$ , the block overturns. It is seen from this figure that the rocking response of the block can be very sensitive to small changes in the system parameters. Small variations in the slenderness ratio  $H/B$  and size parameter  $R$  lead to large changes in response. In contrast to conclusions derived from single pulse excitations, stability of a block does not necessarily increase monotonically with increasing size or decreasing slenderness ratio. Similarly, contrary to what intuition would suggest, decrease in the value of the coefficient of restitution — which implies increase in energy dissipation — does not necessarily lead to smaller response of the block.

Because of the above sensitivity, it became apparent that the influence of system parameters and ground motion properties on rocking response of rigid blocks should be studied from a probabilistic point of view. Therefore, time-histories of response  $\theta(t)$  were obtained for many blocks, each having fixed parameters and each subjected separately to 20 simulated base excitations of the form previously described but scaled by an appropriate factor  $\alpha$ . Thus, in each case 20 values of  $\bar{\theta}_{\max}$  defined by  $\bar{\theta}_{\max} \equiv \theta_{\max}/\theta_c$  were obtained which when plotted in ascending order provide cumulative probability distribution functions (CDF) for extreme values of response as shown in Figs. 4-7. Each CDF in these figures shows that a large dispersion exists in the extreme values of response. Comparing all results in each of these figures shows reasonably consistent statistical trends with respect to parameters  $e$ ,  $\alpha$ ,  $H/B$  and  $R$ , but it is shown that when vertical ground motion is added to the horizontal component, increased levels of response result in some cases but not in others.

As indicated in Figs. 4-7, a block may overturn when subjected to some members of the ensemble of simulated ground motions but remain stable under the action of other members of the same ensemble. From these results, the probability that a block will overturn when subjected to ground motion of specified intensity can be roughly estimated as the fractional number of



ground motions that overturn the block. The influence of system parameters and ground motion intensity on the overturning probability is shown in Figs. 8-10. It is seen that the probability of overturning increases with increasing slenderness ratio for fixed size parameter and ground motion intensity, decreases with increase in size for fixed slenderness ratio and ground motion intensity, and increases with ground motion intensity for fixed size parameter and slenderness ratio. Again it is shown that the influence of vertical ground motions is quite erratic making it difficult to establish statistical trends.

#### GROUND MOTION INTENSITY

The results presented herein show that systematic trends are observed when the rocking response of rigid block is studied from a probabilistic point of view with the ground motion modelled as a random process. The probability of a block exceeding any response level, as well as the probability that a block overturns, increases with increase in ground motion intensity, with increase in slenderness ratio of the block, and with decrease in its size.

Probabilistic estimates of the intensity of ground shaking may be obtained from its observed effects on monuments, minarets, tombstones, and other similar objects provided suitable data in sufficient quantity are available, and provided the estimates are based on probabilistic analyses of the rocking response of rigid blocks, considering their nonlinear dynamic behavior. These estimates will not be precise because the response of rocking blocks is extremely sensitive to variations in system parameters, contact conditions between base of blocks and their support, and ground motion details. For the same reasons, it should be recognized that a deterministic estimate of the intensity of ground motion from its observed effects on a single object is totally unreliable.

#### OVERTURNING OF MONUMENTAL STRUCTURES

Important historical monuments in regions of high seismicity are gradually being destroyed by strong motion earthquakes. Recent events have caused severe damage at many sites including Burma, 1975, Italy and Guatemala, 1976, and Romania, 1977. This is a problem of great concern to the ICOMOS (International Council on Monuments and Sites) Committee on Protection of Monuments and Sites in Seismic Areas.

Because of their inherent structural complexities, variabilities of materials, and levels of damage, each historical monument must be treated as a special case when assessing future damage potential and developing effective protective measures. There is however one class of structural elements common to these sites, namely free standing columns, walls, and other isolated segments, which respond under earthquake conditions in a manner similar to the rigid block previously described. Thus, after having developed expected ground motion intensity levels for a given site through seismic risk studies, results similar to those shown in Fig. 8-10 can be very useful in estimating probabilities of survival of such elements and in selecting protective measures which are rationally sound.

## ACKNOWLEDGMENT

Financial support for the investigation reported herein was provided by the Division of Problem Focused Research, National Science Foundation, under Grant No. PFR-78-08261-ZNF.

## REFERENCES

1. Galitzin, F. B., "Über eine dynamische Skala zue Schätzung von Makroseimischen Bewegungen," 25 pp., St. Petersburg, 1911. Summarized in English by H. O. Wood in Bulletin of the Seismological Society of America, Vol. 3, No. 2, pp. 90-94, 1913.
2. Milne, J., "Seismic Experiments," Transactions of the Seismological Society of Japan, Vol. 8, pp. 1-82, 1885.
3. Milne, J. and Omori, F., "On the Overturning and Fracturing of Brick and Columns by Horizontally Applied Motion," Seismological Journal of Japan, Vol. 17, pp. 59-86, 1893.
4. Kirkpatrick, P., "Seismic Measurements by the Overthrow of Columns," Bulletin of the Seismological Society of America, Vol. 17, pp. 95-109, 1927.
5. Omote, S., Miyake, A., and Narahashi, H., "Maximum Ground Acceleration in the Epicenter Area - Field Studies on the Occasion of the Ohita Earthquake, Japan, of April 21, 1975," Bulletin of the International Institute of Seismology and Earthquake Engineering, Vol. 15, pp. 62-82, 1977.
6. Housner, G. W., "The Behavior of Inverted Pendulum Structures During Earthquakes," Bulletin of the Seismological Society of America, Vol. 53, No. 2, pp. 404-417, 1963.
7. Aslam, M., Godden, W. G., and Scalise, D. T., "Earthquake Rocking Response of Rigid Bodies," Journal of the Structural Division, ASCE, Vol. 106, No. ST2, February 1980; also see Report No. LBL-7539, Lawrence Berkeley Laboratory, University of California, Berkeley, California, November 1978.
8. Ruiz, P., and Penzien J., "Probabilistic Study of the Behavior of Structures During Earthquakes," Report No. EERC 69-3, Earthquake Engineering Research Center, University of California, Berkeley, California, March 1969.
9. Jennings, P. C., Housner, G. W., and Tsai, N. C., "Simulated Earthquake Motions," Earthquake Engineering Research Laboratory, California Institute of Technology, Pasadena, California, April 1968.

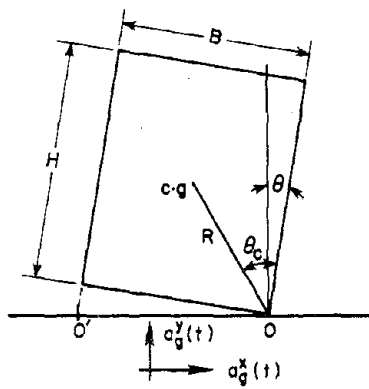


FIG. 1 ROCKING BLOCK

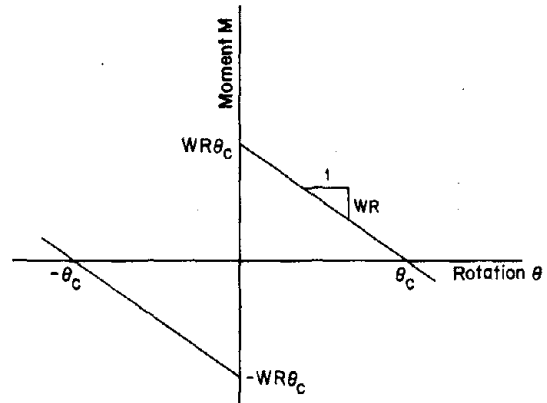


FIG. 2 MOMENT-ROTATION RELATION FOR SLENDER BLOCKS ( $H/B \geq 3$ )

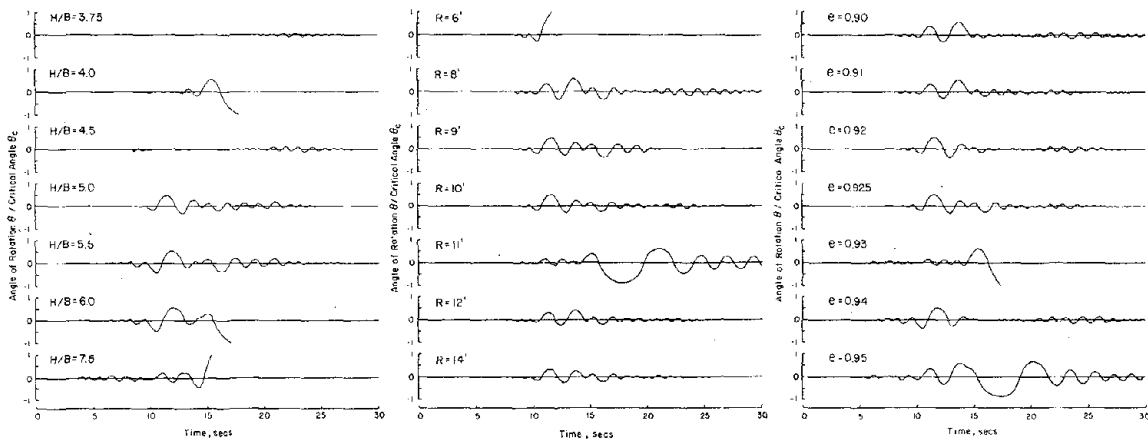


FIG. 3 RESPONSE OF SEVERAL BLOCKS TO THE SAME SIMULATED MOTION. PARAMETERS: SLENDERNESS RATIO  $H/B$ , SIZE  $R$ , AND COEFFICIENT OF RESTITUTION ARE VARIED ONE AT A TIME

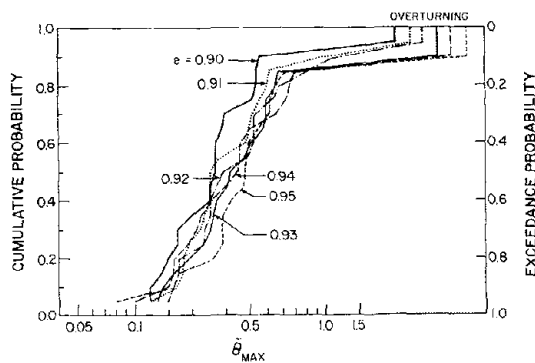


FIG. 4 CUMULATIVE PROBABILITY DISTRIBUTION FUNCTIONS FOR MAXIMUM ROTATION OF A BLOCK,  $R = 10$  FT. AND  $H/B = 5$ , FOR VARIOUS VALUES OF THE COEFFICIENT OF RESTITUTION  $e$ . ENSEMBLE AVERAGE OF PEAK HORIZONTAL GROUND ACCELERATION  $\approx 0.4g$  ( $Q=0.4$ )

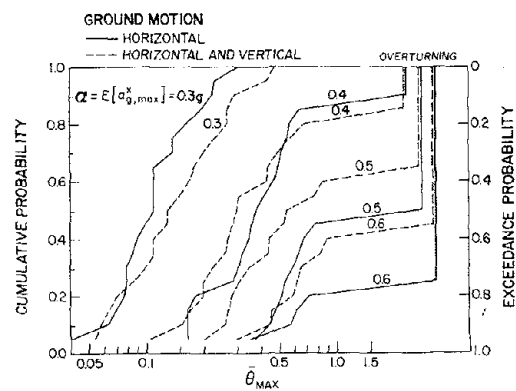


FIG. 5 CUMULATIVE PROBABILITY DISTRIBUTION FUNCTIONS FOR MAXIMUM ROTATION OF A BLOCK,  $R = 10$  FT., AND  $H/B = 5$ . ENSEMBLE AVERAGE OF PEAK ACCELERATION IS VARIED:  $0.3g, 0.4g, 0.5g$ , AND  $0.6g$  FOR HORIZONTAL GROUND MOTION:  $0.18g, 0.24g, 0.30g$ , AND  $0.36g$  FOR VERTICAL GROUND MOTION

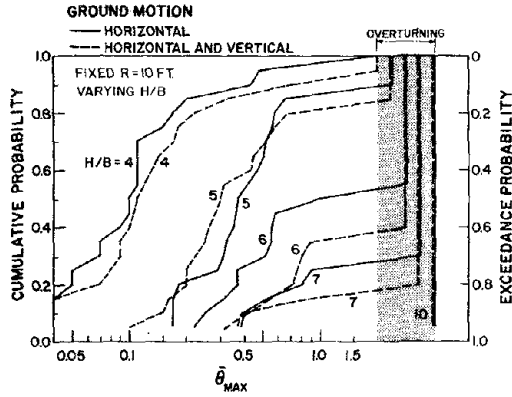


FIG. 6

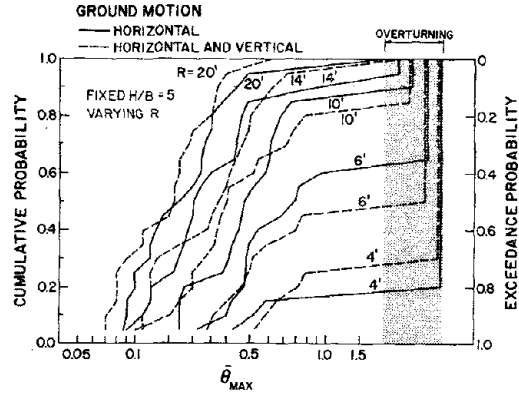


FIG. 7

CUMULATIVE PROBABILITY DISTRIBUTION FUNCTIONS FOR MAXIMUM ROTATION OF BLOCKS SUBJECTED TO ENSEMBLES OF HORIZONTAL AND VERTICAL GROUND MOTIONS, WITH AVERAGE VALUES OF PEAK ACCELERATION = 0.4g AND 0.24g, RESPECTIVELY.

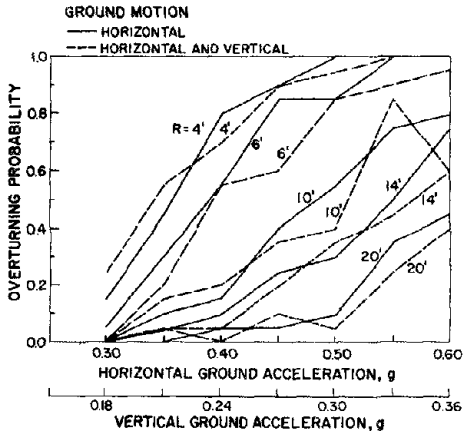


FIG. 8

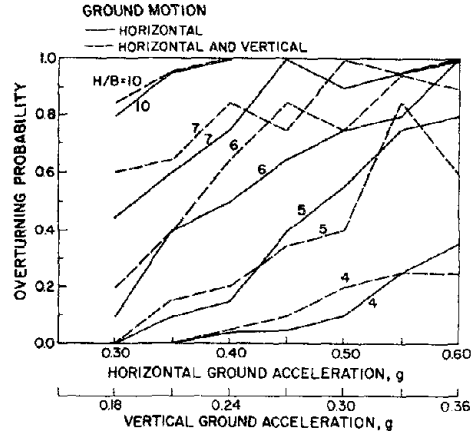


FIG. 9

OVERTURNING PROBABILITY FOR BLOCKS SUBJECTED TO ENSEMBLES OF HORIZONTAL AND VERTICAL GROUND MOTIONS, WITH AVERAGE VALUES OF PEAK ACCELERATION VARIED AS SHOWN.

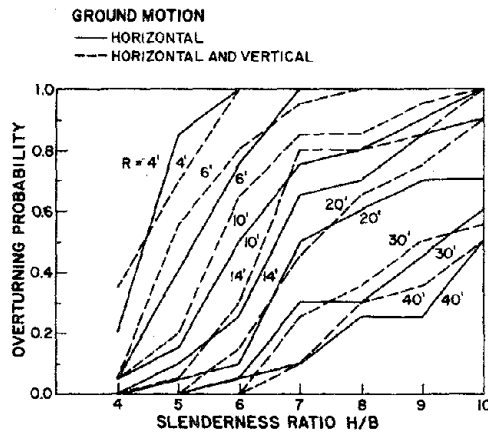


FIG. 10 OVERTURNING PROBABILITY FOR BLOCKS SUBJECTED TO ENSEMBLES OF HORIZONTAL AND VERTICAL GROUND MOTIONS, WITH AVERAGE VALUES OF PEAK ACCELERATION = 0.4g AND 0.24g, RESPECTIVELY.

# DYNAMIC PROPERTIES OF PREFABRICATED APARTMENT BUILDINGS

by

J. G. Bouwkamp<sup>I</sup> and R. M. Stephen<sup>II</sup>

## SYNOPSIS

The paper describes the results of experimental forced and ambient vibration studies of a 12-story apartment building, constructed with prefabricated wall panel and slab elements. Dynamic characteristics, such as resonant frequencies, vertical and horizontal mode shapes and damping capacities of the structure are presented and correlated with analytical studies using the computer program TABS. The fundamental periods of this structure and of an 8-story apartment building with basically the same floor plan and construction are also presented.

## INTRODUCTION

For the last 15 years, a number of full-scaled tests using both forced and ambient vibration techniques have been conducted on multistory structures with distinctly different structural systems (1,2). The collected dynamic data have been used to evaluate the accuracy of analytical modelling and computer programs used in predicting the structural response to known vibration inputs. This led to improved computational procedures and resulted in more reliable predictions of the structural response to actual earthquake ground motions. In order to gain information about the dynamic behaviour of prefabricated apartment buildings, field tests have been performed on the 8-story Los Partales Building and the 12-story Wesley Manor Building located in Oakland and Campbell, California, respectively.

## DESCRIPTION OF THE WESLEY MANOR BUILDING

The 105 foot high building (Fig. 1) has an overall plan of approximately 80 by 164 feet. It is designed as a housing development and is therefore modular in concept. The foundation layout and typical floor plan are shown in Figures 2 and 3, respectively. The building is serviced by two elevators, located in the center, and two stairwells on the north side at either end of the structure. The structure is a "Forest City Dillon" prefabricated building system. The vertical and horizontal load-carrying system consists of reinforced concrete shear walls in both the transverse and the longitudinal directions. These walls rise from the first floor and run upward to the roof in the same dimensions. On the first floor, there are some openings in the walls as noted by solid lines on the foundation plan (Fig. 2). These wall elements rest on spread footings which in turn are placed on 24" diameter piles varying in length from about 30 to 52 feet.

The "Forest City Dillon" system uses solid reinforced floor elements and hollow wall elements. The floor elements have a thickness of 4" and plan dimensions of 8 by 22 feet. At the site, a 4" concrete topping is placed on these elements, with reinforcing at the joints between single floor elements. Preassembled kitchen and bathroom units have an 8" thick slab and are constructed so that reinforcing bars protrude enough to tie into the 4" topping of the adjacent floor panels. The cells of the wall panel elements are reinforced and filled with concrete. Fig. 6 shows a

---

I Professor of Civil Engineering, University of California, Berkeley, USA.  
II Principal Development Engineer, University of California, Berkeley, USA.

typical wall panel element with reinforcing. Examples of an exterior and interior joint are shown in Fig. 7.

#### EXPERIMENTAL STUDIES

Forced vibrations were produced by two rotating mass vibration generators mounted on the twelfth floor at the center of the east and west sides of the building. Linear accelerometers ( $\pm 0.25g$ ) were used to measure the horizontal floor accelerations. Frequency-response curves were determined by increasing the frequency incrementally and measuring the vibration response of the structure at each step. Frequency-response data for different forcing directions and levels of excitations are shown in Figure 4. Using the bandwidth method damping capacities may be found from the normalized frequency-response curves near resonances as  $\zeta = \Delta f/2f$ , where  $f$  = resonant frequency, and  $\Delta f$  = frequency difference of two points on the response curve with amplitudes of  $1/\sqrt{2}$  times the resonant amplitude. Once the resonant frequencies have been found, the mode shapes at each of these frequencies may be determined. Typical mode shapes are shown in Fig. 5. The vertical mode shapes in Fig. 5 show the relative motions at the center and the west end of the building. The horizontal floor modes for the 6th and 12th story are plotted to the right of the corresponding vertical mode shape. Six accelerometers were used to detect the horizontal mode shapes. The floor slab behaved basically as a rigid diaphragm; an observation used specifically in the development of the analytical model of this structure.

The ambient vibration study of dynamic properties uses field measurements based on wind and micro-tremor induced vibrations. An assumption in the analysis technique is that the exciting forces are a stationary random process possessing a reasonably flat frequency response spectrum. A structure subjected to this input will respond in all its normal modes. Wind produces the largest ambient vibrations for multistory structures. The wind induced vibrations were measured using Seismometers. Modal frequencies were obtained by seismometers placed near the outer walls on the north, south, east, and west sides of the 12th floor of the building. The orientation of the seismometers on the north and south sides allowed evaluation of the E-W frequencies; those on the east and west sides the N-S frequencies. In this way, translational frequencies were obtained by averaging the sum of the seismometer readings and torsional frequencies by averaging the difference of those readings. For measurement of the translational and torsional modes, two of the seismometers remained at the twelfth floor and two were placed in pairs at each successive floor. As in the case for determining the modal frequencies, the sum of the two seismometers was averaged to give the translational modes and the difference of the seismometers was averaged to give the torsional modes. Fourier transforms were used to analyze the low level structural vibrations and, thus, to identify the modal frequencies. Comparing vibration amplitude and phase for various floor levels provides an estimate of the mode shape.

The resonant frequencies obtained from the forced vibration tests are in the average 3% smaller than those from the ambient vibration tests and are compared in Table 1. This nonlinear aspect may be due to larger excitations under forced vibrations. The ambient vibration tests gave an equivalent viscous damping factor, determined by using the bandwidth method, of about 1%.

### ANALYTICAL MODEL

An analytical computer model of the Wesley Manor Building was developed to assess the dynamic characteristics. The model was formulated using both a rigid and a flexible base. TABS, a general purpose computer program, was used to calculate the frequencies and mode shapes of the structure. The program considers the floors to act as rigid diaphragms with zero transverse stiffness. All elements are assembled initially into planar frames and then transformed, using the rigid-diaphragm assumption to three degrees of freedom (2 translational and 1 rotational) at the center of rigidity or each story level.

The basic model of the building was formulated as a system of frames and shear wall elements interconnected by floor diaphragms which were rigid in their own plane and fixed at the first floor level. All walls were treated as "wide columns". This required a reduction of properties (I, A) to the elastic centroid of each wall. Moments of inertias of the shear walls included flange areas, with a maximum effective width of one third of the building height or 35'. A value of 4,000 ksi was used for the modulus of elasticity of the concrete and 29,000 ksi for the reinforcing steel. The reinforcing steel area was included in calculating the moment of inertia of the shear walls. Wherever shear walls were positioned in one line parallel to the direction of motion, it was assumed that those walls would be coupled by a portion of the floor slab, which was chosen to be 18 times the thickness of the floor. The effective span of the coupling girders were identical to the clear distance between the walls. Also, the effective height was taken as the clear height between two stories. Fig. 9 shows how two panel elements were idealized for the analytical model.

During the experimental phase of the work, significant horizontal motion was recorded at the first floor level. Therefore, a second analytical model was developed to reflect the flexible base condition. Based on the measurements of the horizontal ground accelerations and the base rotations, estimated from the mode shapes, the following approach was used. The measured floor accelerations times the floor masses gave the elastic forces for each floor level, from which the base shear and the overturning moment could be computed. Comparing base shear and moment with the experimentally determined displacement and rotation at the first story allowed an assessment of the translational and rotational stiffness of the foundation for both directions. An additional dummy base story with stiffness properties as calculated was added to the structure to account for foundation and soil flexibility.

The frequencies for the rigid base model, as well as for the flexible base model, are compared with the experimental results in Table 1. Good agreement with the experimental frequency values can be noted for the model with flexible base, although it seems that the real foundation is stiffer than the "dummy story".

### CONCLUSIONS

The results presented herewith clearly show that forced and ambient vibration studies can be carried out effectively. In comparing experimental and analytical solutions, good agreement can be noted for frequencies and mode shapes. Only the three fundamental modes of vibration could be found from the forced (up to 6.75 Hz) and ambient vibration tests (up to 20 Hz), thus indicating that the building would respond in a first mode motion to

seismic excitation. The predominant feature which came out of the dynamic tests was the high coupling between E-W and torsional modes. This highly coupled response indicates the need to revise the floor plan in order to separate the modes. The same behavior was observed during the tests of the 8-story Los Portales Building with almost the same floor plan. The periods of the two structures are plotted versus building height and reveals, as shown in Fig. 8, an almost linear increase with height.

The frequencies for a standard code analysis, based on overall building dimensions, are 22% low in the N-S (transverse) direction and 40% high in the E-W (longitudinal) direction. These inconsistent results clearly indicate the need for a detailed dynamic analysis, considering the actual wall layout, stiffness distribution, and foundation conditions. Neglecting the foundation flexibility, as done in the rigid base model, yields an over-estimation of the frequencies by 30% to 50%. Thus, in the analysis of rigid structures on flexible foundations, the soil-structure interaction must be considered.

#### ACKNOWLEDGEMENT

The authors gratefully acknowledge the financial support provided by the National Science Foundation under Grant NSF PFR79-08257-ZNF.

#### REFERENCES

1. Wiegel, R. L., Earthquake Engineering, Prentice Hall, Inc., 1970.
2. Stephen, R. M., Wilson, E. L., Bouwkamp, J. G., and Button, M., "Dynamic Behavior of a Pedestal-Base Multistory Building," Report No. EERC-78/13, Earthquake Engineering Research Center, University of California, Berkeley, 1978.
3. Wilson, E. L., and Dovey, H. H., "Three-Dimensional Analysis of Building Systems - TABS", Report No. EERC-72/8, Earthquake Engineering Research Center, University of California, Berkeley, 1972.

TABLE 1 (Frequencies)

Forcing Direction	Experiment		Analysis		Code
	Forced Vibration	Ambient Vibration	Rigid Base	Flexible Foundation	
E-W/Torsion	1.76	1.82	2.27	1.71	—
E-W/Torsion	2.08	2.14	2.74	2.08	2.44
N-S	2.18	2.24	3.14	2.19	1.69





FIG. 1 WESLEY MANOR BUILDING, CAMPBELL, CA

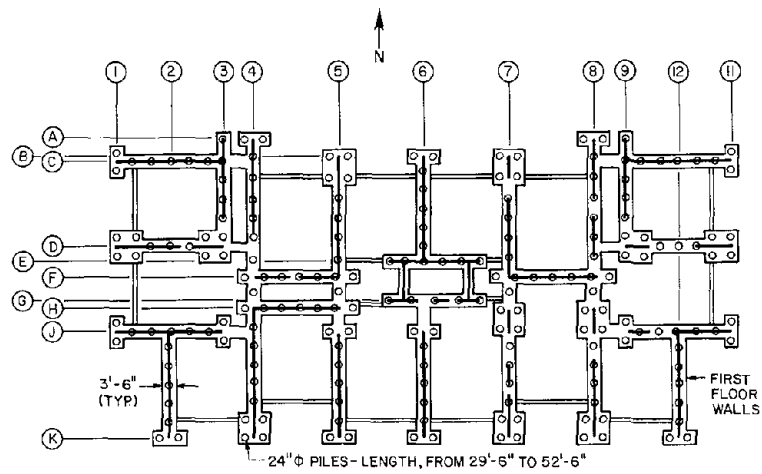


FIG. 2 FOUNDATION PLAN

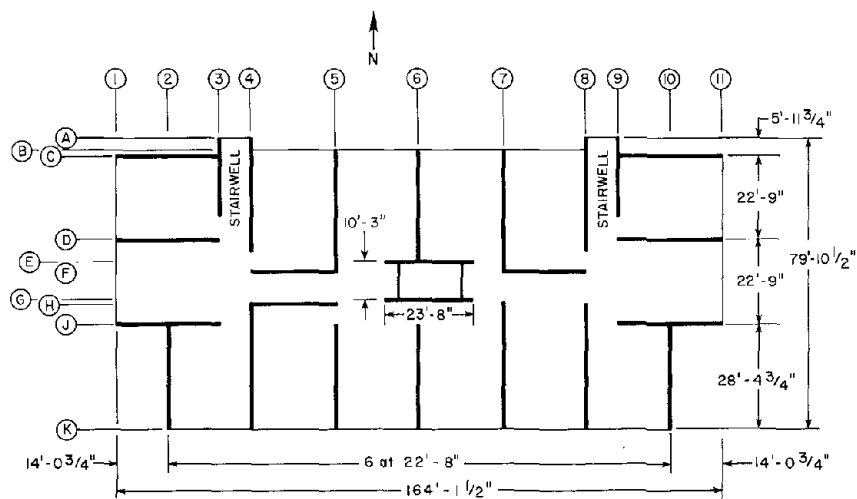


FIG. 3 TYPICAL FLOOR PLAN - 2ND THRU 12TH FLOORS

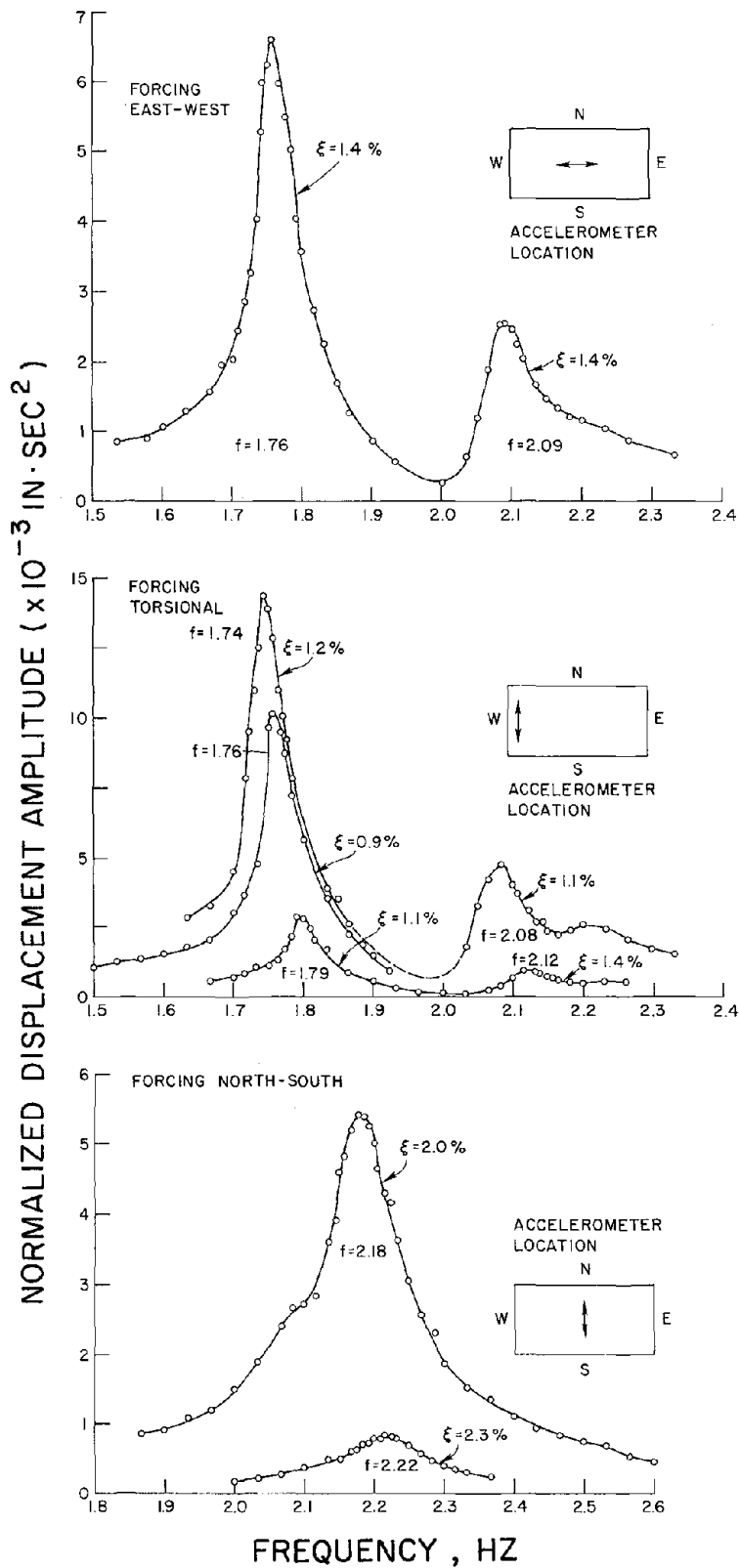


FIG. 4 FREQUENCY RESPONSE CURVES

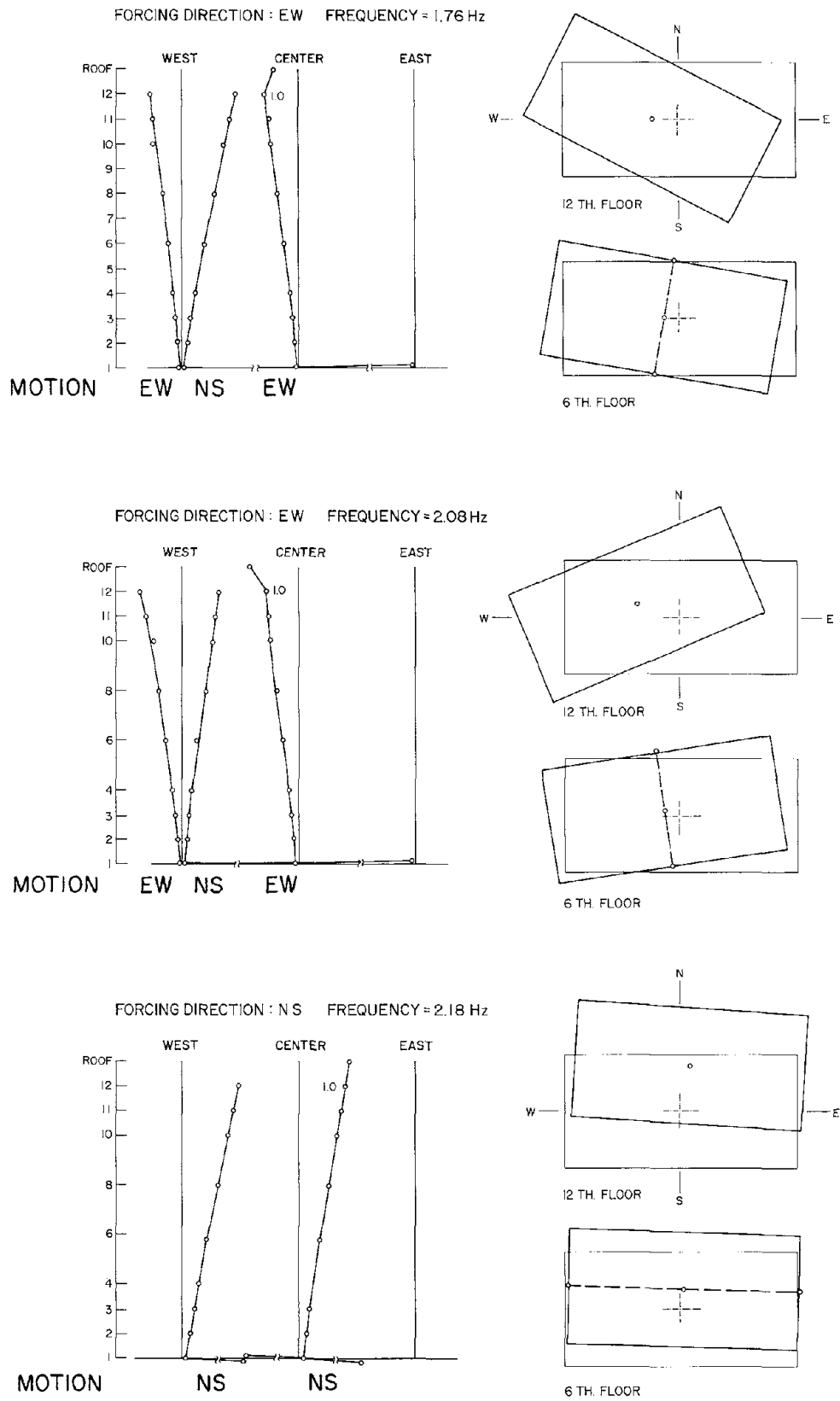


FIG. 5 TYPICAL MODE SHAPES

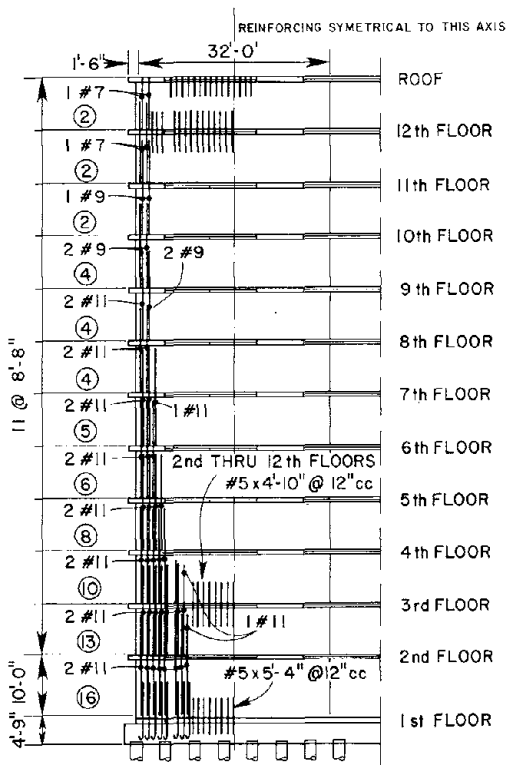


FIG. 6 TYPICAL WALL PANEL ELEMENT

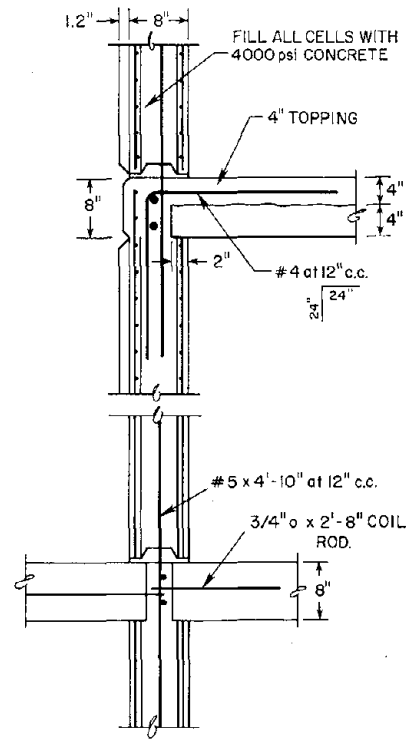


FIG. 7 TYPICAL WALL-FLOOR JOINT CONNECTION

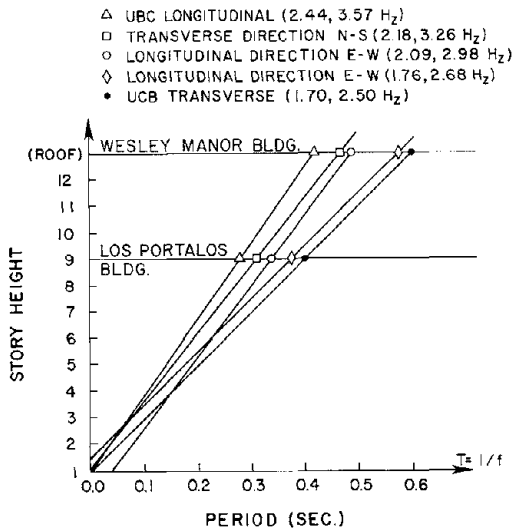


FIG. 8 PERIOD VS STORY HEIGHT

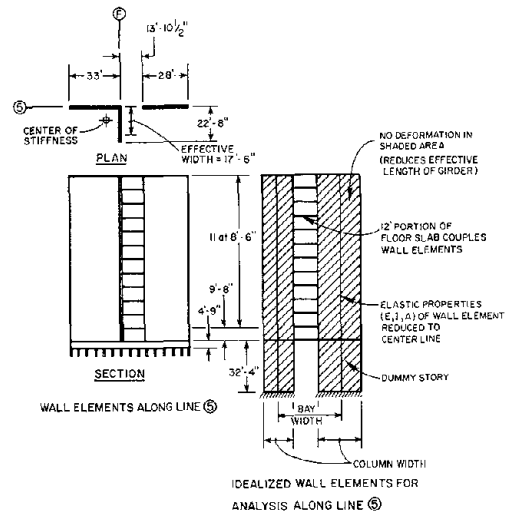


FIG. 9 TYPICAL WALL ELEMENTS

MODELING THE STIFFNESS CONTRIBUTION OF INFILL PANELS  
TO FRAMED STRUCTURES BY A CONSTRAINT APPROACH

James W. Axley<sup>I</sup>

SUMMARY

A means to model the stiffness contribution of infill panels to framed structures, based upon a simplifying constraint assumption, is presented. The accuracy of the method, the development of "infill elements" based upon the method, and the generality of the method are discussed.

INTRODUCTION

Infilled frame structural systems, wherein conventional frames of reinforced concrete or steel are filled, in their plane, with construction usually of masonry, have resisted analytical modeling, although they have been studied experimentally for many years [1,3,4]. Yet, or perhaps because of this, buildings utilizing frame-infill systems have consistently performed poorly in past earthquakes. Frame-infill systems continue to be used throughout the world, however, as they provide an economic and direct means to enclose and partition space that suits many local building traditions.

THE CONSTRAINT APPROACH

Frame-infill systems have been modeled by either an "equivalent strut" approach or by refined finite element discretization [4,5,6,8,9]. The former method is intuitively and computationally attractive, yet theoretically weak and relatively unsuccessful while the latter approach is computationally prohibitive although apparently effective. This paper presents a modeling approach that falls between these two extremes that may be thought to be an extension of the idealization suggested by Newmark [7] where the infill is assumed to act as if it is constrained by a rigid linkage.

Constraint Assumption. Here it is assumed that the frame constrains the form, but not the degree, of the deformation of the infill. This assumption follows naturally from the consideration of a system that has a very stiff frame and relatively soft infill. Clearly, if the infill is sufficiently soft, relative to the frame, then the posed assumption will be valid. The assumption suggests a general approach of modeling the structural behavior of other "secondary" structural elements (eg. stairways, floor slabs, windows, etc.) where it may be reasonably assumed that the primary structural system acts to constrain the form of deformation of the secondary structural system. Three questions remain, however; (1) How may this assumption be implemented practically? (2) What form of constraint is to be assumed? and (3) Is typical infill construction 'sufficiently soft' to be accurately modeled this way?

Implementation. This kinematic assumption may be realized by constraining a suitable mesh of plane stress elements to the nodal degrees of freedom of

---

<sup>I</sup>Assistant Professor of Architecture, University of California, Berkeley

of the surrounding frame composed of conventional beam elements. For rectangular geometry (Fig. 1) the system is modeled by separate assemblages of finite elements for the frame and infill. The separate stiffnesses are formed and the stiffness of the infill alone is reduced, by condensation, to the boundary degrees of freedom. A constraint relation is assumed between the 12 frame degrees of freedom and the infill boundary degrees of freedom thereby allowing a congruent transformation of the separate systems to a composite approximate frame-infill system with only 12 degrees of freedom. It is seen that the infill contribution is distinct and is simply added (in a direct stiffness assembly sense) to the frame stiffness. Frame-infill systems of greater complexity may then be modeled in a similar manner.

Constraints. Although a wide range of constraints may be considered [1] two types of constraints are of particular interest as they offer conformation of the infill and frame deformations. In the first constraint the boundary of the infill is constrained to deform transversely to the flexural beam shape function, the cubic hermitian polynomial shape function, and longitudinally to the truss shape function, the linear shape function, as these two shape functions define the deformation of the general beam element. The second constraint utilizes only the transverse constraint. The first constraint may, then, be thought to approximate the behavior of "stiff" infill panels monolithic with the frame while the second constraint will result in a "soft" infill panel that may better approximate the behavior of typical masonry panels.

Infill Elements. In effect, the approach is an approximate finite element substructuring technique that leads naturally to the development of infill elements that may simply be "plugged" into conventional frame analysis programs. The use of such elements will not substantially increase the size of the system of equations that would be solved for the frame alone. The approach allows the development of a large variety of infill elements including elements to model completely as well as partially infilled frames, unusual infill geometry, possibly with openings, as well as unusual infill material properties or constraint conditions.

Four homogeneous linear elastic infill elements corresponding to completely and partially infilled frames with either "stiff" or "soft" constraint assumptions assumed have been studied. The complete and partial "stiff" infill elements may be reasonably compared to a conventional finite element idealization (the "exact" scheme of Fig. 1). Such a comparison reveals that (1) the assumption is indeed more accurate with softer infill panels, (2) the assumption is reasonably accurate for practical infill construction, and (3) framing member forces as well as infill stress levels are captured reasonably well, albeit, in only a best-fit-mean sense (Fig. 2).

Comparison with experimental test results (Fig. 3 is one example) has proven to be encouraging also. These four infill elements were used in a detailed dynamic analysis of a relatively complex building damaged during the 1976 Guatemalan earthquake with some success (see Ref. 2, a paper presented at this conference).

Computational Efficiency. The generation of the infill elements, as suggested, represents a computationally costly task that may be justified when few

infill panels or many identical infill panels are to be modeled. To avoid this computationally difficult task a nondimensional parameter study may be used to relate individual nondimensional infill stiffness terms to the aspect ratio of the infill panel by polynomial approximation [1]. Using these polynomial approximations infill stiffnesses may be computed with little effort. This was done but the approach demands further development.

#### CONCLUSION

It is believed that infilling frames may provide an effective means to stiffen and strengthen framed structures, even though experience suggests the contrary, if (1) an effective means to model the seismic response of frame-infill systems is developed and (2) frame-infill design details are sought that will improve the hysteretic behavior of these systems. Klingner and Bertero [4] have addressed this latter need and the constraint approach presented in this paper addresses the former need.

Frame-infill system response behavior is not yet well understood. The constraint approach aids only in predicting the initial elastic behavior of such systems. Additional research may most effectively be directed toward improving and predicting the inelastic response of these systems, the constraint approach may, conceivably, be adapted to these purposes as the method is theoretically consistent and yet very flexible in the types of elements that may be developed.

For the purposes of modeling the initial elastic response of frame-infill systems the constraint approximation appears to provide a degree of accuracy well within the inevitable uncertainty of the infill material stiffness, homogeneity, and continuity. It is important to note, finally, that in every case considered the infill had a primary, even dramatic, influence upon system behavior that cannot, reasonably, be ignored.

#### ACKNOWLEDGEMENT

The research behind this paper was sponsored by the National Science Foundation and encouraged as well as supervised by Professor V. Bertero of the University of California, Berkeley.

#### REFERENCES

1. Axley, J.W., Bertero, V.V., "Infill Panels: Their Influence On Seismic Response of Buildings", EERC Report No. UCB/EERC-79/28, Sept. 1979
2. Bertero, V.V., Mahin, S.A., & Axley, J.W., "Lessons From Structural Damages Observed in Recent Earthquakes", 7th WCEE, Istanbul, 1980
3. Dowrick, D.J., Earthquake Resistant Design: A Manual for Engineers and Architects, John Wiley & Sons, London 1977
4. Klingner, R.E., Bertero, V.V., "Infilled Frames In Earthquake-Resistant Construction", Report No. 76-32, College of Engineering, U. of Ca., Dec. 76
5. Kost, E.G., "Nonlinear Dynamic Analysis of Frames with Filler Panels", John A. Blume & Assoc., Nov. 1972, San Francisco
6. Mainstone, R.J., "On the Stiffness and Strengths of Infilled Frames", Current Paper CP2/72, Building Research Station, Britain, Feb. 1974
7. Newmark, N.M., Rosenbleuth, E., Fundamentals of Earthquake Engineering, Prentice-Hall Inc., Englewood Cliffs, N.J. 1971

8. Riddington, J.R., Smith, B.S., "Analysis of Infilled Frames Subject to Racking With Design Recommendations", The Structural Engr., June 77, No. 6, Vol. 55
9. Smith, B.S., Riddington, J.R., "The Design of Masonry Infilled Steel Frames for Bracing Structures", The Structural Engr., Mar. 78, No. 1, Vol. 56B
10. Vallenias, Jose M., "Hysteretic Behavior of R/C Structural Walls", PhD Dissertation, University of California, Berkeley 1979

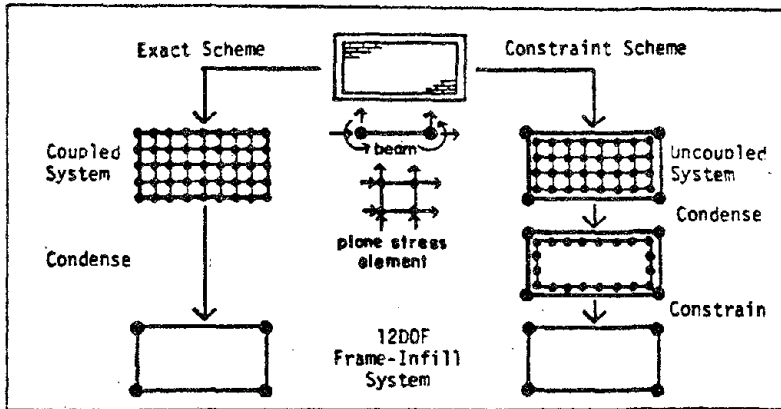


Figure 1. Comparison of the Constraint Approach to a Conventional Finite Element Idealization

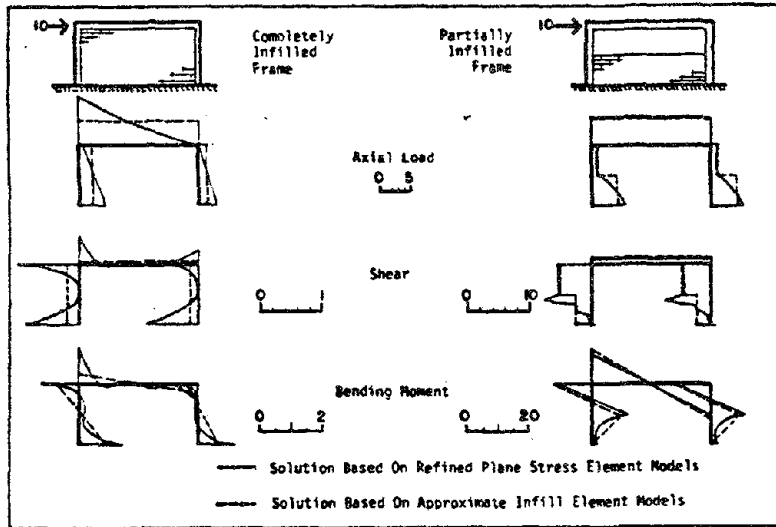


Figure 2. Accuracy of the Constraint Approach: Member Force Evaluation

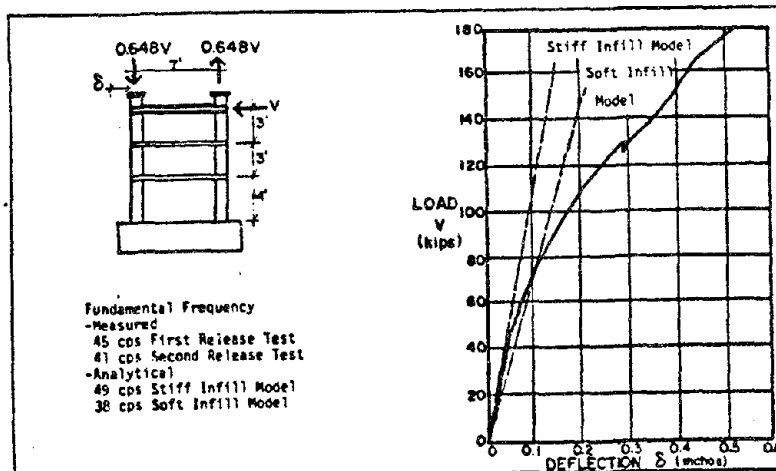


Figure 3. Accuracy of the Constraint Approach: Comparison to Vallenias' [10] Experimental Results



## LESSONS FROM STRUCTURAL DAMAGES OBSERVED IN RECENT EARTHQUAKES

Vitelmo V. Bertero<sup>I</sup>, Stephen A. Mahin<sup>II</sup>, and James W. Axley<sup>III</sup>

## SUMMARY

After reviewing present knowledge in seismic-resistant building construction, the objectives of a research program on post-earthquake damage inspection and analysis are presented. Results and observations of investigations of several buildings in four different earthquakes are summarized. The lessons learned from these investigations reiterate both the importance of proper selection of building layout, of recognizing possible interacting effects of non-structural components with the structure, and of detailing and workmanship, and the limitations of present analytical methods of estimating demands.

## INTRODUCTION

Introductory Remarks. The last few decades have witnessed many advances in the field of earthquake engineering; however, many researchers and most professionals working in this field feel that the design and construction of earthquake-resistant structures is still an art and not a science [1-3]. One critical ingredient in such design and construction is seasoned engineering judgment; the best way to develop such judgment is by field surveys of the performance of actual structures during earthquakes and in-depth analyses of the damages observed. These observations and analyses provide invaluable evidence concerning the effectiveness of seismic codes and procedures used in design and of available analytical methods.

In view of the importance of studying the performance of structures during earthquakes, a research program based on post-earthquake damage inspection and analysis was started in Berkeley several years ago [4-13]. The specific objectives of this program are (1) to identify the reasons for the observed damage, and in this way to assess the reliability of various analytical models and techniques for predicting structural response to earthquake ground motions; (2) to assess possible improvements in design and construction practice which might minimize the observed types of damage in future earthquakes; (3) to investigate ways of strengthening, stiffening, toughening, and/or modifying existing structures to minimize the danger of significant damage during future earthquakes; and (4) to assess the efficiency of present methods of repairing structures damaged during earthquakes and to search for more efficient methods. A summary of some of the results obtained in this program is presented herein.

Objectives. The main purposes of this paper are (1) to review the different factors that can affect the seismic behavior of buildings; (2) to summarize the reasons for damages observed in several buildings during recent earthquakes; and (3) to develop lessons from these observed damages and to assess their implications with respect to present methods of design, analysis, construction and maintenance of earthquake-resistant buildings.

---

<sup>I</sup>Professor and <sup>II</sup>Assistant Professor of Civil Engineering, University of California, Berkeley.

<sup>III</sup>Assistant Professor of Architecture, University of California, Berkeley.

## FACTORS CONTROLLING EFFICIENCY OF SEISMIC-RESISTANT CONSTRUCTION

General Factors. In-depth studies of the performance of buildings during recent damaging earthquakes [4-13] point out that efficient seismic-resistant construction necessitates careful attention to the total seismic design, construction, and maintenance process. The phases of this process include: evaluating the seismic threat, selecting the structural layout, predicting the mechanical behavior of the whole soil-building system, proportioning and detailing the structural components with their connections and supports, analyzing the reliability of the design obtained, and constructing and maintaining the building during its service life [1-3].

The inelastic response of a building is extremely sensitive to its initial dynamic characteristics, and those of the ground motion, and to the hysteretic behavior of its nonstructural and structural components, which depends on their detailing. This sensitivity is shown in studies of the response of concrete structures to severe earthquakes, and must be recognized to properly interpret results which will be presented later. Performance of a structure depends on its state when the earthquake strikes, which may differ significantly from the state the designer envisioned. Thus, construction and maintenance, which includes modification and repair, must also be considered in addition to general design aspects. The importance of these factors is illustrated by results obtained in the following studies.

## STUDIES OF SEISMIC PERFORMANCE OF BUILDINGS

1972 Managua, Nicaragua, Earthquake. Two reinforced concrete buildings, the 15-story Banco Central and the 18-story Banco de America, were located on adjacent sites in Managua at the time of the earthquake (Fig. 1). Due to extensive earthquake damage, the top 12 stories of the Banco Central were demolished. However, only moderate structural repairs were required in the Banco de America. To determine the reasons for this difference in performance, a number of detailed dynamic analyses were performed [7,11,12]. Accelerograms from the Esso Refinery, about 5 km from the buildings, were used in these analyses.



FIG. 1. VIEW OF BANCO CENTRAL AND BANCO DE AMERICA, MANAGUA

concrete walls, were eccentrically located in the west end of the tower.

Banco Central [11]. The configuration and structural system used for the Banco Central were complex (Fig. 2). In the upper portions of the tower, the floor system consisted of a 0.05 m slab supported by 14 m-long joints having a total depth of only 0.45 m. Closely spaced columns located along the north, east and south sides of the tower were replaced by ten 1 x 1.55 m columns below the third floor. In the bottom two stories, waffle slabs were used to extend the plan of the building considerably to the south. Four elevator shafts, enclosed by reinforced

The perimeter columns between the fourth and fifteenth story suffered extensive cracking. The walls around the elevator shafts suffered cracking and spalling of the concrete and buckling of the reinforcement in the fourth and fifth stories. Transverse cracks, sometimes wider than 10 mm, were observed

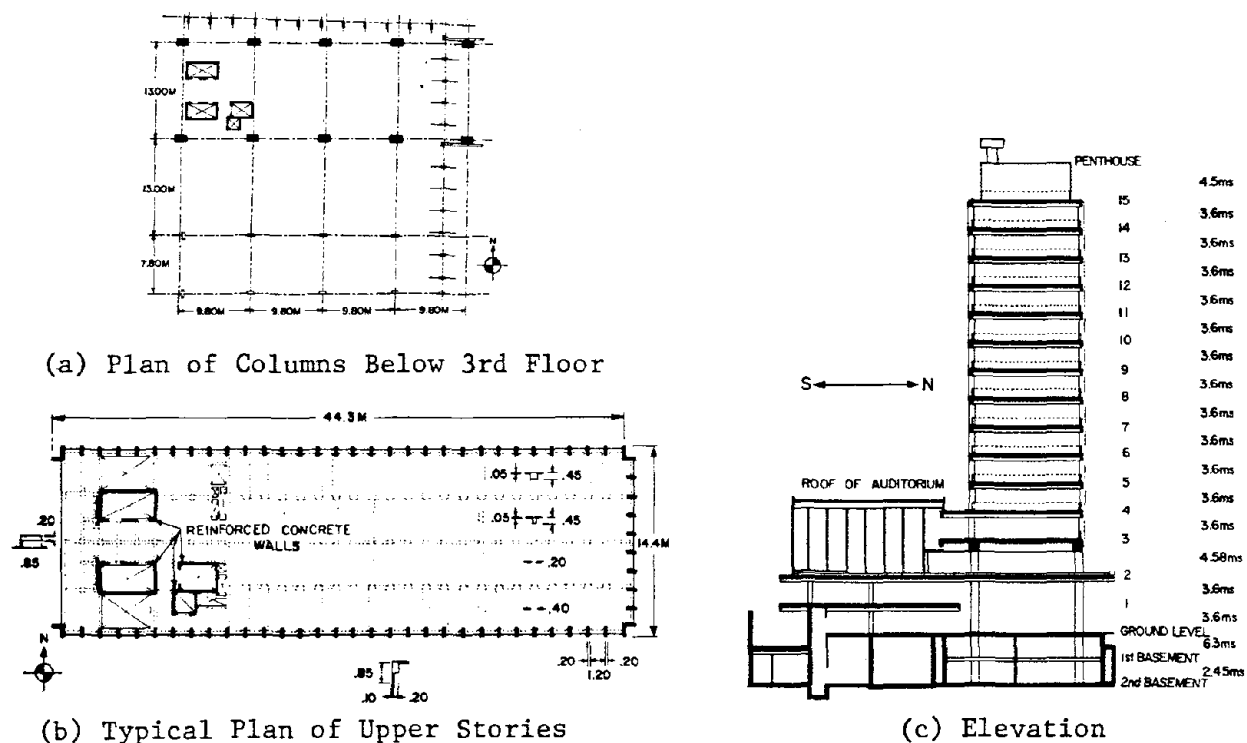


FIG. 2. PLANS AND ELEVATION OF BANCO CENTRAL

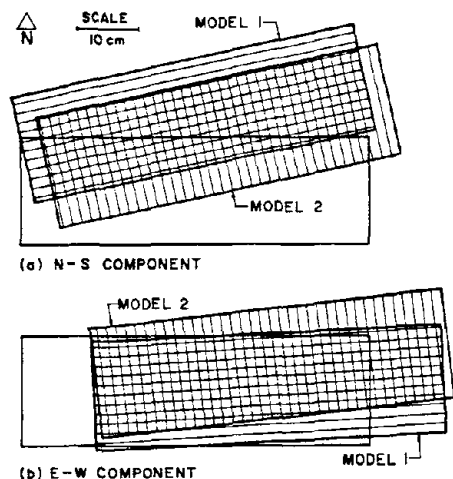


FIG. 3. ROOF DISPLACEMENT OF BANCO CENTRAL FOR ESSO REFINERY RECORDS

across all slabs above the third floor just to the east of the elevator shafts. Hollow clay tile infilled walls (located on the west face of the tower, beneath the windows on the other faces of the tower and around the stairwells) and other nonstructural elements suffered substantial damage.

Three elastic analytical models were considered. Model 1 was three-dimensional and included all structural elements as well as the hollow clay tile infilled walls. Model 2 was similar but the nonstructural elements were disregarded. In Model 3, inertial forces resulting from horizontal and/or vertical ground excitations, on a representative transverse frame, could be accounted for. Based on the results of these elastic analyses, the following observations can be made: (1) the substantial change in structural configuration as well as the eccentric location of the elevator shaft walls resulted in substantial torsional response (Fig. 3); (2) the tile partitions lowered the fundamental period about 20% and significantly modified the response (Fig. 3); however, computed elastic forces in these members far exceeded their capacities and they would begin to fail very early in the response; (3) the shear capacity of most columns along the north and south sides of the tower above the third floor would be exceeded assuming peak EW ground accelerations only 40% of those recorded at the Esso refinery; (4) due to the relative stiffnesses of the remaining uncracked members, any additional inertial forces developed in the eastern portion of the tower were transferred primarily back

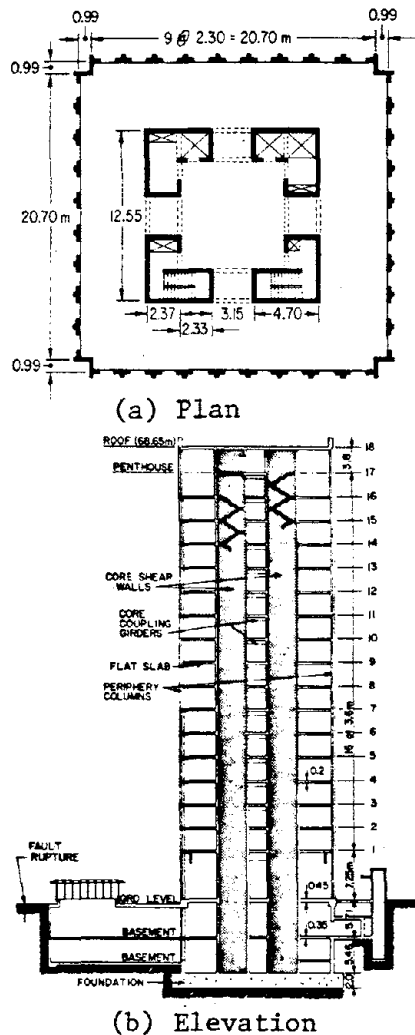


FIG. 4. PLAN AND ELEVATION OF BANCO DE AMERICA

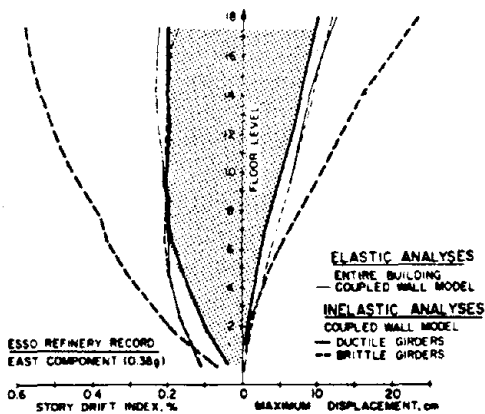


FIG. 5. ENVELOPES OF MAXIMUM FLOOR DISPLACEMENTS AND STORY DRIFTS--BANCO DE AMERICA

to the elevator shaft walls by means of in-plane diaphragm forces resulting in transverse slab cracks and damage to the elevator shaft walls; (5) even for horizontal excitations, the long, flexible floor joists developed significant vertical motion contributing substantially to the damage in the nonstructural elements they supported.

Banco de America [7,12]. As indicated in Fig. 4, the structural system of the Banco de America is essentially symmetric. The primary lateral force resisting system consisted of four large L-shaped wall cores, symmetrically coupled by pairs of girders. Because of duct openings placed at the center of the coupling girders, their shear capacities were generally only about 35% of the values required to develop their flexural capacities. Shear failures in these girders were the primary structural damage observed in the building. Elastic three-dimensional analyses of the whole building and inelastic two-dimensional analyses of the coupled wall system indicate that (1) the symmetric structural configuration and relatively stiff and strong coupled wall system effectively limited displacements and drifts (Fig. 5) and prevented any significant torsional influence; (2) avoidance of long floor spans and masonry partitions reduced nonstructural damage; and (3) when coupling girder shear failures were accounted for, displacements significantly increased (Fig. 5) but were limited due to the considerable remaining lateral stiffness and strength provided by the walls.

1976 Guatemalan Earthquake [9]. During this earthquake a relatively modern three-story reinforced concrete building, La Escuela De Niñeras (Nursery School) (Fig. 6), which utilized structural frames infilled with masonry, suffered seismic damage characteristic of this type of frame-infill construction, i.e., "captive column" failures due to infill panel restraint, "explosive" shear failures of infill panels, and masonry debris blocking exits and stairways (Fig. 7).

The post-earthquake study of this building reviewed its construction and its seismic behavior and investigated its dynamic character through a series of linear elastic studies. The structural contribution of the infill to the frame was modeled analytically by a constraint approach [13] and the influence of the infill upon the structural response to different earthquake excitations, including the 1976 Guatemalan record, was considered in detail. These analytical studies indicated that the infill had the effect of shortening the natural periods of the building, tuning the structure to a

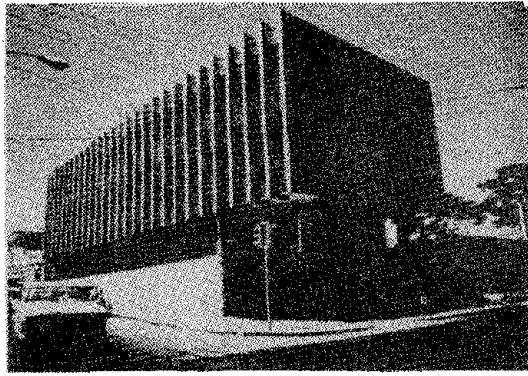


FIG. 6. VIEW OF ESCUELA DE NIÑERAS

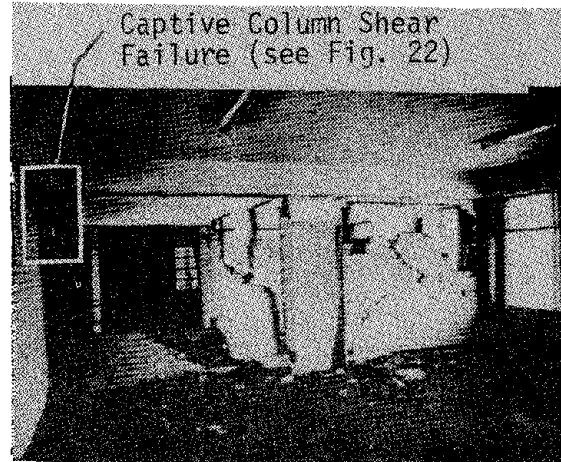


FIG. 7. WALL DAMAGE AT TRANSVERSE FRAME

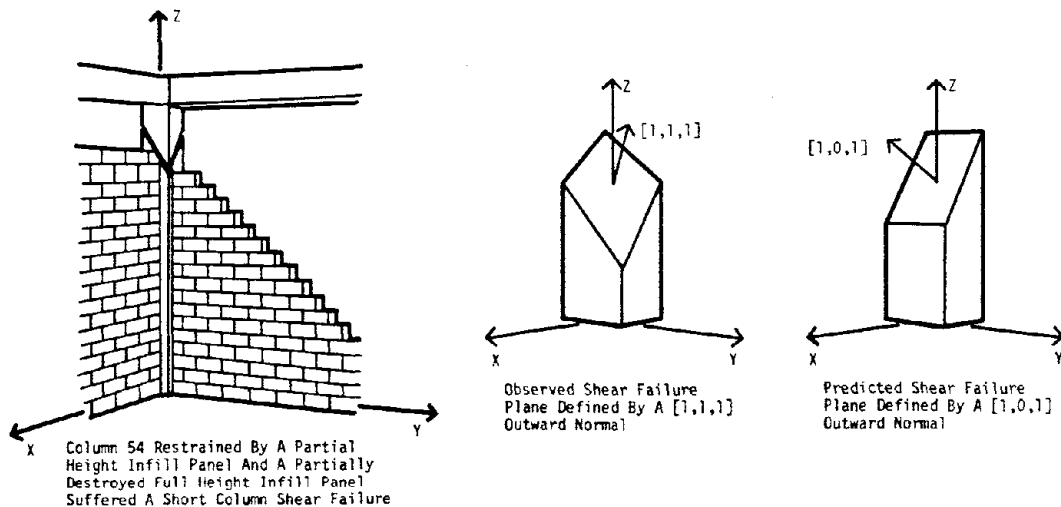


FIG. 8. DETAIL OF THE SHEAR FAILURE OF THE CAPTIVE COLUMN 54

dominant frequency content of the Guatemalan record. The highly irregular and asymmetric distribution of infills in the otherwise relatively regular and symmetric frame introduced significant torsional response and thus a concentration of (computed) stress in two of the seven transverse frames that correlated well with the observed damage. The constraint approach provided a sufficiently detailed estimation of member forces and local infill stresses to indicate the probable nature of failure of a critically damaged column (Fig. 8), insofar as the brittle nature of the building response allowed realistic modeling elastically. Furthermore, the combined evidence of the observed damage and analytically predicted behavior (1) suggested one probable failure mechanism for completely infilled frames, and (2) demonstrated a positive correlation between observed infill damage levels and predicted infill stress levels, encouraging consideration of a damage limit state based upon a parameter of infill stress (or strain) rather than drift.

1977 Cauçete (San Juan, Argentina) Earthquake [10]. Regarding the performance of structures, the main features of this earthquake were (1) the poor behavior of cylindrical liquid storage tanks; (2) the excellent behavior of one- to three-story dwellings constructed (according to code regulations developed after the destructive earthquake of 1944) using masonry properly restrained by R/C beams and columns; and (3) the relatively poor performance of some school buildings due to poor construction, poor selection of building layout, and, in some cases, due to a disregard for the interaction of nonstructural elements

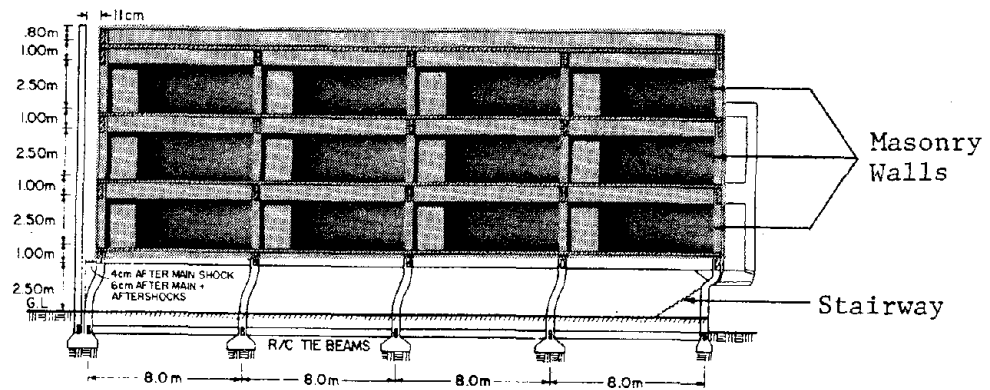


FIG. 9. LONGITUDINAL ELEVATION OF THE ENET NO. 2 BUILDING ILLUSTRATING PERMANENT DISPLACEMENT AFTER EARTHQUAKE

with the structure. A good illustration of this poor performance was that of the Escuela (School) ENET No. 2. This building consisted of a four-story R/C moment-resisting space frame. The first story was left completely open in the longitudinal direction, while the frames in the upper three stories were infilled with masonry walls to provide several classrooms (Fig. 9). These decisions and resulting construction led to a soft first-story building type response to the earthquake. The first-story columns underwent significant inelastic deformations resulting in a permanent horizontal displacement of 40 mm after the main shock and increasing to 60 mm due to aftershocks. Three-dimensional linear elastic analyses were performed assuming different models (neglecting and including nonstructural elements) and using the earthquake ground motion recorded 2 km from the building. Nonlinear dynamic analyses were also conducted. The above analyses lead to the following observations: (1) the linear elastic analyses show the significant effect of the masonry walls located in the upper stories, which not only increased the overall stiffness of the building but, more importantly, significantly changed the modes of vibration, practically converting it to a soft first-story building; (2) the columns of the first story exceeded their "elastic" range; (3) the nonlinear analysis predicted a permanent deformation of 38 mm which is very close to the measured 40 mm; and (4) the columns as designed and constructed were just capable of developing the ductility required which was about 2.5.

1979 Imperial Valley (California) Earthquake. As far as performance of structures is concerned, the main features of this earthquake were (1) significant damage to cylindrical liquid storage tanks, either ground supported or elevated, and (2) the recorded performance of the modern six-story Imperial County Services Building in El Centro (Fig. 10). Thirteen accelerograms recorded the motion at various locations in the building, which suffered significant structural damage. This six-story building is rectangular in plan (23 x 42 m). Lateral resistance is provided by moment-resisting frames in the longitudinal direction (EW), and shear walls were used in the transverse direction (NS). Shear walls in the upper five stories were provided for the full width of the building on its east and west faces. Four considerably narrower shear walls were asymmetrically placed in the first story. Damage to the building consisted of the failure of the four columns along the east side at the ground level (Fig. 11), spalling of concrete cover and buckling of longitudinal steel in other columns at the ground level, and cracking in slabs, beams, columns, and shear walls throughout the building. A detailed field survey of the damages and preliminary study of the design and detailing indicate that the observed failure of the columns was due to a combination of factors: (1) discontinuities in the

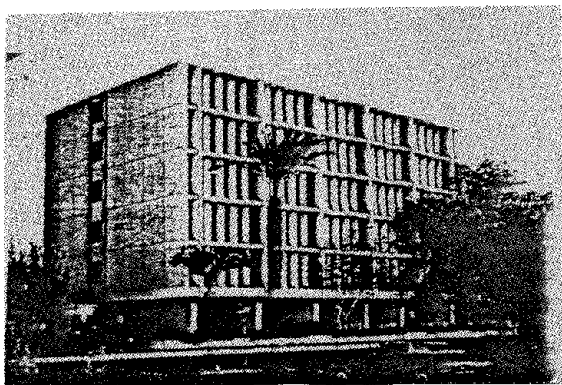


FIG. 10. VIEW OF THE IMPERIAL COUNTY SERVICES (ICS) BUILDING, EL CENTRO, CALIFORNIA

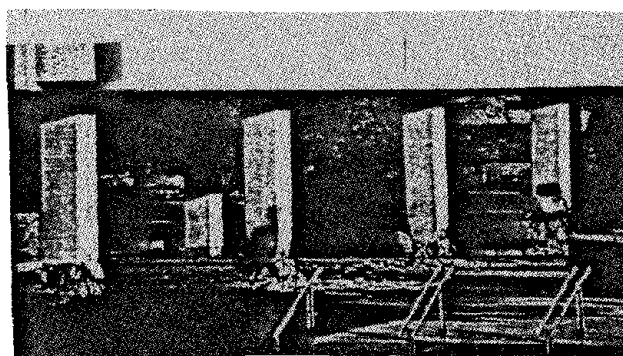


FIG. 11. FAILURE OF THE FOUR GROUND-STORY COLUMNS LOCATED AT THE EAST SIDE OF BUILDING OF FIG. 10

structural system at the second-floor level; (2) interruption of the special lateral reinforcement at the "created" critical regions near the lower end of the columns; and (3) bending of the column main reinforcement at these critical regions.

#### LESSONS LEARNED

Based on the performance and analyses of the buildings studied, the following lessons regarding seismic-resistant design and construction were learned: (1) Proper selection of structural layout and systems is essential. Compact symmetrical layouts and the avoidance of discontinuities in mass, stiffness, strength and/or ductility are crucial. Multiple lines of defense are desirable; (2) Flexible long span floor systems can result in large horizontal and vertical displacements which can contribute to nonstructural damage; (3) Failure of nonstructural components can result in serious threat to life and contribute significantly to the cost of repair; (4) Nonstructural infill elements often have a primary effect on seismic response and should be considered in design or adequately isolated. If ignored in design, such infills can lead to unanticipated, and potentially catastrophic, modes of structural behavior; (5) Members and connections should be detailed and constructed to have a large ductility capacity due to the uncertainty in ductility demands; (6) Analytical studies should include the effects of vertical inertial forces and of nonstructural components where appropriate. Inelastic analyses are needed to estimate ductility demands.

Conclusions. These lessons clearly indicate that at present, because of large uncertainties in estimating the demands in earthquake-resistant design of buildings, it is of paramount importance to pay more attention to "conceptual" than to "numerical" design. Sophistication in selection of building layout (structural system, structural material, nonstructural components) is at present more important than sophistication in estimating demands (analysis). The inertial forces depend upon the interacting effects of the ground motions with the mass, damping, and structural characteristics of the building. Therefore, designers need to understand how design and construction decisions may create serious seismic effects. Guidelines for selecting a proper structural layout are discussed in Refs. 2, 3 and 14.

#### ACKNOWLEDGMENT

Most of the research reported has been supported by National Science Foundation grants. Thanks are also due to E. Matthews and D. Ullman for their help in preparing this paper.

## REFERENCES

1. Bertero, V.V., Organizer, Proceedings, Workshop on Earthquake-Resistant Reinforced Concrete Building Construction, Univ. of Cal., Berkeley, July 1977, 3 vols., 1941pp.
2. Bertero, V.V., "An Overview of the State-of-the-Art in Earthquake-Resistant Reinforced Concrete Building Construction," Proceedings of the 2nd U.S. Nat'l Conf. on Earthquake Engineering, Aug. 22-24, 1979, Stanford Univ., pp.838-52.
3. Bertero, V.V., "Seismic Performance of Reinforced Concrete Structures," Anales, Argentina Academy of Exact Sciences, Vol. 31, 1979, pp. 75-144.
4. Bertero, V.V. et al., "Seismic Analysis of the Charaima Building, Caraballeda, Venezuela," Report No. EERC 70-4, Univ. of Cal., Berkeley, 1970.
5. Bertero, V.V., & Collins, R.G., "Investigation of the Failures of the Olive View Stairtowers During the San Fernando Earthquake and Their Implications on Seismic Design," Report No. EERC 73-26, Univ. of Cal., Berkeley, 1973.
6. Bresler, V., & Bertero, V.V., "Olive View Medical Materials Studies, Phase I," Report No. EERC 73-19, Univ. of Cal., Berkeley, 1973.
7. Mahin, S.A., & Bertero, V.V., "An Evaluation of Some Methods for Predicting Seismic Behavior of Reinforced Concrete Buildings," Report No. EERC 75-5, Univ. of Cal., Berkeley, 1975.
8. Mahin, S.A. et al., "Response of the Olive View Hospital Main Building during the San Fernando Earthquake," Report No. EERC 76-22, Univ. of Cal., Berkeley, 1976.
9. Axley, J.W., & Bertero, V.V., "Infill Panels: Their Influence on Seismic Response of Buildings," Report No. EERC-79/28, Univ. of Cal., Berkeley, 1979.
10. Lara, O., "Nonlinear Seismic Response of the ENET No. 2 Building During the 1977 San Juan Earthquake," Proceedings of the XX Jornadas Sudamericanas de Ingenieria Estructural, Cordoba, Argentina, July 1979, Vol. III, pp. B18.1-.30.
11. Lara, O. et al., "Performance of Banco Central During the 1972 Managua Earthquake," Research Report, SESM Division, Univ. of Cal., Berkeley, 1978 (to be published as an EERC report).
12. Mahin, S.A., & Bertero, V.V., "Nonlinear Seismic Response of a Coupled Wall System," J. of the Structural Division, ASCE, Vol. 102, ST9, Sept. 1976, pp. 1759-80.
13. Axley, J.W., "Modeling the Stiffness Contribution of Infill Panels to Framed Structures by a Constraint Approach," Proceedings of the 7th World Conference on Earthquake Engineering, Istanbul, 1980.
14. Dowrick, D.J., Earthquake Resistant Design, A Manual for Engineers and Architects, New York: John Wiley & Sons, Inc., 1977.



# A LIFETIME COST APPROACH TO AUTOMATED EARTHQUAKE RESISTANT DESIGN

by

Norman D. Walker, Jr.<sup>I</sup> and Karl S. Pister<sup>II</sup>

## SUMMARY

A lifetime cost approach to the design of earthquake resistant multistory steel building frames is presented. The development begins with the design objective: minimized lifetime cost including construction and earthquake-induced damage. Standard design constraints are then formulated for operating loads and a dual design constraint for earthquake loading. Finally, the design problem thus formed is explored through the example of a one-story frame.

## INTRODUCTION

The problem addressed here is selection of member sizes for single-bay, multistory, unbraced steel frames with fully rigid connections. Uniformly distributed beam loads and earthquake-generated horizontal ground motion will be considered. A typical member of this class of design problems is shown in Fig. 1. The frame is symmetric about its vertical mid-plane, and members are to be selected from the set of A-36 rolled steel wide flange economy sections. Performance constraints for operating loads will be introduced through typical code requirements, while for earthquake loads a dual criterion based on selection of moderate and strong design earthquakes is adopted. As a design criterion, we take lifetime cost of the structure, which we assume to be composed of initial (construction) cost and the cost of earthquake-induced damage over its lifetime. The following sections briefly sketch a methodology for formulating the problem and supply an example. More detailed information can be found in [1].

## DESIGN OBJECTIVE

To compare alternative choices of a given structure, a design objective must be quantified. Here, we choose minimum lifetime cost (LC), a choice obviously dependent upon the selection of design variables (design vector). Only those costs strongly related to the design variables need be calculated; costs which are relatively independent of the design vector merely add a constant to the cost, producing no effect on the outcome of the design process. Obviously, care must be exercised in selecting design variables compatible with the design objective (cost). Here, we select

---

<sup>I</sup>Staff Research Engineer, Kaiser Aluminum & Chemical Corporation, Center for Technology, Pleasanton, CA 94566.

<sup>II</sup>Professor of Engineering Science, Division of Structural Engineering and Structural Mechanics, Department of Civil Engineering, University of California, Berkeley, CA 94720.

moment of inertia of the member cross-section for this purpose.

The LC associated with multistory framed buildings separates into two categories: (1) cost of construction and (2) cost of damage associated with structural overload, here assumed to result from earthquake exposure.

### Construction Costs

Design vector dependent construction costs include costs of members, beam-column connections, including welding, transportation, size extra charges, painting, etc. We will indicate the form of these cost functions. If  $C_s$  denotes the unit cost of steel, the total frame cost can be written

$$\text{Total Cost} = C_s \gamma \sum_{m_i} A_i L_i \quad (1)$$

where  $A_i$ ,  $L_i$  denote cross-sectional area and length of each member,  $\gamma$  the unit weight of steel and the summation is taken over all frame members. In many studies of optimal structural design, Eq. 1 represents the design objective function. To account for cost of connections, welding and other member-related charges, it is possible to develop empirical equations relating costs to section properties. Thus, the total construction cost  $C_c$  can be expressed in the form

$$C_c = \gamma \sum_{m_i} [C_s A_i + C'_s f_s (A_i)] L_i + \gamma \sum_{g_i} [C'_c f_c (I_i) + C_w f_w (I_i)] \quad (2)$$

In Eq. 2, the following definitions have been introduced:

$C'_s$  = unit cost of additional charges for members (transportation, etc.)

$C'_c$  = unit cost of connection steel

$C_w$  = unit cost of welding connections

The functions  $f_s$ ,  $f_c$ ,  $f_w$  can be determined by curve-fitting, [1]. Symbols  $m_i$  and  $g_i$  on the summations denote "all members" and "all girders", respectively.

### Damage Costs

To develop a model for damage costs resulting from earthquake-induced overload, it is necessary to relate damage to structural response parameters and identify an expected earthquake exposure hazard for the building lifetime. In a complete treatment of costs of future damage, certain economic assumptions dealing with the cost of money, etc., would have to be incorporated. To avoid departing from the main objective of our work here, a "constant dollar", unencumbered by economic considerations, is used.

We assume that damage costs can be divided into three categories: structural damage, non-structural damage, and down-time costs. The definition of structural damage is elusive. Fortunately, for steel framed buildings structural, as opposed to non-structural, damage is relatively unimportant, assuming the design prevents collapse of the structure. A suggested model, based on restoration of member ductility, can be found in [1].

Included in the category of non-structural damage are items such as interior and exterior walls, partitions, glazing, plumbing, electrical fixtures, etc. Taken collectively, the cost of damage for these items is much more significant than structural damage in steel framed buildings. From the above list, the principal contributions are from interior drywalls, glazing and masonry, if present. There is evidence to support the choice of story drift as an appropriate measure of non-structural damage. Utilizing data from [2], it has been found that the damage ratio  $D_n$ , defined as the cost of damage repair, divided by the cost of construction of the damaged items can be expressed as [1]:

$$D_n = 8.52 \delta \quad (3)$$

where  $\delta$  is the story drift in feet. Using Eq. 3 to compute the non-structural damage ratio,  $D_n$ , the cost of damage per story can be developed. The total cost of non-structural damage is then obtained by summing over all the floors.

Repair of non-structural damage frequently requires temporary shut-down or relocation of activities, with resulting costs and revenue losses which affect the LC. Review of data from [3] reveals a range of down-time costs from zero to 300 per cent of the total damage cost. In order to estimate this type of cost, some assessment of the susceptibility of the function of a building to such inconvenience costs must be made.

#### Lifetime Cost

The damage cost models developed apply to individual earthquakes. To obtain lifetime cost, it is necessary to make assumptions about the intensity and frequency distributions of earthquakes for the particular site and sum the damage costs over all expected earthquakes to obtain a lifetime exposure profile. This is accomplished as follows: we develop a model for the annual frequency of earthquakes with a given peak acceleration at a site utilizing a linear relation between log frequency and magnitude in connection with Housner "affected area" curves [4, 5] for a fixed fault direction. A least squares fit of the resulting simulation gives

$$n = 3.44 e^{-15.25a} \quad (4)$$

where  $a$  is the acceleration normalized by gravity. The constants reflect seismicity appropriate to a Southern California site. To obtain damage costs, we must relate the proposed damage models to structural response,

i.e., in Eq. 3,  $\delta$  is a function of  $a$ : The lifetime cost of non-structural damage per story can then be written as

$$C_{NS} = \int_0^{a_{\max}} Nn D_n da = \int_0^{a_{\max}} d_t da \quad (5)$$

where  $n$  is determined by Eq. 4,  $N$  is the structural life in years,  $D_n$  is obtained from Eq. 3 and  $d_t = Nn D_n$  will be called the "lifetime damage profile". As an example, consider a one-story frame with beam and column moments of inertia of 223 in.<sup>4</sup> and 235 in.<sup>4</sup>, respectively, with a span and height of 300 inches and 150 inches, assuming 5% of critical damping. Use of Newmark-Hall response spectra [6] gives story drift  $\delta = 3.7a$ , where  $\delta$  is in inches. Using this in Eq. 3 with an assumed non-structural cost of 10% of the construction cost and employing Eq. 4 with a 50-year service life yields an expected lifetime damage profile

$$d_t = 4540 a e^{-15.25a} \quad (6)$$

Eq. 6 is shown in Fig. 2. Note that most of the structural damage results from ground accelerations of less than 25%  $g$  with the peak in the curve occurring at 6.56%  $g$ . The area under this curve is easily computed from Eq. 6, in the general case, however, numerical integration is necessary to obtain the lifetime cost of non-structural damage defined by Eq. 5. For multistory frames, story drifts at each floor level can be found from appropriate dynamic analysis, e.g., employing modal analysis and maximum modal response estimates for the assumed response spectra. Eq. 5 is then evaluated at each story and the total damage cost obtained by summation. This result, together with Eq. 2, provides the design objective in terms of a lifetime cost.

#### PERFORMANCE CONSTRAINTS

Design limitations are typically imposed via building codes. Here we will treat constraints under operating loads in the usual manner; however, criteria for earthquake loading will follow a different course. Only the general outline of the constraint formulation scheme will be given; details are in [1].

#### Constraints Under Operating Loads

Maximum moments in members are required to satisfy the condition

$$|M| \leq c M_p \quad (7)$$

where  $M$  is the moment under operating loads,  $M_p$  the section plastic moment and  $c$  a reduction coefficient, typically  $\approx 0.6$ . For columns  $M_p$  must be modified to reflect axial loading. Limitations on maximum beam deflection are also incorporated.

Because of the lateral strength requirements of earthquake resistant frames, it is assumed here that sidesway stability requirements will not play a prominent role in the design process. This requirement, along with any other limitations thought to be necessary, can be easily incorporated.

### Constraints Under Dynamic Loading

For response to earthquake loads, we adopt the following dual design criterion:

- (1) The structure should respond elastically to a moderate earthquake of an intensity reasonably anticipated within its lifetime.
- (ii) During a maximum credible (strong) earthquake, the structure may yield significantly but must avoid collapse.

Design earthquakes representative of the above conditions are typically selected on the basis of their probability of occurrence. A sample probability of occurrence curve is shown in Fig. 3, generated on the basis of a 50-year life expectancy for a Southern California site [4]. Moderate earthquakes are chosen with a 50-80% probability of occurrence in mind, whereas strong earthquakes are picked in the 5-10% probability of occurrence range. Both are selected on the basis of a 50-70 year building life expectancy. Thus, two peak ground acceleration values, referred to as design earthquakes, are chosen to represent a moderate and strong earthquake. This is consistent with analysis procedures which employ response spectra. In the specification of dynamic constraints, dead/live load effects on the beams are accommodated in addition to those resulting from the earthquake. No reduction of the live load from that specified for the static operating constraints is introduced. For a moderate earthquake, the structure is to respond elastically, hence, the maximum member moments throughout must be less than each corresponding member yield moment,  $M_y$ .

In general, the same form of constraints on maximum beam and column moments carries over to the case of the moderate earthquake, i.e., constraints have the form of Eq. 7 where now  $M$  is obtained by combining the separate effects of operating loads and earthquake loading.

The strong earthquake design criterion requires avoidance of structural collapse. We adopt the strong column-weak girder design constraint and utilize the ductility ratio defined as the maximum total end rotation of a member divided by its elastic limit end rotation. In terms of ductility ratio, the strong column-weak girder philosophy means that the ductility demands of each member must be less than some specified allowable, which for columns is close to unity. Let  $M_T$  represent the total maximum moment (i.e., the sum of the static and dynamic moments) in a particular member. Then the form of strong earthquake constraints can be written

$$M_T \leq \mu M_p, \quad (8)$$

where  $\mu$  is the allowable ductility. As can be seen, this equation is identical in form to Eq. 7 with  $c = \mu$ . Hence, all of the constraint devel-

opments for the moderate earthquake apply to the strong earthquake with  $c$  equal to the allowable ductility in each member.

### EXAMPLE

To illustrate the methodology, we select a one-story frame with the span and height used to obtain Eq. 6. The intent is to identify the optimal design easily and to illustrate the characteristics of the objective and constraint functions. The beam supports a 40 kip distributed load. Moderate and strong design earthquakes are taken to have 0.12 g and 0.35 g peak ground accelerations (corresponding to 80% and 5% probabilities of occurrence, Fig. 3), respectively. In Eq. 7, reduction coefficients  $c$  are given values 0.60 for operating loading and 0.85 for dynamic loading associated with the moderate earthquake. A deflection of one inch is permitted at the center of the beam span under operating loads. For the strong design earthquake ductility factors  $\mu$  of 1 for columns and 6 for beams are assigned. Typical construction cost rates for California are assumed, along with allowances of 10% of construction cost for overhead and profit and 10% of total damage cost for down-time costs. Structural damage is not accounted for, on the basis of earlier computational experience [1].

Using these assumptions, the design space is shown in Fig. 4. Hatched lines denote system constraints with the unhatched side of the curves representing usable designs. Constraint  $c$  corresponds to a static (operating load) beam constraint, while  $a$  and  $b$  are column constraints. For clarity, only constraints which bound the usable design region of the design space are shown. The cost lines given in the figure are computed as follows:

$$\text{Cost} = \frac{100 [\text{LC}(X) - \text{LC}(X^*)]}{\text{Construction Cost at Optimal}} \quad (9)$$

where  $\text{LC}(X)$  is the lifetime cost as a function of the present design vector  $X$  and  $X^*$  is the optimal (minimum LC) design vector.

The following features deserve comment: the optimal design is unconstrained. This would not be expected for multistory frames where strong earthquake column constraints would become active. Another interesting feature is that the objective function has the rough appearance of an uncoupled function. That is, the principal directions in the cost surface (eigenvectors of the Hessian of the cost function) are nearly parallel to the axes. This characteristic grows especially strong as the optimal is approached. Since coupling is greatest between adjacent members in a structure, this uncoupled feature of the objective function should become stronger as multistory frames are considered. Finally, the constraint functions are also nearly uncoupled. That is, each constraint depends essentially upon one variable, lying approximately parallel to one axis or the other. This feature in conjunction with the uncoupled objective function leads to the important conclusion that the sizing of the various members can take place nearly independently of one another, i.e., member sizing decisions are uncoupled. This has major ramifications in the selection of an automated design procedure, to be presented in a forthcoming paper.

In conclusion, we note that the frame designed on the basis of least weight (equivalent to minimum initial construction cost) is 25% cheaper in terms of construction cost, but when its lifetime cost is considered, it is actually 23% more expensive than the LC optimal frame. Thus, a clear choice in design philosophy exists.

#### ACKNOWLEDGMENT

This research was sponsored by the National Science Foundation under grants to the University of California, Berkeley.

#### REFERENCES

1. Walker, Jr., N. D., "Automated Design of Earthquake Resistant Multistory Steel Building Frames," University of California, Berkeley, Report No. EERC 77-12 (1977).
2. Czarnecki, R. M., "Earthquake Damage to Tall Buildings," Department of Civil Engineering Research Report R 73-8, MIT, Cambridge, Mass., (1973).
3. Whitman, R. V., Hong, S., and Reed, J. W., "Damage Statistics for High-Rise Buildings In The Vicinity of the San Fernando Earthquake," Department of Civil Engineering Research Report R 73-24, MIT, Cambridge, Mass. (1973).
4. Housner, G. W., "Strong Ground Motion," Chapter 4, Earthquake Engineering, R. L. Wiegel, Ed., Prentice-Hall, (1970).
5. Housner, G. W., "Engineering Estimation of Ground Shaking and Maximum Earthquake Magnitude," 4th World Conference on Earthquake Engineering (1969), Vol. 1, Section A-1, pg. 1.
6. Newmark, N. M., and Hall, W. J., "Procedures and Criteria for Earthquake Resistant Design," Building Practices for Disaster Mitigation, Building Science Series 46, National Bureau of Standards, February 1973.

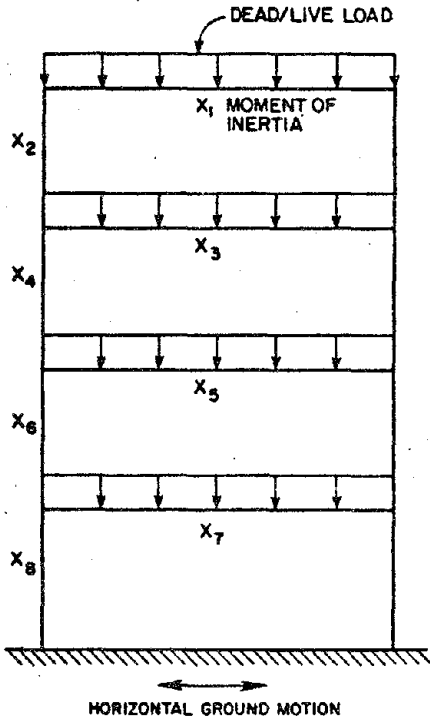


FIG. 1. STRUCTURE WITH LOADS AND MEMBER DESIGN VARIABLE LABELS

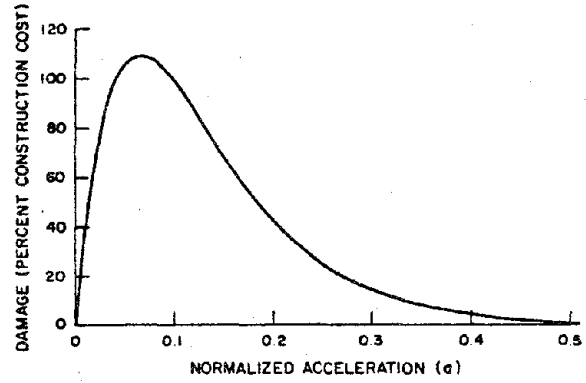


FIG. 2. LIFETIME DAMAGE PROFILE FOR ONE STORY FRAME

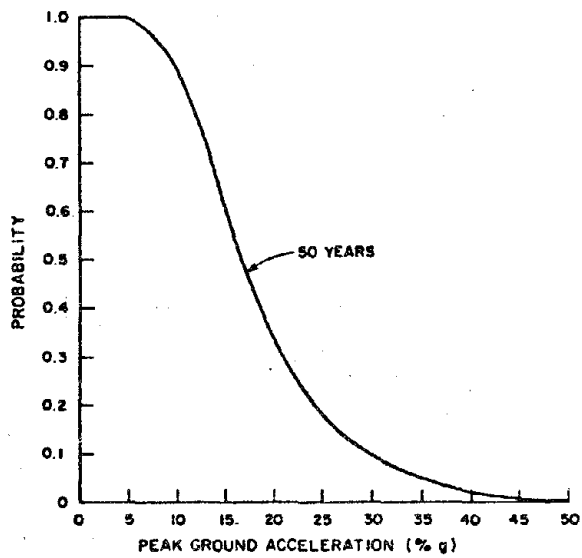


FIG. 3. PROBABILITY OF OCCURRENCE OF PEAK GROUND ACCELERATION

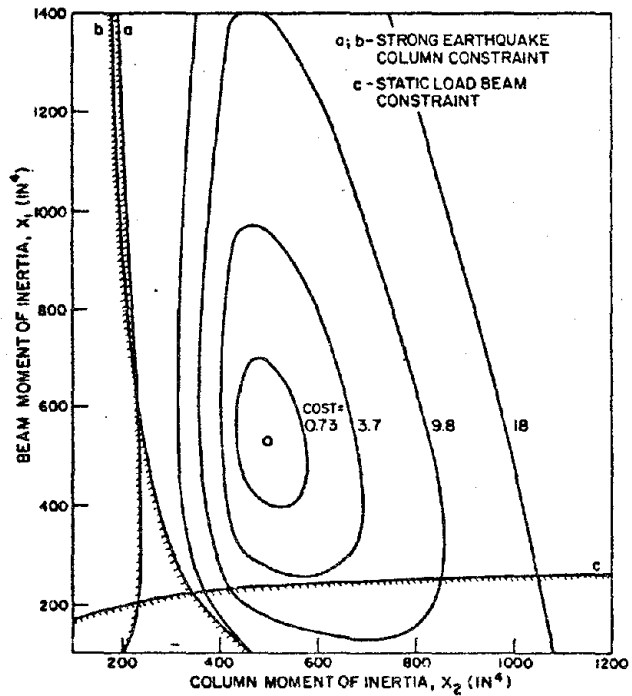


FIG. 4. ONE-STORY FRAME DESIGN SPACE



## EARTHQUAKE ANALYSIS OF COUPLED SHEAR WALL BUILDINGS

by

T. Srichatrapimuk<sup>I</sup> and Anil K. Chopra<sup>II</sup>

## SUMMARY

An efficient technique especially suited for computer analysis of coupled shear wall buildings is outlined. Application of the technique to analysis of earthquake-damaged buildings is demonstrated.

## INTRODUCTION

Coupled shear wall buildings have usually been analyzed by computer programs based on standard methods of building frame analysis. These analysis methods, in determining responses to horizontal ground motions, neglect inertia forces in vertical and rotational degrees of freedom. By static condensation of these degrees of freedom, the dynamic equations are formulated in terms of lateral displacement and the problem size is greatly reduced. However, such a formulation is generally inappropriate for coupled shear wall buildings because vertical inertia effects of walls can be significant in the dynamics of such structures.

Because the stiffness, strength, and stability of coupled shear wall buildings is largely due to the walls, they should be designed to remain essentially undamaged in the event of an earthquake. The benefits of energy dissipation through inelastic action can be provided by yielding of the coupling beams. Therefore, this investigation assumes that the walls are linearly elastic, thus confining yielding to the coupling beams.

The objectives of this paper, which summarizes some results from the complete report<sup>1</sup> on this study, are: (1) to present an efficient technique especially suited for computer analysis of coupled shear walls; and (2) to demonstrate application of the technique to analysis of earthquake-damaged buildings.

## OUTLINE OF ANALYTICAL PROCEDURE

The end shear wall of the building shown in Fig. 1 may be idealized as the structural assemblage shown in Fig. 2, with three wide-column lines (located at the respective neutral axes of the walls), and beams at every floor level coupling adjacent walls. The corner spandrel beams may be neglected; the wall-beam panel zone is idealized by rigid links.

Coupling beams in coupled shear wall buildings are usually deep and subject to high shear, resulting in shear cracking, normally accompanied by yielding of stirrups and flexural reinforcement. Shear cracks and subsequent yielding are not localized at end sections of beams, but are

I Faculty of Engineering, Chieng Mai Univ., Chieng Mai, Thailand;  
formerly Graduate Student, Univ. of Calif., Berkeley

II Prof. of Civil Engineering, Univ. of Calif., Berkeley.

spread over a substantial portion of the span. Therefore, instead of using the end sectional moment capacities,  $M_{y1}$  or  $M_{y2}$ , to signify a change in beam stiffness - as is done with flexural beams - the shear  $P_v = (M_{y1} + M_{y2})/s$ , which directly reflects nonlinearities due to diagonal shear cracking or stirrup yielding, is used to decide whether or not a change in stiffness has occurred. A bilinear hysteretic force-deformation relation is assumed for coupling beams, controlled by a bilinear shear-average end rotation relation (Fig. 3a) which can be obtained from laboratory experiments.<sup>2</sup> This model implies simultaneous changes in stiffness in the moment-rotation relation at both ends of the beam, reflecting nonlinear effects distributed throughout the beam span, not just at the ends (Fig. 3b).

By considering bending and axial deformations in walls; bending, axial, and shear deformations in coupling beams; including inertia forces associated with lateral as well as vertical motions; and using variational principles, the equations of motion were first formulated in the nodal point degrees of freedom (DOF): vertical, horizontal, and rotational displacements at each beam-wall (wide column) joint in Fig. 2. The number of these equations increases rapidly as the number of walls and stories increase and their solution requires large computational effort.

In Fig. 4, the first 10 natural vibration mode shapes computed for the McKinley Building<sup>3</sup> are compared to the vibration mode shapes of the individual walls of the building. The general similarity of the two sets of mode shapes suggests that displacements of the structure may be effectively expressed as a linear combination of the natural mode shapes of vibration of individual walls. Thus, the displacements at the nodal points on the  $j$ th wall are expressed as a linear combination of the first few natural mode shapes of the  $j$ th wall, considered as an individual cantilever. Local plastic rotation at the base of a wall may be considered by including the associated rigid body displacement of the structure as an additional shape function. The equations of motion are transformed to the associated generalized coordinates. If a small number of generalized coordinates suffice to predict response accurately, the number of equations and the computational effort would be reduced considerably, as discussed in the next section.

Not only does the numerical step-by-step integration of the reduced system of equations require considerably less computational effort than does the original system, but a larger time step may be used in the integration, because the higher vibration modes, having very short vibration periods and contributing negligibly to structural response, are eliminated by the transformation to generalized coordinates.

#### EVALUATION OF REDUCTION TECHNIQUE

The simple idealization presented in Ref. 3 for the McKinley Building (Fig. 1) was employed to evaluate the effectiveness of the above-described technique for reducing the number of DOF. Coupling beams were assumed to span the two end walls and the middle pier was ignored. A reduced system of equations is designated by  $H_m V_n$ , where  $m$  and  $n$  denote the number of modes of lateral (horizontal) and longitudinal (vertical) vibration, respectively, of each wall included in the analysis. The natural frequencies and mode shapes of the coupled shear wall system, modal stress resultants, and the nonlinear response of the system are computed from the original system

("exact" analysis) of equations in nodal point coordinates, and from the reduced system of equations in generalized coordinates.

The first six natural frequencies and mode shapes of the structure were satisfactorily reproduced by the  $H_4V_4$  system, whereas the first nine modes were more accurately reproduced by the  $H_6V_3$  system (Fig. 5). Because the more significant displacements in the lower modes of vibration of the structure are in the lateral direction, it is effective to include a larger proportion of lateral vibration modes of the walls.

Although the deflected shape of the first antisymmetrical mode was very accurately reproduced by solving the eigenvalue problem for the  $H_{16}V_8$  reduced system, to within 2%, predictions of the associated shear and bending moments in the walls were extremely inaccurate (Fig. 7). Stress resultants were inaccurate because the moments in the walls associated with the deformations in vibration modes of individual walls vary gradually along the height, whereas their actual distribution is discontinuous due to the moments at the ends of coupling beams. However, the predicted wall moment smoothly averaged the discontinuity in moments at the beam level. Shear in coupling beams, however, was predicted accurately (Fig. 7).

The stress resultants for the walls obtained by analyzing the reduced system were corrected by distributing, as shown in Fig. 6, the beam end-moments to the wall above and below each beam-wall joint. A correction was also necessary at the base of the structure. Shear forces in the wall are then correspondingly adjusted to equilibrate corrected bending moments. By applying the above adjustment procedure, the corrected bending moments and shears obtained from analyzing the  $H_6V_3$  reduced system -- a much less refined system than the  $H_{16}V_8$  one -- satisfactorily agreed with the "exact" values (Fig. 7). The  $H_6V_3$  reduced system, with this adjustment, also satisfactorily predicts the stress resultants associated with the third antisymmetrical mode shape (Fig. 8).

Two approaches were used to determine the nonlinear response of the simple idealization for the Mt. McKinley building, wherein yielding of the coupling beams is considered, to a simple ground motion, described by a half-cycle of displacement<sup>4</sup>, with maximum acceleration = 0.5 g in the horizontal direction and one-third of that in the vertical. The  $H_6V_3$  reduced system was analyzed by the procedures outlined earlier and the equations in nodal point coordinates were solved by DRAIN-2D<sup>5</sup>, a computer program based on standard frame analysis procedures. The results (Figs. 9 and 10) indicate that the two analyses lead to essentially the same displacement response, but the forces determined from DRAIN-2D analysis oscillate about those determined from analysis of the reduced system. These oscillations do not disappear even when the integration time step in the DRAIN-2D analysis is reduced to half the value used in analysis of the reduced system. An operation count indicates that the computational effort required for analysis of the reduced system is 20% to 50% of that required for the original system in nodal point coordinates. Obviously, with the use of generalized coordinates, not only is the size of the problem and computational effort greatly reduced but, by eliminating the unimportant higher modes of vibration, the spurious oscillations in the numerical calculations are eliminated.

## ANALYSIS OF EARTHQUAKE-DAMAGED BUILDINGS

Some of the damage to McKinley Building caused by the 1964 Alaska earthquake is apparent in Fig. 1. The response of the mathematical model of an end wall of the building (Fig. 2) to a simulated motion<sup>6</sup>, intended to represent the ground shaking in Anchorage, was determined by the procedure outlined earlier. The results are summarized in Figs. 11-13.

Beams on the second through eighth stories underwent the most extensive yielding, each of which accumulated a total plastic rotation of more than 0.02 radians during more than 20 yielding excursions (Fig. 11). Cyclic rotation ductility demand exceeded 10, an excessive demand for an ordinarily reinforced deep beam. The analysis thus predicted severe inelastic action in these beams which failed due to inadequate ductility. The prediction was generally consistent with the observed damage, beams from the second through the ninth stories having been severely damaged during the earthquake.

Axial force envelopes for walls (Fig. 12) indicate no resulting axial tension, and therefore no possibility of uplifting of the foundation or failure of walls in tension. A significant difference in the magnitude of developed axial compression in two identical walls gave rise to substantially different sectional moment capacities. Therefore, one of the two identical walls with smaller moment capacity was more vulnerable to yielding than the other wall; this is consistent with the observed damage.

Although yielding in walls was not considered in the analysis, it can be examined by studying the force distribution at selected time steps. For example, at  $t = 16.9$  seconds, beams in the third through eighth stories had just undergone three large, consecutive yielding cycles. They were assumed to fail at this point and part of the resistance to story overturning moment, formerly offered by axial forces in the walls, was no longer available at these stories. Wall sections across affected stories had therefore to resist more moment to compensate for the loss of the axial-force couple. This additional moment was assumed to be resisted equally by the two outside walls. The resulting moment distribution is presented in Fig. 13, indicating that wall sections from the fourth story down were stressed beyond yielding capacity. Although actual redistribution of the couple due to axial forces in the walls after some beams have failed is much more complicated, this simple analysis of redistribution of moments indicates a yielding tendency in these lower story wall sections. In fact, yielding did occur in the third story wall section (Fig. 1).

A similar analytical investigation<sup>1</sup> of the performance of the Banco de America building during the Mangua earthquake led to conclusions consistent with the actual damage. Coupling beams underwent significant yielding but the walls were essentially undamaged. The excellent performance of this building suggests that, for coupled shear walls to be most effective as a structural system, walls should be designed to remain elastic, thus justifying the assumption of linearly elastic walls in this analytical procedure.

## CONCLUSION

Under the assumption that inelastic action is confined to the coupling beams, coupled shear wall buildings can be most effectively analyzed by

expressing the deflections as a linear combination of the first few natural mode shapes in lateral (horizontal) and longitudinal (vertical) vibration of individual cantilever walls. In this approach, the vertical inertia, important in the dynamics of coupled shear walls, need not be neglected; and any mechanical model for the coupling beams can be employed. This analysis procedure requires considerably less computational effort than standard computer programs do. Using the technique presented earlier, results were given of earthquake response analyses of two existing coupled shear wall buildings damaged during earthquakes. It was shown that damage predictions based on analytical results are generally consistent with observed damage.

#### ACKNOWLEDGEMENT

This paper is based on a report<sup>1</sup> on research conducted under Grants GI-36387, AEN73-07732, and ENV76-04264 from the National Science Foundation.

#### REFERENCES

1. Srichatrapimuk, T., Report No. EERC 76-27, Univ. of Calif., Berkeley, Nov., 1976.
2. Paulay, T., Ph.D. Thesis, Univ. of Canterbury, New Zealand, 1969.
3. Skattum, K.S., Ph.D. Thesis, Calif. Inst. of Tech., Pasadena, Calif., 1971.
4. Veletsos, A.S., and Vann, W.P., Journal of the Structural Division, ASCE, Vol. 97, No. ST4, April, 1971, pp. 1257-1281.
5. Kaanan, A.E., and Powell, G.H., Report No. EERC 73-6, Univ. of Calif., Berkeley, Calif., 1973.
6. Housner, G.W. and Jennings, P.C., The Greater Alaska Earthquake of 1964 - Engineering, National Academy of Sciences, Washington, D.C., 1973, pp. 43-48.



FIG. 1 MCKINLEY BUILDING:  
EARTHQUAKE DAMAGE  
IN NORTH END WALL

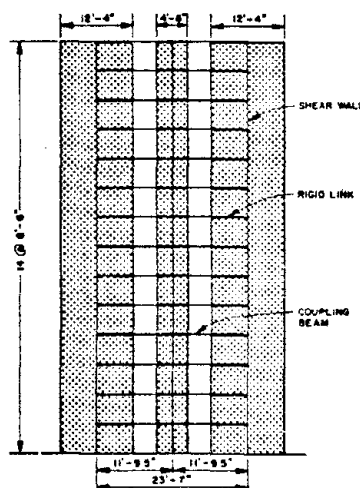


FIG. 2 MCKINLEY BUILDING:  
STRUCTURAL IDEALIZATION  
OF NORTH END WALL

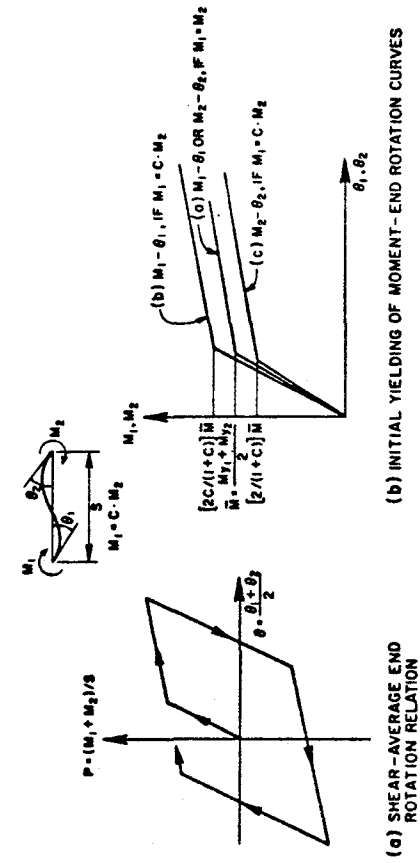


FIG. 3 MECHANICAL MODEL OF COUPLING BEAM

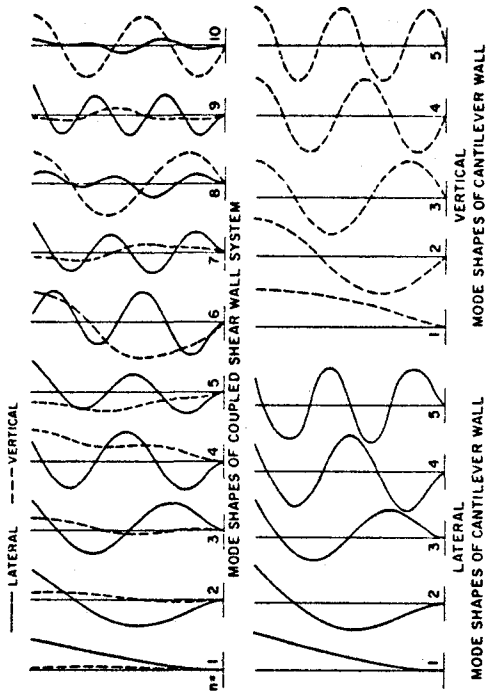


FIG. 4 STRUCTURAL MODE SHAPES AND CANTILEVER WALL MODE SHAPES

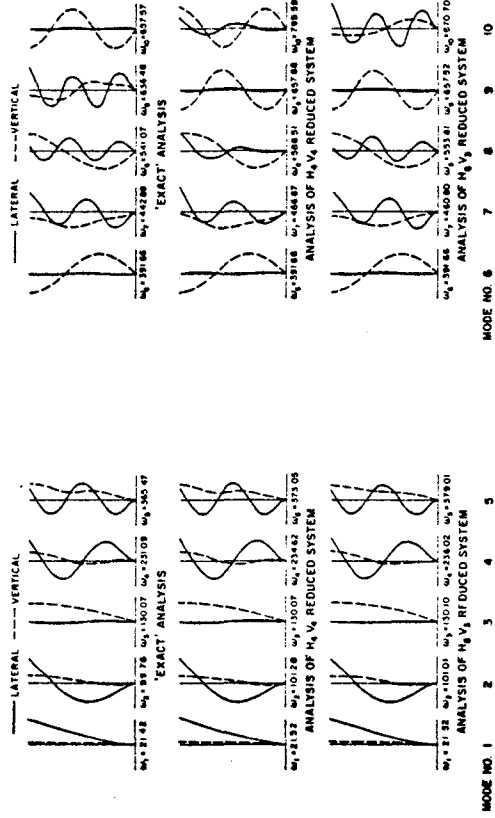


FIG. 5 NATURAL FREQUENCIES AND MODE SHAPES OF VIBRATION OF MCKINLEY BUILDING COMPUTED FROM THREE ANALYSES

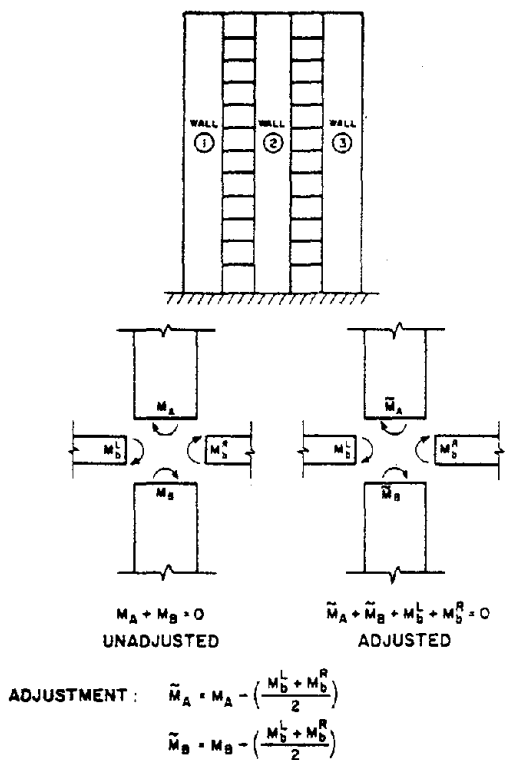


FIG. 6 ADJUSTMENT OF BENDING MOMENT IN WALL

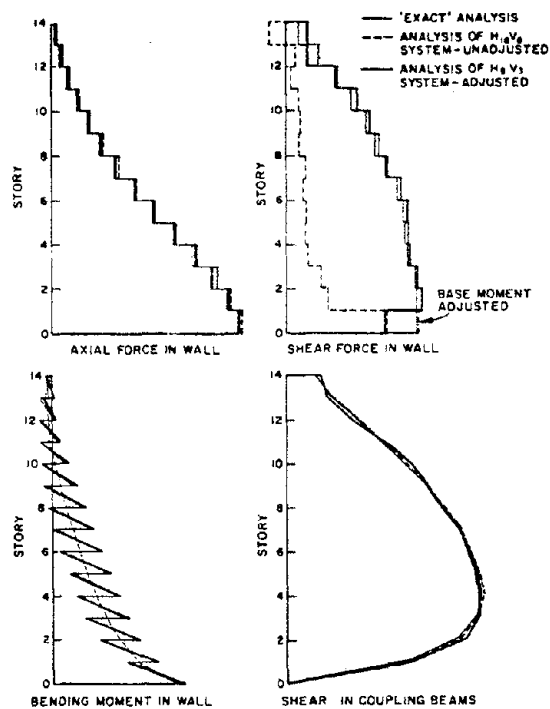


FIG. 7 STRESS RESULTANTS IN FIRST MODE OF VIBRATION OF MCKINLEY BUILDING

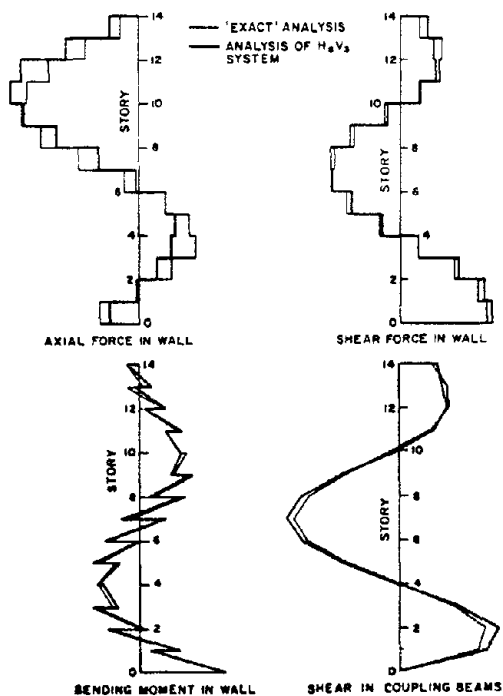


FIG. 8 STRESS RESULTANTS IN THIRD MODE OF VIBRATION OF MCKINLEY BUILDING

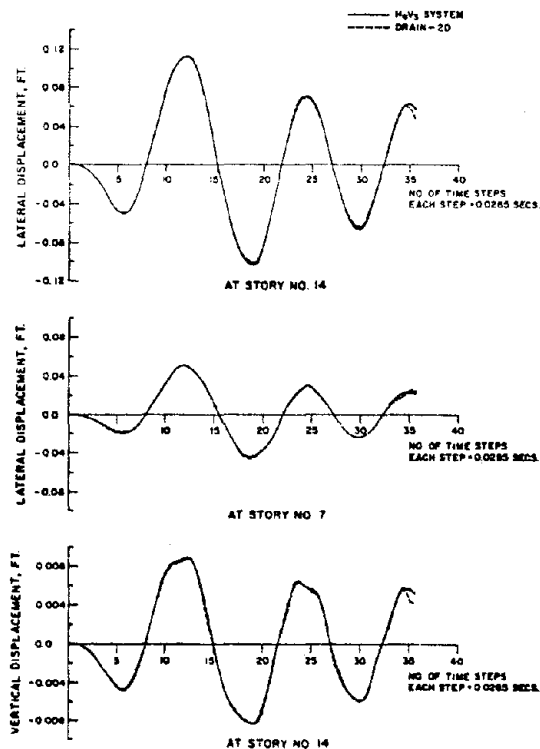


FIG. 9 DISPLACEMENT HISTORY OF WALL 1 OF MCKINLEY BUILDING

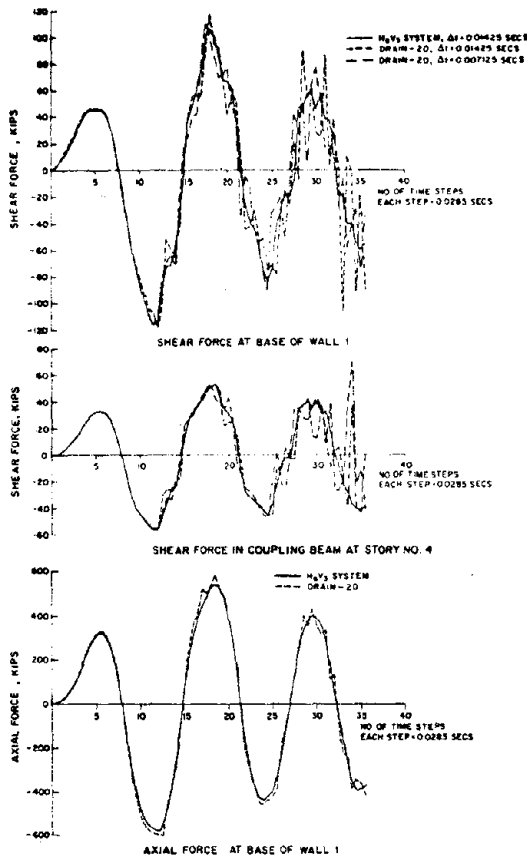


FIG. 10 STRESS RESULTANT HISTORY FOR MCKINLEY BUILDING

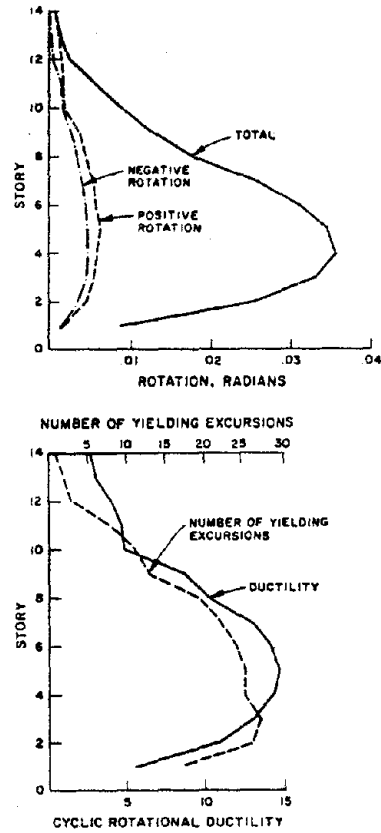


FIG. 11 PLASTIC END ROTATION, CYCLIC ROTATIONAL DUCTILITY DEMAND, AND NUMBER OF YIELDING EXCURSIONS IN COUPLING BEAMS OF MCKINLEY BUILDING

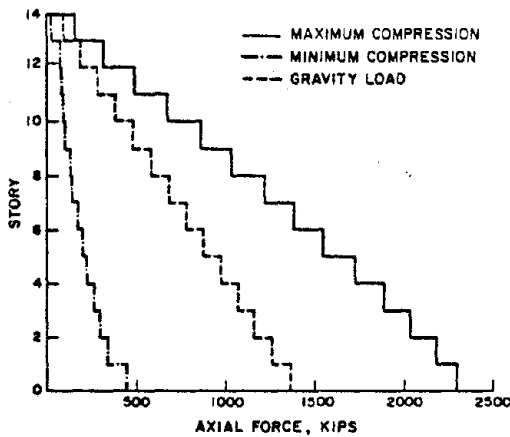


FIG. 12 ENVELOPES OF AXIAL FORCES IN AN END WALL OF MCKINLEY BUILDING

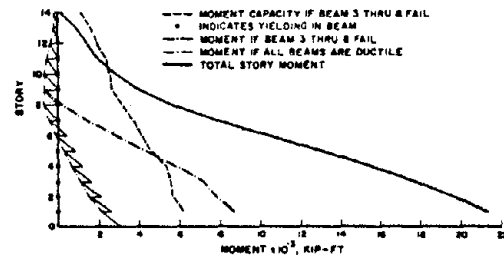


FIG. 13 DISTRIBUTIONS OF MOMENT IN AN END PIER AT TIME = 16.90 SECS.



## EFFECTS OF DURATION AND AFTERSHOCKS ON INELASTIC DESIGN EARTHQUAKES

by Stephen A. Mahin<sup>I</sup>

## SUMMARY

Some basic problems in defining design earthquakes for structures that can be allowed to yield during severe, long duration ground shaking are examined. Results of inelastic dynamic analyses of systems with different mechanical characteristics are presented for ensembles of synthetic accelerograms with durations ranging up to 60 sec., for recorded aftershock sequences and for other commonly used records. It is shown that duration effects must be considered in certain cases to limit lateral displacements and energy dissipation demands.

## INTRODUCTION

Field surveys following recent major earthquakes indicate that aftershocks can substantially increase structural damage and that it is not unusual for this damage to accumulate during aftershock sequences resulting in structural collapse. Damage may also accumulate during severe, long duration ground motions associated with a great earthquake as well as during several severe earthquake events which may occur at different times during the service life of a structure. Since cumulative damage from such seismic events may exceed that predicted using records commonly employed in seismic response analyses, more stringent design criteria may be necessitated where long duration motions can occur. As part of an overall evaluation of current seismic-resistant design methods [1,2], analytical studies have been performed to assess the effect of duration of shaking on inelastic seismic response and some results for single degree-of-freedom (SDOF) systems are reported herein.

## RESPONSE OF INELASTIC SDOF SYSTEMS

Several analytical studies indicate that the maximum displacement ductility,  $\mu$ , does not substantially increase with increasing duration of ground shaking, e.g. [3]. Even if  $\mu$  is bounded, cycles of reversed inelastic deformations may result in excessively large energy dissipation demands. To study this possibility, it is convenient to define an equivalent energy dissipation ductility factor,  $\mu_E$ , equal to the maximum displacement ductility of a monotonically loaded elasto-perfectly plastic (EPP) system that dissipates the same hysteretic energy as the actual system. As indicated in Fig. 1, EPP SDOF systems, designed according to [4] and subjected to 10 standard duration accelerograms, develop values of  $\mu_E$  significantly larger on average than can be inferred from  $\mu$  alone [1].

A number of other studies indicate that displacements can significantly increase with duration of shaking, e.g. [2,5], resulting in an incremental-type failure (Fig. 2). Following an initial seismic excitation a structure may retain a permanent deflection. For systems considered in Fig. 1, permanent deformations averaged more than 40% of the maximum displacements [1]. As discussed in Ref. 2, repetition of severe, long duration acceleration pulses and deformation softening tendencies of the system (representative

---

<sup>I</sup>Assistant Prof. of Civil Engineering, Univ. of California, Berkeley, CA.

of P- $\Delta$  effects or strength deterioration) may preferentially orient further inelastic deformations in the direction of the initial offset. For example, P- $\Delta$  effects reduce the effective stiffness of a SDOF system by an amount equal to its weight divided by its effective height. Because of this reduction (expressed herein as a fraction,  $p$ , of the initial stiffness), the yield strength of the system will decrease for loads in the direction of the offset (Fig. 2) and will correspondingly increase for loads in the opposite direction.

The sensitivity of inelastic response to post-yield stiffness can be seen in the nondimensional maximum displacement ductility spectra shown in Fig. 3 for the derived Pacoima Dam base rock (DPD) record. In this figure, parameter  $\eta$  equals the system's yield resistance divided by the product of its mass and the peak ground acceleration. While moderate amounts of deformation hardening have minor effects, moderate deformation softening results in significant increases in ductility demands in all but the most flexible systems. For example, according to Fig. 3, deformation softening systems with strengths corresponding to an  $\eta$  value of 0.5 and an initial period less than 0.8 sec. would collapse (while EPP systems would not).

#### EFFECT OF LONG DURATION GROUND MOTIONS

To assess the effect of long duration ground motions, average ductility spectra were constructed based on the response of bilinear hysteretic SDOF systems to five, 60 sec. long, synthetic accelerograms. These records were generated to be representative of severe ground motions recorded at moderate epicentral distances on firm ground [6].

Displacement Ductilities. Average displacement ductility spectra for systems with  $\eta$  equal to 0.2 are plotted at 10 sec. intervals in Fig. 4. Average ductility demands generally decrease with increasing period for systems with constant strength. The maximum displacement ductility demands of EPP systems tend to increase only slightly in the last half of the records, and the greatest increase occurs within the first 10 sec. (Figs. 4 and 5(a)). This trend is maintained for all  $\eta$  values (Fig. 5(b)). Deformation softening substantially increases ductility demands in general (Fig. 4). The increase is usually small during the initial portion of the excitation, but becomes larger as time progresses. This is particularly true for systems in which  $\mu$  values exceed 4-6. Small amounts of deformation softening have catastrophic effects on weak structures with low initial periods. Coefficients of variation for  $\mu$  are generally much larger for softening systems.

Energy Dissipation Demands. Although  $\mu$  values for EPP SDOF systems tend to remain constant with time,  $\mu_E$  tends to increase with continued shaking (Figs. 4 and 5). Thus, the duration of potential ground shaking must be carefully considered in the design of systems with limited energy dissipation capacities.

#### EFFECT OF AFTERSHOCK SEQUENCES

To assess the effect of the accumulation of damages due to successive ground motions, a number of earthquake aftershock sequences have been investigated. For example, the 1972 Managua earthquake main shock was followed by two large aftershocks. Cumulative ductility spectra for the east component of the Esso Refinery records are presented in Fig. 6. Depending

on the initial period and strength, the main shock (351 gal) would have induced significant inelastic deformations in EPP SDOF systems. The first aftershock (120 gal) had relatively little effect. However, inelastic deformations during the second aftershock (277 gal) predominantly occurred in the same direction as in the main shock, more than doubling  $\mu$  for many systems (especially those with relatively low  $\eta$  values). Energy dissipation demands were similarly increased. As shown in Fig. 7, small amounts of deformation softening again have a significantly adverse effect on ductility demands.

#### CONCLUSIONS

Duration of severe ground shaking can have a significant effect on inelastic deformational and energy dissipation demands. This is especially true of relatively weak, short period structures which may be expected to develop significant inelastic deformations. Particular attention must be devoted to determination of the total duration of shaking if a structure may exhibit deformation softening or has a limited capacity to dissipate energy. Additional research is needed to devise reliable design methods for such systems and to assess the effect of duration of stiffness and strength degrading systems.

#### ACKNOWLEDGEMENTS

The financial support of the NSF is gratefully acknowledged. The numerical computations were performed by M. Williams and A. Ziegler.

#### REFERENCES

1. Mahin, S. and Bertero, V., "An Evaluation of Inelastic Seismic Design Spectra," submitted to J. of the Str. Div., ASCE.
2. Bertero, V., "Establishment of Design Earthquakes," Proceedings, Int. Symp. on Earthquake Struct. Engineering, St. Louis, 1976.
3. Murikami, M. and Penzien J., "Nonlinear Response Spectra for Probabilistic Seismic Design of R/C Structures," Proceedings, 6WCEE, New Delhi, 1977.
4. Newmark, N. and Hall, W., "Procedures and Criteria for Earthquake Resistant Design," Building Science Series 45, NBS, Washington, D.C., 1973.
5. Sun, C., Berg, G. and Hanson, R. "Gravity Effect on a Single-Degree Inelastic System," J. of Eng. Mech. Div., ASCE, Vol. 99, No. EM1, 1973.
6. Ruiz, P. and Penzien, J., "Stochastic Seismic Response of Structures," J. of Eng. Mechanics Div., ASCE, No. 97, Vol. EM2, 1971.

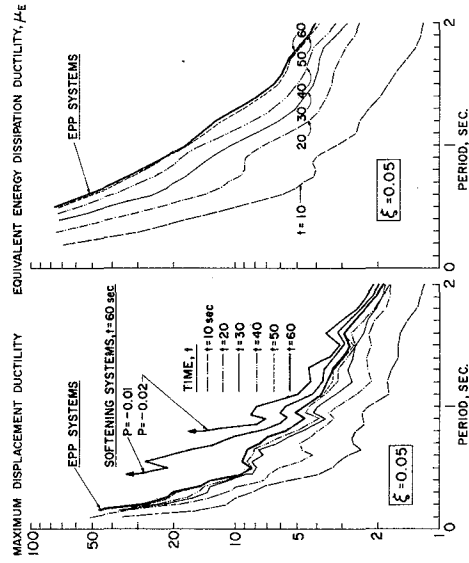


FIG. 1 AVE. RESPONSE FOR TEN RECORDS--EPP SYSTEMS DESIGNED USING [4];  $\xi = 5\%$

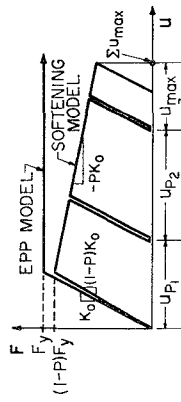


FIG. 2 INCREMENTAL TYPE FAILURE

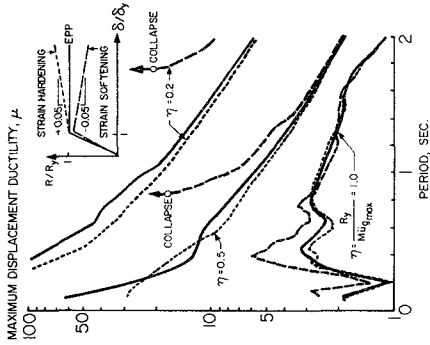


FIG. 3 EFFECT OF HARDENING AND SOFTENING ON  $\mu$ :DPD RECORD (SI6E)

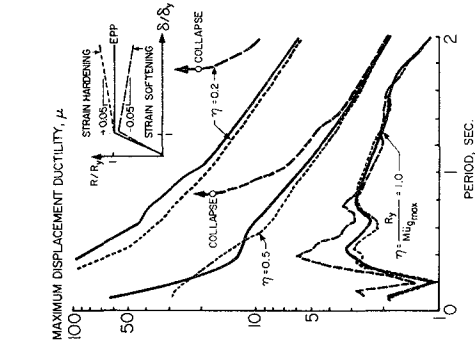


FIG. 4 EFFECT OF DURATION ON DUCTILITY SPECTRA--AVE. FOR 5 SYNTHETIC RECORDS

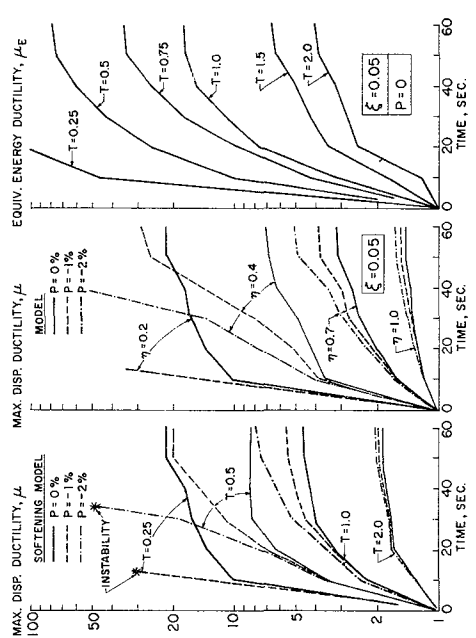


FIG. 5 VARIATION OF  $\mu$  WITH TIME--AVE. FOR 5 SYNTHETIC RECORDS

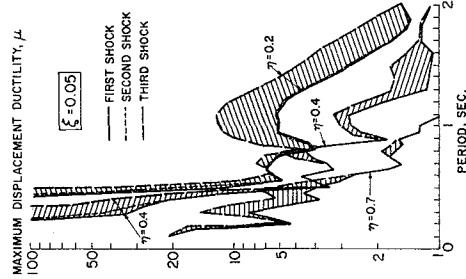


FIG. 6 EFFECT OF ESSO REFINERY AFTERSHOCKS (EW) ON  $\mu$ ; P = 0. ESSO REFINERY AFTERSHOCK SEQUENCE (EW)

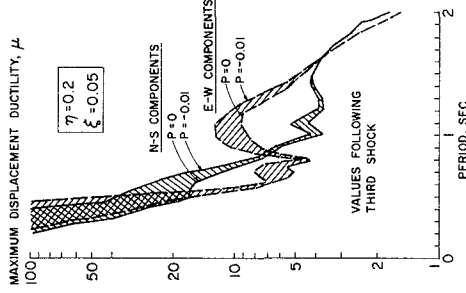


FIG. 7 EFFECT OF SOFTENING ON  $\mu$ ; AFTERSHOCKS (EW) ON  $\mu$ ; P = 0. ESSO REFINERY AFTERSHOCK SEQUENCE (EW)

ADDRESS TO STATE-OF-THE-ART PANEL NO. 6

SYSTEM IDENTIFICATION  
IN  
EARTHQUAKE ENGINEERING

by

Hugh D. McNiven

Professor of Engineering Science  
University of California  
Berkeley, California

## SYSTEM IDENTIFICATION IN EARTHQUAKE ENGINEERING

## 1. Introduction

The instructions accompanying the invitation to submit a paper on this topic call for the paper to be devoted to the state of the art. As the topic is so enormous and space is limited, I will bend the assignment a little and present a survey of what I have found about mathematical modeling of earthquake-resistant structures in general, and about system identification in particular. As my involvement covers a period of only five years, the space allowed seems appropriate.

One of the major efforts of structural engineers in the field of earthquake engineering is directed to trying to predict how a structure will respond to seismic forces. In order to make this prediction, the engineer needs a mathematical model of the structure. As system identification is a rational, systematic method for formulating mathematical models, my various colleagues and I have used it in almost all of our formulations to date. In doing so we have learned a great deal about system identification, but also a fair amount about the general art of formulating mathematical models.

Engineers have for years used mathematical models to predict the seismic response of a structure and have realized a great deal of success. However, we are entering an era when it is becoming necessary to model structures beyond the scope of many present methods. Further, it is generally recognized that it is not economically feasible to design a structure that will respond entirely elastically to strong motions, and that it is acceptable to expect some inelastic behavior in the response. This brings us into the domain of nonlinear models, and it is fair to say that we are in the infancy of our ability to formulate such models. We are beginning an era that will require all of the sophistication we can muster to formulate mathematical models that will accommodate these new demands. I think that system identification as we now know it, and as our knowledge of how to use it grows, offers the most sensible method for formulating models in this new era.

A definition of system identification might be "A rational, systematic method for constructing a mathematical model to represent a physical system." The method is explicit, and must consist of the following three parts.

1. The form of the mathematical model.
2. The cost or error function.
3. The optimization algorithm.

The method though simple in concept is extremely powerful. It allows for a great deal of ingenuity when modeling a particular system, so that it is in the details that one formulation may differ significantly for one system from that of another. It is the details that are interesting, and it is a discussion of the details that will form the bulk of this presentation.

The most difficult aspect of writing this paper has been the choice of a format which allows me to present what I wish to say. After discarding

several, I have decided to talk at length about each of the three parts of system identification and to convey to you what we have learned of system identification, segregated accordingly. There are a few things about the subject which do not suit this format, so they will be gathered together at the end under "General Comments."

## 2. The Form of the Mathematical Model

When we began using system identification, we considered that this part deserved the least attention of the three. We now feel that it deserves the most. The reasons for this reappraisal will become apparent in what follows.

One of the fundamental misunderstandings about mathematical modeling is that a particular structure has "a mathematical model." In theory there are an infinite number of possible models; in reality there is usually a small family. The models are distinguished from one another by the order of their complexity. The order of a model, reflected in the number of parameters involved, derives from the number of degrees of freedom which the model accommodates. The task of the person constructing models is to ensure that the model of a particular order is the best possible of all models of that order.

For example, to predict the seismic responses of a symmetric, three-story, steel frame<sup>[1]</sup>, we constructed three different models, containing five, eight and nine parameters, which allowed respectively three, six and seven degrees of freedom. All are useful for a dynamic analysis. In choosing which is appropriate for a particular analysis, one must be aware that there is always a trade-off. The higher the order of the model, the more accurate it is, but the more costly to use.

In choosing the form for a particular model, we have pointed out that the number of degrees of freedom which one wishes to accommodate is one decision. There are others. The model we are constructing is the mathematical expression of the physics of the problem. Particularly when we consider that the response of the structure will be nonlinear, it is not always clear at the outset what physical contributions to include in the model and what can safely be neglected. It is when addressing this fundamental consideration that we can point to one of the great benefits of system identification. The usefulness of system identification in this situation is that it allows for appraisal of the form of the model. By definition (understood by what follows), the parameters which we find using the optimization algorithm are the best set possible for achieving the purpose of the model (as expressed by the error function). If the model, at the completion of system identification, is judged to be inadequate in predicting responses, the fault must be with the form of the model. If the form is "inadequate" more physical influences must be added or introduced mathematically in a different way. Adding the influence of one physical contribution may improve the predictions of the model considerably, in which case the term in the model that reflects it should be retained. If on the other hand the improvement is minor, the complication is not worth the improvement, allowing for the judgement that the physical influence can be neglected. Just as with the order of the model, a number of models can be constructed each containing a different set of physical influences, and with system identification the relative merits, that is their ability to predict, are carefully calibrated.

### 3. The Cost or Error Function

The error function is a mathematical statement of what it is you want the model to do. In all of our work we have had as the end product a mathematical model of a physical structure that will predict responses as close as possible to those recorded experimentally, when both the structure and the model are subjected to the same earthquake input. At a particular instant of time, a chosen response quantity (say a floor acceleration) has one value as recorded experimentally ( $y_j$ ) and another which is predicted by the model ( $x_j$ ). The difference is the "error." The error function is a measure of the accumulation of errors of all response quantities ( $n$ ) over the full duration of the excitation or part of it ( $T$ ). We have used the squared error in formulating our error function which is not mandatory, but widely used. The form we have used is

$$J(\beta_1, T) = \sum_{j=1}^n \int_0^T k_j [x_j(\beta_1, t) - y_j(t)]^2 dt$$

If one wishes to match one response quantity more closely than another, he can use the weighting factors ( $k_j$ ) for this purpose.

We are fortunate at the Earthquake Engineering Research Center of the University of California at Berkeley to have a shaking table that can accommodate large-scale physical models of structures and subject them to a large family of earthquake excitations. With this facility it is possible to record accurately the forcing function and a variety of response quantities.

The most important part of formulating the error function, and perhaps not fully appreciated, is the choice of response quantities to be included. To understand the importance of the choice, we recall that the selection is made when the form of the model and the number of degrees of freedom it is to accommodate have already been made. The family of response quantities must be consistent with the number and kind of degrees of freedom. The selection of response quantities dictates whether the values of the parameters resulting from optimization will be unique, and also whether the optimization algorithm will in fact converge. These are major considerations.

In selecting response quantities for a model of a three-story steel frame that would allow both floor translations and joint rotations, we found that, for one set of response quantities the algorithm would not converge, for another it would. So far as we can tell, a family of response quantities will be effective when each of its members imposes an independent constraint or influence on the deformed shape allowed by the chosen degrees of freedom. A puzzling circumstance is that a unique set of parameters can be derived when the appropriate family is incomplete, but incomplete in a particular way. For the same three-story frame, the effective family of response quantities consists of the floor accelerations and the joint rotations. The optimization algorithm converges to the same set of parameters when accelerations and rotations at only the first and third floors are used. However, it converges for no other pair of floors. At the present time we are trying to establish a way of selecting a priori the minimum set of incomplete data that will lead to a unique set of parameters when the number and kind of degrees of freedom are specified, and when the set includes joint rotations. I add this last about rotations, because Sharma and Udwadia<sup>[2]</sup> have already shown



that, when the model treats a building as a shear building, translational response quantities at the first floor only are sufficient to construct a unique mathematical model for the building. One last point regarding responses. Kinematical response quantities are desirable because they can be used when the behavior is elastic or inelastic. Unfortunately no very elegant device has yet been perfected to measure joint rotations. In one set of experiments we are measuring joint rotations using lasers, but this requires a remote reference frame.

#### 4. The Optimization Algorithm

The parameters which appear in the model affect the responses that are included in the error function. Optimization therefore is the process of choosing that particular set of parameters which will minimize the error function. The best way of understanding optimization in this context is to visualize the error function as a surface in  $(n+1)$  dimensional space when there are "n" parameters. Optimization consists of starting at some point on the surface and traversing it step by step until the global minimum, or more realistically a point in some neighborhood of the global minimum, is established. The coordinates of this point form the set of parameters to be introduced into the model. With this insertion the model is complete.

The scheme used to traverse the surface is called the algorithm. The choice of algorithm is dictated by the number of parameters to be established. When the number is modest (say up to 10), we have found the modified Gauss-Newton algorithm to be powerful and efficient. When the number is large we have resorted to a program called POWBRE, which is a modification of Powell's method of minimizing a function without having to use analytical expressions for the derivatives or sensitivity coefficients. Time forces me to seek refuge in references for these methods. A very complete treatment of optimization is given in a report we issued on the modeling of a reinforced concrete beam<sup>[3]</sup>.

Optimization has attracted immense activity in mathematics and engineering, and perhaps the major effort in system identification has been in this last part, optimization. It is an attractive field. Devising an algorithm that is elegant and powerful is very satisfying. So much attention has been paid to optimization that many refer to system identification as parameter estimation. To me this puts a false emphasis on the values of the parameters and on the elegance of the method used to establish them. The mathematical model, which is the end product of the whole exercise, is only as good as its form. Whether the set of parameters is found using an elegant method or by brute force is not unimportant, but affects the final model very little.

As anyone with experience in optimization knows, rate of convergence to the global minimum is greatly enhanced by a good starting point. By a good starting point we mean initial values of the parameters that are based on enlightened insight rather than on a blind guess. This is not always possible but even the form of the model can be altered to allow for this insight.

When we constructed a model to mimic stress-strain behavior far into the work hardening range for mild steel<sup>[3]</sup>, we chose the Menegotto and Pinto model rather than the Ramberg-Osgood. The parameters in the Menegotto and Pinto model can be estimated quite accurately from the shape of the hysteresis

loops as the parameters represent geometric properties of the loops. The parameters in the Ramberg-Osgood model do not lend themselves to this enlightened estimation. Also the Menegotti and Pinto equations express the displacement (or strain) as an explicit function of the force (or stress) so that the dependent variable appears in each term of the governing differential equation. In the Ramberg-Osgood equation the reverse is true which complicates the algorithm needed to solve the equation.

## 5. General Comments

The comment that must be made when discussing system identification is that it is simple in concept and is extremely powerful. The first time we used system identification[4] we were amazed that a method so simple could give a model that predicts behavior so accurately.

Even though I come here to praise system identification and not to bury it, I must point out a weakness that it shares with most other methods of constructing mathematical models. The weakness can only be understood after a little elaboration.

The real structure has a number of physical features that identify it. These can include its geometry, the sizes of the members, the properties of the materials of which it is made, etc. We will call these family (A).

Now the parameters that appear in the mathematical model we will call family (B). For linear models the two families usually either coincide or are related in a simple way. However, for nonlinear models the families are usually distinct.

The problem with system identification is that it finds the values for the members of family B without in any way relating them to family A. Let me explain why this is a disadvantage. Suppose that using system identification we construct a model of a particular three-story steel frame and that the model predicts the frame's responses to an earthquake extremely well. If we want to change the physical structure in any single way (family A) by, for example, changing the orientation of the columns, there is no way to change the parameters of the model (family B) to accommodate this change. This significantly reduces the generality of the way in which our mathematical model can be used to predict. To further explain this limitation I will describe briefly a mathematical model we constructed to predict the linear, dynamic response of masonry[5]. The model is complicated and the physical bases for its form are not pertinent here. What is pertinent is that, when we attempted to make the model behave dynamically as the prototype, we chose particular characteristics such as cut off frequencies and asymptotic phase velocities of waves traveling through both the model and the prototype. These characteristics are expressible in terms of both family A and family B. When the characteristics were matched, family A was related to family B in a variety of ways. The equations thus formed constituted a well-formulated algebraic system. Therefore, whereas the mathematical model of a particular masonry might not predict its dynamic behavior as well as if the parameters were found using system identification, when a minor change is made in a property of the masonry (say the properties of the mortar), a mathematical model for the new prototype is quickly constructed.

I must point out that whereas a model constructed using system identification lacks one kind of generality it possesses another. We have recently established that a model of a one-story steel frame, constructed using the responses to a particular earthquake, predicts accurately the non-linear responses of the frame to a variety of other earthquake inputs<sup>[6]</sup>.

In formulating mathematical models, we have found that there is a constant temptation to be drawn into the detailed aspects of the process at the expense of the fundamental purposes of modeling and the details are often in conflict with these purposes. We have had to remind ourselves to attempt the simplest model possible and to satisfy ourselves of its limitations before proceeding to a more complicated one. We have found it useful to be cognizant about what can be derived from formulating a mathematical model. We feel that there are three objectives. The first and foremost is a model or models that will mimic the response behavior of the physical structure in some specified way. The second is to gain from the model insight into the physics of the structure, usually from the values of the parameters that appear in the final model. The third is to learn something about the mathematical technique used in formulating the models, in our case, system identification. It is seldom that all three objectives are realized, but they should always dominate one's thinking.

These last two objectives have helped to formulate our philosophy about model building, which is to undertake first a relatively simple model and exhaust from it all there is to learn before proceeding to the next more difficult model. As an example we started with models, both linear and non-linear, of a one-story steel frame. After we thought we had learned all that we could about the model and the details of system identification used in the process, we moved to a three-story steel frame. This problem introduced the question of effective and ineffective response data that had not been pertinent to the one-story frame. It also introduced, but did not solve, the matter of minimum incomplete data. To try to resolve this question, we are now working on the problem of constructing models of a six-story frame.

Whenever there are rules like these, there are exceptions. We departed from this philosophy when we constructed a model to predict the flexural behavior of a reinforced concrete, cantilever beam when it is subjected to cyclic, quasi-static loading<sup>[3]</sup>. Because we were not at all sure that this complicated behavior could in fact be reproduced by a mathematical model, we included all the physical contributions we could think of that would influence the beam's behavior. We included the cyclic behavior of the reinforcing steel far into the work hardening range, the behavior of the concrete itself, and even possible bond-slip. We introduced each of these into the global behavior of the beam by dividing the beam cross section into horizontal layers to arrive at the resisting moment. We ended with a model that predicts the experimental results extremely accurately but the model is too complicated for reasonable use. It remains therefore to systematically simplify the model first by eliminating those physical contributions whose inclusion does not warrant the computational cost, and then for the surviving contributions, trying to select from the family of parameters associated with each those that influence the behavior in the most pronounced way.

One might gather from all of this that we understand a great deal about constructing mathematical models. I for one am much more aware of what we don't know and what our limitations are. If there is a similar session devoted to this topic nine or ten years from now, the participants will probably be amused by the naiveté of the state of the art in 1980.

#### References

1. I. Kaya and H.D. McNiven, "Investigation of the Elastic Characteristics of a Three Story Steel Frame Using System Identification," Report No. UCB/EERC-78/24, Nov. 1978.
2. D.K. Sharma and F.E. Udwadia, "On Uniqueness of Identification in Damped Building Structures," S.I.A.M. Journal of Applied Mathematics, Vol. 34, No. 1, Jan. 1978.
3. J.F. Stanton and H.D. McNiven, "The Development of a Mathematical Model to Predict the Flexural Response of Reinforced Concrete Beams to Cyclic Loads, Using System Identification," Report No. UCB/EERC-79/02, Jan. 1979.
4. V.C. Matzen and H.D. McNiven, "Investigation of the Inelastic Characteristics of a Single Story Steel Structure Using System Identification and Shaking Table Experiments," Report No. UCB/EERC-76/20, Aug. 1976.
5. Y. Mengi and H.D. McNiven, "A Mathematical Model of Masonry for Predicting its Linear Seismic Response Characteristics," Report No. UCB/EERC-79/04, Feb. 1979.
6. B.I. Sveinsson and H.D. McNiven, "General Applicability of a Nonlinear Model of a One Story Steel Frame," Report No. UCB/EERC-80/10, May 1980.

EVALUATION OF NONLINEAR STRUCTURAL RESPONSE TO SEISMIC EXCITATIONS  
BY SYSTEM IDENTIFICATION

Bojidar S. Yanev<sup>1</sup>

SUMMARY

The evaluation of the response of a one story steel frame with partitions to earthquake type excitations is discussed. Modeling of the structure is attempted by means of system identification techniques. Alternatives are sought for a model, suitable in representing nonlinear inelastic response. Conclusions are formed concerning the applicability and the limitations of the Kelvin model as the analogy of a single degree of freedom oscillating structure and the Gauss-Newton numerical procedure as a means of performing system identification of such a model.

INTRODUCTION

The Earthquake Simulator of the Earthquake Engineering Research Center at the University of California, Berkeley provides the opportunity to investigate structural behaviour under earthquake type excitations. During the last few years experiments have been performed on the shaking table of the simulator with one and multistory steel frames, reinforced concrete frames, masonry buildings etc.

A large variety of structural responses have been obtained, ranging from linear elastic to nonlinear inelastic ones. The evaluation of this experimental data involves a search for meaningful parameters characterizing the structural behaviour and linking it to an idealized model with analogous performance. System identification techniques are helpful in this process.

SYSTEM IDENTIFICATION

The identification of a system with a given parametric model usually involves the minimization of an error function in search of the optimal parameters. Experimental data and a numerical procedure are required. The modified Gauss-Newton method has been applied in the studies of one (1) and three (2) story steel frames. The following error functions are considered:

$$J_1(\bar{a}, T) = \int_{T_1}^T (\dot{y}(\bar{a}, t) - \ddot{x}(t))^2 dt \quad (a)$$

$$J_2(\bar{a}, T) = \int_{T_1}^T (y(\bar{a}, t) - x(t))^2 dt \quad (b) \quad (1)$$

$$J_3(\bar{a}, T) = J_1(\bar{a}, T) + b J_2(\bar{a}, T) \quad (c)$$

where  $x$  and  $\ddot{x}$  are measured structural displacements and accelerations,  $y$  and  $\dot{y}$  are simulated values obtained from the model,  $\bar{a}$  is the parameter vector and  $b$  is a weighting factor.

Error  $J_3$  is eventually abandoned since it implies a relationship between displacements and accelerations, which is the subject of the modeling.

1) Research Engineer, EERC, University of California, Berkeley.

Reported in (3) and (4) are some of the results of applying the above procedure to data obtained during the tests of a one story steel frame with various infill partitions. The primary concern in this case was with the increased complexity of the behaviour expected of the partitioned frame. The deteriorating stiffness of the partitions and their buffeting against the frame for instance would require adequate energy dissipation devices in the model. Modeling the yield of the bare frame alone falls short of simulating nonlinear displacements as pointed out in (1), where Eq. 2 is applied.

$$C \dot{x} + P(x) = - M \ddot{x}_{abs} \quad (2)$$

where  $P(x)$  is the chosen load-displacement function,  $M$  is the concentrated mass,  $C$  is the viscous damping and  $\ddot{x}_{abs}$  is the absolute acceleration.

A preliminary inspection of the test data usually consists of obtaining 'pseudo' load-displacement relationships by neglecting the velocity term in Eq. 2. Fig. 1 illustrates a typical response of a partitioned frame. Another estimate of the structural behaviour is provided by Eq. 2 in the form:

$$\begin{aligned} C_i \dot{x}_i + K_i x_i &= - M \ddot{x}_{abs,i} \\ C_i \dot{x}_{i+1} + K_i x_{i+1} &= - M \ddot{x}_{abs,i+1} \end{aligned} \quad (3)$$

where  $K$  is the structural stiffness and  $i, i+1$  refer to consecutive timesteps in the test history, which is usually recorded at frequency of 100 Hertz.

System (3) is solved for  $C$  and  $K$ . The result corresponding to the relationship of Fig. 1 is shown on Fig. 2. It is noted that changes of  $K$  occur systematically and are always accompanied by changes in  $C$ .

In order to accommodate this behaviour, the identification procedure described in (3) and (4) is carried out over individual cycles of motion, allowing for a change of  $C$  and  $K$  at given points during the cycle. For the test of Fig. 1 the resulting parameters are shown on Fig. 3 along with a comparison between the measured and simulated acceleration. The identification uses error  $J_1$ . Average values in agreement with the results of elastic analysis are discernible but the abrupt changes of both parameters at points of motion reversal persist. This can not be solely attributed to data noise. A closer examination of the initial model is indicated.

#### MODELING OF THE SDOF STRUCTURE

The modeling of a system by numerical identification of parameters serves two purposes:

Quantitatively, the values of the parameters are obtained.

Qualitatively, if a good fit is demonstrated between measured and simulated responses, the model assumption is substantiated.

Eqs. 1, 2 and 3 are based on the Kelvin model of Table 1, Column 2, which is the standard assumption for a single degree of freedom structure. Non-linearity is built in the system by replacing  $K$  with  $P(x)$  in Eq. 2. Two objections to such a model are raised:

Changes in the stiffness do not lead to changes in the damping.

No provision is made for permanent eccentricities due to inelastic behaviour.

Viscous damping can not be discredited as a means of representing the global effects causing decay of oscillatory motion. On the other hand yield in structures involves a different type of energy dissipation. Hysteretic damping has been suggested in view of the generally hysteretic shape of non-linear load-displacement relationships. Coulomb damping, which is a function of the displacement rather than the velocity can account for friction.

Rather than speculate on the nature of the damping independent of the model configuration, the present study reexamines other possible analogies available from viscoelasticity (5) as shown in Table 1. Column 1 contains the basic alternative to the Kelvin solid, i.e. the Maxwell fluid. If such a model is to be considered for structural purposes, the damping acquires a new significance. Instead of being too small and hence possibly negligible, it becomes too large to affect the linear oscillations of the spring element. Only if the spring's capacity is exceeded does it come into effect, resulting in permanent displacements.

Such reasoning is not entirely foreign to solids. Yielding of metals has been modeled as a slip between molecules already stressed to their elastic limit. It appears that while the parallel action of the damping and the spring elements of a Kelvin model is typical of elastic oscillations, during yield their position may be in sequence. Columns 3 and 4 of Table 1 show two of the possible Kelvin-Maxwell combinations allowing the oscillator to display the flexible behaviour suggested by the tests. The model of Column 3 can be used as follows: with  $C_2$  tending to infinity it is reduced to a Kelvin model with an increased stiffness;  $K_2$  tending to infinity produces another Kelvin model with a higher damping. Such behaviour has been observed during the test of the relatively flexible frame with a stiffer partition. In this case the bond between frame and partition can be modeled as a damper of the  $C_2$  type. Internal modeling of the partition would be required for its nonlinearities.

The model of Column 4 also has its applications. The yield in an internally statically indeterminate structure (such as the partitioned frame) corresponds to the action of an internally positioned damper, such as  $C_2$  of Column 3. The forming of yielding areas and the ensuing permanent eccentricities of the bare frame however are more accurately represented by an external damper, such as  $C_2$  of Column 4. The above considerations can be summed up in the following conclusions.

#### CONCLUSIONS

The Kelvin model on which the standard SDOF equation of motion is based fails to represent structural yield regardless of the provisions made for a nonlinear spring behaviour. Also required is a damping device in sequence, rather than in parallel with the spring. The damper itself need not be necessarily a viscous one.

Qualitative modeling of the parameters requires a numerical procedure which, unlike the Gauss-Newton method would allow parameters to vanish. Identification would then consist not only of establishing the values of the parameters, but also of determining the number of the significant ones. As in viscoelasticity (5), the general model would be of the following form:

$$M (\ddot{x} + p_1 \dot{x} + \dots) = q_0 x + q_1 \dot{x} + \dots \quad (4)$$

In general the parameters of a system obtained by identification, such as  $p_i$  and  $q_i$  of Eq. 4 need not necessarily have physical significance. In the case of Eq. 4 however, they do. The model is generated on the basis of certain physical analogies and the physical compatibility of the results has to be maintained. Furthermore, the physical significance of a parameter may vary, depending on the configuration of the model as can be seen by a comparison between Columns 3 and 4 of Table I. It has been noted that a structural response containing local nonlinear behaviour can be roughly approximated by a linear model. Once the parameters of such a model are determined, it is still of interest to identify the elastic and the damping characteristics of which they consist in order to judge the form of the model and to draw conclusions on its subsequent performance.

The need for more information on structural motion, particularly the velocity and the rate of change of the acceleration is stressed. The concept of parsimony which requires that the model parameters should be necessary as well as sufficient extends to the identification procedure as well. The search for the significant parameters should not be encumbered with irrelevant data. The models of Table I with four parameters, one of which is allowed to vanish limit the requirements for data on the motion to the above.

#### ACKNOWLEDGMENTS

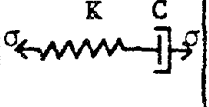
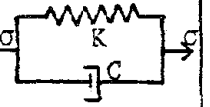
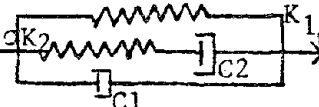

This work is part of a research program conducted at the EERC, UC, Berkeley under a grant from the National Science Foundation.

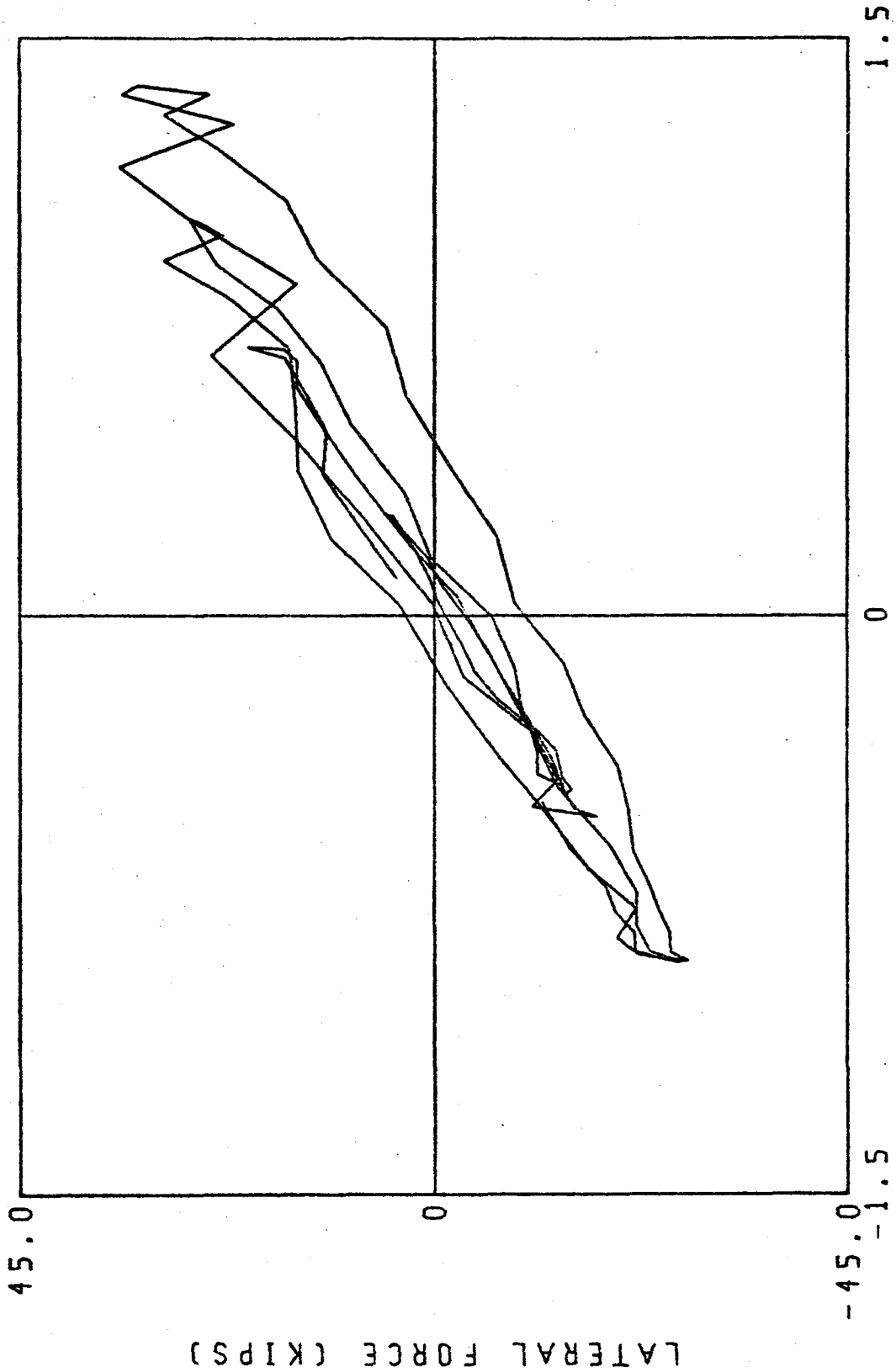
#### REFERENCES

1. Matzen, V., McNiven, H. D., "Investigation of the Inelastic Characteristics of a Single Story Steel Structure Using System Identification and Shaking Table Experiments", Report No. EERC 76-20, University of California, Berkeley, August 1976.
2. Kaya, I., McNiven, H. D., "Investigation of the Elastic Characteristics of a Three Story Steel Frame Using System Identification", Report No. UC/EERC 78/24, University of California, Berkeley, November 1978.
3. Yanev, B. S., McNiven, H.D., "Mathematical Modelling of the Seismic Response of a One Story Steel Frame With Infill Partitions", Third Canadian Conference on Earthquake Engineering, June 1979, Tome 2, pp. 829-846.
4. Yanev, B. S., McNiven, H.D., "Nonlinear Structural Response to Earthquakes Investigated by System Identification", Seventh Canadian Congress of Applied Mechanics, Sherbrooke, May 27 - June 1, 1979, pp. 405-406.
5. Flugge, W., "Viscoelasticity", Springer-Verlag, New York, Heidelberg, Berlin, 1975.



Table 1. Models of an Oscillating System.

	1	2	3	4
Model				
Viscoelastic Equation	$\sigma + \frac{C}{K} \dot{\sigma} = C \dot{\epsilon}$	$\sigma = K \epsilon + C \dot{\epsilon}$	$\sigma + \frac{C_2}{K_2} \dot{\sigma} =$ $= K_1 \epsilon + (C_1 + C_2 (1 + \frac{K_1}{K_2})) \dot{\epsilon} +$ $+ \frac{C_1 C_2}{K_2} \ddot{\epsilon}$	$\sigma + (\frac{C_1}{K_1} + \frac{C_2}{K_2} + \frac{C_2}{K_1}) \dot{\sigma} +$ $+ \frac{C_1 C_2}{K_1 K_2} \ddot{\sigma} =$ $= C_2 \dot{\epsilon} + \frac{C_1 C_2}{K_1} \ddot{\epsilon}$
Structural Analogy	$-M \ddot{x}_{abs} =$ $-\frac{MC}{K} \ddot{x}_{abs} =$ $= C \dot{x}$	$-M \ddot{x}_{abs} =$ $= Kx + C \dot{x}$	$-M \ddot{x}_{abs} - \frac{C_2}{K_2} \dot{x}_{abs} =$ $= K_1 x + (C_1 + C_2 (1 + \frac{K_1}{K_2})) \dot{x} +$ $+ \frac{C_1 C_2}{K_2} \ddot{x}$	$-M \ddot{x}_{abs} - M(\frac{C_1}{K_1} + \frac{C_2}{K_2} + \frac{C_2}{K_1}) \dot{x}_{abs} -$ $\frac{C_1 C_2}{K_1 K_2} x_{abs} =$ $= C_2 \dot{x} + \frac{C_1 C_2}{K_1} \ddot{x}$
Reduced Order	$A - M \ddot{x}_{abs} =$ $= K(x + \frac{M}{C} \dot{x}_{abs})$	-	-	$A - M \frac{K_1}{C_2} \dot{x}_{abs} - M \frac{C_1}{K_2} \ddot{x}_{abs} -$ $- M(1 + \frac{C_1}{C_2} + \frac{K_1}{K_2}) \dot{x}_{abs} =$ $= K_1 x + C_1 \dot{x}$
$\infty$ $K_2$	-	-	$-M \ddot{x}_{abs} =$ $= K_1 x + (C_1 + C_2) \dot{x}$	$A - M \frac{K_1}{C_2} \dot{x}_{abs} -$ $- M(1 + \frac{C_1}{C_2}) \ddot{x}_{abs} =$ $= K_1 x + C_1 \dot{x}$
$\infty$ $C_2$	-	-	$A - M \ddot{x}_{abs} =$ $= (K_1 + K_2) x + C_1 \dot{x}$	$A - M(1 + \frac{K_1}{K_2}) \ddot{x}_{abs} -$ $- M \frac{C_1}{K_2} \dot{x}_{abs} =$ $= K_1 x + C_1 \dot{x}$
$\infty$ $K_2, C_2$	-	-	Rigid Body	$A - M \ddot{x}_{abs} = K_1 x + C_1 \dot{x}$



RELATIVE DISPLACEMENT OF PLATFORM (IN)  
Figure 1. 'Pseudo' Response of a Partitioned Single Story Steel Frame

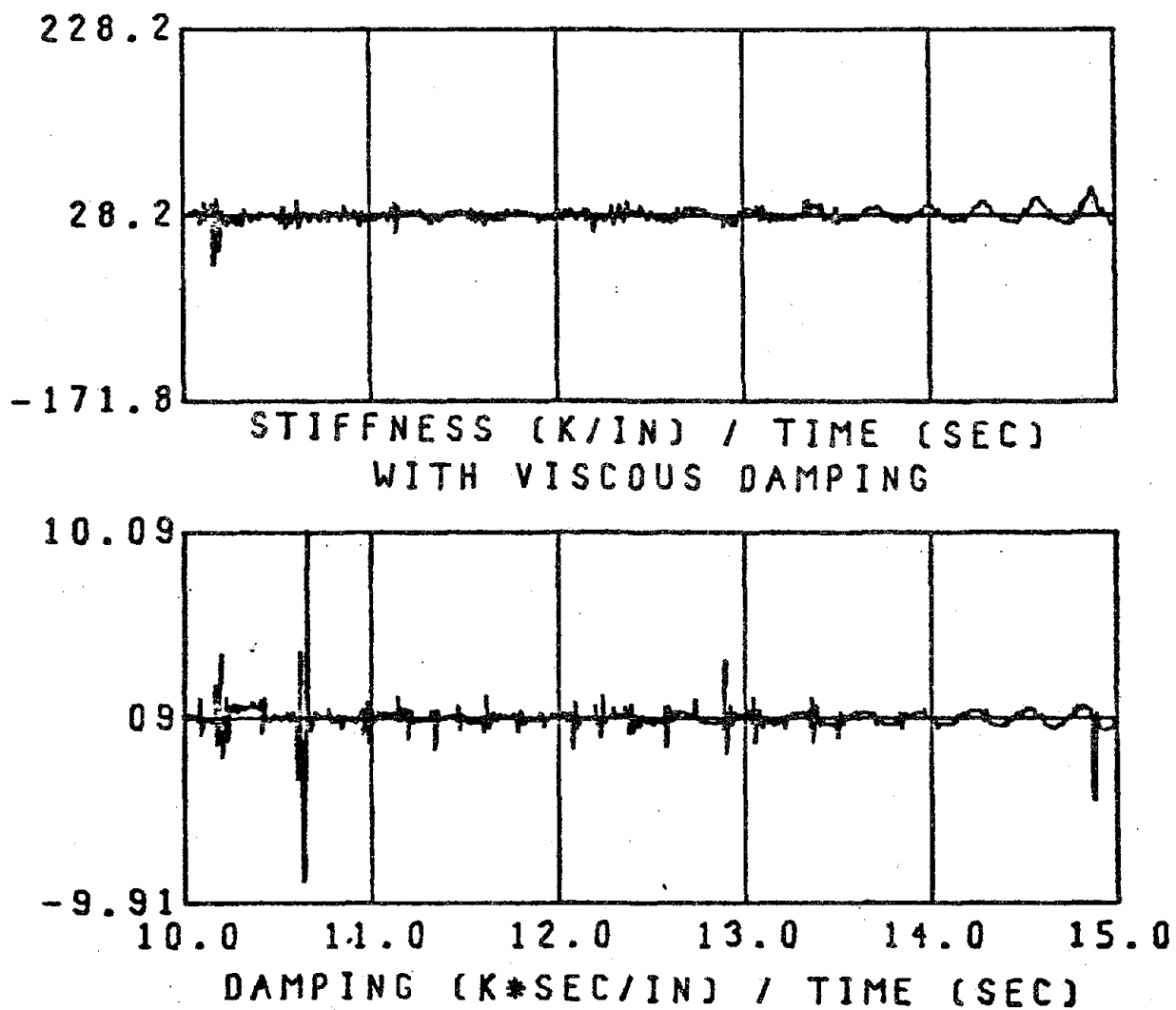


Figure 2.  $C_1$  and  $K_1$  Directly Obtained From the Experiment of  
Figure 1.

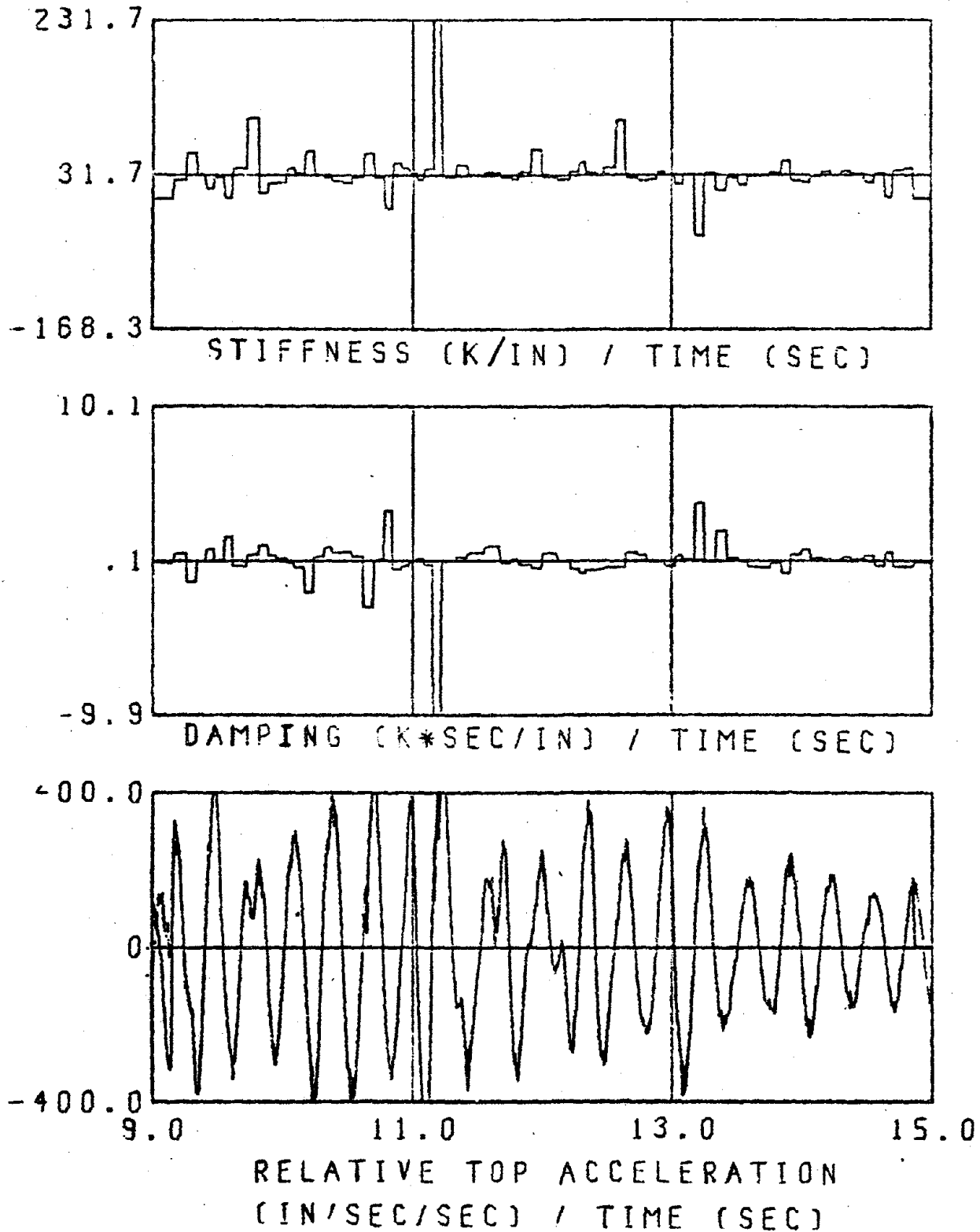


Figure 3.  $C_1, C_2, K_1, K_2$  obtained by Identification Over Individual Cycles of Motion.

--- measured acceleration  
 ——— simulated acceleration

LINEAR MATHEMATICAL MODELS TO PREDICT THE SEISMIC  
RESPONSE OF A THREE-STORY STEEL FRAME

by

Hugh D. McNiven<sup>I</sup> and Izak Kaya<sup>II</sup>

SUMMARY

Mathematical models are constructed to predict the linear seismic response of a three-story steel frame using system identification. The experimental data used are from tests performed on a shaking table by Clough and Tang. The models accommodate both floor translations and joint rotations and they predict the time histories of these responses with exceptional accuracy.

INTRODUCTION

In this study we construct mathematical models, using system identification, to predict the linear seismic response of a three-story steel frame. As the models are linear, many will no doubt feel that models presently in use are adequate. We show in what follows that this is not so.

In earlier studies using system identification for constructing mathematical models to predict seismic response, such as McNiven and Matzen [1], we have argued that the major value of system identification is derived from the fact that using it enables one to appraise the form of the model. This is not its value here. In this study we have accepted the usual form for a set of simultaneous, linear differential equations. System identification has been invaluable, however, in arriving at sets of parameters which, when introduced into a set of equations, give models that predict accurately the seismic response of the frame.

There is no such thing as a single mathematical model for a physical frame. There are large numbers of models of different orders of complexity. The job of the person constructing the models is to ensure that each model of a particular order is the best possible of all models of that order. The order of a model, reflected in the number of parameters involved, derives from the number of degrees of freedom which the model accommodates. In this paper we construct only an eight parameter model accommodating six degrees of freedom. A nine parameter model is constructed only to gain physical insight into the behavior of the frame.

System identification needs experimental response data. We are fortunate in having an excellent set of data from experiments performed in 1975 on the shaking table at the Earthquake Engineering Research Center of the University of California, Berkeley, and reported by Clough and Tang [2]. The frame, the experiments performed on it; and the test results are described briefly in the paper.

The eight and nine parameter models predict response quantities that match all of the experimental responses with exceptional accuracy. We learn

---

<sup>I</sup> Professor of Engineering Science, Univ. of Calif., Berkeley, Calif. 94720.

<sup>II</sup> Professor of Civil Engineering, University of Ismir, Turkey.

what it is about the engineering of the frame that must be understood in formulating the models and what constitutes complete data for a model of a particular order. We find that each response quantity in that data must impose a constraint on the structure independent of all of the others.

In the interest of brevity, we do not describe system identification as we used it, nor the problems encountered in the numerical analysis. We refer for a detailed account to a report by Kaya and McNiven [4].

### THE TEST STRUCTURE

Details of the test structure are shown in Fig. 1. It is sufficient here to note that the frame is forced in a direction parallel to its major

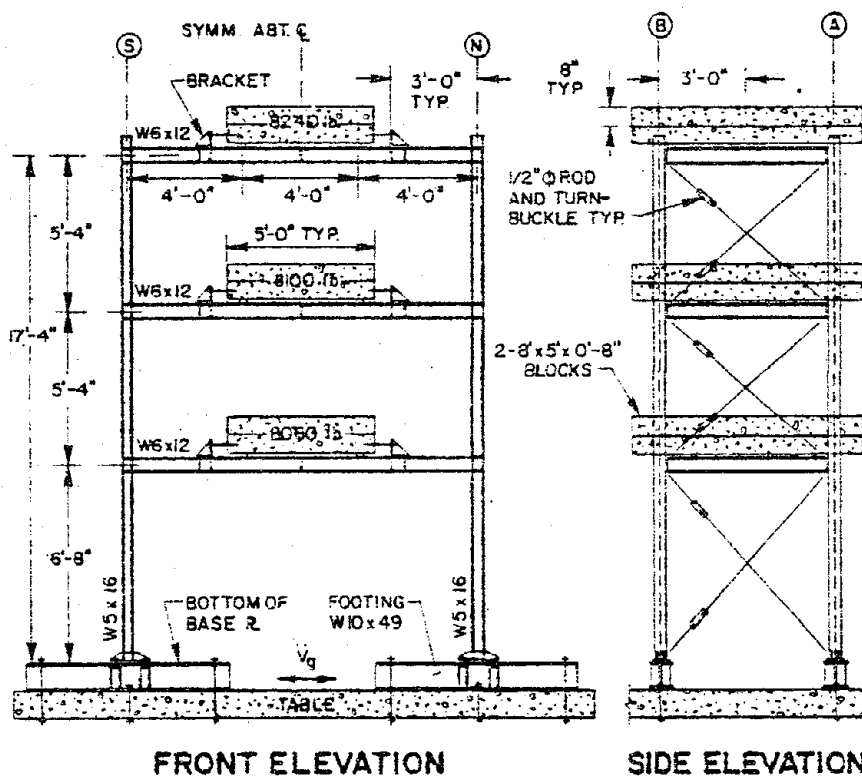


FIGURE 1: ELEVATIONS OF TEST STRUCTURE

axis and that response data are the time histories of the floor accelerations, displacements and strains close to the ends of the members.

### AN EIGHT PARAMETER MODEL

The form of the model consists of the usual set of equations appropriate to a multistory frame:

$$\begin{aligned}
 [M] \{\ddot{u}\} + [C] \{\dot{u}\} + [K] \{u\} &= -[M] \{I\} \ddot{u}_g \\
 \{\dot{u}\}_0 &= \{u\}_0 = \{0\}
 \end{aligned}
 \tag{1}$$

where  $[M]$  is the mass matrix and  $[C]$  and  $[K]$  are the damping and stiffness matrices for the structure.  $\{I\}$  is a unit vector;  $\ddot{u}_g$  is the base acceleration and  $\{u\}$ ,  $\{\dot{u}\}$  and  $\{\ddot{u}\}$  are vectors for relative nodal displacement, velocity and acceleration, respectively.

The mass of the structure is assumed to be lumped at the nodal points, so that  $[M]$  is a diagonal matrix, taken here to be constant. The damping is taken in the form

$$[C] = A_0 [M] + A_1 [K].$$

We assume a stiffness matrix that will accommodate six degrees of freedom, three translational and three rotational. Examination of the frame leads us to anticipate that the joints will in fact rotate. As the frame is symmetrical, the joint rotations on each end of a girder will be the same.

Construction of the stiffness matrix begins by writing the complete 6 x 6 matrix.

$$\begin{Bmatrix} \bar{M} \\ \bar{P} \end{Bmatrix} = \begin{bmatrix} [K_{11}] & [K_{12}] \\ [K_{21}] & [K_{22}] \end{bmatrix} \begin{Bmatrix} \bar{\omega} \\ \bar{\Delta} \end{Bmatrix} \quad (2)$$

where  $\bar{M}$  and  $\bar{P}$  are external joint moments and forces while  $\bar{\omega}$  and  $\bar{\Delta}$  are the rotations and displacements of the joints.

For our frame there are no external moments at the joints, so

$$\{\bar{M}\} = \{0\}. \quad (3)$$

This circumstance allows for the condensation of the 6 x 6 matrix into a 3 x 3, giving the reduced equation

$$\{\bar{P}\} = [\bar{K}] \{\bar{\Delta}\} \quad (4)$$

where 
$$[\bar{K}] = [-[K_{21}] [K_{11}]^{-1} [K_{12}] + [K_{22}]] \quad (5)$$

Resulting from the condensation is the equation

$$\{\bar{\omega}\} = - [K_{11}]^{-1} [K_{12}] \{\bar{\Delta}\}. \quad (6)$$

This relationship will turn out to be of major significance in what follows and we will return to it in the appropriate context.

The form of the model is now complete, but before continuing the system identification we must introduce eight parameters into the model and assume initial values of all of the quantities that are candidates for optimization. As the stiffness matrix is symmetrical, we assign one parameter to each independent element and evaluate each of the elements using Eq. (5) and the E, I and L for each member where L is the center to center distance. The stiffness matrix resulting is

$$[K] = \begin{bmatrix} \beta_1 \times 23.15 & -\beta_2 \times 33.10 & \beta_3 \times 11.52 \\ -\beta_2 \times 33.10 & \beta_4 \times 71.89 & -\beta_5 \times 49.64 \\ \beta_3 \times 11.52 & -\beta_5 \times 49.64 & \beta_6 \times 69.48 \end{bmatrix} \quad (7)$$

The remaining two parameters are associated with  $A_0$  and  $A_1$  whose initial values we found appropriate for a five parameter model of the same frame. The damping components are

$$A_0 = \beta_7 \times 0.2340 \text{ and } A_1 = \beta_8 \times 0.0003.$$

We begin with the parameter vector  $\beta_1 = \langle 1 \ 1 \ 1 \ 1 \ 1 \ 1 \ 1 \ 1 \rangle$  so that our initial model corresponds to existing practice. The ability to predict response of this model can be seen in Fig. (2) designated "before optimization". Examination of the figure shows that it models the frame poorly.

The response quantities we use in the cost function are the floor accelerations and displacements of Frame II to the El Centro, Span 400. Even though the duration of the disturbance is about eleven seconds, we use only the first six seconds to reduce the cost of optimization. This first six seconds contains the "rich" part of the input and trial showed that the values of the parameters obtained using only the first six seconds change only slightly when the full duration is used.

For optimization of the parameters we use the Modified Gauss-Newton algorithm which is described in [1].

The final values of the parameters are  $\langle 1.147, 1.175, 1.080, 1.131, 1.024, .998, .575, .607 \rangle$ . The ability of the initial model and the model after optimization are shown in Fig. [2] comparing response time histories for the MEC 600. The improvement is significant and the predicted responses for the improved model matched the experimental so closely that at this stage we felt that the model was complete.

One thing, however, still bothered us. Examination of final values of the parameters shows that during optimization the stiffness parameters change by as much as 18% and the damping parameters even more. We wanted to know, if possible, the physical reason that would account for this significant adjustment. This uneasiness led to the formulation of a second eight parameter model.

#### SECOND EIGHT-PARAMETER MODEL

The first impulse in trying to account physically for the significant change in the parameters, was to try to trace backwards the relationship between the parameters and the individual members of the frame, where the physical significance would be found. It quickly became apparent that, because the condensation of the stiffness matrix cannot be reversed, physical insight would be gained only by constructing an entirely new model in which the parameters are introduced in association with each individual member of the frame.

The stiffness of each member is derived from its E, I and L and we felt that of the three, the L is the most vulnerable to change during optimization, so that we associated a new parameter  $\delta_i$  ( $i = 1-6$ ) with each L, one with each column and each girder. The 6 x 6 matrix was formulated as before, condensed as before giving a new 3 x 3 stiffness matrix in which the  $\delta$ 's appear in each element in a somewhat complicated way. The damping parameters were taken in the same form as the first eight parameter model with  $\delta_7$  and  $\delta_8$  replacing  $\beta_7$  and  $\beta_8$ .

Using the floor accelerations and displacements in the cost function, optimization was begun with the new model, and to our surprise the iterative process did not converge. After a fruitless search for errors, we sought mathematical and physical reasons for the lack of convergence. We had



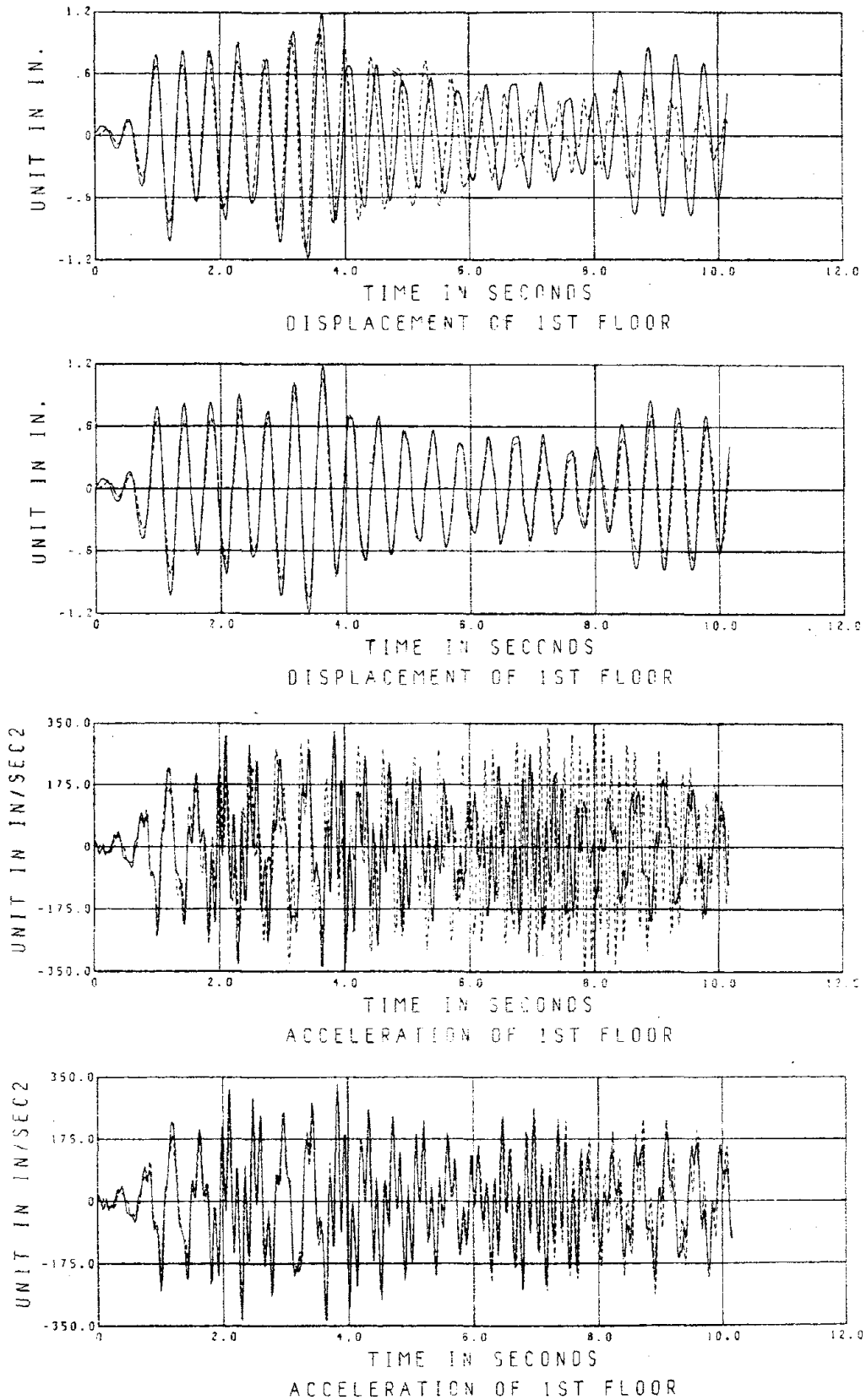


FIGURE 2: MEC 600-II COMPARISON OF MEASURED AND COMPUTED RESPONSE TIME HISTORIES BEFORE AND AFTER OPTIMIZATION OF PARAMETERS (FIRST EIGHT PARAMETER MODEL)

already noted for the first eight parameter model that the same set of values were obtained if in the cost function we used only the acceleration or only the displacements. We concluded from this that they are not independent response quantities perhaps accounting for the lack of convergence.

We recognized that we had strain gage readings on the columns and by using the moments derived from these and moment area we could calculate the joint rotation. Here we recall, however, that due to the absence of external joint moments, the joint rotations are linearly related to the floor displacements. This relationship depends on two assumptions, first that the deformations are elastic, which is applicable here, but also that there is perfect continuity between beams and columns, which might not be applicable to our frame. Feeling that this last point was worth pursuing, we introduced the three joint rotations and the three floor accelerations into the cost function. To our gratification convergence was as rapid as it was in the first eight parameter model.

With the new set of parameters, the second eight parameter model was complete and we were pleased that the model predicts very accurately both the floor translation time histories and the time histories of the joint rotations. This is displayed in Fig. [3].

However, as we were anxious to gain physical insight into the improvement and as the set of parameters gives an effective length for each of the members, it bore close scrutiny. As the effective lengths for the columns were about five percent less than the center to center distances we thought this was reasonable and accounted for the improvement in matching, but the effective lengths of the girders turned out to be about twenty percent longer than their geometric length which was not. We reasoned that the girders were trying to account for vertical motion that they were not in fact responsible for.

At this stage we benefited from work done by Tang [3] in formulating a model of the same frame. Tang found that his model was improved by accounting for the rigid body pitching of the shaking table during excitation. We decided therefore to formulate one more model including the possible pitching, not particularly to improve the ability to predict response time histories, but to see if the effective lengths of the girders would adjust to reasonable values.

#### THE NINE PARAMETER MODEL

Pitching of the shaking table is accounted for by introducing a ninth parameter  $\delta_g$  associated with the rigid body rotational stiffness ( $k$ ) of the shaking table and letting  $k = \delta_g \times 100^k/\text{in.}$  and taking  $\delta_g = 1$  as the initial value. When the model was completed, it predicted responses little better than the final eight parameter model. However, it showed  $\delta_g = 1.845$  indicating that the table probably does pitch and it lowered the effective length parameters for the girders to about 1.10, a more sensible value.

Both the fact that joint rotations and floor translations are independent response quantities, and that the model is significantly improved by using effective rather than geometric member lengths, indicate that there is

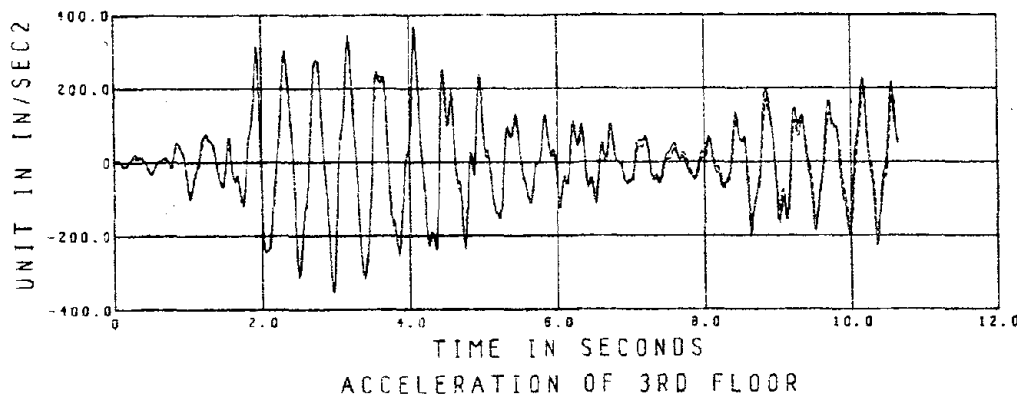
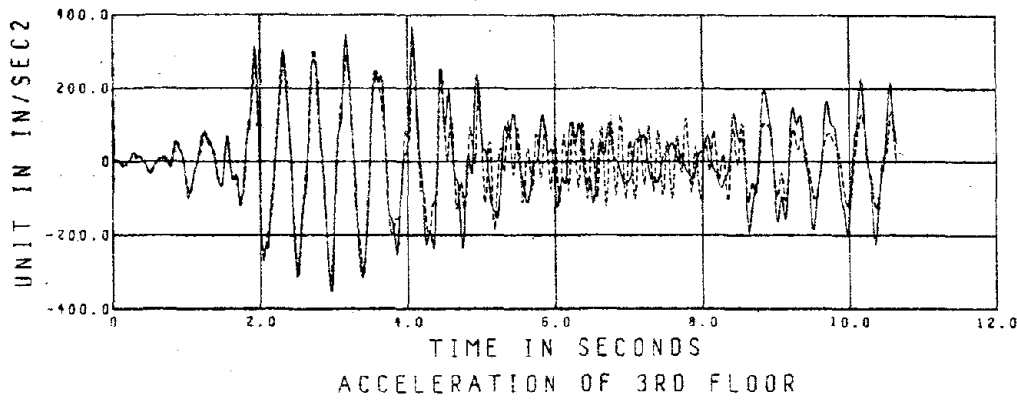
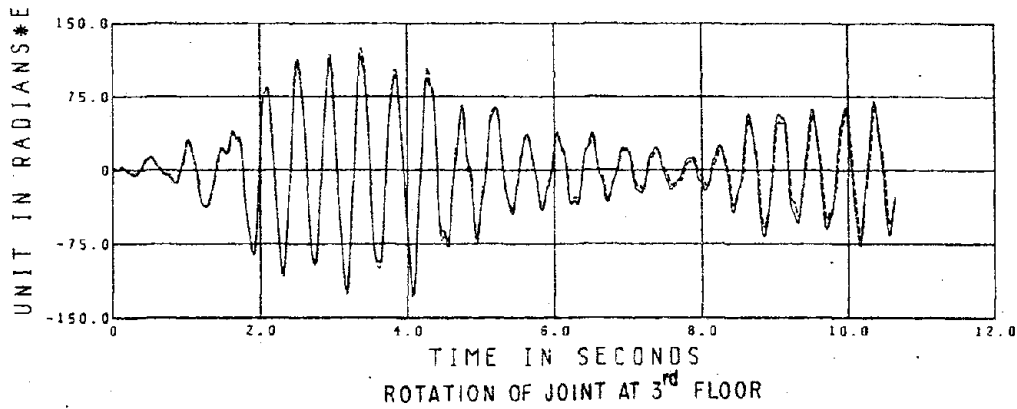
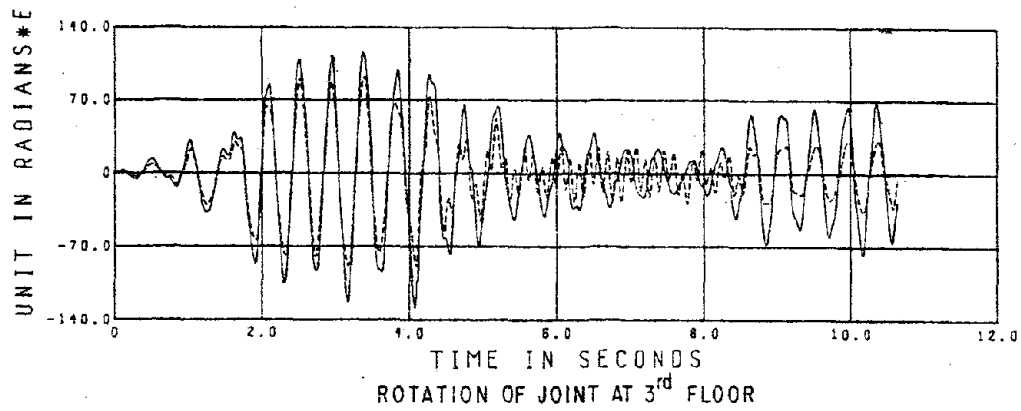


FIGURE 3: EC 400-II COMPARISON OF MEASURED AND COMPUTED RESPONSE TIME HISTORIES BEFORE AND AFTER OPTIMIZATION OF PARAMETERS (SECOND EIGHT PARAMETER MODEL)

not perfect continuity between columns and girders, that the panels at the joints do in fact deform.

We are fortunate in that the testing program allows us to substantiate this conclusion. When the frame was first tested linearly and the response quantities recorded, the joint panels were stiffened and the altered frame was tested and its response data recorded. We formulated nine parameter models based first on the response data of the first frame, and another based on the data from the stiffened frame. For the stiffened frame the effective length factors are closer to 1.0 than those of the first frame.

#### REFERENCES

1. Hugh D. McNiven and Vernon C. Matzen, "A Mathematical Model to Predict the Inelastic Response of a Steel Frame: Formulation of the Model," Earthquake Engineering and Structural Dynamics, Vol. 6, 189-202 (1978).
2. R. W. Clough and D. T. Tang, "Earthquake Simulator Study of a Steel Frame Structure, Vol. I: Experimental Results," Report No. EERC 75-6, Earthquake Engineering Research Center, University of California, Berkeley (1975).
3. D. T. Tang, "Earthquake Simulator Study of a Steel Frame Structure, Vol. II: Analytical Results," Report No. EERC 75-36, Earthquake Engineering Research Center, University of California, Berkeley (1975).
4. I. Kaya and H. D. McNiven, "Investigation of the Elastic Characteristics of a Three Story Steel Frame Using System Identification," Report No. EERC 78-24, Earthquake Engineering Research Center, University of California, Berkeley (1978).

#### ACKNOWLEDGEMENT

The research described in this paper was supported by a research grant from the National Science Foundation to the University of California at Berkeley. The support is gratefully acknowledged.

## SEISMIC BEHAVIOR OF R/C WALL STRUCTURAL SYSTEMS

Vitelmo V. Bertero<sup>I</sup>

## SUMMARY

The state-of-the-practice in the design and construction of R/C ductile moment-resistant space frame buildings is compared with that of shear wall buildings, and it is concluded that frame-coupled wall systems offer great potential for seismic-resistant building construction. Experimental and analytical research results on seismic behavior of isolated walls and coupling girders indicate excellent hysteretic behavior. Problems in designing coupled wall systems are examined. Recommendations are formulated for research to realize the great potential of these systems.

## INTRODUCTION

General Remarks. Analysis of the 1976 UBC [1] shows that, of buildings having the same dynamic characteristics, those with shear walls must be designed for seismic forces about 20% to 100% higher than those having ductile moment-resisting space frames (DMRSF). Furthermore, the UBC design provisions for the shear walls against shear are inconsistent with the philosophy of the design for shear of members of DMRSF. As a consequence of the excellent performance of shear wall structures in recent destructive earthquakes, the following questions have been raised: Is there any new information to justify the modifications of these high seismic forces and the apparent inconsistency in requirements for shear design? Also, can a building whose structural system is based on use of walls be designed with the same distribution of inertial forces along its height as a building whose structural system is a DMRSF, as specified in the present UBC? These questions were the motives for an investigation that began several years ago at Berkeley [2,3,4] with the ultimate objectives described below and which motivated this paper.

Objectives. The ultimate objective of the investigation being conducted at Berkeley is to develop practical methods for the seismic design of combined wall-frame structural systems. The specific objectives of this paper are to summarize the state-of-the-practice and state-of-the-art in predicting seismic behavior and in the design and construction of R/C structural wall systems, to ascertain whether there is sufficient data to recommend modifications in current practice, to analyze problems that still remain without satisfactory solutions, and to formulate research needs to solve them.

## STATE-OF-THE-PRACTICE OF SEISMIC-RESISTANT DESIGN OF SHEAR-WALL SYSTEMS

Introductory Remarks. To recognize problems that are still present in the design of seismic-resistant buildings having shear wall structural systems in comparison with the design of DMRSF buildings, it is convenient to analyze all the main steps that are involved in trying to satisfy the basic design equation, i.e., the DEMAND (on stiffness, strength, stability, durability, ductility, and energy absorption and energy dissipation capacity) shall be exceeded by the SUPPLY.

Estimation of Demands. It has been shown [5-8] that the major uncertainties in the whole design process are involved in this estimation, usually

<sup>I</sup>Professor of Civil Engineering, University of California, Berkeley.

conducted through numerical analysis, due to the difficulties in predicting what the critical seismic loading would be during the service life of the structure (proper establishment of design earthquakes) and the state of the building when the critical seismic ground motion at the site of the building occurs (proper selection of the building model that should be analyzed).

1. Seismic Loading. Present seismic code [1] defines this loading by specifying the value of the total lateral force or shear at the base,  $V$ , and its distribution over the height of the building. According to this code, shear wall buildings must be designed for a total  $V$  20% to 100% higher than a DMRSF building having the same fundamental period of vibration,  $T$ . Why are R/C wall structural systems penalized? Usually it is claimed that R/C walls lack ductility. As will be shown later, properly designed and constructed R/C walls can develop large ductility and, even more importantly, dissipate large amounts of energy through stable hysteretic behavior. Furthermore, since the modeling of a building having as a structural system a proper layout of walls (particularly coupled walls) offers considerably less uncertainty than a DMRSF building (due largely to the sensitivity of the latter to the interacting effects of the nonstructural elements), it seems illogical to require that a properly designed R/C wall building be designed for higher loads than DMRSF buildings. The ATC [9] recognizes, through a response modification coefficient  $R$ , that properly designed and constructed walls can dissipate more energy than a DMRSF. While for an R/C special moment frame, which is a DMRSF,  $R$  is specified as 7, for a dual system based on use of R/C shear walls,  $R$  is 8, i.e., the seismic forces for which it should be designed are about 15% less than those of the DMRSF having the same dynamic characteristics. Regarding the distribution of the lateral force over the height of the structure, the UBC [1] specifies just one set of formulas for all buildings no matter what structural system is used. While the code distribution appears justified for those types of structures in which the effects of moments (overturning moment) are controlling the design, it does not seem to be a conservative pattern for cases in which shear can be a problem, as it is in the case of R/C walls.

2. Modeling. A design can only be effective if it can be constructed, i.e., the model used for conducting the estimation of the demands in the design process should be realistic. An analysis of the uncertainties that exist in developing realistic models for a R/C DMRSF vs. a R/C shear wall building indicates that the uncertainties involved in the first are larger than in the second. The main reasons follow: (1) Effect of Higher Modes and Inelastic Moment Redistribution on Actual Response of a Building--The design and construction of a DMRSF building is based on the philosophy of strong columns-weak girders. Column hinging should be allowed at the base of the bottom columns only after all the girders' plastic hinges have been developed (Fig. 1a). Although this requirement can be satisfied by designing the columns to have a flexural strength larger than that required at the joint considering the ultimate flexural capacity of the girders (as it is specified in the codes), in reality due to effects of higher modes and unequal distribution of beam input moments at a joint between the column above and below the joint, early and significant column hinging can develop. To avoid this, Paulay in Ref. 5 has suggested that columns be designed to resist the moment computed according to the girder capacity by a dynamic moment magnification factor which is a function of the computed fundamental period,  $T$ , and can vary from 1.2 to 1.8. It is obvious, then, that while the actual behavior of a DMRSF can lead to early formation of column hinging, this could not happen in coupled wall systems, since the walls act as a column having a flexural strength considerably higher than that of the

girders. Thus, the development of inelastic deformation at the girder can be controlled with higher reliability in coupled wall structural systems than in DMRSF systems. (2) Effect of Nonstructural Elements. The seismic response of DMRSF systems is considerably more sensitive to the effects of nonstructural elements than wall systems. The effects can be grouped in two categories: (a) walls, partitions, stairways, etc. can considerably change the dynamic characteristics of the whole DMRSF system, particularly increasing the fundamental period and modifying the torsional response of the building; and (b) these walls, partitions, stairways, etc. can create "soft story" and/or "short columns and/or girders" in the DMRSF, as illustrated in Fig. 1. The effect of such nonstructural elements will be considerably less in the case of coupled wall structural systems.

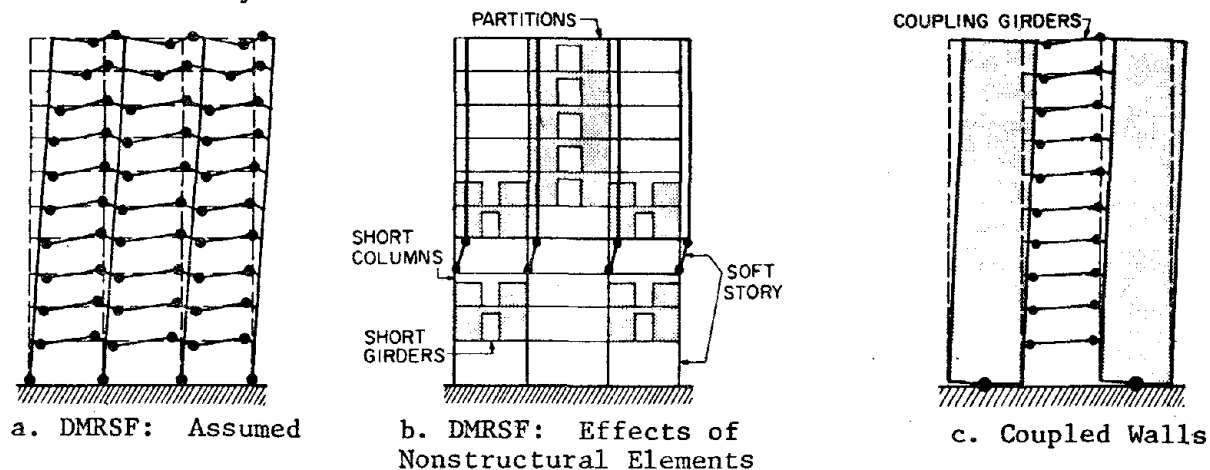


FIG. 1. COMPARISON OF BEHAVIOR OF DMRSF AND COUPLED WALLS

Concluding Remarks. Use of coupled walls in seismic-resistant design seems to have great potential. To realize this potential it would be necessary to prove that it is possible to design and construct "ductile coupling girders" and "ductile walls" that can SUPPLY the required strength, stiffness, and stability and dissipate significant amounts of energy through stable hysteretic behavior of their critical regions. A review of present knowledge in these matters is presented below.

#### STATE-OF-THE-ART OF SEISMIC BEHAVIOR OF SHEAR-WALL SYSTEMS

Introductory Remarks. The state-of-the-art in seismic behavior of shear-wall structural systems in several countries, particularly Japan, New Zealand and the U.S., up to 1977 has been discussed in detail in Ref. 5. The experimental and analytical studies presented in this reference, as well as those studies carried on to date, have been reviewed by the author in light of the previous discussion, i.e., to ascertain whether it is possible to design and construct shear walls and coupling girders with sufficient energy dissipation capacity to permit the construction of efficient seismic-resistant frame-coupled wall structural systems. The main observations obtained from this review follow.

Isolated Walls. The behavior of walls under loading histories simulating those that can develop during the response of a shear wall building to severe seismic ground motions has recently been extensively studied, experimentally and analytically, particularly at the laboratories of the Portland Cement Association (PCA) [10] and of the University of California, Berkeley [2-4]. A total of 34 experiments have been conducted (16 at PCA and 18 at Berkeley) to study the effects of several parameters on the hysteretic behavior of these walls. A brief discussion of the effects of some of these parameters follows.

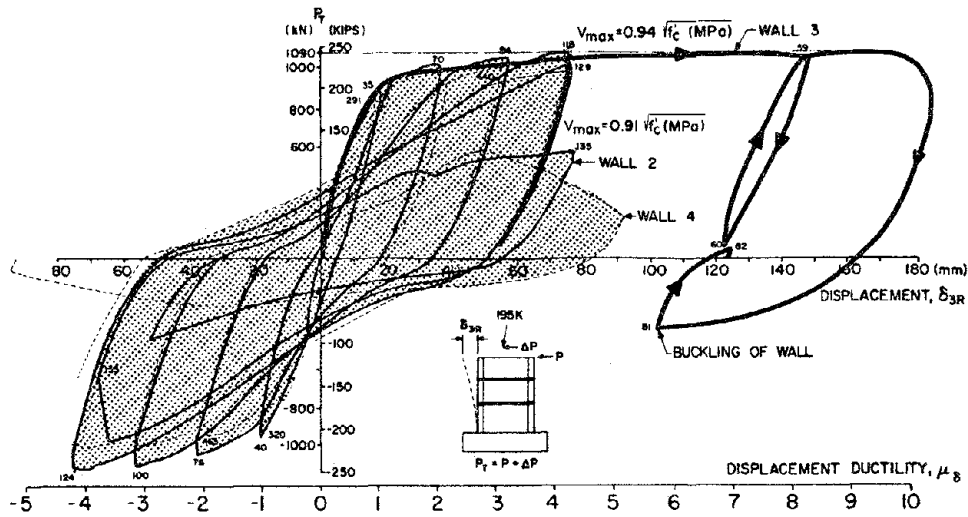


FIG. 2. R/C WALLS: COMPARISON OF BEHAVIOR UNDER MONOTONICALLY INCREASING LOADING (WALL 3) WITH HYSTERETIC BEHAVIOR UNDER INCREASING DISPLACEMENT REVERSALS (WALLS 2 AND 4).

1. Loading History. A larger displacement ductility is obtained when the wall is subjected to monotonically increasing lateral load. As can be seen in Fig. 2, before any significant reduction in strength was observed (1090 KN), wall 3 deformed up to nearly 180 mm, giving a displacement ductility,  $\mu_{\delta}$ , of 10 (the  $\mu_{\delta}$  of the first story was 14). However, when the load was reversed, the wall buckled under a lateral load of only 356 KN. Therefore, this large displacement ductility cannot be used for seismic-resistant design. Stability under load reversal can control the maximum ductility that can be used. The main effects of cyclic loading inducing reversals of loads are to reduce the  $\mu_{\delta}$  and originate a degradation in the initial stiffness (pinching of the hysteretic loops). The larger the deformation reversals, the larger the reductions. For example, cycling under full deformation reversals reduces the  $\mu_{\delta}$  from 10 to about 4 (which corresponds to a cyclic ductility ratio of about 7), and the initial stiffness during reloading is reduced so drastically that the energy dissipated in one cycle is only about 50% of that which will result if the hysteretic loop is that of an elasto-perfectly plastic type. However, in spite of these reductions, the total amount of energy dissipated by walls 2 and 4, which were subjected to cyclic loading with full deformation reversals, was more than three times that dissipated by the walls subjected to monotonically increasing loads, i.e., wall 3, Fig. 2. Furthermore, at the reduced  $\mu_{\delta} = 4$  and after the wall panel failed completely, the edge members of the barbell cross-section walls remained sound and capable of resisting the effects of the axial forces imposed by the gravity loads combined with the effect of lateral loads at working load level.

2. Cross-Section Type: Barbell vs. Rectangular. Figures 3 and 4 compare the behavior of these two types of cross sections under monotonic and cyclic loading. The better behavior of the barbell is clear from these figures. The main reason is the earlier lateral buckling of the rectangular with respect to the barbell, due to the smaller thickness of the rectangular wall (114 mm) with respect to the thickness of the barbell edge member (254 mm). Spalling of the concrete cover in the rectangular wall results in a 48% reduction in the out-of-plane stiffness, leading to its failure by out-of-plane buckling.

3. Edge Member Confinement. Three different types of lateral reinforcement



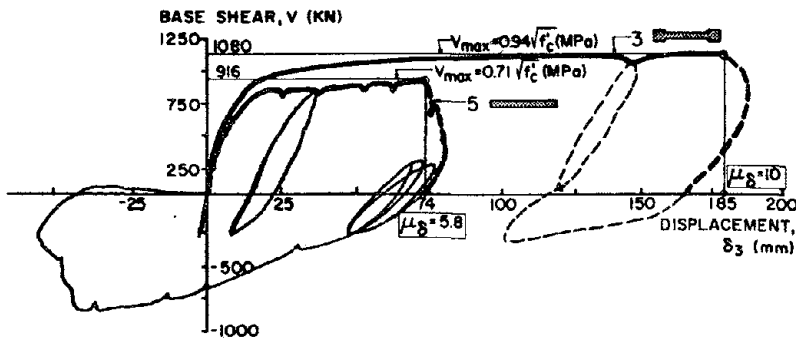


FIG. 3. BARBELL VS. RECTANGULAR CROSS-SECTION WALLS: COMPARISON OF BEHAVIOR UNDER MONOTONICALLY INCREASING LOAD

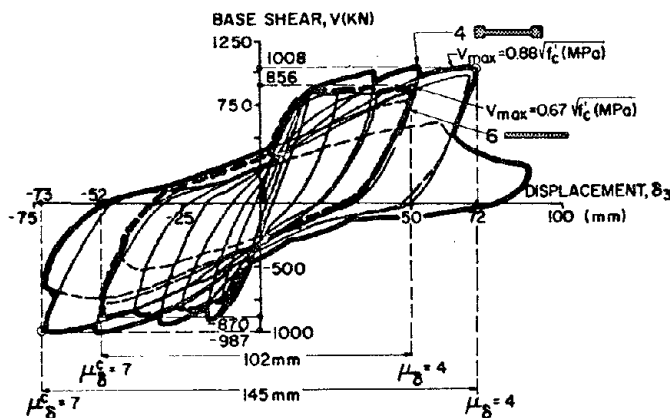


FIG. 4. BARBELL VS. RECTANGULAR CROSS-SECTION WALLS: COMPARISON OF BEHAVIOR UNDER CYCLIC LOADING

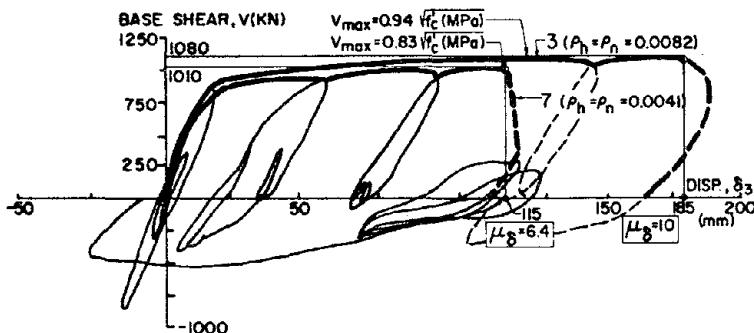


FIG. 5. BARBELL CROSS-SECTION WALLS: EFFECT OF AMOUNT OF WALL-PANEL REINFORCEMENT

were studied: (1) circular spiral; (2) square ties; and (3) rectangular ties. Confinement and overall behavior of the edge members where spiral and square ties were used were better than that obtained with rectangular ties. Protection against buckling of the longitudinal reinforcement offered by the rectangular ties was less effective than that offered by the square ties; the best protection was that offered by the spiral.

4. Wall Reinforcement: Amount and Arrangement. *Amount,  $\rho$ :* The strength capacity is practically unaffected by the amount of wall reinforcement (Fig. 5). The larger the amount and particularly the closer the spacing of the wall panel reinforcement, the more ductile the behavior. However, the degree of improvement is not in direct proportion to  $\rho$  but is significantly smaller. The plots of Fig. 5 illustrate these observations, although it should be noted that wall 7 was submitted to a series of cycles with full deformation at yielding level which could affect (decrease) the actual  $\mu_\delta$  under monotonically increasing loads [4]. *Arrangement:* Diagonal arrangement of the reinforcement (i.e., inclined at  $45^\circ$ ) results in better behavior than the vertical and horizontal reinforcing bar arrangement (Fig. 6).

5. Shear Stress,  $v$ . The nominal shear stress,  $v$ , is usually computed as  $V/hd$ ,

where  $h$  is the thickness of the wall panel and  $d$  is the effective depth between the extreme compression fiber and the centroid of the rebars in tension. Code requirements allow use of the value  $0.8 \ell_w$  as  $d$ , where  $\ell_w$  is the total length of the wall. Using this last value, the  $v_{max}$  in the tests carried out by the PCA varied from  $0.12$  to  $1.15\sqrt{f'_c}$  (MPa). On the other hand, during the 18 tests conducted at Berkeley, this value ranged from  $0.71$  to  $1.12\sqrt{f'_c}$  (MPa). Analyses of

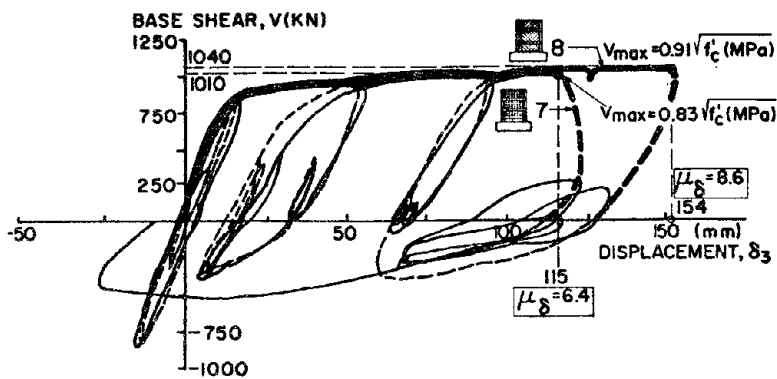


FIG. 6. BARBELL CROSS-SECTION WALLS: EFFECT OF WALL-PANEL REINFORCEMENT ARRANGEMENT

these results indicate that for similar walls the smaller the value of  $v_{max}$ , the better the overall behavior under monotonically, and particularly under cyclic, loading with full deformation reversals. Barbell cross-section can resist lateral loading inducing higher  $v$  than the rectangular one, and still results in significantly better overall behavior (see Figs. 3 and 4), emphasizing the importance of providing well-confined edge members.

6. Axial Load,  $N$ . The value of  $N$  significantly affects the stiffness, strength, ductility and energy dissipation capacity of the walls, the presence of moderate compression being highly beneficial.

7. Construction Joints. Concrete and complete concrete and steel construction joints performed satisfactorily, although lap splicing of the reinforcement did not satisfy minimum code requirements and it was located in critical regions which were subjected to  $v_{max} = 1.08\sqrt{f'_c}$  (MPa).

8. Flexibility at the Construction Joints. The more flexible the foundation, the closer to it failure of the wall panel begins. However, this change did not affect either the strength or deformation capacity of the isolated wall. Further experimental studies should be conducted to determine how much flexibility is required to induce any significant effects. Recent studies [11] indicate that the flexibility, as well as any movement, of the foundation can have very important effects on the overall response. Rocking of the foundation of each wall of a coupled wall system can increase significantly the inelastic rotation demands on the coupling girders [11].

From the above observations, it becomes clear that, if barbell cross-section walls are proportioned and detailed according to present UBC seismic provisions, they can be very "ductile" and dissipate sufficient energy through stable hysteretic loops to survive the demands of extreme earthquake ground shakings. This holds true even if they are subjected to shear forces above those presently permitted by code, i.e.,  $V_{max} = \phi 0.83\sqrt{f'_c}$  (MPa)  $hd$ , which, considering the specified value of  $\phi = 0.85$ , gives  $V_{max} = 0.71\sqrt{f'_c}$  (MPa)  $hd$ . (Values up to  $V_{max} = 1.15\sqrt{f'_c}$  (MPa)  $hd$  have been resisted.) The amount of displacement ductility that can be used is limited by instability problems. Present code and Paulay's [5] suggested dimensional limitations to avoid instability are not adequate when the required  $\mu_\delta$  under cyclic loading including reversals of deformations exceeds 6 for barbell cross sections and 3 for rectangular cross sections. Dimensional limitations should depend upon the required rotation capacity of the critical region of the wall and type of loading history.

Coupling Girders. The performance of coupling girders during the 1964 Alaska and 1972 Managua earthquakes demonstrated that a conventional approach to designing and detailing these girders results in poor performance. This is not surprising because these girders are often deep in relation to their span.

Thus, significant interaction between shear and flexure--usually disregarded in conventional design procedures--may be present. Furthermore, the deformation capacity, the number of yielding excursions, and the number of plastic rotation reversals demanded from these coupling beams are very large compared with those encountered in beams of ductile moment-resistant frames [7]. Analysis of the experimental data available indicates the following: (1) Compliance with code requirements results in satisfactory hysteretic behavior when  $v_{\max} \leq 0.25\sqrt{f'_c}$  (MPa); (2) When  $v_{\max}$  is in the range of 0.25 to  $0.5\sqrt{f'_c}$  (MPa), it is necessary to use special web reinforcement. Although the use of intermediate longitudinal bars improves hysteretic behavior, the addition of diagonal reinforcement seems to be more effective in controlling sliding shear at critical regions; (3) The use of conventional reinforced beams where the nominal unit shear stress,  $v_{\max}$ , can exceed  $0.5\sqrt{f'_c}$  (MPa) should be avoided; (4) When  $v_{\max} > 0.25\sqrt{f'_c}$  (MPa) and particularly when it exceeds  $0.5\sqrt{f'_c}$  (MPa) as is usual for coupling beams, the energy dissipation capacity can be improved significantly by placing the main reinforcement diagonally in the beams as has been demonstrated by Paulay [5]. The superior response of diagonally reinforced coupling beams has also been shown in tests carried out by the PCA [12]. Therefore, even in cases of short-deep coupling beams, it is possible to design and construct them so they can offer excellent ductility and hysteretic dissipation of energy.

Concluding Remarks. Ample experimental and analytical evidence indicates it is possible to design and construct very "ductile walls and coupling girders" which could supply frame-coupled wall buildings with stiffness, strength, ductility and energy dissipation capacity in excess of the actual demands, even when these buildings are subjected to recorded or estimated extreme ground motions. This observation is strongly supported by the results of experiments conducted on frame-walls and coupled walls by Paulay [5] and on coupled walls by the PCA [13], and by the observed performance of these types of building structural systems during recent destructive earthquakes. However, there are still several problems requiring further study before specific guidelines and/or reliable code provisions can be recommended for the seismic-resistant design of R/C frame-coupled wall buildings. Some of these are enumerated below.

#### RESEARCH NEEDS

1. Problems in Estimating Demands. There is a need to develop more reliable methods for estimating the maximum shear that can occur in each story of a complete frame-coupled wall building, of its frame and coupled walls, and of its individual walls. This will require investigation of the (1) effects of foundation movements; (2) variation in coupling girders' flexural and shear stiffness and strength; (3) effects of wall axial forces in the variation of their flexural and shear strength and stiffness (particularly the latter); and (4) interacting effects of frame and coupled walls.

2. Problems in Estimating Supply. For any given or selected wall, there is a need to improve present methods of predicting its shear strength, flexural and shear stiffnesses, particularly in the inelastic range. Conventional methods are inadequate.

3. Problems in Design. Developing optimal methods for the design of coupled wall and frame-coupled wall systems will require investigation into the optimal selection of stiffness and strength of the coupling girders, and the optimal selection of thickness of walls and size of edge members, considering the possibility of using different sizes for the outside and inside edge members.

## ACKNOWLEDGMENT

The Berkeley research was supported by grants from the National Science Foundation. The cooperation of Prof. E.P. Popov and Dr. A. E. Aktan with this research is appreciated. Thanks are also due to E. Matthews and D. Ullman for their help with this report.

## REFERENCES

1. Uniform Building Code Standards, 1973, 1976, and 1979 editions, International Conference of Building Officials, Whittier, CA.
2. Wang, T.Y., Bertero, V.V., & Popov, E.P., "Hysteretic Behavior of Reinforced Concrete Framed Walls," Report No. EERC 75-23, Univ. of Cal., Berkeley, 1975.
3. Vallenias, J.M., Bertero, V.V., & Popov, E.P., "Hysteretic Behavior of Reinforced Concrete Structural Walls," Report No. EERC-79/20, Univ. of Cal., Berkeley, 1979.
4. Iliya, R., & Bertero, V.V., "Effects of Amount and Arrangement of Wall-Panel Reinforcement on Hysteretic Behavior of Reinforced Concrete Walls," Report No. EERC-80/04, Univ. of Cal., Berkeley, 1980.
5. Bertero, V.V., Organizer, Proceedings, Workshop on Earthquake-Resistant Reinforced Concrete Building Construction, Univ. of Cal., Berkeley, July 1977, 3 vols., 1941p.
6. Bertero, V.V., "Seismic Performance of Reinforced Concrete Structures," Anales of the Argentina Academy of Science, Vol. 31, Buenos Aires, 1979, pp. 75-144.
7. Bertero, V.V., "Seismic Behavior of Structural Concrete Linear Elements (Beams, Columns) and Their Connections," Proceedings of the A.I.C.A.P.-C.E.B. Symposium on "Structural Concrete Under Seismic Actions", Rome, May 25-28, 1979, Vol. 1, pp. 123-212.
8. Bertero, V.V., "An Overview of the State-of-the-Art in Earthquake-Resistant R/C Building Construction," Proceedings of the 2nd U.S. Nat'l Conf. on Earthquake Engineering, Aug. 1979, Stanford Univ., Stanford, CA, pp. 838-52.
9. "Tentative Provisions for the Development of Seismic Regulations for Buildings," prepared by the Applied Technology Council, Nat'l Bureau of Standards, 510, Washington, D.C., June 1978.
10. Oesterle, R.G. et al., "Earthquake-Resistant Structural Walls--Tests of Isolated Walls--Phase II," Portland Cement Association, Report PCA R/D Ser. 1629, Skokie, IL, Oct. 1979.
11. Tong, S.T., "Behavior of R/C Coupled Walls," Individual research report, SESM, Univ. of Cal., Berkeley (in preparation).
12. Barney, G.B. et al., "Earthquake-Resistant Structural Walls--Tests of Coupling Beams," Portland Cement Association, Report PCA R/D Ser. 1583, Skokie, IL, Jan. 1978.
13. Aristizabal-Ochoa, J.D., Skin, K.N., & Corley, W.G., "Effects of Beam Strength and Stiffness on Coupled Wall Behavior," Proceedings of the 2nd Nat'l Conf. on Earthquake Engineering, Aug. 1979, Stanford Univ., Stanford, CA, pp. 323-32.

# SEISMIC BEHAVIOR OF REINFORCED CONCRETE MOMENT-RESISTING FRAMES

Egor P. Popov<sup>I</sup>

## SUMMARY

At severe random cyclic loadings, bond failure may occur and slippage may take place between the reinforcing bars and concrete. Some experimental evidence of this kind of behavior at interior joints of moment-resisting reinforced concrete frames is examined. Selected test results on one-half scale cruciform subassemblages of normal and lightweight aggregate concrete specimens are presented. Practical means of avoiding the bar slip in an interior column joint by designing for plastic hinges to occur away from the column faces are then described. A discussion of a mathematical model for the analysis of reinforced concrete frames when the main beam bars slip in a joint and plastic zones extend along a beam concludes the paper.

## INTRODUCTION

Moment-resisting reinforced concrete frames are widely used as prime elements or in conjunction with structural (shear) walls for resisting seismic forces. The analysis of such frames has not been fully perfected because of several complicating features in the behavior of reinforced concrete. The most difficult aspects of the problem pertain to shear transfer across severely cracked sections and bond failure accompanied by bar slippage. Analytical models for predicting such behavior under cyclic loading are far from being satisfactory. This paper addresses itself primarily to the question of main beam bar slippage in an interior joint and a possibility of including in the analysis the zones of alternating plasticity along the beams.

## SPECIMEN DESIGN

A 20-story, four-bay reinforced concrete frame of an office building designed as a ductile moment-resisting space frame in accordance with the most severe requirements of the 1970 UBC [1], 1971 ACI Code [2], and 1971 SEAOC Recommendations [3] served as the prototype for this study [4]. A strong column-weak beam design approach, which meant that under gravity and code seismic lateral loadings yielding would occur only in the beams, was adopted.

The location of the selected subassemblage at the third floor level of a 20-story frame prototype is shown in Fig. 1 [5]. The subassemblage beams were hinged at mid-span, since the inelastic behavior of the third floor beams is influenced primarily by the lateral rather than gravity forces. The columns were hinged at mid-height. The geometry and reinforcement of the half-scale typical test specimen are shown in Fig. 2 [5]. Typical beams were 9 × 16 in. (230 × 400 mm) with #6 (19 mm) main bars at the top and #5 (16 mm) bars at the bottom. For some specimens four #6 (19 mm) bars were used both at the top and at the bottom of the beams. For all specimens  $L = h$  was 72 in. (1.8 m).

---

<sup>I</sup>Professor of Civil Engineering, University of California, Berkeley, California, USA, 94720.

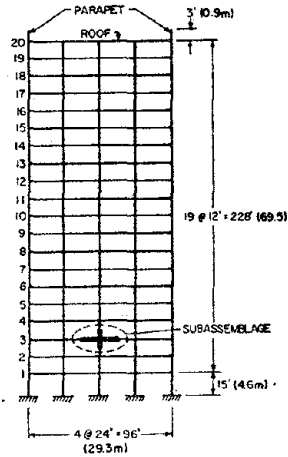


Fig. 1 20-Story Prototype Frame and Selected Subassemblage [8]

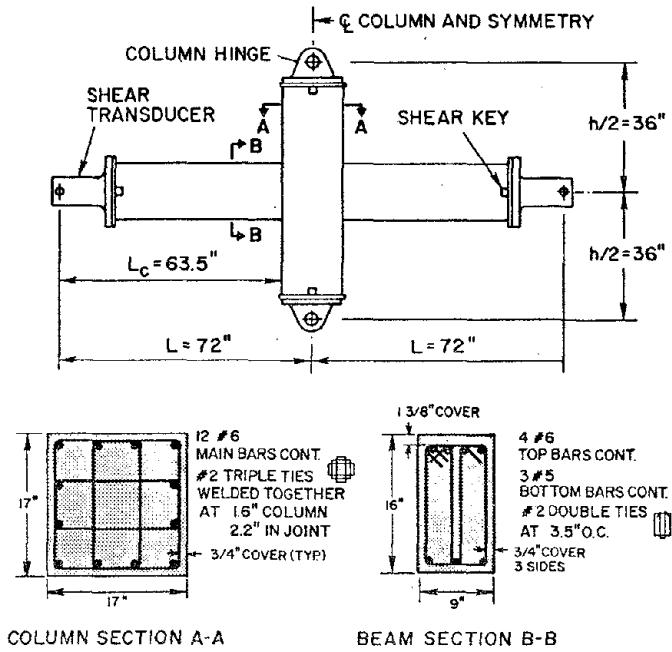


Fig. 2 Beam-Column Test Specimen [5]

EXPERIMENTAL PROCEDURE AND RESULTS

On placing the specimens into a test frame, the columns were loaded axially to 470 kips (2090 kN), and the beam ends were deflected downward developing reactions of 3.5 kips (16 kN). The application of these forces simulated gravity effects. A horizontal double-acting jack at the bottom hinge of the specimen simulated the effect of seismically induced forces by applying specified displacements in a quasi-static manner. A free-body diagram for a subassemblage for these conditions is shown in Fig. 3. At large

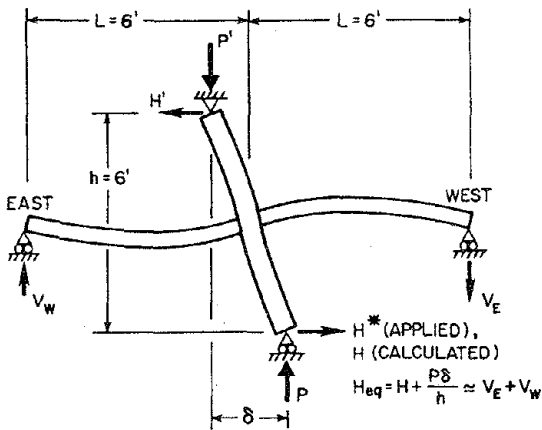


Fig. 3 Free-Body Diagram for Subassemblage [5]

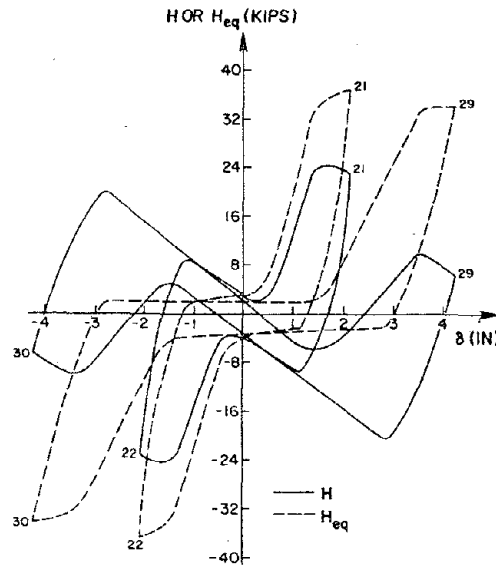


Fig. 4 Comparison of H-δ with Heq-δ for Specimen BC2 [5]

column displacement  $\delta$ , due to the presence of a large axial column force  $P$ , the  $P$ - $\delta$  effect becomes important and must be considered.

A portion of a hysteretic diagram for the horizontal force  $H$  applied by a jack vs. displacement  $\delta$  for Specimen BC2 is shown in Fig. 4. In the same diagram an equivalent horizontal force  $H_{eq}$  vs.  $\delta$  is also shown. The force  $H_{eq}$  was found by adding to the applied horizontal force  $H$  a term  $P\delta/h$  which accounts for the  $P$ - $\delta$  effect. The  $H_{eq}$ - $\delta$  diagram shows the actual strength demands placed on a joint. Because of attaching an excessive number of strain gages to the beam bars within the joint, the bar anchorage length in Specimen BC2 was reduced resulting in an early bond failure generating very poor hysteretic loops. A similar situation may develop in actual construction due to poor workmanship. Because of steel congestion at the joints of ductile moment-resisting frames, the occurrence of rockpockets in such locations is a distinct possibility. In these cases significant beam fixed-end rotations can take place at large ductilities.

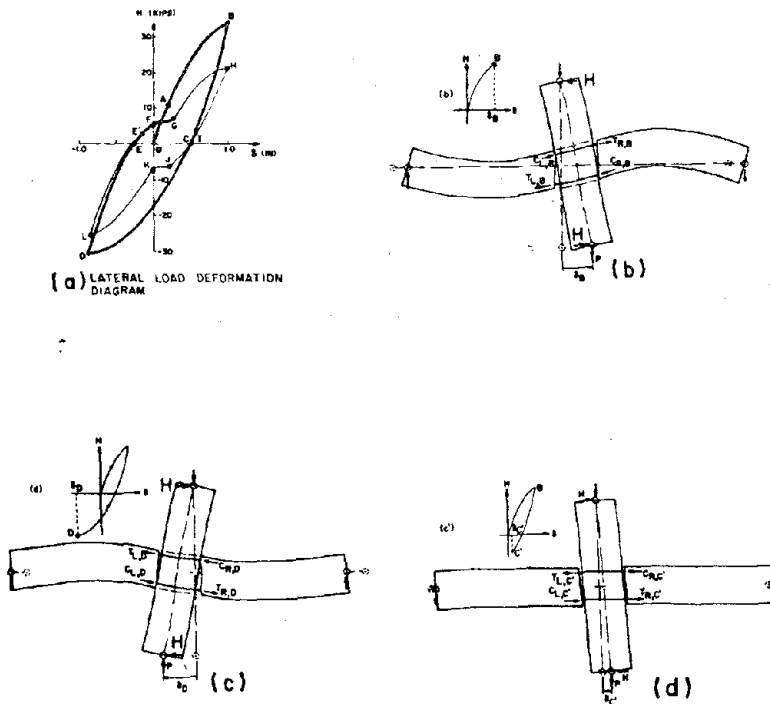


Fig. 5 Mechanism of Stiffness Degradation [6]

ity, and a progressive breakdown in bond within a joint was observed. Of course bond deterioration does not occur as rapidly nor is it as extreme in the example first cited. Nevertheless it should be remarked that although the beam fixed-end rotations for BC3 are substantially smaller than those for Specimen BC2, at large displacements they contribute 20 to 35% to the total horizontal displacement of the subassembly.

The tendency for an anchorage failure at the beam bars within an interior joint can be greatly reduced or even completely eliminated. This is most easily done by requiring a larger amount of reinforcement at the bottom of a beam at a joint than is customary. Thus, instead of merely complying

The mechanism of stiffness degradation at a joint is illustrated in Fig. 5 [6]. On complete load reversal cracks are formed on both sides of a column, and, due to plastically strained steel, these cracks can remain open and the beam bars can become subjected simultaneously to pull and push. This imposes severe demands on the bar anchorage within a joint. Vestiges of this behavior can occur in specimens with no construction defects. Such an example is shown in Fig. 6 for Specimen BC3 [5]. In this case some pinching of the hysteretic loops can be noted at relatively low values of ductility,

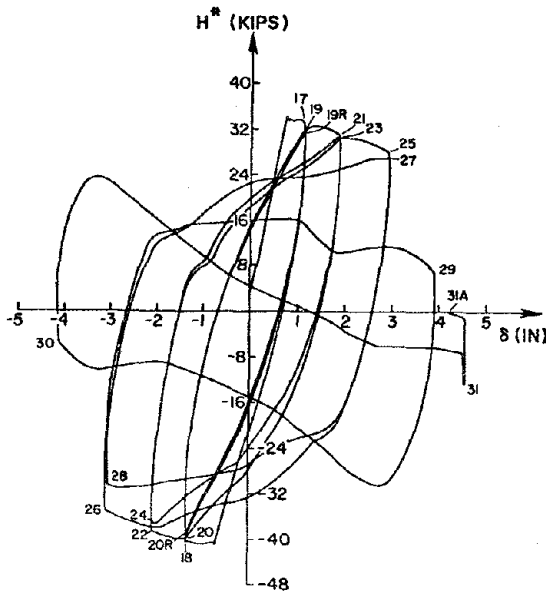


Fig. 6  $H^*-\delta$  Diagram for Specimen BC3 [5]

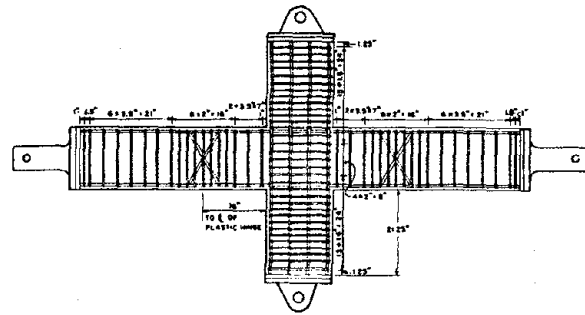


Fig. 7 Subassemblage with Inclined Bars in the Plastic Hinge Region. Specimen BC5 [8]

with the current practice [2] of providing as little as 50% of the top steel area in the bottom bars of a beam, one could specify the same amount of top and bottom reinforcement. Experiments have shown this to be very effective [7,8].

A somewhat costlier but superior method

of detailing for avoiding bond failure within a joint is shown in Fig. 7. In this scheme [8] some of the beam bars are bent at points of the anticipated plastic hinges. The hysteretic loops for a specimen made in this manner are shown in Fig. 8. Note particularly the slow rate of deterioration of the loops in the important inelastic range of displacements from 0.75 to 2 or 3 in. (20 to 50 or 75 mm). This can be compared with the poorer performance of BC3 shown in Fig. 6. The cracking of Specimen BC5 was remarkably well distributed along the beam resulting in narrow cracks.

A comparison of hysteretic behavior between two dimensionally identical subassemblages with the same amount of reinforcement, but made with concrete having different aggregates is shown in Fig. 9 [9,10]. Specimen

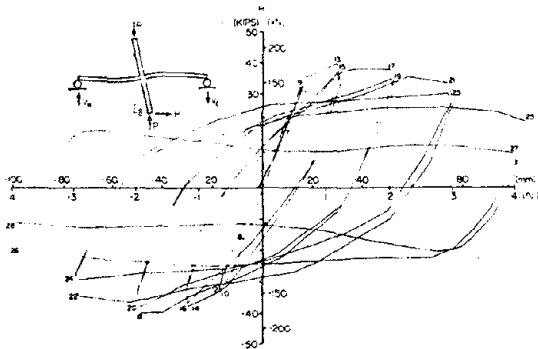


Fig. 8  $H-\delta$  Diagram for Specimen BC5 [8]

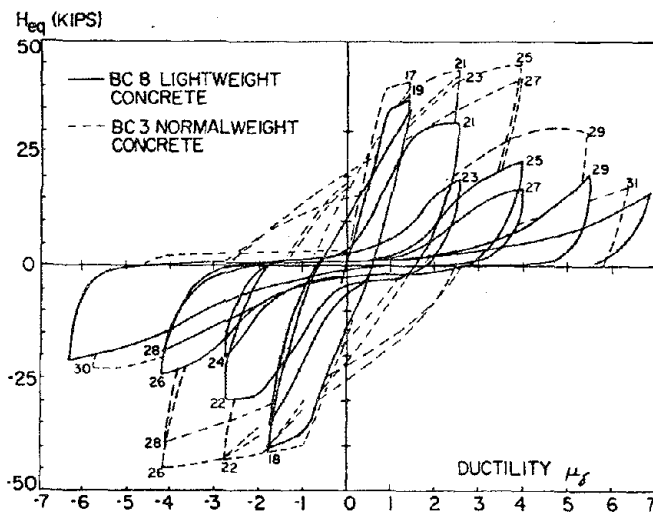


Fig. 9 Comparison of Hysteretic Behavior of Normal with Lightweight Aggregate Specimens [10]



BC8, which was made of lightweight concrete, deteriorated under the application of cyclic loading much more rapidly than BC3 made of a normal weight concrete. No such difference in behavior was noted for monotonic application of the loads [10]. This clearly points to rapid bond deterioration in lightweight concrete under cyclic loading.

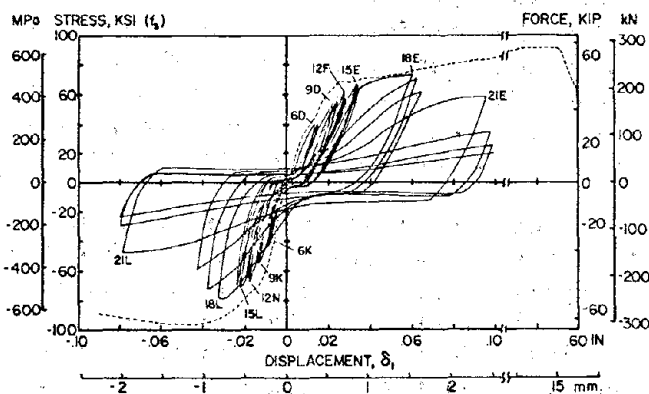


Fig. 10 End Displacements of a Bar under Cyclic Loadings [11]

experience during a cycling process. It is significant to note that some slip of a bar occurs from the earliest stages of loading. Progressively this slip becomes larger until the bar pulls through the column stub. Some success was achieved in modeling cyclic behavior analytically [12]. A much simpler model for bar pull-out leading to satisfactory results has been proposed for monotonic application of loads [13]. Further work remains to be done to determine the interaction between parallel bars.

#### ANALYTICAL STUDIES OF FRAME BEHAVIOR

In order to evaluate the contribution of the inelastic beam fixed-end rotations as well as the effect of finite length plastic hinges at beam ends on the cyclic behavior of subassemblages and frames, two computer programs were written [4,14]. One of these programs was for the static analysis of frames; the other, for the dynamic analysis. The principal features for these two programs which are common to both are briefly outlined next.

Since the developed computer programs are intended for the analysis of reinforced concrete frames designed on the basis of the strong columns - weak beams concept, the columns were assumed to remain elastic throughout a time-history analysis. However, in order to allow for the formation of a sidesway mechanism, rotational springs with a yielding feature were provided at the column bases.

The beams were idealized as shown in Fig. 11 [14]. To account for the fixed-end rotations of the beams at the column faces during the inelastic cyclic excursions, rotational springs were provided at the beam ends. Finite lengths of Zones of Alternating Plasticity (ZAP) were assumed to extend over the end portions of the beams. This assumption contrasts with the

Because of the importance of bond behavior under cyclic loading, this problem was isolated and investigated in some detail [11]. By applying different patterns of loading to a bar embedded in a reinforced concrete block simulating a column, numerous hysteretic loops were obtained. One such case for a #8 (25 mm) bar embedded in a column stub 25 in. (635 mm) deep is shown in Fig. 10. In this experiment pull at one end of a bar was simultaneously applied with a push at the other end. This corresponds to the most severe loading condition a bar may

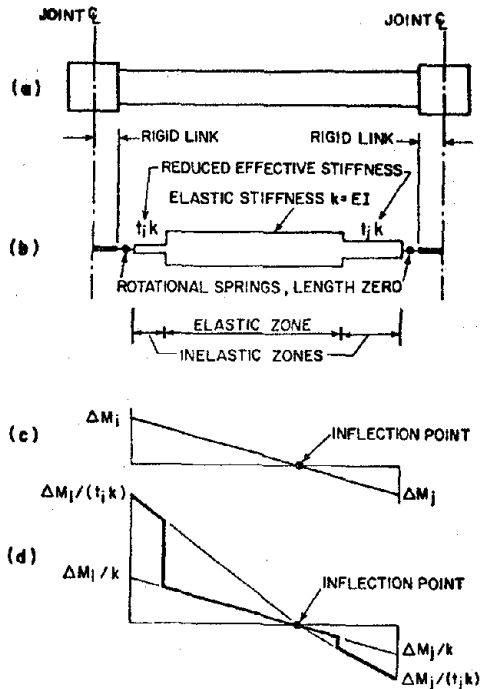


Fig. 11 ZAP Model Characteristics:  
 (a) Actual Member; (b)  
 Idealized Member; (c)  
 Incremental Moments; (d)  
 Incremental Curvatures

usual practice of taking plastic point hinges at the ends of beams. Time-step analyses of a frame show that the lengths of the inelastic regions of a beam (ZAP) vary with time. The incremental beam curvatures were taken as shown in Fig. 11(d) in order to symmetrize the stiffness matrices. A degrading moment-curvature model, which included stiffness degradation and strain hardening features, was used to relate the beam moments with their curvature.

The developed computer program for the static analysis of frames subjected to cyclic loading was used to compare the analytical with the experimental results. Such a comparison for a hysteretic loop for Specimen BC3 is shown in Fig. 12 [14]. The agreement between the two is seen to be excellent. If the fixed-end rotation of the beam ends is not permitted in the analysis, the agreement of the analytical results with the experimental ones is poorer.

The dynamic computer program developed on the same basis was used to analyze the prototype structure shown in Fig. 1. For some severe earthquakes this analysis indicates a number of interesting results. As to be expected, the nonlinear behavior of the frames reduces the story shears by a factor on the order of three, but even then significantly exceeds the level of the lateral loads currently prescribed in the codes [1]. The increase in displacements caused by fixed-end rotation of beams appears to be surprisingly small, being approximately 8% for the derived Pacoima earthquake. For the same earthquake the base shear decreases about 10% if the beam ends rotate. These tentative results need further verification, and it must be recognized that the developed programs do not include a provision for a complete bar pull-through in the joints. In some situations the latter condition may be the most critical.

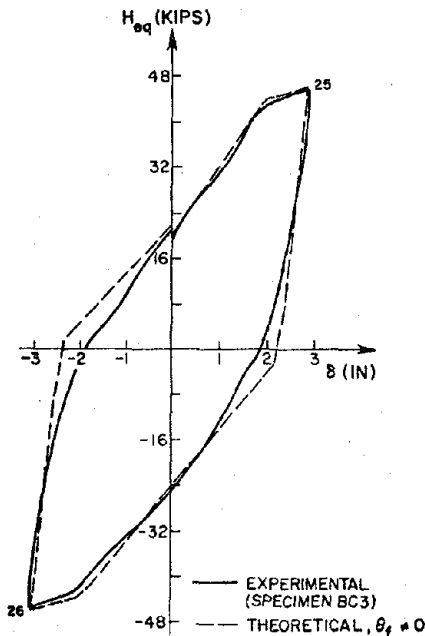


Fig. 12 Experimental and Theoretical  $H_{eq}-\delta$  Diagrams [14]

## ACKNOWLEDGEMENTS

The findings reported are a result of research extending over several years of joint effort with Professor V. V. Bertero, and were supported by the National Science Foundation (current Grant No. PFR-7908984). Any opinions, findings, and conclusions expressed in the paper are those of the author and do not necessarily reflect the views of the Foundation. A number of graduate students participated in the projects described, and several of them are co-authors of the cited papers; Philip Filippou assisted with the preparation of this paper. It is a pleasure to acknowledge all of this help with gratitude.

## REFERENCES

- [1] Uniform Building Code, 1970 Ed., Vol. 1, International Conference of Building Officials, Whittier, California.
- [2] Building Code Requirements for Reinforced Concrete (ACI 318-71), American Concrete Institute, Detroit, Michigan, 1971.
- [3] Seismology Committee, Recommended Lateral Force Requirements and Commentary, Structural Engineers Association of California, San Francisco, 1968, and Appendix F-1969, 1970, 1971 Revisions.
- [4] Soleimani, D., "Reinforced Concrete Ductile Frames Under Earthquake Loadings with Stiffness Degradation," Ph.D. Dissertation, University of California, Berkeley, Dec. 1978.
- [5] Soleimani, D., Popov, E. P., and Bertero, V. V., "Hysteretic Behavior of Reinforced Concrete Beam-Column Subassemblages," ACI Journal, Vol. 76, No. 11, Nov. 1979, pp. 1179-1195.
- [6] Bertero, V. V., and Popov, E. P., "Seismic Behavior of Ductile Moment-Resisting Reinforced Concrete Frames," Reinforced Concrete Structures in Seismic Zones, SP-53, American Concrete Institute, Detroit, Michigan, 1977.
- [7] Popov, E. P., Bertero, V. V., Galunic, B., and Lantaff, G., "On Seismic Design of R/C Interior Joints of Frames," 6WCEE, New Delhi, India, January 1977, Vol. 7, pp. 5-191 to 5-196.
- [8] Galunic, B., Bertero, V. V., and Popov, E. P., "An Approach for Improving Seismic Behavior of Reinforced Concrete Interior Joints," Report UCB/EERC-77/30, University of California, Berkeley, 1977.
- [9] Forzani, B., Popov, E. P., and Bertero, V. V., "Hysteretic Behavior of Lightweight Reinforced Concrete Beam-Column Subassemblages," Report UCB/EERC-79/01, University of California, Berkeley, April 1979.
- [10] Bertero, V. V., Popov, E. P., and Forzani, B., "Seismic Behavior of Lightweight Concrete Beam-Column Subassemblages," ACI Journal, February 1980 (in press).

- [11] Popov, E. P., Bertero, V. V., and Viwathanatepa, S., "Bond in Interior Joints of Ductile Moment-Resisting R/C Frames, Part I: Experiments," ACI Symposium, Houston, Texas, October 1978 (in press).
- [12] Viwathanatepa, S., "Deterioration of Bond in Reinforced Concrete Under Generalized Loading," Ph.D. Dissertation, University of California, Berkeley, California, 1978.
- [13] Bertero, V. V., Popov, E. P., and Viwathanatepa, S., "Bond of Reinforcing Steel: Experiments and a Mechanical Model," Preliminary Reports, Vol. 2, IASS Symposium, July 1978, Darmstadr, W. Germany, pp. 3-17.
- [14] Soleimani, D., Popov, E. P., and Bertero, V. V., "Nonlinear Beam Model for R/C Analysis," Seventh Conference on Electronic Computations, St. Louis, Missouri, August 1979, ASCE, New York, 1979, pp. 483-509.

## PROBABILISTIC MODAL COMBINATION FOR EARTHQUAKE LOADING

Armen Der Kiureghian<sup>1</sup>

### SUMMARY

A probabilistic method for evaluating the earthquake response of multi-degree-of-freedom structures using the response spectrum approach is developed. Various statistical quantities of the response, including the root-mean-squares of the response and its time derivative and the cumulative distribution and the mean and variance of the peak response, are directly obtained in terms of the response spectral ordinates and the modal properties of structure. The procedure is applicable to structures with closely spaced frequencies for which the existing SRSS method for the mean response is in gross error. For an example structure with closely spaced frequencies, the proposed response spectrum method produces results that are in close agreement with simulation results based on time-history computations.

### INTRODUCTION

Earthquake induced loads on structures are stochastic in nature. Therefore, a probabilistic approach for the analysis of structural response to earthquakes and the assessment of safety is essential. Random vibration techniques have successfully been used to determine the statistical quantities of response to stochastic inputs typical of earthquake motions [1,6]. In this approach, the input excitation is usually described through a power spectral density function. This description, however, is not the most convenient in earthquake engineering practice. Instead, a description of the ground motion in terms of an average response spectrum is found to be more convenient and is commonly used in design applications and code specifications. Based on concepts from the theory of random vibrations, Rosenblueth et al. [7] were the first to develop a method for determining the responses of multi-degree-of-freedom (MDF) structures to earthquakes using the response spectrum approach. Their method, as well as other methods that were subsequently developed [8,10], are limited to a determination of the mean value of the maximum response.

In this paper, a probabilistic method for evaluating the responses of linear MDF structures to earthquakes using the response spectrum approach is developed. Various statistical quantities of the response, including the root-mean-squares of the response and its time derivative and the cumulative distribution and the mean and variance of the peak response, are directly obtained in terms of the response spectrum ordinates and the modal properties of the structure. The method includes the correlation between modal responses; thus, it is applicable to structures with closely spaced frequencies. The required expressions are all in closed form and require little computational effort.

The development in this paper is based on the previous works of Vanmarcke [11,12] and the author [3]. In Ref. 11, it is shown that most statistical quantities of interest for a stationary process are obtained in terms of the first three moments of the power spectral density function. In Ref. 12, these moments are used to determine the cumulative distribution of the first-passage time for a Gaussian process, which is also the distribution of the peak over a specified duration. In Ref. 3, closed-form expressions for the first three spectral moments of the response of MDF structures to white-noise and filtered white-noise input excitations are derived. The significance of closely spaced modes, which result in correlated modal responses, is included in this derivation. Through comparisons of results for the two types of inputs, the range of applicability of the white-noise model as an approximation for wide-band inputs is also

1. Assistant Professor, Department of Civil Engineering, University of California, Berkeley, California.

determined in this reference. These results will subsequently be used in developing the response spectrum method.

### RESPONSE OF MDF SYSTEMS TO STATIONARY GAUSSIAN EXCITATION

Consider an  $n$ -degree-of-freedom, viscously damped, linear system having classical modes. Let  $\omega_i, \zeta_i, i=1, 2, \dots, n$ , represent its natural frequencies and damping coefficients, respectively. Any response of such a system can be expressed in terms of its modal responses as

$$R(t) = \sum_i R_i(t) = \sum_i \Psi_i S_i(t) \quad (1)$$

where  $R_i(t) = \Psi_i S_i(t)$  is the response in mode  $i$ , in which  $\Psi_i$  is the effective participation factor, a constant in terms of the modal vectors and the mass matrix, and  $S_i(t)$  is the  $i$ -th normal coordinate representing the response of an oscillator of frequency  $\omega_i$  and damping coefficient  $\zeta_i$  to the given input [1]. For a zero-mean stationary Gaussian input,  $F(t)$ , described through a one-sided power spectral density,  $G_F(\omega)$ , the corresponding power spectral density for the stationary response is

$$G_R(\omega) = \sum_i \sum_j \Psi_i \Psi_j G_F(\omega) H_i(\omega) H_j^*(\omega) \quad (2)$$

where  $H_i(\omega) = 1/(\omega_i^2 - \omega^2 + 2i\zeta_i\omega_i\omega)$  is the complex frequency response function of mode  $i$  and the asterisk denotes a complex conjugate. Using this relation, the first three moments of the response power spectral density, as defined by Vanmarcke [11], are

$$\lambda_m = \int_0^\infty \omega^m G_R(\omega) d\omega = \sum_i \sum_j \Psi_i \Psi_j \lambda_{m,ij}, \quad m=0, 1, 2 \quad (3)$$

where

$$\lambda_{m,ij} = \text{Re} \left[ \int_0^\infty \omega^m G_F(\omega) H_i(\omega) H_j^*(\omega) d\omega \right], \quad m=0, 1, 2 \quad (4)$$

are the cross-spectral moments of the normal coordinates associated with modes  $i$  and  $j$  [3]. Introducing the coefficients  $\rho_{m,ij} = \lambda_{m,ij} / \sqrt{\lambda_{m,ii} \lambda_{m,jj}}$ ,  $m=0, 1, 2$ , Eq. 3 can be written in terms of uni-modal spectral moments as

$$\lambda_m = \sum_i \sum_j \Psi_i \Psi_j \rho_{m,ij} \sqrt{\lambda_{m,ii} \lambda_{m,jj}}, \quad m=0, 1, 2 \quad (5)$$

It is noted that  $\rho_{0,ij}$  and  $\rho_{2,ij}$  are the correlation coefficients between  $S_i(t)$  and  $S_j(t)$  and between their time derivatives,  $\dot{S}_i(t)$  and  $\dot{S}_j(t)$ , respectively. A similar interpretation of  $\rho_{1,ij}$  is not possible; however, the behavior of this coefficient is also similar to a correlation coefficient. Whereas the spectral moments,  $\lambda_{m,ii}$ , are in general sensitive to the shape of the input power spectral density, the coefficients,  $\rho_{m,ij}$ , remain relatively indifferent for wide-band inputs. For the response to a white-noise input, approximate expressions for these coefficients from Ref. 3 are

$$\rho_{0,ij} = \frac{2\sqrt{\zeta_i \zeta_j} \left[ (\omega_i + \omega_j)^2 (\zeta_i + \zeta_j) + (\omega_i^2 - \omega_j^2) (\zeta_i - \zeta_j) \right]}{4(\omega_i - \omega_j)^2 + (\omega_i + \omega_j)^2 (\zeta_i + \zeta_j)^2} \quad (6)$$

$$\rho_{1,ij} = \frac{2\sqrt{\zeta_i \zeta_j} \left[ (\omega_i + \omega_j)^2 (\zeta_i + \zeta_j) - 4(\omega_i - \omega_j)^2 / \pi \right]}{4(\omega_i - \omega_j)^2 + (\omega_i + \omega_j)^2 (\zeta_i + \zeta_j)^2} \quad (7)$$

$$\rho_{2,ij} = \frac{2\sqrt{\zeta_i \zeta_j} \left[ (\omega_i + \omega_j)^2 (\zeta_i + \zeta_j) - (\omega_i^2 - \omega_j^2) (\zeta_i - \zeta_j) \right]}{4(\omega_i - \omega_j)^2 + (\omega_i + \omega_j)^2 (\zeta_i + \zeta_j)^2} \quad (8)$$

A comparison of these results with the corresponding values for response to filtered white-noise inputs has demonstrated that these expressions can be used for responses to wide-band inputs

typical of earthquake ground motions [3]. These expressions for  $\rho_{m,ij}$  are plotted in Fig. 1 against the frequency ratio for selected values of damping.

In terms of the moments of the response power spectral density,  $\lambda_m$ , the statistical quantities of response are: the root-mean-square (rms) response,  $\sigma_R = \sqrt{\lambda_0}$ ; the rms of the time derivative of the response,  $\sigma_{\dot{R}} = \sqrt{\lambda_2}$ ; the response mean zero-crossing rate,  $\nu = \sqrt{\lambda_2/\lambda_0}/\pi$ ; and the cumulative distribution of the maximum absolute response over duration  $\tau$ ,

$$R_\tau = \max_t |R(t)| \quad (9)$$

as

$$F_{R_\tau}(r) = \left[ 1 - \exp(-s^2/2) \right] \exp \left[ -\nu\tau \frac{1 - \exp(-\sqrt{\pi/2}\delta_e s)}{\exp(s^2/2) - 1} \right], \quad r > 0 \quad (10)$$

in which  $s = r/\sigma_R$ ,  $\delta_e = \delta^{1.2}$ , and  $\delta = \sqrt{1 - \lambda_1^2/\lambda_0\lambda_2}$  [11,12]. The mean and standard deviation of the maximum response may, in general, be obtained as  $\bar{R}_\tau = p\sigma_R$  and  $\sigma_{R_\tau} = q\sigma_R$ , respectively, where  $p$  and  $q$  are peak factors. Empirical expressions for  $p$  and  $q$  that are consistent with the distribution in Eq. 10 were obtained in Ref. 3 as

$$p = \sqrt{2 \ln \nu_e \tau} + \frac{0.5772}{\sqrt{2 \ln \nu_e \tau}} \quad (11)$$

$$q = \begin{cases} \frac{1.2}{\sqrt{2 \ln \nu_e \tau}} - \frac{5.4}{13 + (2 \ln \nu_e \tau)^{3.2}}, & \nu_e \tau > 2.1 \\ 0.65, & \nu_e \tau \leq 2.1 \end{cases} \quad (12)$$

where

$$\nu_e = \begin{cases} (1.63\delta^{0.45} - 0.38)\nu, & \delta < 0.69 \\ \nu, & \delta \geq 0.69 \end{cases} \quad (13)$$

is an equivalent rate of statistically independent zero crossings. These expressions are valid in the ranges  $0.1 \leq \delta \leq 1$  and  $5 \leq \nu\tau \leq 1000$ , which are of interest in earthquake engineering. Fig. 2 shows plots of  $p$  and  $q$  versus  $\nu\tau$  for selected values of  $\delta$ . (It is noted that the distribution in Eq. 10 and the peak factors in Eqs. 11 and 12 include the effect of the dependence between crossings of the response process and, in this respect, are superior to similar results previously given by Davenport [2]).

#### DEVELOPMENT OF THE RESPONSE SPECTRUM METHOD

Let  $\bar{S}_\tau(\omega, \zeta)$  represent the mean of the maximum absolute response of an oscillator of frequency  $\omega$  and damping  $\zeta$  to a given input,  $F(t)$ , over duration  $\tau$ . A plot of  $\bar{S}_\tau(\omega, \zeta)$  for all  $\omega$  and  $\zeta$  is defined herein as the response spectrum associated with the input  $F(t)$  and the duration  $\tau$ . It is the intention here to develop a method for approximate evaluation of the response of an MDF structure when the input is described through its response spectrum. This development is based on the assumption that the input is a wide-band process, i.e., that it has a smoothly varying power spectral density over a wide range of frequencies.

From the definition of the response spectrum, it is clear that  $\bar{S}_\tau(\omega_i, \zeta_i)$  is the mean of the absolute maximum of the  $i$ -th normal coordinate,  $S_i(t)$ . Thus, if  $p_i$  denotes the peak factor for this process, using the relation  $\bar{S}_\tau(\omega_i, \zeta_i) = p_i \sqrt{\lambda_{0,ii}}$ , one has

$$\lambda_{0,ii} = \frac{1}{p_i^2} \bar{S}_\tau^2(\omega_i, \zeta_i) \quad (14)$$

It is shown in Ref. 3 that for responses to a wide-band input

$$\nu_i = \frac{1}{\pi} \left( \frac{\lambda_{2,ii}}{\lambda_{0,ii}} \right)^{\frac{1}{2}} \approx \frac{\omega_i}{\pi} \quad (15)$$

$$\delta_i = \left[ 1 - \frac{\lambda_{1,ii}^2}{\lambda_{0,ii}\lambda_{2,ii}} \right]^{\frac{1}{2}} \approx \left[ 1 - \frac{1}{\sqrt{1-\zeta_i^2}} \left( 1 - \frac{2}{\pi} \tan^{-1} \frac{\zeta_i}{\sqrt{1-\zeta_i^2}} \right) \right]^{\frac{1}{2}} \approx 2 \left( \frac{\zeta_i}{\pi} \right)^{\frac{1}{2}} \quad (16)$$

These relations are exact for responses to white-noise inputs and are close approximations for responses to earthquake-type, wide-band inputs. Using these expressions in Eqs. 11 and 13, the peak factor,  $p_i$ , for the  $i$ -th normal coordinate is computed in terms of the corresponding modal frequency and damping coefficient. Substituting this factor in Eq. 14, the first moment,  $\lambda_{0,ii}$ , is obtained directly in terms of the response spectrum ordinate associated with mode  $i$ . Furthermore, using Eqs. 14-16, the second and third spectral moments are also obtained in terms of the response spectrum ordinate as

$$\lambda_{1,ii} = \frac{\omega_i \sqrt{1-4\zeta_i/\pi}}{p_i^2} \bar{S}_\tau^2(\omega_i, \zeta_i) \quad (17)$$

$$\lambda_{2,ii} = \frac{\omega_i^2}{p_i^2} \bar{S}_\tau^2(\omega_i, \zeta_i) \quad (18)$$

Thus, substituting Eqs. 14, 17, and 18, together with the previously given expressions for  $\rho_{m,ij}$ , in Eq. 5, the moments of the response power spectral density are obtained directly in terms of the response spectrum ordinates and the modal properties of the structure. With these moments known, the statistical quantities of response are evaluated as described in the preceding section. In particular, if  $\bar{R}_{i\tau} = \Psi_i \bar{S}_\tau(\omega_i, \zeta_i)$  denotes the maximum response in mode  $i$ , this development yields

$$\sigma_R = \left( \sum_i \sum_j \frac{1}{p_i p_j} \rho_{0,ij} \bar{R}_{i\tau} \bar{R}_{j\tau} \right)^{\frac{1}{2}} \quad (19)$$

$$\sigma_{\dot{R}} = \left( \sum_i \sum_j \frac{\omega_i \omega_j}{p_i p_j} \rho_{2,ij} \bar{R}_{i\tau} \bar{R}_{j\tau} \right)^{\frac{1}{2}} \quad (20)$$

$$\bar{R}_\tau = p \sigma_R = \left( \sum_i \sum_j \frac{p^2}{p_i p_j} \rho_{0,ij} \bar{R}_{i\tau} \bar{R}_{j\tau} \right)^{\frac{1}{2}} \quad (21)$$

$$\sigma_{R_\tau} = q \sigma_R = \left( \sum_i \sum_j \frac{q^2}{p_i p_j} \rho_{0,ij} \bar{R}_{i\tau} \bar{R}_{j\tau} \right)^{\frac{1}{2}} \quad (22)$$

where  $p$  and  $q$  are the peak factors for the response process,  $R(t)$ , and are obtained from Eqs. 11-13 using  $\nu = \sqrt{\lambda_2/\lambda_0}/\pi$  and  $\delta = \sqrt{1-\lambda_1^2/\lambda_0\lambda_2}$ . Another useful response quantity is the mean response frequency,  $\bar{\omega} = \pi\nu$ , which is of interest in problems of structural fatigue. Using Eqs. 19 and 20,

$$\bar{\omega} = \frac{\sigma_{\dot{R}}}{\sigma_R} = \left( \frac{\sum_i \sum_j \frac{\omega_i \omega_j}{p_i p_j} \rho_{2,ij} \bar{R}_{i\tau} \bar{R}_{j\tau}}{\sum_i \sum_j \frac{1}{p_i p_j} \rho_{0,ij} \bar{R}_{i\tau} \bar{R}_{j\tau}} \right)^{\frac{1}{2}} \quad (23)$$

Observe that this frequency is a weighted average of the modal frequencies.

It is important to note in the preceding expressions that, since  $\bar{S}_\tau(\omega_i, \zeta_i)$  by definition is positive, the sign of  $\bar{R}_{i\tau}$  is always the same as that of  $\Psi_i$ . This sign could be positive or negative, depending on the modal characteristics of the structure and on the direction of input. It follows, then, that the cross terms in Eqs. 19-23 would have negative values when the effective participation factors for the two modes assume opposite signs.

In many practical applications, the mean of the maximum response is all that is needed. A simplification of Eq. 21 is, therefore, of special interest. It is first noted that the ratios  $p/p_i$



in this equation are all near unity. (This ratio is nearest to unity for the mode which has the closest frequency to the average frequency,  $\bar{\omega}$ , and it decreases with increasing mode number.) This is because of the slow variation of the peak factor with the parameter  $\nu\tau$ ; see Fig. 2. Neglecting these ratios in Eq. 21, which is equivalent to assuming a constant peak factor, is therefore a possible simplification. This yields

$$\bar{R}_\tau = \left( \sum_i \sum_j \rho_{0,ij} \bar{R}_{i\tau} \bar{R}_{j\tau} \right)^{\frac{1}{2}} \quad (24)$$

Note that with this simplification, the mean response is directly given in terms of the modal responses and the coefficients  $\rho_{0,ij}$ , i.e., there is no need to compute the spectral moments from Eq. 5. Also note that this expression for the mean response is independent of the duration, except that which is implicit in the specified response spectrum. A corresponding simplification for the other response quantities is not possible except for  $\bar{\omega}$ , which after multiplying the numerator and the denominator in Eq. 23 by  $p$ , and neglecting the ratios  $p/p_i$ , yields

$$\bar{\omega} = \left( \frac{\sum_i \sum_j \omega_i \omega_j \rho_{2,ij} \bar{R}_{i\tau} \bar{R}_{j\tau}}{\sum_i \sum_j \rho_{0,ij} \bar{R}_{i\tau} \bar{R}_{j\tau}} \right)^{\frac{1}{2}} \quad (25)$$

Observe that with this simplification,  $\bar{\omega}$  becomes the average of the modal frequencies as weighted by the maximum modal responses.

Another simplification in the response expressions is possible when the structural frequencies are well separated. As shown in Fig. 1, the coefficients  $\rho_{m,ij}$  diminish in such cases. Therefore, all cross terms in the expressions for the response, i.e. Eqs. 5 and 19-25, can be dropped. In particular, Eq. 24 in this case reduces to

$$\bar{R}_\tau = \left( \sum_i \bar{R}_{i\tau}^2 \right)^{\frac{1}{2}} \quad (26)$$

This is the well known square-root-of-sum-of-squares (SRSS) rule for modal combination. It is clear from this derivation that the SRSS rule for the mean response is only adequate for structures with well spaced frequencies. When modal frequencies are closely spaced, this rule may lead to erroneous results and should not be used.

### APPLICATION TO EARTHQUAKE LOADING

In applying the above procedure to earthquake loading, the validity of several assumptions inherent in the derivation of the method must be examined. These assumptions are: (a) the input is stationary; (b) the input is Gaussian; (c) the input is wide banded; and (d) the response is stationary. Whereas earthquake-induced ground motions are inherently nonstationary, the strong phase of such motions is often nearly stationary. Since the peak response usually occurs during this phase, it is reasonable, at least for the purpose of a response spectrum method, to assume a stationary process. This assumption would clearly become less accurate for short-duration, impulsive earthquakes. The assumption of Gaussian input is acceptable on the basis of the central limit theorem, since the earthquake ground motion is the accumulation of a large number of randomly arriving pulses [1]. The wide-band assumption for the earthquake motion is acceptable based on investigations in Refs. 3 and 5. Finally, for the assumption of stationary response, it is well known (e.g., Ref. 6) that the response of a not-too-lightly damped oscillator to a wide-band input reaches stationarity in just a few cycles. Thus, this assumption should be acceptable for structures whose fundamental periods are several times shorter than the strong-phase duration of the ground motion. These considerations also suggest that the duration of the strong phase of the ground motion is the appropriate value for the parameter  $\tau$  in the response spectrum method.

It is clear from the above discussion that the response spectrum method for earthquake loadings will be most accurate for earthquakes with long, stationary phases of strong shaking and for not-too-lightly damped structures whose fundamental periods are much longer than the duration of earthquake. Through a large number of example studies, it has been found that the procedure is quite accurate for typical structures and earthquakes (see the example below). It has also been found in these studies that Eq. 24 for the mean response closely approximates the maximum response for a deterministic ground motion with a non-smooth response spectrum. Maximum errors in such applications are expected to be within 10 to 30 percent, depending on the response frequency.

As was indicated before, several formulations for the mean of the peak response have previously been given [7,8,10]. These are generally similar to Eq. 24 of the present formulation with different expressions given for  $\rho_{0,ij}$ . In the method of Rosenblueth et al. [7], which is the most widely known, this coefficient is given as a function of the modal frequencies and damping ratios as well as the duration of input. Unfortunately, no specific definition of the duration (i.e., total duration or strong-phase duration) was given in their development. This ambiguity remains to be a shortcoming of their formulation. (Note that in the present formulation  $\rho_{0,ij}$  is independent of duration.) In the methods of Refs. 8 and 10, no closed-form expressions for this coefficient were given. These methods require much more computational effort and, therefore, are less desirable.

#### EXAMPLE APPLICATION

As an example application of the proposed procedure, the responses of a 5-story building structure to a set of 20 simulated ground motions are studied. The building has uniform floor masses and story stiffnesses with the typical floor plan and properties as shown in Fig. 3. It is subjected to ground motions in the  $x$  direction only; however, because of asymmetry about the  $x$  axis, the center of mass at each floor has a rotational as well as a translational degree of freedom. As a consequence of this, the structure has closely spaced frequencies, as shown in Fig. 3. The ground motions were simulated using a computer program by Ruiz et al. [9]. These were generated as samples of filtered, Gaussian shot noise with a Kanai-Tajimi [5] power spectral density. An intensity function similar to that of a type-B earthquake, as defined by Jennings et al. [4], was used for this purpose. It includes a stationary strong-motion phase of 11 seconds and is scaled to produce a mean peak ground acceleration of 0.5g. A sample of the simulated ground motions is illustrated in Fig. 4.

Using numerical integration, the response spectrum associated with each individual ground motion was computed. These were averaged to obtain the mean spectra shown in Fig. 5. These spectra were used with the proposed method to compute the various responses of the structure. To examine these results, time-history analyses were made of the building responses to each individual ground motion. Samples of such results were used to compute simulated values of the means and standard deviations of peak responses. Table 1 summarizes these results for several selected responses of the building. Numbers inside parenthesis in this table denote percent errors relative to the simulated values. As can be observed, the response spectrum method for the mean (Eqs. 21 or 24) and the standard deviation (Eq. 22) of peak responses closely predicts the simulated values. For the mean response, Eq. 24 appears to give results nearly as good as Eq. 21. However, Eq. 26, which is equivalent to the SRSS method, is in gross error. This is clearly due to the closeness of frequencies for the structure under consideration.

#### ACKNOWLEDGEMENT

This research was supported by the U. S. National Science Foundation under Grant No. ENG-7905906. This support is gratefully acknowledged.

## REFERENCES

- [1] Clough, R. W., and Penzien J., *Dynamics of Structures*, McGraw-Hill, New York, N.Y., 1975.
- [2] Davenport, A. G., "Note on the Distribution of the Largest Value of a Random Function with Application to Gust Loading," *Proceedings*, Institution of Civil Engineers, London, Vol. 28, 1964, pp. 187-196.
- [3] Der Kiureghian, A., "On Response of Structures to Stationary Excitation," *Report No. EERC 79-32*, Earthquake Engineering Research Center, University of California, Berkeley, CA., December, 1979.
- [4] Jennings, P. C., Housner, G. W., and Tsai, N. C., "Simulated Earthquake Motions," Earthquake Engineering Research Laboratory, California Institute of Technology, Pasadena, CA, April, 1968.
- [5] Kanai, K., "Semi-Empirical Formula for Seismic Characterization of the Ground," *Bulletin of Earthquake Research Institute*, University of Tokyo, Japan, Vol. 35, June 1967.
- [6] Lin, Y. K., *Probabilistic Theory of Structural Dynamics*, McGraw-Hill, New York, N.Y., 1967.
- [7] Rosenblueth, E. and Elorduy, J., "Responses of Linear Systems to Certain Transient Disturbances," *Proceedings*, Fourth World Conference on Earthquake Engineering, Vol. I, Santiago, Chile, 1969, pp. 185-196.
- [8] Ruiz, P., "On the Maximum Response of Structures Subjected to Earthquake Excitations," *Proceedings*, Fourth Symposium on Earthquake Engineering, Roorkee, India, 1970, pp. 272-277.
- [9] Ruiz, P. and Penzien, J., "PSEQGN - Artificial Generation of Earthquake Accelerograms," *Report No. EERC 69-3*, Earthquake Engineering Research Center, University of California, Berkeley, CA, March, 1968.
- [10] Singh, M. P., and Chu, S. L., "Stochastic Considerations in Seismic Analysis of Structures," *Earthquake Engineering and Structural Dynamics*, Vol. 4, No. 3, March, 1976, pp. 295-307.
- [11] Vanmarcke, E. H., "Properties of Spectral Moments with Application to Random Vibration," *Journal of the Engineering Mechanics Division*, ASCE, Vol. 98, No. EM2, Proc. Paper 8822, April 1972, pp. 425-446.
- [12] Vanmarcke, E. H., "On the Distribution of the First-Passage Time for Normal Stationary Random Processes," *Journal of Applied Mechanics*, Vol. 42, March 1975, pp. 215 -220.

Table 1. Summary of Results for Example Structure

Response Description	$R_{\tau}$						$\sigma_{R_{\tau}}$		
	simul.	Eq. 21	Eq. 24	Eq. 26	simul.	Eq. 22			
Roof displ., ft.	0.264	0.261 (-1)	0.256 (-2)	0.196 (-26)	0.052	0.048 (-8)			
Roof rot. $\times 10^2$ , rad.	0.231	0.245 (+6)	0.263 (+14)	0.536 (+132)	0.044	0.044 (+1)			
Roof accel., g.	1.430	1.416 (-1)	1.387 (-3)	1.044 (-27)	0.278	0.250 (-10)			
Roof ang. accel., rad/sec <sup>2</sup> .	0.402	0.430 (+7)	0.446 (+11)	0.929 (+131)	0.068	0.074 (+9)			
Base shear, kip.	1848	1840 (-0)	1830 (-1)	1386 (-25)	352	318 (-10)			
Base torque, kip-ft.	5454	5781 (+6)	6163 (+13)	12599 (+131)	1116	1037 (-6)			

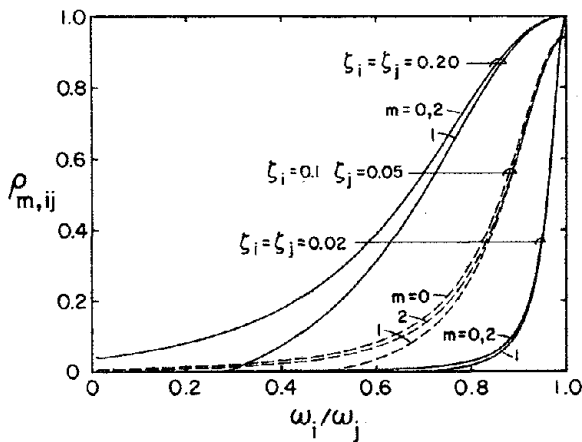


Fig. 1. Coefficients  $\rho_{m,ij}$  for Response to White Noise

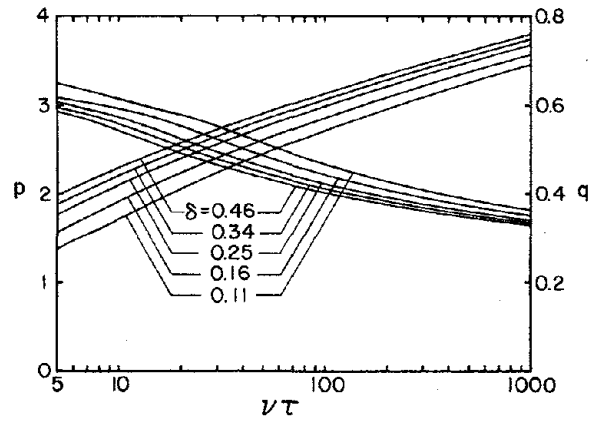


Fig. 2. Peak Factors for Stationary Gaussian Process

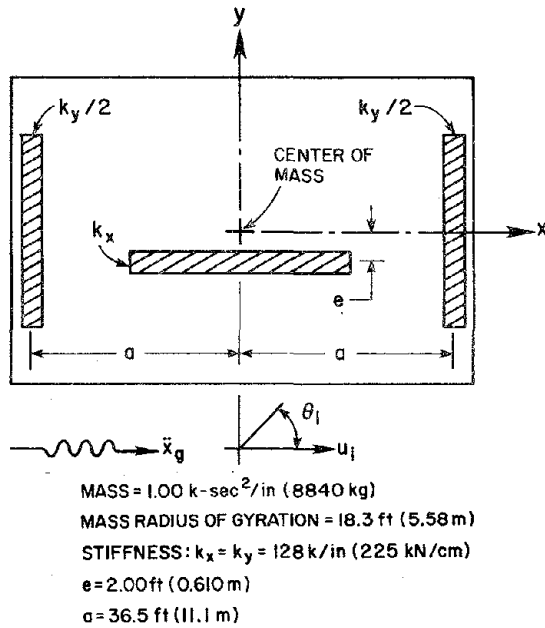


Fig. 3. Typical Floor Plan and Properties of Example Structure

Modal Properties

Mode	Freq., cps	Damp. ratio
1	2.00	0.05
2	2.11	0.05
3	5.84	0.05
4	6.17	0.05
5	9.20	0.05
6	9.72	0.05
7	11.80	0.05
8	12.50	0.05
9	13.50	0.05
10	14.20	0.05

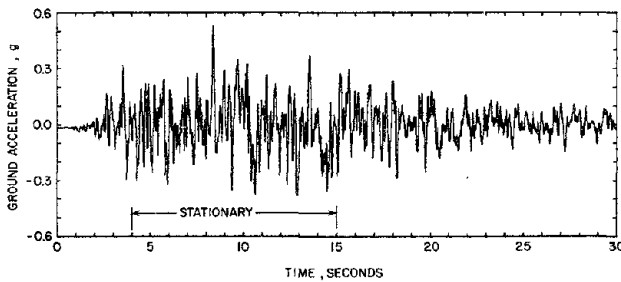


Fig. 4. Sample of Simulated Ground Motion

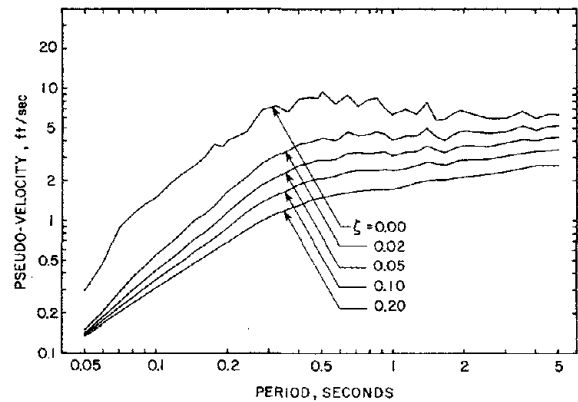


Fig. 5. Mean Response Spectra for Simulated Ground Motions

## BIAXIAL SHAKING TABLE STUDY OF A R/C FRAME

By M. G. Otiiva<sup>I</sup> and R. W. Clough<sup>II</sup>

## SUMMARY

Experimental earthquake testing of a large scale reinforced concrete frame with inelastic biaxial response was undertaken on the University of California shaking table. Comparison of results with response measured in a previous uniaxial test showed decreased capacity and greater stiffness degradation in the rectangular columns under biaxial loading. Evaluation of local bending mechanisms demonstrated a considerable degree of biaxial interaction when non-linear response occurred.

## INTRODUCTION

In the event of a major earthquake, large lateral forces will be induced in the structural framework of a typical building. The dynamic nature of the loading may produce biaxial inelastic bending in the columns at one moment, and then reverse the moments as well as the contribution to axial loading due to overturning effects, all within a fraction of a second. Yet, most buildings are designed only on the basis of static lateral loads (specified by code), applied independently to frames oriented parallel with the two principal axes of the structure.

Can a design based on such simplistic concepts resist the actual combination of peak bending moments and axial loads developed in the members, considering the entire history of deformation? While the structure is in the elastic state, the two biaxial concurrent loadings induce no interaction between the responses along their two axes; hence the code assumption may be valid for linear behavior. However, if inelastic response due to loading along one axis changes the resisting mechanism for motion along the other axis, then load independence between the axes ceases and the code design procedure would be highly questionable. The extent that such biaxial coupling occurs in the earthquake response of real structures is presently a matter of conjecture, and it was the purpose of this research to shed some light on this question.

Although the results of static biaxial tests on square columns with constant axial loads have shown varying amounts of interaction (1) (2) (3), they may not reflect the total influence that coupling could have when all load components vary randomly during inelastic earthquake response. Aktan, et al (4), tested a square column with lumped mass under earthquake motion and reported unexpected permanent displacement drift due to biaxial interaction effects when the yield displacement was exceeded by a factor of two or more. Jirsa (5) reviewed various other biaxial test programs and summarized similar results and conclusions.

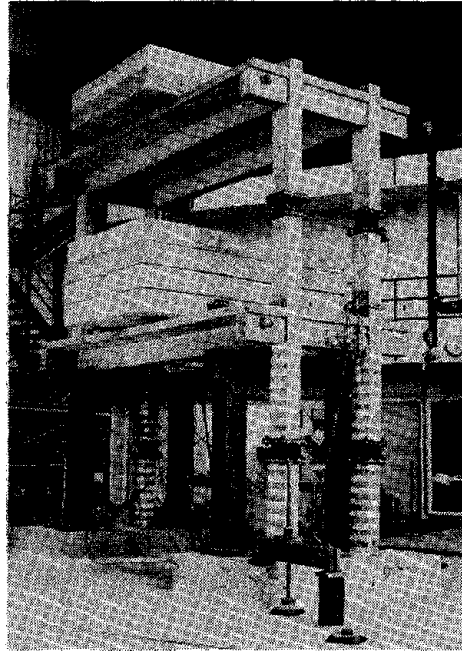
---

I. Research Assistant, University of California, Berkeley

II. Professor of Civil Engineering, University of California, Berkeley

All of the reported tests either neglected the effects of axial load or considered only square column sections. Varying axial load may have serious effects on the strain history of the reinforcing and on the instantaneous effective concrete section. Square columns have no specific principal axes of flexural rigidity and would be expected to exhibit less biaxial response coupling than rectangular columns. The very nature of the rectangular column, with different moments of inertia along its principal axes, can be expected to induce exaggerated interaction effects under biaxial loading.

Fig. 1 Model Test Structure On the Shaking Table



#### EXPERIMENTAL STUDY

In the present investigation, this biaxial response interaction mechanism was studied by means of experimental testing of a two-story reinforced concrete frame on the University of California, Earthquake Engineering Research Center's 20 ft. square shaking table. The seven-tenths scale model was subjected to intense earthquake motions applied at a skew angle relative to the structure's principal axes, thereby inducing significant biaxial column bending and overturning moments. The test structure, shown in Fig. 1, is identical to a frame tested previously under uniaxial motion applied along the model's major principal axis (6). Results of the previous tests thus serve as a control for comparison with the biaxial response of the frame in the present study.

Overall dimensions of the frame are illustrated in Fig. 2; the 7/10 scale allowed the use of normal reinforced concrete materials and fabrication procedures, and avoided the problems associated with modeling nonlinear behavior at small scales. The frame has a single bay in each direction; the four columns are connected by longitudinal and transverse 'T' beams cast integrally with the floor slab at each level. The columns have four

5/8 in. (1.6 cm.) diameter longitudinal reinforcing bars with 1/4 in. stirrups at 1-3/8 in. spacing, as shown in Fig. 3. The model was mounted on the shaking table with its longitudinal axis at a twenty-five degree angle to the horizontal excitation axis of the shaking table. A plan view of the frame and table layout is shown in Fig. 4; also indicated are the pretest first mode vibration frequencies along the longitudinal "stiff" axis and the transverse "weak" axis.

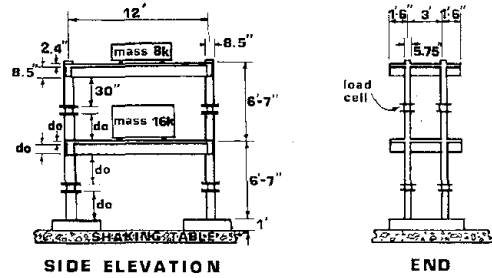


Fig. 2 Test Structure Dimensions

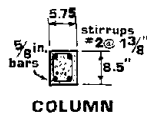


Fig. 3 Column Dimensions

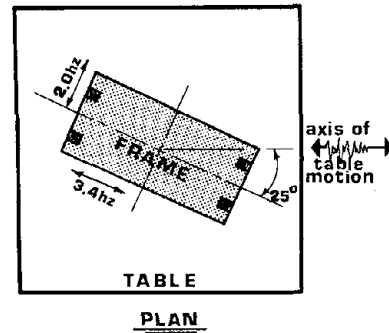


Fig. 4 Orientation on Table

The major excitation signal applied to the structure by the shaking table (Fig. 5) was derived from the Taft, California 1952 earthquake accelerogram. The maximum velocity applied in the strongest intensity test was 32.5 in/sec. (82.6 cm. sec.); the corresponding peak table acceleration was .7g and the maximum table displacement was 5 in. (12.7 cm.). More than one hundred forty transducers of various types were used to monitor the shaking table motion and frame response; measured quantities included accelerations, displacements, column forces, member curvatures and strains in reinforcing bars.

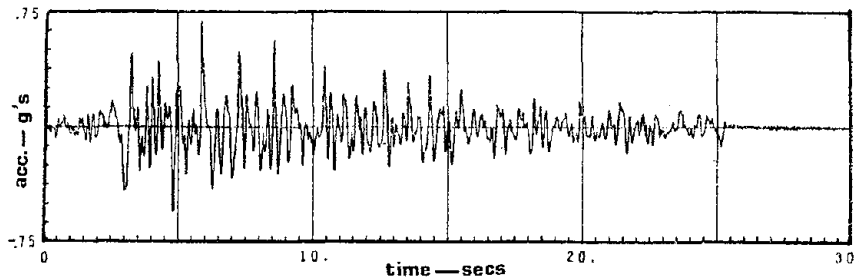


Fig. 5 Taft Earthquake - Table Acceleration History

## DYNAMIC RESPONSE BEHAVIOR

The biaxial nature of the response displacements is apparent in the trace of the motion shown in Fig. 6 as viewed from above. Indicated displacements were measured at the top of the first floor column shown as a darkened rectangle at the far left in Fig. 4 and show motions relative to the shaking table. The column's strong and weak axes coincide with the longitudinal and transverse axes of the frame. The maximum displacement loop toward the lower right in Figure 6 is in a direction nearly perpendicular to the axis of table motion; that axis is 25 degrees counter-clockwise from the horizontal plot axis.

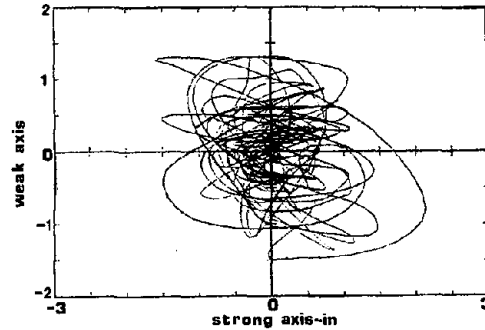


Fig. 6 Displacement Trace of Top of Column

If the first floor longitudinal component of this biaxial response (measured on Test Structure RCF5) is compared with the first floor displacements measured in the previous equivalent uniaxial tests (Structure RCF2) the two records are remarkably similar. The only major difference between the longitudinal displacement histories of the two frames is the increased degradation of stiffness resulting from biaxial damage. This degradation is evidenced by the increased first mode longitudinal vibration period, shown marked on the response spectrum for the test motion (Fig. 7). The uniaxial test frame (RCF2) showed a smaller change of period (0.32 to 0.49 sec.) in the corresponding test, thus demonstrating a lesser degree of damage.

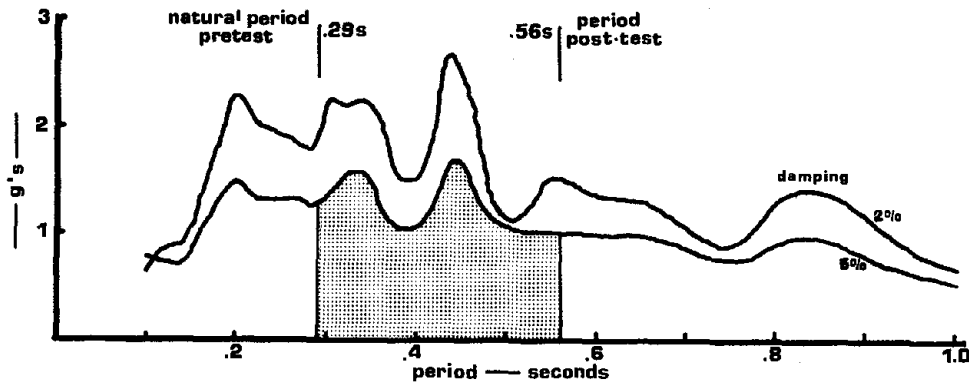


Fig. 7 Pseudo-acceleration Response Spectrum of Table Motion and Variation of Model Period

Most of the inelastic deformation and damage to the structure occurred at the extremities of the lower columns, with spalling and concrete crushing initiated at the corners (Figure 8). Greater visible column damage was apparent in the present biaxial frame than was seen in the earlier uniaxial



test. However, there was virtually no visible beam damage in the present frame, whereas cracking was evident through the full depth of the beams in the previous tests; hence it may be inferred that less force was transferred between beams and columns in the biaxial test.

The smaller column forces developed in the biaxial test (RCF5), as compared with the uniaxial test (RCF2) are apparent in Fig. 9, where column shear along the longitudinal axis is plotted against longitudinal displacement of the test structure. Though the initial column stiffness ( $k$ ) was



Fig. 8 Damage at Column Base

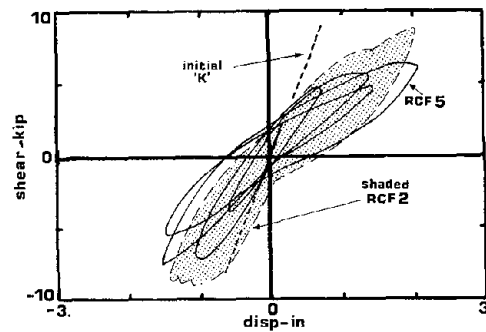
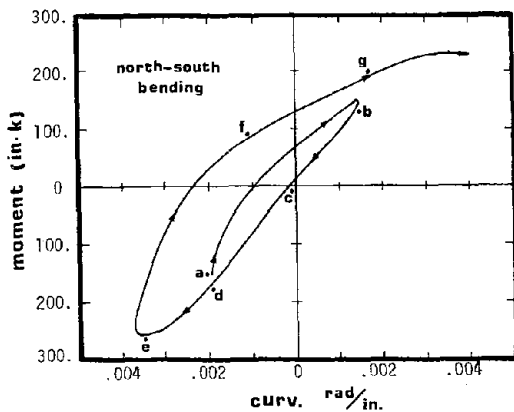


Fig. 9 Column Force-Displacement

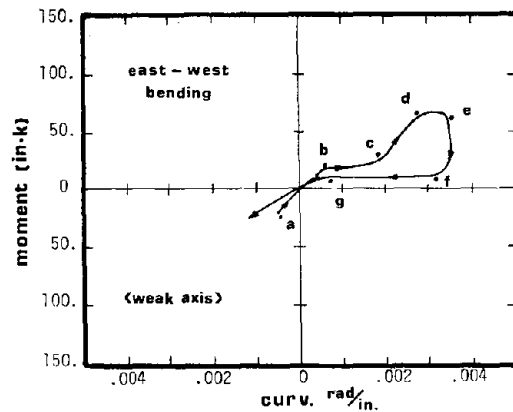
identical for both frames, greater stiffness degradation is apparent in the biaxial loading test of RCF5. Moreover, the multiaxial load combination obviously decreases the yield capacity of the frame below that available in uniaxial loading.

EVALUATION OF RESPONSE MECHANISM

Detailed studies of the local column response in terms of the moment-curvature relationship indicate a considerable amount of coupling occurring between the response in the two axes. Figures 10a and b are plots of the moment-curvature history at the column base during a period of intense motion.



(a) North-South Axis



(b) East-West Axis

Fig. 10 Moment-Curvature Variation at Column Base

The bending response is separated into components along the major (north-south) axis and minor (east-west) axis. Positive moments correspond with compression on the south and west column faces respectively. Letters indicate corresponding points in time on each of the plots. The interval plotted extends from 5.68 seconds to 6.38 seconds in the earthquake record, but similar behavior, indicating significant strong axis influence on weak axis moments is evident in the entire response history after the first large displacement excursion at 3.14 seconds.

The nature of the response interaction becomes understandable if the moment-curvature results of Figs. 10a and b are considered in conjunction with the axial load variation, with the cracking condition of the confined and cover concrete, and with the reinforcing bar strain history and instantaneous stiffness. Prior to the start of the interval at 5.68 seconds, the reinforcing bars already have permanent residual strains ranging from 0.3% to 1.0% and have been strained to a maximum of 1.5%. The concrete has developed open residual cracks through the entire concrete cross section (in the absence of significant compression forces.) Loss of bond between concrete and steel was detected over at least a 3 in. length on one of the bars and the steel strains listed above justify assumption of bond loss over segments of all of the bars at the column-to-footing joint. Calculated concrete strains indicate that crushing of some of the concrete cover has occurred at the two corners on the north column face.

In the interval shown between points 'b' and 'c', for instance, the weak axis east-west bending plot has a plateau of low apparent stiffness while the north-south (strong) component is unloading from a southerly peak at 'b'. The north-south component bending moment changes from positive 145 in.-k (16.4kN-m) to a value of zero, while the east-west component increases slightly from positive 11 in.-k (1.2kN-m) to 21 in.-k (2.4kN-m). During the short 'b-c' period (0.12 sec.) the axial load increases from 3.0 kips (13kN) to 21.8 kips (97kN) as a result of changing overturning moments.

At point 'b', under low axial load and high residual bar strains, the entire column was cracked open and the bar in the south-west corner was yielding in compression, while the bar in the southeast corner was near compressive yielding. By the time of point 'c', the open crack along the north face of the column resulting from the south moment at 'b' had closed at its west corner under the increased axial load and relatively constant west moment. The reinforcing bar at the northwest corner was yielding in compression, the southwest bar was under elastic compression and the southeast bar changed from near compressive yield to tension. The large change of strain in the southeast bar and the yielding northwest bar caused a rotation in the column about an axis running roughly through the northeast and southwest corners.

Thus an apparent east-west component of rotation occurred while the column was under constant moment, and produced the flat segment in the east-west moment curvature diagram. Similar changes in apparent stiffness have been detected when the concrete cover at a corner reached its crushing strain, effectively reducing the section size along both axes.

Unexpected deformations also occurred when decreasing axial loads affected the yield strain in specified bars, while other bars remained elastic under constant moment.

#### CONCLUSION

Studies of the test data have verified that the resisting capacities of the structure are reduced under multiaxial loading as expected; also a marked degree of response interaction has been demonstrated when non-linear motion involving changes in the section stiffness occurred. In the test structure which has rectangular columns with distinct strong and weak axes, the biaxial coupling occurred predominantly in the form of a significant strong axis influence on weak axis response.

Correlation studies are now being undertaken to compare the experimental test results with predictions from various types of computer analysis. Methods considered include combining 2-D frame analyses along separate axes and using 3-D degrading stiffness modeling of the entire structure. The vast amount of test data that has been obtained during this investigation warrants extensive study, and the final report on the project will not be completed for several months.

#### REFERENCES

1. Takiguchi, K., and Kokoshu, S., "Hysteretic Behavior of Reinforced Concrete Members Subjected to Biaxial Bending Moments," Sec. 11, Dynamic Behavior of Structural Elements, 6th World Conference on Earthquake Engineering, 1977.
2. Okada, Seki, Asai, "Response of Reinforced Concrete Columns to Bi-Directional Horizontal Force and Constant Axial Force," BULL. ERS No. 10, Earthquake Resistant Structural Research Center, Institute of Industrial Science, University of Tokyo, 1976.
3. Takizawa, and Aoyama, H., "Earthquake Response of R/C Structures," J. Earthquake Engineering and Structural Dynamics, Vol 4, 523-552, 1976.
4. Aktan, A.E., Pecknold, D.A., Sozen, M.A., "R/C Column Earthquake Response in Two Dimensions," J. Structural Division, ASCE, Vol 100, No. ST10, 1999-2015, 1974.
5. Jirsa, J.O., Maruyama, K. and Ramiroz, H., "Reinforced Concrete Columns Under Three-Dimensional Loading Histories", Symposium on Nonlinear Behavior of Reinforced Concrete and Prestressed Concrete Structures, ACI Fall Convention, Houston, Nov. 1978.
6. Clough, R.W., and Gidwani, J., "Reinforced Concrete Frame 2 - Seismic Testing and Analytical Correlation," Earthquake Engineering Research Center, EERC Report No. 76-15, University of California, June, 1976.



## SLOSHING OF LIQUIDS IN RIGID ANNULAR CYLINDRICAL AND TORUS TANKS DUE TO SEISMIC GROUND MOTIONS

M. Aslam,<sup>I</sup> W. G. Godden,<sup>II</sup> and D. T. Scalise<sup>III</sup>

### SUMMARY

Sloshing response and impulsive hydrodynamic pressures in rigid axisymmetric tanks due to horizontal ground motions are predicted by theoretical solutions based on series and finite element analysis. Results are compared with experimental data from model tests conducted on a 20 ft × 20 ft earthquake simulator.

### INTRODUCTION

The general problem of sloshing of liquid in containers due to dynamic excitation is one that has received considerable attention in the literature, and selected references are given [1,2,3,4]. This paper deals with sloshing in annular cylindrical and torus tanks due to horizontal seismic ground motions. Tanks of this type are used as pressure-suppression pools in Boiling Water Nuclear Reactors and have the following typical overall dimensions: annular tank - 120 ft. OD, 80 ft. ID, water depth - 20 ft.; torus tank - 140 ft. OD, 80 ft. ID, water depth - 15 ft.

Sloshing could lead to the danger of superheated steam escaping if, under dynamic conditions, the water level was to drop below Section C-C on the Mark III Suppression Pool of Fig. 1. Hence, it is important to be able to predict maximum water surface displacements for any prescribed seismic ground motion.

This paper presents the results of both experimental and analytical studies on the sloshing of water in both types of tanks subjected to arbitrary ground motions. Tests were done on model tanks on a shaking table. Two analytical procedures were developed; one based on a series solution and the other on the finite element method.

### ANALYSIS

Assumptions: The analysis is based on three assumptions:

(1) displacements are small and thus linear theory is applicable; (2) the tank is assumed to be rigid (the heavy structures used for suppression pools makes this a realistic assumption and even in more flexible tanks the assumption may still be valid as the primary sloshing response is a low frequency phenomenon); (3) water is assumed to be an incompressible and nonviscous fluid. Thus the flow remains irrotational.

- 
- I Senior Engineer, Bechtel Corporation, San Francisco, California.
  - II Professor of Civil Engineering, University of California, Berkeley, California.
  - III Department Head, Engineering Sciences Department, Lawrence Berkeley Laboratory, University of California, Berkeley.

This work was supported by the U. S. Department of Energy under Contract W-7405-ENG-48.

The first solution (series solution) which involves Bessel functions is applicable to annular tanks. The second solution, based on the finite element method is applicable to all axisymmetric tanks. The velocity potential  $\phi$  is taken as the primary variable and the sloshing displacements and impulsive pressures are derived from it. The equations of motion and both solutions are briefly described as follows:

Series Solution for Annular Tanks: In the annular tank of Fig. 2, as the flow is assumed to be irrotational there exists a velocity potential  $\phi$  that must satisfy the Laplace equation,

$$\frac{\partial^2 \phi}{\partial r^2} + \frac{1}{r} \frac{\partial \phi}{\partial r} + \frac{1}{r^2} \frac{\partial^2 \phi}{\partial \theta^2} + \frac{\partial^2 \phi}{\partial z^2} = 0 \quad (1)$$

Let  $a$  and  $b$  be the outer and inner radii of the annular tank and  $h$  be the depth of water, then the following boundary conditions must be satisfied:

$$\left. \frac{\partial \phi}{\partial r} \right|_{r=a} = \dot{x} \cos \theta, \quad \left. \frac{\partial \phi}{\partial r} \right|_{r=b} = \dot{x} \cos \theta, \quad \left. \frac{\partial \phi}{\partial z} \right|_{z=-h} = 0 \quad (2-4)$$

in which  $\dot{x} = dx/dt =$  tank wall velocity; and  $t =$  time. Also, the linearized free-surface boundary conditions is [5]

$$\frac{\partial^2 \phi}{\partial t^2} + g \frac{\partial \phi}{\partial z} = 0 \quad \text{at } z=0 \quad (5)$$

in which  $g =$  the acceleration of gravity. The solution to Eq. 1 subject to the above boundary conditions and at rest initial conditions is

$$\phi = \cos \theta \left[ r\dot{x} - a \sum_{n=0}^{\infty} A_n \frac{\cosh \xi_n \left( \frac{z}{a} + \frac{h}{a} \right) C_1 \left( \xi_n \frac{r}{a} \right)}{\omega_n \cosh \left( \xi_n \frac{h}{a} \right)} T_n(t) \right] \quad (6)$$

in which

$$T_n(t) = \sin \omega_n t \int_0^t \ddot{x} \cos \omega_n \tau d\tau - \cos \omega_n t \int_0^t \ddot{x} \sin \omega_n \tau d\tau \quad (7)$$

$$C_1 \left( \xi_n \frac{r}{a} \right) = J_1 \left( \xi_n \frac{r}{a} \right) Y_1'(\xi_n) - J_1'(\xi_n) Y_1 \left( \xi_n \frac{r}{a} \right) \quad (8)$$

$$A_n = \frac{2 \left[ \frac{2}{\pi \xi_n} - K C_1(K \xi_n) \right]}{\frac{4}{\pi^2} \xi_n^2 (\xi_n^2 - 1) + C_1^2(K \xi_n) (1 - K^2 \xi_n^2)} \quad (9)$$

and  $\xi_n$  are the roots of the equation

$$J_1'(\xi_n)Y_1'(K\xi_n) - J_1'(K\xi_n)Y_1'(\xi_n) = 0 \quad (10)$$

with  $K = b/a$ . The mode shapes are given by Eq. 8 and the frequencies  $\omega_n$  are given by:

$$\omega_n = \frac{g}{a} \xi_n \tanh\left(\xi_n \frac{h}{a}\right) \quad (11)$$

In Eq. 8,  $J_1$  and  $Y_1$  are Bessel functions of the first and second kind and primes indicate their derivatives. Eq. 6 is the general expression for the velocity potential in an annular-circular tank. Once the expression for velocity potential is known, the surface displacements  $\delta(r, \theta, z, t)$  and the impulsive hydrodynamic pressures  $p(r, \theta, z, t)$  anywhere in the fluid are derived from  $\phi$  and given by the following expressions.

$$\delta(r, \theta, z, t) = -\frac{\cos\theta}{g} \left[ r\ddot{x} - a \sum_{n=0}^{\infty} A_n \frac{\cosh\xi_n \left(\frac{z}{a} + \frac{h}{a}\right) C_1 \left(\xi_n \frac{r}{a}\right)}{\cosh\left(\xi_n \frac{h}{a}\right)} \left( \cos\omega_n t \int_0^t \ddot{x} \cos\omega_n \tau d\tau + \sin\omega_n t \int_0^t \ddot{x} \sin\omega_n \tau d\tau \right) \right] \quad (12)$$

$$p(r, \theta, z, t) = -\rho \cos\theta \left[ r\ddot{x} - a \sum_{n=0}^{\infty} A_n \frac{\cosh\xi_n \left(\frac{z}{a} + \frac{h}{a}\right) C_1 \xi_n \frac{r}{a}}{\cosh\left(\xi_n \frac{h}{a}\right)} \left( \cos\omega_n t \int_0^t \ddot{x} \cos\omega_n \tau d\tau + \sin\omega_n t \int_0^t \ddot{x} \sin\omega_n \tau d\tau \right) \right] \quad (13)$$

#### Finite Element Analysis

Figure 4 shows a rigid wall tank of arbitrary shape filled with a liquid and whose free surface area is  $B_2$ .  $B_1$  represents the surface area of liquid in contact with the solid boundary of the container.  $V$  is the volume of the liquid and  $\delta$  is the surface water displacement. The velocity potential  $\phi$  which must satisfy Laplace equation is written in rectangular coordinates as:

$$\frac{\partial^2 \phi}{\partial x^2} + \frac{\partial^2 \phi}{\partial y^2} + \frac{\partial^2 \phi}{\partial z^2} = 0 \quad (14)$$

If  $v_n(t)$  = velocity of the tank wall along its outward normal to the boundary at any point, then:

$$\frac{\partial \phi}{\partial n} = v_n(t) \quad \text{on } B1 \quad (15)$$

For the finite element analysis we assume that

$$\phi = \sum_1^N N_j(x,y,z) \phi_j(t) \quad (16)$$

in which  $N_j$  are the shape functions and  $\phi_j(t)$  are the nodal values of the field variable  $\phi$ . Substituting Eq. 16 into Eqs. 14, 15 and 5, using the Galerkin principle [7,8,9,10,11] and applying the Divergence theorem we obtain:

$$\begin{aligned} & \int_B N_i \left[ \sum_1^N \frac{\partial N_j}{\partial x} l_x \phi_j + \sum_1^N \frac{\partial N_j}{\partial y} l_y \phi_j + \sum_1^N \frac{\partial N_j}{\partial z} l_z \phi_j \right] ds \\ & - \int_V \left[ \frac{\partial N_i}{\partial x} \sum_1^N \frac{\partial N_j}{\partial x} \phi_j + \frac{\partial N_i}{\partial y} \sum_1^N \frac{\partial N_j}{\partial y} \phi_j + \frac{\partial N_i}{\partial z} \sum_1^N \frac{\partial N_j}{\partial z} \phi_j \right] dv \\ & = \int_{B1} N_i \sum_1^N \frac{\partial N_j}{\partial n} \phi_j ds - \int_{B1} N_i v_n ds \\ & \quad + \frac{1}{g} \int_{B2} N_i \sum_1^N N_j \ddot{\phi} ds + \int_{B2} N_i \sum_1^N \frac{\partial N_j}{\partial z} \phi_j ds \end{aligned} \quad (17)$$

in which  $\ddot{\phi} = d^2\phi/dt^2$ ,  $B = B1+B2$ , and  $l_x$ ,  $l_y$  and  $l_z$  are direction cosines, and  $\int dv$  and  $\int ds$  represent the integrals over the volume and appropriate surfaces respectively. Using the approximation  $\partial N_i/\partial z = \partial N_i/\partial n$ , Eq. 17 can be simplified to the following form

$$\underline{M} \ddot{\phi} + \underline{K} \phi = \underline{F} \quad (18)$$

in which the elements of matrices  $\underline{M}$ ,  $\underline{K}$  and  $\underline{F}$  are given by

$$M_{ij} = \frac{1}{g} \sum_{EB2} N_i N_j ds \quad (19)$$

$$K_{ij} = \sum_{EV} \left[ \frac{\partial N_i}{\partial x} \frac{\partial N_j}{\partial x} + \frac{\partial N_i}{\partial y} \frac{\partial N_j}{\partial y} + \frac{\partial N_i}{\partial z} \frac{\partial N_j}{\partial z} \right] dv \quad (20)$$

$$F_i = \sum_{EB1} N_i v_n ds \quad (21)$$

where summation for  $M_{ij}$  covers only the elements on the free surface boundary and the integral is carried out on the free surfaces of each



element EB2. Summation for  $K_{ij}$  covers the contribution of each fluid element and EV is the element region. EB1 refers only to the elements which lie on the solid boundary B1, and the loading term thus is associated with the elements that lie on the tank wall boundary. The free surface matrix M and the fluid matrix K are comparable to the mass and stiffness matrices respectively used in structural mechanics.

The finite element equations derived above apply to a general 3-dimensional case. However, in this study these equations were specialized to axisymmetric tanks [6] and the computer code was written to predict the hydrodynamic pressures p and sloshing displacements  $\delta$  for arbitrary horizontal ground motions given by the following

$$\delta = -\frac{1}{g} \frac{\partial \phi}{\partial t} \quad (22)$$

$$p = -\frac{\rho \partial \phi}{\partial t} \quad (23)$$

in which  $\rho$  is the mass density of the fluid.

#### MODEL TESTS AND CORRELATION WITH ANALYSIS

Tests were conducted on a 20-ft  $\times$  20-ft (6-m  $\times$  6-m) shaking table at the University of California, Berkeley [12]. Annular tank tests used a 1/15th scale model of a Mark III suppression pool consisting of an 8 ft. (2.4-m) diameter steel tank with observation windows and an inside diameter of 5 ft. 6 in. (1.7 m) (Fig. 3). Torus tank tests used a 1/60th scale model of a Mark I suppression pool (Fig. 5). In both cases time-scaled accelerograms of the El Centro (1940) and Parkfield earthquakes were applied in increasing amplitudes to determine the range of linear behavior. Wave heights and dynamic pressures were recorded at selected locations.

Analytical results for wave heights as predicted by the series solution for annular tanks are compared with test data in Fig. 6 for two different intensities of the El Centro 1940 ground motion. In Fig. 6a the results are well within the linear range and comparison with theory is accurate, and this also applied to similar results for the ground motion applied at the actual intensity. Increasing the intensity by approximately 40% above actual produced some nonlinear behavior as shown in Fig. 6b. The range of linearity will depend on the predominant response mode as well as on the tank and the water depth: in the case shown the motion was primarily in the first radial mode and the limit of linearity was associated with a maximum water surface gradient of 1/5. The annular tank theory also gave good results for simple cylindrical tanks by letting the inner radius approach zero. Comparison of the finite element solution with the test results for the torus tank are shown in Fig. 7 and indicate a similar level of agreement. In both solutions the correlation between measured and computed hydrodynamic pressures was very close.

## CONCLUSIONS

The correlation between measured and computed data indicate that the linearized small displacement theory developed for annular cylindrical or torus tanks can satisfactorily predict the sloshing displacements and hydrodynamic pressures in typical reactor suppression pools under the action of strong ground motions such as the El Centro 1940 and the Parkfield earthquakes. The theory is also applicable to plain cylindrical tanks by letting the inner radius approach zero.

## REFERENCES

1. Bauer, H. F., "The Dynamic Behavior of Liquids in Moving Containers," National Aeronautics and Space Administration, Washington, D. C., 1966, edited by Abramson, H. Norman.
2. Clough, D. P., "Experimental Evaluation of Seismic Design Methods for Broad Cylindrical Tanks," Ph.D. Dissertation, University of California, Berkeley, 1976.
3. Veletsos, A. S. and Yang, J. Y., "Dynamics of Fixed-Base Liquid Storage Tank," U. S., Japan Seminar on Lifelines, 1976.
4. Luk, C. H., "Finite Element Analysis for Liquid Sloshing Problems," Office of Aerospace Research, U. S. Air Force Report No. 69-1504 TR, 1969.
5. Stoker, J. J., "Water Waves," Interscience Publishers, Inc., New York, N. Y. 1957.
6. Aslam, M., "Earthquake Induced Sloshing in Axisymmetric Tanks," Ph.D. Dissertation, University of California, Berkeley, 1978.
7. Crandall, S., "Engineering Analysis," McGraw-Hill, New York, 1965.
8. Finlaysan, B. A., "The Method of Weighted Residuals," Applied Mechanics Reviews, Vol. 19 No. 9, September 1966.
9. Hutton, S. G., "Finite Element Method-Galerkin Approach," Journal of Engineering Mechanics Division, Vol. 97 No. EM5, October 1971.
10. Zienkiewicz, O. C. and Perekh, C. J., "Transient Field Problems: Two-Dimensional and Three-Dimensional Analysis by Isoparametric Finite Elements," International Journal of Numerical Methods in Engineering, Vol. 2, No. 1, June 1970.
11. Pinder, G. P., "Application of Galerkin Procedure to Aquifer Problems," ASCE Journal of Water Resources, Vol. 8 No. 1, February 1972.
12. Rea, D., and Penzien, J., "Structural Research Using an Earthquake Simulator," Proceedings, Structural Engineering Association of California Conference, Monterey, California 1972.

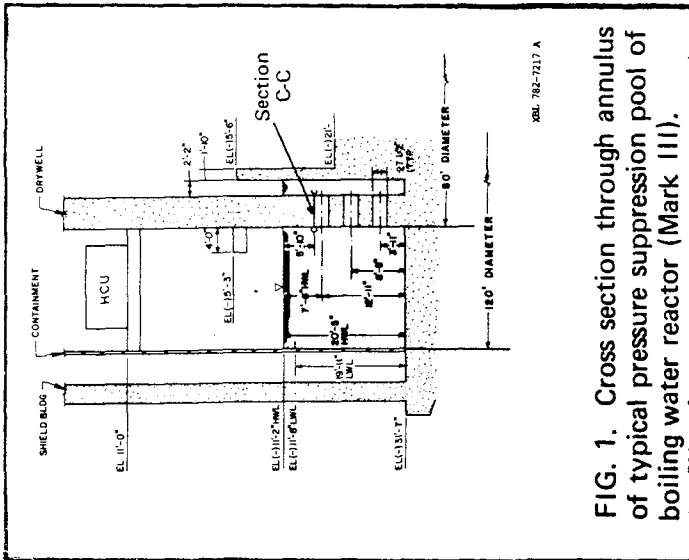


FIG. 1. Cross section through annulus of typical pressure suppression pool of boiling water reactor (Mark III).

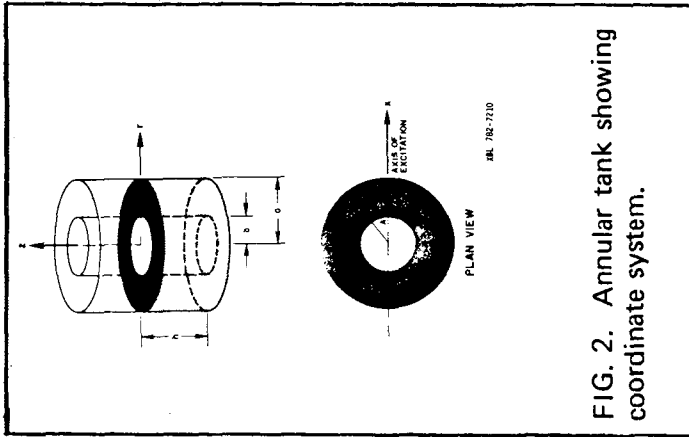
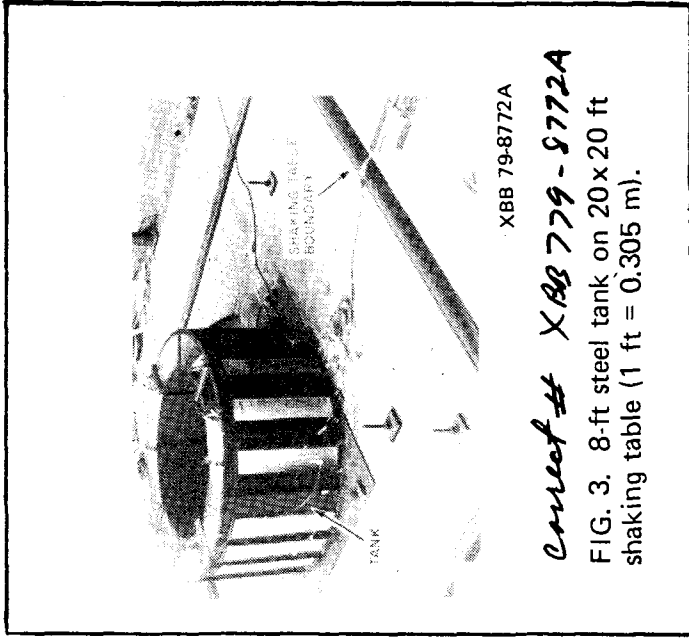


FIG. 2. Annular tank showing coordinate system.



XBB 79-8772A

*Correct # XBB 779-9772A*

FIG. 3. 8-ft steel tank on 20 x 20 ft shaking table (1 ft = 0.305 m).

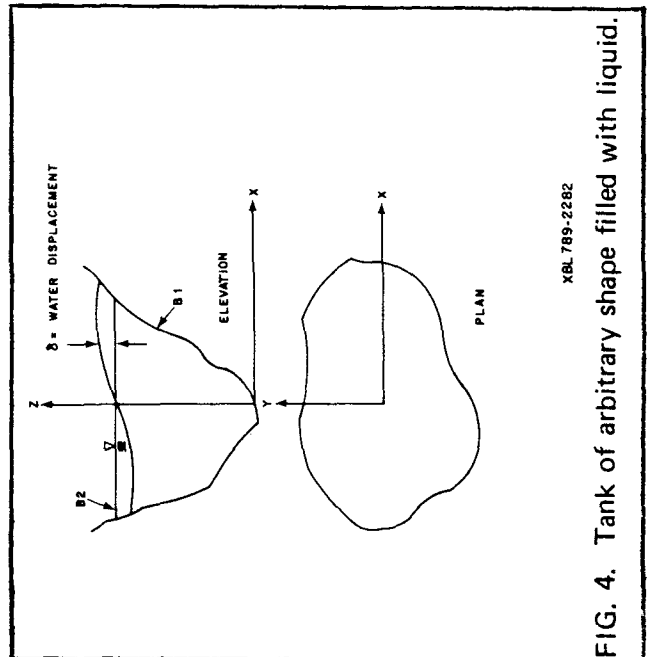
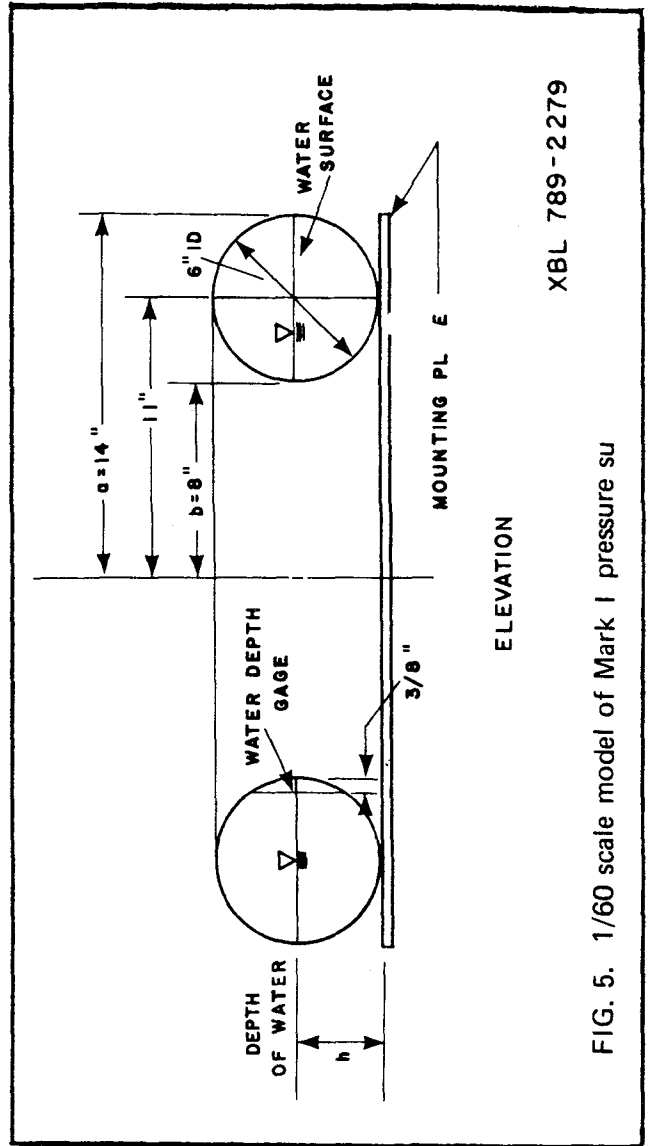


FIG. 4. Tank of arbitrary shape filled with liquid.

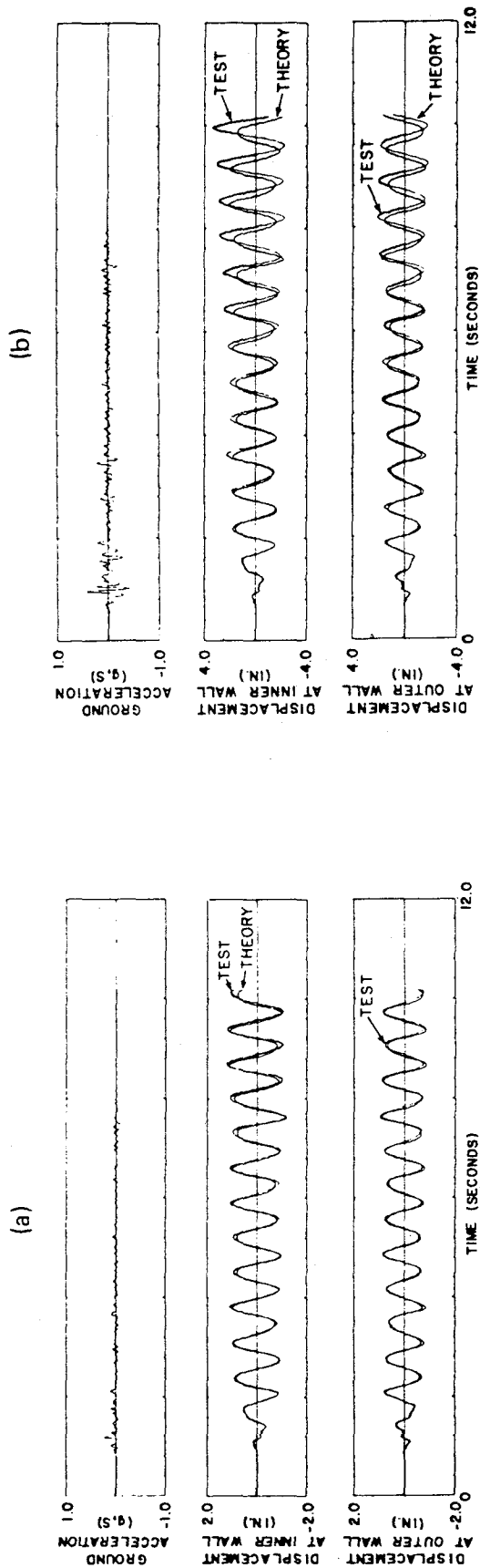
XBL 789-2282



ELEVATION

XBL 789-2279

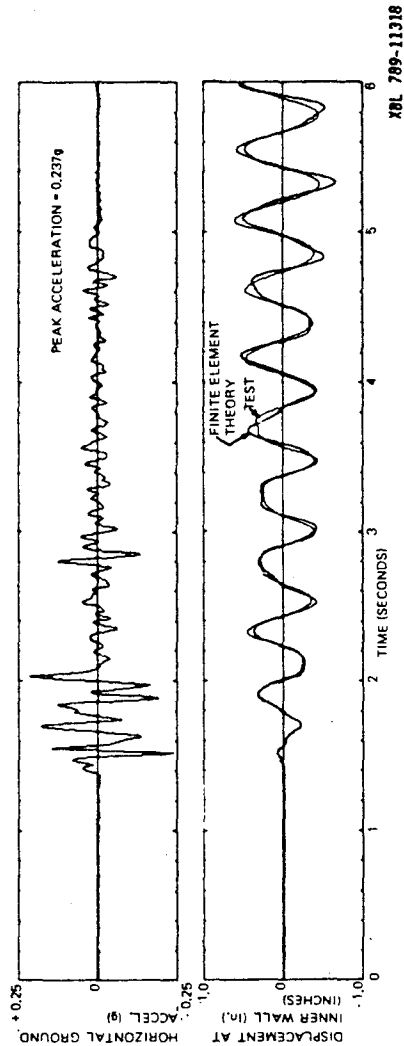
FIG. 5. 1/60 scale model of Mark I pressure su



XBL782 7209A

XBL782-7216A

FIG. 6. Sloshing response of water in annular tank model (inner radius = 33.2 in., outer radius = 48.0 in., depth of water = 16.0 in.) under scaled El Centro 1940 earthquake. [Comparison of theory and test (1 inch = 25.4 mm)] (a) Peak acceleration = 0.24 g; (b) Peak acceleration = 0.44 g.



XBL 789-11318

FIG. 7. Sloshing response of water in Torus Tank Model (inner radius = 8 in., outer radius = 14 in., depth of water = 3 in.). Test and finite element results for surface displacements.

## SEISMIC BEHAVIOR OF MASONRY BUILDINGS

by

Pedro A. Hidalgo<sup>1</sup>, Ronald L. Mayes<sup>2</sup>, and Hugh D. McNiven<sup>3</sup>

## ABSTRACT

Experiments have been conducted to evaluate the seismic behavior of window piers typical of high-rise masonry construction. Sixty-three fixed ended piers were subjected to cyclic, in-plane shear loads. Principal test parameters were the type of masonry construction, the height-to-width ratio, the amount of reinforcement and the effect of full and partial grouting. An identification of the principal modes of failure is presented. Also included is a proposition to predict the ultimate strength associated with the shear mode of failure on the basis of the experimental data, as it becomes available. Finally, the effect of the test parameters on the inelastic characteristic of piers exhibiting the shear mode of failure is discussed.

## INTRODUCTION

This paper describes the main findings of a masonry research program that has been carried since 1972 at the Earthquake Engineering Research Center of the University of California, Berkeley. The first objective of this program is to carry out an experimental study on the inelastic seismic behavior of structural components of shear walls typical of multistory masonry buildings (Fig. 1). The second is to use the experimental data to formulate mathematical models of the inelastic behavior of the structural elements for inclusion in computer programs. These computer programs permit the prediction of the response of multistory masonry buildings to ground earthquake excitation.

Two structural elements can be found in the shear wall panels shown in Fig. 1, the piers and the spandrel beams. The results presented herein only refer to the experimental phase of the research program associated with piers. Initially, a pilot series of seventeen concrete block double pier panels were tested as shown in Fig. 2. Deep spandrel beams at both top and bottom of the piers prevented the rotation of the end sections of the piers. These tests were intended to study the effect of rate of loading, bearing load and types of reinforcing on the inelastic behavior of the piers [1]. The test results [2] validated other results on cantilever piers [3] showing that piers failing in the flexural mode of failure have desirable inelastic behavior. It was also concluded that the rate of loading does not have a significant effect on the ultimate strength of the piers and consequently a low cyclic frequency was adopted for the rest of that program. Moreover, the results demonstrated the need for more extensive tests on piers failing in the shear mode, in order to establish definitive parametric relationships.

---

<sup>1</sup> Visiting Associate Research Engineer, Earthquake Engineering Research Center (EERC), University of California, Berkeley, California.

<sup>2</sup> Assistant Research Engineer, EERC, University of California, Berkeley, Calif. and Principal Computech, Berkeley, California.

<sup>3</sup> Professor of Engineering Science, University of California, Berkeley, Calif.

The cost of the double pier tests, both in time and money, precluded carrying out the extensive parametric study using this test procedure, and consequently a single pier system was devised (Fig.3), which greatly simplified the investigation. In this test setup, two hinged external steel columns restrain the rotation of the top of the pier, forcing it towards the same condition of rotation fixity at top and bottom sections that was developed in the double pier test system (Fig. 2). The parameters of the sixty-three single pier tests included the type of masonry material, the height-to-width ratio of the piers, the type of grouting and the amount of horizontal reinforcement. The test results of the single pier test program have been reported in detail elsewhere [4,5]. This paper presents the major conclusions on how the parameters mentioned above affect the ultimate shear strength and the inelastic behavior of the piers.

Although the bearing load was not included as one of the parameters of the single pier test program, the value of the compressive vertical load acting on the pier increased as the in-plane horizontal displacement of the test specimen increased, due to the natural tendency of the steel columns to maintain a constant length (Fig. 3). This circumstance distorted the results in two ways; first, it changed the mode of failure of some of the piers, and second, the inelastic behavior of the piers, after the major diagonal cracks have occurred, may be different from the behavior observed in the tests reported here. These conclusions have been validated by preliminary tests carried out using a modified single pier test setup that eliminated the additional compressive load on the piers. The modification consisted of replacing the steel columns by vertical actuators; these actuators are commanded to impose forces of equal value but opposite sign at two sides of the pier and the magnitude of the forces is selected to maintain the point of inflection of the deformed shape at the mid-height of the pier. The modified single pier test setup permits the test to be developed under any desired constant bearing load and a series of tests is presently under way to ratify or modify the results concerning the inelastic behavior of the piers after major diagonal cracks have occurred.

#### TEST PROGRAM AND TEST PROCEDURE

Three types of masonry material were used throughout the pier test program, namely hollow concrete block (HCBL), hollow clay brick (HCBR) and double wythe grouted core clay brick piers (CBRC). The HCBL piers were constructed from standard two-core reinforceable hollow concrete blocks, nominally 8 in. (20 cm) wide by 8 in. (20 cm) high by 16 in. (40 cm) long. The HCBR piers were constructed from standard two-core reinforceable hollow clay bricks, nominally 8 in. (20 cm) wide by 4 in. (10 cm) high by 12 in. (30 cm) long. The CBRC piers were constructed from two wythes of solid clay brick units, nominally 4 in. (10 cm) wide by 4 in. (10 cm) high by 12 in. (30 cm) long; the grouted core between the two wythes was nominally 2 in. (5 cm) thick giving the test specimens a thickness of 10 in. (25 cm).

The test program included single piers with three height-to-width ratios. Piers HCBR-21 and CBRC-21 were 80 in. (2.03 m) high by 42 in. (1.07 m) wide, with a height-to-width ratio of 1.90. Piers HCBL-11, HCBR-11 and CBRC-11 were 56 in. (1.42 m) high by 48 in. (1.22 m) wide, with a height-to-width ratio of 1.17. The piers with height-to-width ratio of 0.5 (HCBL-12, HCBR-12 and CBRC-12) were 40 in. (1.02 m) high by 80 in. (2.03 m) wide.

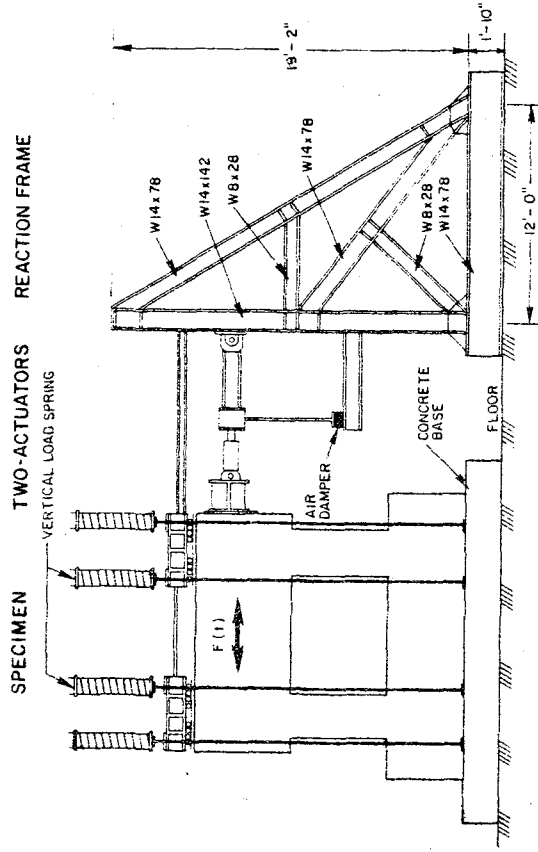


FIG. 2 DOUBLE PIER TEST SETUP

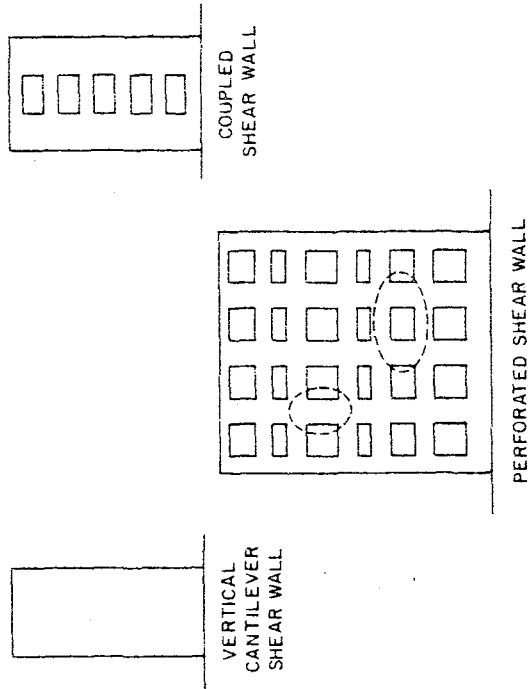


FIG. 1. TYPICAL SHEAR WALLS.

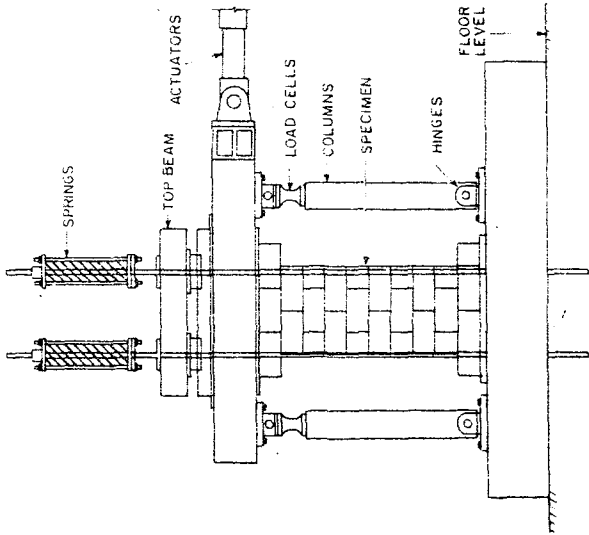


FIG. 3 SINGLE PIER TEST SETUP

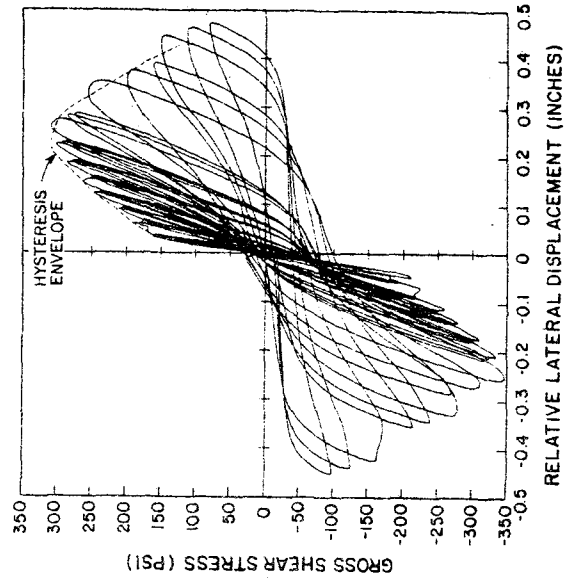


FIG. 4 HYSTERESIS LOOPS AND HYSTERESIS ENVELOPE

Two types of grouting were used in the HCBR-11, HCBR-11 and HCBR-21 piers; in the partially grouted piers only the cells and the bond beams containing reinforcement were grouted; the fully grouted piers had all the cells grouted. All of the other piers were fully grouted.

The test equipment shown in Figs. 2 and 3 permits lateral loads to be applied in the plane of the piers, using displacement controlled actuators with a maximum capacity of 450 kip (203 ton). A vertical load may be applied to the piers through the spring and rollers shown above the spandrel beam in Fig. 2 and above the lateral loading beam in Fig. 3. All the single pier tests had an initial bearing stress of 50 psi (3.5 kg/cm<sup>2</sup>). The lateral loading sequence for each test consisted of sets of three sinusoidal displacement cycles applied at a specified actuator displacement amplitude. The specified amplitude was gradually increased and followed a sequence that varied according to the height-to-width ratio of the piers. The cyclic frequency was generally maintained at 0.02 Hz.

The basic product obtained from the tests was the hysteresis loops diagram, which is a plot of the lateral load against the lateral displacement of the piers as shown in Fig. 4. The strength and deformation properties, the stiffness degradation and the energy dissipation characteristics of the piers can be obtained from the hysteresis loops. The hysteresis envelope, also shown in Fig. 4, is a plot of the absolute average of the maximum positive and negative forces and corresponding displacements, for each of the three cycles of loading at a given input displacement amplitude.

#### MODES OF FAILURE

Two principal modes of failure have been observed during the tests, a flexural and shear mode. Sliding modes associated with either shear or flexural crack were also observed in the piers with height-to-width ratio of 0.5.

A flexural mode of failure was obtained in two of the double pier tests (HCBL-21) and in the preliminary tests using the modified single pier test setup. The specimens have only horizontal cracks at the top and bottom sections and the ultimate strength of the pier is controlled by the tensile yielding strength of the vertical reinforcement. In this case the final mechanism of failure is due to crushing at the compressive toe of the pier.

Most of the piers exhibited a shear mode of failure. This mode is characterized by early flexural cracks at the toes of the pier which are later augmented by diagonal cracks that extend through a partial zone of the pier. As the horizontal load increases, large diagonal cracks (X cracks) form when the diagonal tensile stress in the pier reaches the tensile strength capacity of the masonry. Some of the single piers with height-to-width ratio of 2 or 1 exhibited yielding in the vertical reinforcement before the occurrence of the major diagonal cracks. However, as the vertical compressive load induced by the single pier test setup (Fig. 3) increased, the flexural moment capacity of the pier sections also increased while the tension vertical reinforcement continued to yield. This effect allowed the lateral load on the pier to increase until the diagonal tensile stress reached the tensile strength of the masonry and a shear failure developed. The same test was later repeated using the modified single pier test setup and a typical flexural mode of failure was obtained. This fact shows how important the compressive axial load may be in shifting the mode of failure from the flexural to shear.



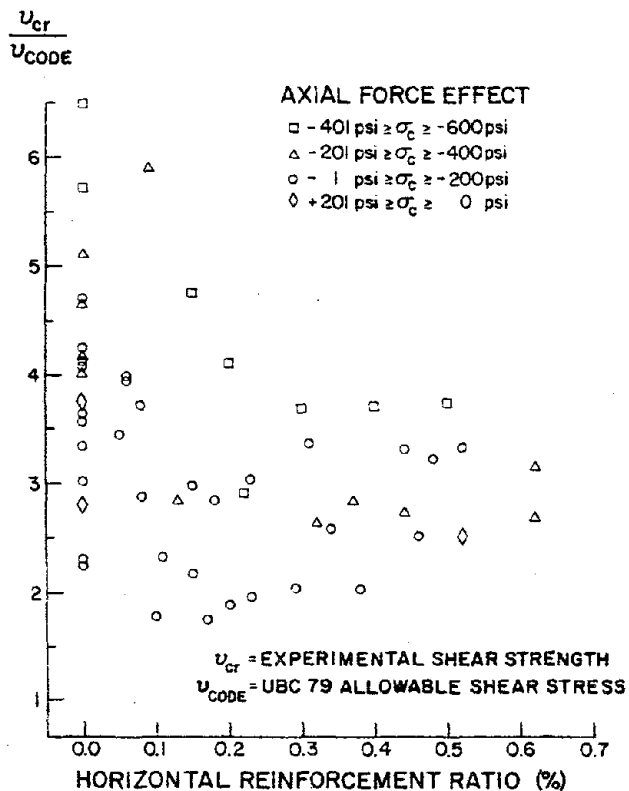


FIG. 5 COMPARISON BETWEEN EXPERIMENTAL SHEAR STRENGTH AND UBC 1979 ALLOWABLE SHEAR STRESS

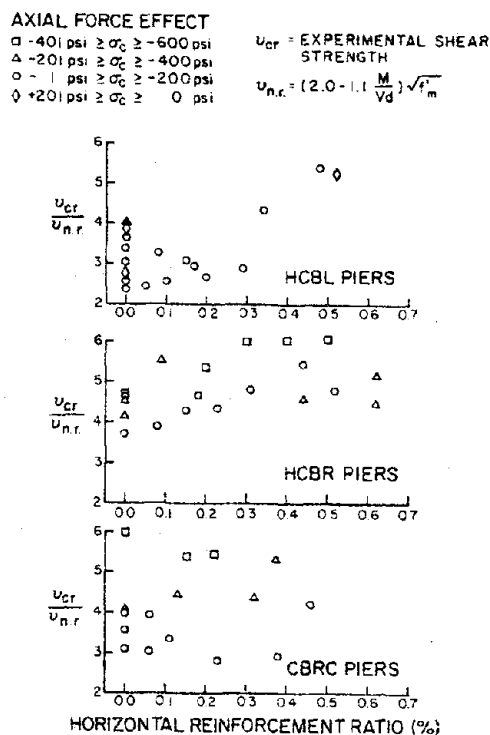


FIG. 7 EFFECT OF HORIZONTAL REINFORCEMENT AND AXIAL FORCE ON SHEAR STRENGTH OF MASONRY PIERS

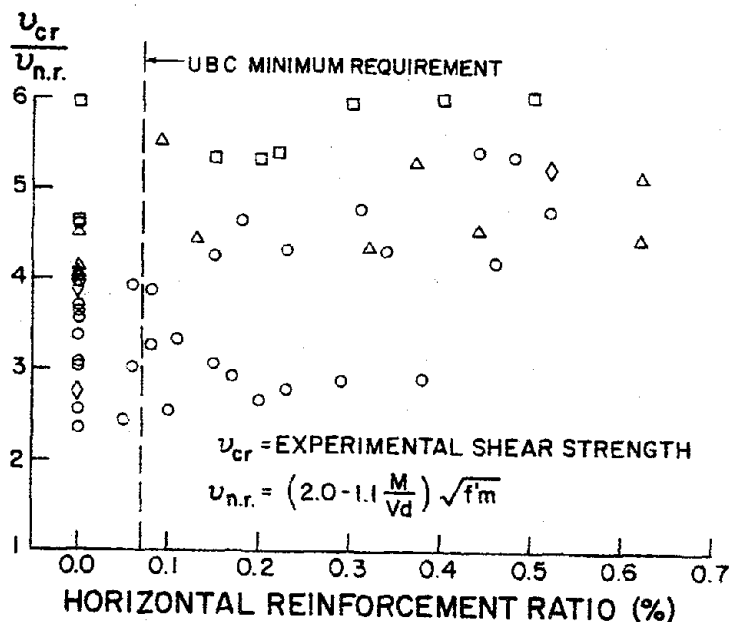


FIG. 6. EFFECT OF HORIZONTAL REINFORCEMENT AND AXIAL FORCE ON SHEAR STRENGTH OF MASONRY PIERS.

## ULTIMATE STRENGTH ASSOCIATED WITH THE SHEAR MODE OF FAILURE

The ultimate lateral load strength of each pier is determined by the lesser of the lateral load capacities associated with each of the modes of failure. The ultimate strength associated with the two sliding modes of failure described above proved to be quite similar to that obtained with the shear mode of failure.

The lateral load capacity associated with the flexural mode of failure is reasonably predicted by current analytical methods, which can be found in reference [2].

The lateral load capacity associated with the development of the first major diagonal crack (shear strength), will be analyzed in detail using the experimental data obtained throughout the test program. This lateral load capacity usually, but not always [4], coincides with the ultimate (maximum) shear strength of the piers.

Figure 5 presents a comparison between the experimental shear strength of the piers and the allowable shear stress that the pier would have according to the Uniform Building Code (UBC), 1979 Edition. Both the percentage of horizontal reinforcement and the axial stress developed concurrently with the major diagonal crack have been used as parameters, even though the axial force effect is not considered by the UBC. The code allowable shear stress is also a function of the compressive strength of the corresponding masonry prism and the height-to-width ratio of the piers (or  $M/Vd$ ). Both effects have proved to be significant factors to the shear capacity of the piers. Except for unreinforced or very lightly reinforced piers, the allowable stress given by the UBC appears to be a good basis to predict the shear strength of masonry piers.

Based on the previous result, Fig. 6 presents the experimental shear strength as a function of  $v_{n,r}$ , which is the basic expression proposed by the UBC to evaluate the allowable shear stress of an unreinforced pier. Fig. 6 illustrates the improvement in strength that can be obtained through the use of horizontal reinforcement and the beneficial effect of compressive load on the shear strength. As more experimental data becomes available, it will be possible to predict with more confidence the shear strength of masonry piers. Fig. 7 presents the same data separated by masonry material. It is interesting to observe the different effect of the horizontal reinforcement depending on the type of masonry.

## INELASTIC BEHAVIOR OF PIERS FAILING IN THE SHEAR MODE

In order to simplify the analysis, the inelastic characteristics of the piers exhibiting a shear mode of failure are discussed using the area A of the hysteresis envelope, as defined in Fig. 8. The area A is directly proportional to the ultimate strength and the ductility developed by the piers, but other parameters like the energy dissipated per cycle and the comparison of crack patterns at equal displacements must be considered to fully evaluate the inelastic characteristics of the pier behavior.

Figure 9 presents the effect of horizontal reinforcement and height-to-width ratio on the inelastic behavior of the piers. It can be observed that increasing amounts of horizontal reinforcement improve the inelastic behavior; however, this improvement is not large and presents more consistency for the HCBL and HCBR piers than for the CBRC piers. The squat piers (height-to-width

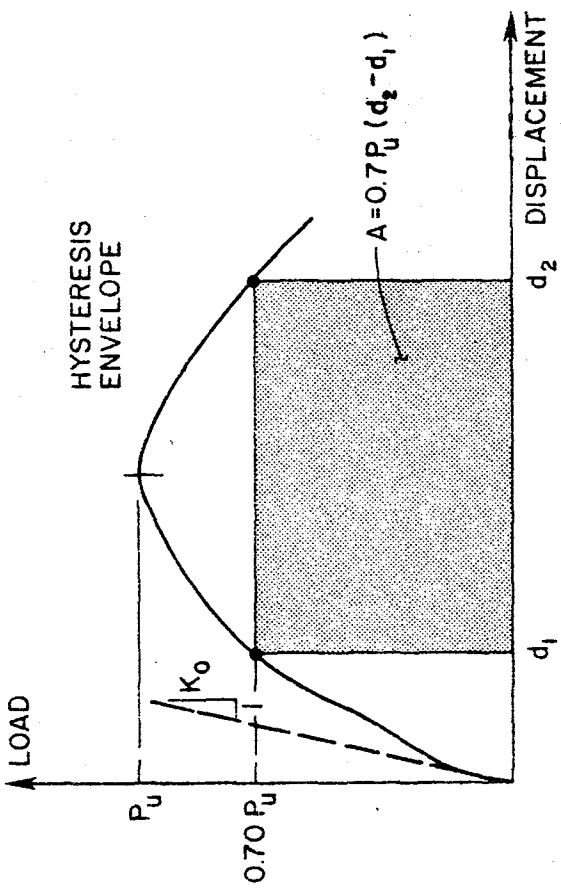


FIG. 8. DEFINITION OF PARAMETER A.

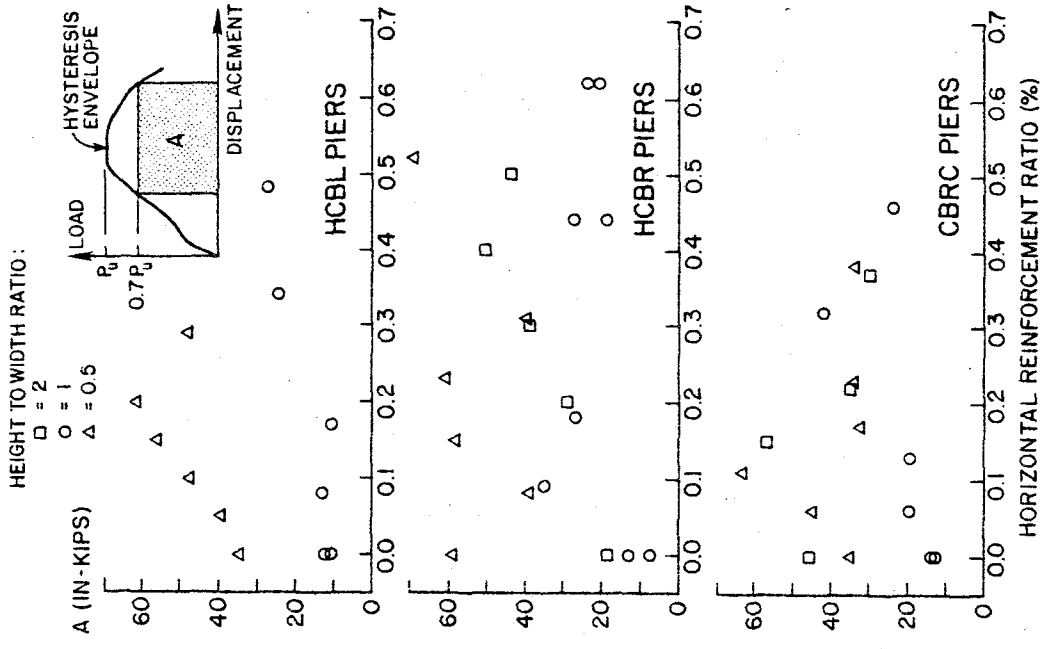


FIG. 9. EFFECT OF HORIZONTAL REINFORCEMENT AND HEIGHT-TO-WIDTH RATIO ON INELASTIC BEHAVIOR OF PIERS.

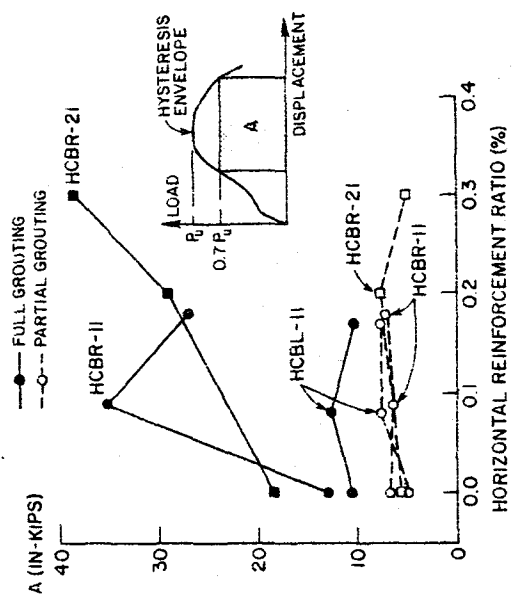


FIG. 10. EFFECT OF TYPE OF GROUTING ON INELASTIC BEHAVIOR OF PIERS.

ratio of 0.5) generally show better inelastic behavior than the more slender piers.

The effect of partial grouting as compared with full grouting is shown in Fig. 10, using shear forces for the comparison. The behavior of partially grouted HCBL piers is not significantly less desirable than that of fully grouted piers, but definitively worse in the case of the HCBR piers.

#### SUMMARY OF RESULTS

1. Two principal modes of failure may occur in a masonry pier, flexure and shear. In addition, the piers with height-to-width ratio of 0.5 showed a tendency to develop a sliding mode of failure.
2. The strength associated with the shear mode of failure is a function of the compressive strength of the masonry material and the ratio  $M/Vd$  of the pier. This strength may be improved with increasing amounts of horizontal reinforcement and increasing values of the compressive axial load acting on the pier.

#### ACKNOWLEDGEMENTS

The research reported in this paper has been jointly funded by the National Science Foundation, the Masonry Institute of America, the Western States Clay Products Association and the Concrete Masonry Association of California and Nevada. The sponsorship of these institutions is gratefully acknowledged.

#### REFERENCES

- [1] Mayes, R. L., Omote, Y. and Clough, R. W., "Cyclic Shear Tests of Masonry Piers, Volume I - Test Results", EERC Report No. 76-8, University of California, Berkeley, California, 1976.
- [2] Mayes, R. L., Omote, Y. and Clough, R. W., "Cyclic Shear Tests of Masonry Piers, Volume II - Analysis of Test Results", EERC Report No. 76-16, University of California, Berkeley, California, 1976.
- [3] Priestley, M.J.N. and Bridgemann, D.O., "Seismic Resistance of Brick Masonry Walls", Bulletin of the New Zealand National Society for Earthquake Engineering, Vol. 7, No. 4, 1974.
- [4] Hidalgo, P. A., Mayes, R. L., McNiven, H. D., and Clough, R. W., "Cyclic Loading Tests of Masonry Single Piers, Volume I - Height to Width Ratio of 2", EERC Report No. 78/27, University of California, Berkeley, California, 1978.
- [5] Hidalgo, P. A., Mayes, R. L., McNiven, H. D., and Clough, R. W., "Cyclic Loading Tests of Masonry Single Piers, Volume 3 - Height to Width Ratios of 0.5", EERC Report No. 79/12, University of California, Berkeley, California, 1979.

# AN INVESTIGATION OF THE SEISMIC BEHAVIOR AND REINFORCEMENT REQUIREMENTS FOR SINGLE-STORY MASONRY HOUSES

by

R. W. Clough<sup>I</sup>, P. Gülkan<sup>II</sup>, and R. L. Mayes<sup>III</sup>

## ABSTRACT

An investigation undertaken to determine the reinforcement requirements for single-story masonry houses in Uniform Building Code Seismic Zone 2 areas of the U. S. is described. The investigation consisted of testing four masonry house models measuring 16 ft. (4.90 m) square in plan dimensions on a two-component shaking table capable of horizontal and vertical motions. The dynamic response of each house was measured and careful observations enabled tentative recommendations to be made for two subregions defined within the current Zone 2 on the basis of effective peak ground accelerations. The tentative recommendations are that no reinforcement is necessary for single-story residences made from brick or concrete block in those subareas of Zone 2 where the effective peak ground acceleration is less than 0.1 g. Partial reinforcement is recommended for the remainder of Zone 2. Final recommendations will await the results of an additional test in which the walls of the house will be subjected to combined in-plane and out-of-plane loads.

## BACKGROUND

Seismic design requirements specified by the U.S. Department of Housing and Urban Development (HUD) are referenced to "seismic risk zones" defined by the Uniform Building Code (UBC). Changes in the UBC maps were incorporated into HUD requirements and this resulted in the requirement for partial reinforcement for masonry houses in newly specified Zone 2 areas. These requirements were considered overly conservative by the construction industry in Phoenix, Arizona, one of the affected locations, and it was decided to study the question experimentally by subjecting assembled components of masonry houses to simulated earthquakes on the EERC shaking table. The primary objective was to determine the maximum earthquake intensity that could be resisted satisfactorily by an unreinforced house, and to evaluate the additional resistance that would be provided in the structure by partial reinforcing. Details of four of the test houses are given in [1] and [2]. The major conclusions and recommendations will be presented in a report after a fifth test is performed in which the walls will be subjected to both in-plane and out-of-plane forces.

## STRUCTURES TESTED

The unique feature of the study was the testing of full scale components of typical masonry houses subjected to motions recorded in actual earthquakes. Masonry walls 8 ft - 8 in. (2.64 m) in height and up to 16 ft (4.90 m) long were constructed with commercially available 6 in. wide concrete block or clay

---

<sup>I</sup> Professor of Civil Engineering and Assistant Director, Earthquake Engineering Research Center, University of California, Berkeley, U.S.A.

<sup>II</sup> Associate Professor of Civil Engineering, Middle East Technical University, Ankara Turkey.

<sup>III</sup> Asst. Research Engineer, Earthquake Engineering Research Center, University of

brick units. The walls were assembled to form 16 ft. (4.90 m) square test "houses" built on strip footings. The individual wall units were connected at the top by a timber roof structure of standard construction. Concrete slabs were bolted to the roof structure to compensate for the reduction of mass resulting from scaling the plan dimensions. The weight of the slabs were chosen so that the ratio of total roof load to total wall peripheral length was similar to that of a 40 x 50 ft. (12 x 15 m) house with a specified roof load of 20 psf ( $1 \text{ kN/m}^2$ ).

Fig. 1 shows a three-dimensional view of a typical test house, one of four specimens tested. All models were designed so that transverse and in-plane response of both unreinforced and partially reinforced panels could be observed in a single test. All partial reinforcement consisted of vertical bars. In the last house a series of tests were conducted when all four wall panels were initially unreinforced; during the subsequent phase, all walls were partially reinforced with two No. 3 (10 mm) bars.

The test structures were generally subjected to a series of base motions with progressively increasing intensity. Some tests performed on Houses 3 and 4 included both horizontal and vertical components of motion. Three earthquake motions were used derived from the 1940 El Centro, 1952 Taft and 1971 Pacoima Dam accelerograms. Roof truss orientation and local repair of cracked walls were also included as test parameters.

#### OBSERVATIONS ON THE RESPONSE BEHAVIOR

The specimens used in this study were typical of "box" structures which derive their lateral force resistance from "membrane" action of the walls. The major part of the lateral force developed in these tests resulted from the concrete blocks bolted to the roof. Resistance to this force was provided by a mechanism dependent on the relative in-plane shear rigidity of the roof and wall components; the out-of-plane rigidity of the wall panels and the flexural stiffness of their connections to the roof were of negligible value in resisting the roof loads. The roof structure simply provided the top support for out-of-plane forces.

From this description it is clear that the out-of-plane walls of a masonry house must have sufficient flexural strength to resist their own inertia forces when acting as vertical beams, while the in-plane walls must have the capacity to resist the inertia forces of the entire roof system plus the top half of the walls.

In general, the observed behavior was consistent with this description of box structures subjected to lateral forces. During the tests, roof displacement amplitudes were directly related to the behavior of the in-plane walls (designated as A and B in Fig. 1). Differential displacements of the two in-plane walls were accommodated by "racking" distortions of the roof; relatively little in-plane distortion was observed in the out-of-plane walls, so it may be concluded that the roof structure did not rotate as a rigid unit. This is consistent with the usual design assumption that plywood diaphragms are much more flexible in shear distortion than are masonry walls.

A significant observation made from these experiments was that typical single-story masonry houses are so rigid that they do not develop complicated response mechanisms during an earthquake. Motions of the test structures

followed the shaking table motions very closely, with distortions generally proportional to, and in phase with, the base accelerations. The peak input acceleration may therefore be cited as the dominant quantity controlling response. The most significant features of the observed response of the test structures taken as a whole may be summarized as follows:

For Unreinforced Wall Units:

(1) No cracking was observed in any major unreinforced wall unit for tests with peak accelerations less than 0.2 g. The lowest intensity shaking that caused cracking of a non-bearing in-plane wall occurred during tests with peak accelerations of 0.21 g; the minimum intensity to cause cracking of an out-of-plane wall was 0.25 g.

(2) Unreinforced out-of-plane walls continued to perform satisfactorily after cracking during several tests of increased intensity, but the displacements of these walls generally became excessive during tests with accelerations greater than 0.4 g. These large displacements involved hinging at the horizontal crack line and exhibited potential instability.

(3) Cracking of unreinforced in-plane walls was of two-types: horizontal cracks in panels without openings, and a diagonal crack extending downward from the window corner in the wall units with window penetrations. Permanent displacements generally were not associated with the horizontal cracks; however, the diagonal cracks led to permanent displacements which became unacceptably large with further testing.

For Partially Reinforced Wall Units:

(1) Nearly all partially reinforced wall units performed satisfactorily in all tests. None of the partially reinforced out-of-plane components developed any significant cracks during any test, including several with peak accelerations in excess of 0.5 g.

(2) Partially reinforced in-plane walls also performed satisfactorily although some cracked when peak accelerations exceeded 0.3 g. Cracking in the pier units without window openings was associated with rigid body rocking, and included a horizontal crack due to uplift near the base of the wall. Residual cracks were easily repairable.

(3) The only partially reinforced wall which exhibited unsatisfactory behavior was the window wall of House 4 (unit A in Fig. 1). A typical diagonal crack extending from the window corner to the "toe" of the wall developed during the first phase of testing when this house was unreinforced. After the addition of two undowelled bars, the wall resisted a 0.32 g test without additional cracking. However, in subsequent tests with peak accelerations in the range of 0.47 to 0.68 g further cracking did develop as a result of uplift at the undowelled corner.

Extrapolation to Prototype Conditions

This general description of the observed behavior provides the basis for the tentative recommendations presented below concerning seismic design criteria for single-story masonry houses. However, before these observations may

be applied, it is necessary to estimate the extent to which they represent the performance of real houses subjected to real earthquakes. Comparisons of shaking table test conditions with those existing in a prototype response to earthquakes were considered with regard to: (1) seismic input, (2) roof load, (3) foundation flexibility, (4) geometric effects, (5) roof diaphragm flexibility, (6) pre-existing state of stress in walls, (7) torsional response mechanisms, and (8) progressive damage. After evaluating each of these factors in detail, it was concluded that the behavior observed in the shaking table tests was quite similar to the performance expected of a real house subjected to a real earthquake with a similar peak acceleration. The only significant shortcoming of the shaking table tests was that only a single horizontal component of earthquake motion was applied, so that walls were subjected to either in-plane or out-of-plane forces. It is believed that the out-of-plane response of unconfined walls might have an unfavorable influence in their resistance to a simultaneous in-plane excitation, and it was decided that this negative effect should be investigated in an additional test before final recommendations are presented.

#### TENTATIVE DESIGN RECOMMENDATIONS

##### Seismic Input for Zone 2

From the earliest stages of this investigation, one of the most critical questions related to the intensity of shaking table accelerations that should be used to represent the maximum earthquake motions expected in UBC Zone 2. This correlation of shaking table motions to field excitation is required to relate the damage observed in the test structures to the expected behavior of real houses in Zone 2.

The best current estimate of expected earthquake intensity for the U.S. was developed by the Applied Technology Council (ATC) in preparing proposed seismic design regulations for buildings [3]. Figure 2 shows the ATC map of effective peak acceleration (EPA) contours superimposed on the 1976 UBC Seismic Zoning Map. The EPA contours are intended to represent effective ground motions with a 10 percent probability of being exceeded during a 50 year period. The EPA of a given ground motion is defined in terms the response spectrum of the motion evaluated for 5 percent of damping by drawing a line of constant spectral acceleration approximating the peaks and valleys of the spectrum in the period range of 0.1 to 0.5 seconds. The EPA is given by this spectral acceleration divided by 2.5, where the divisor is typical of the amplification for Western U.S. earthquakes. The concept of EPA was introduced in [3] to avoid overemphasizing the peak ground acceleration, the value of which often does not relate well with the damage induced by a given motion.

It will be noted in Fig. 2 that Zone 2 includes a wide range of EPA values from 0.05 to 0.2 g. It is not reasonable to impose design requirements suitable for the maximum EPA value of 0.2 g for all of Zone 2, and accordingly, two subzones were defined within it. Zone 2A is the part of Zone 2 indicated by the ATC map to have an EPA of less than 0.1 g while Zone 2B is the areas with EPA values of 0.1 to 0.2 g.

EPA values of the shaking table motions were determined by applying the above definition to the shaking table response spectrum. Because the tests were conducted with widely varying intensities, the table motions were all



normalized to 1 g before the response spectra were constructed. The resulting combined average EPA value was 0.82 g for the three types of base motions used in the experiments. This means that a table motion having a peak acceleration of 1 g is assumed to have an EPA of 0.82 g, or conversely, the maximum EPA of 0.2 g indicated by the ATC map for Zone 2 is represented by a peak shaking table acceleration of 0.24 g.

### Test Structure Amplification

Although masonry houses are relatively rigid, they do exhibit some vibratory amplification so that peak accelerations recorded on the structure are greater than the peak input acceleration. This amplification effect is represented in the definition of the EPA by the 2.5 divisor; that is, ATC has tacitly assumed an amplification factor of 2.5 to be appropriate for typical building structures.

Experimental data obtained during the course of this study demonstrated that the amplification varied considerably, from point to point on the test structures, and with differing test conditions. Amplification factors are important in the design of structures to resist earthquakes because the seismic load induced in any part of a structure is given by the product of the mass of that part multiplied by its local acceleration. In a single-story masonry house the principal seismic force results from the mass of the roof structure. Hence, the seismic load to which a house is subjected is given by the roof acceleration amplification factor multiplied by the product of the roof mass and the table acceleration. Careful review of test data indicated that an amplification factor of 2.5 was appropriate for estimating the seismic forces induced in the test structures by the given peak table acceleration.

### Tentative Design Criteria

As noted earlier, the principal purpose of this investigation was to determine the amount and type of reinforcing that should be provided in single-story masonry houses constructed in Zone 2, and to recommend design provisions that will satisfy these requirements. Because two subzones having different earthquake intensities have been identified in Zone 2, it was necessary to formulate different recommendations for each subzone.

#### A. Criteria for Zone 2A

The maximum effective peak acceleration to be expected in this subzone is 0.1 g; this EPA is provided by shaking table tests with a peak table acceleration of 0.12 g. Concern about the performance of unreinforced walls subjected to combined in-plane and out-of-plane forces led to the recommendation for an additional test with the walls subjected to combined forces. The combined force effect was accounted for in the tentative recommendations by increasing the intensity of the single component by 30 to 50 percent. Thus, a single shaking table test with a peak acceleration of 0.16 g to 0.18 g is assumed to simulate the effects of a maximum Zone 2A earthquake on an unreinforced wall.

Review of test data [1] and [2] shows that no damage of any type occurred in any wall of any test structure during tests not exceeding this peak value of 0.18 g. Unreinforced walls which had been cracked during more severe tests performed satisfactorily in subsequent tests of 0.18 g or less. Based on this

observation, the following tentative code provision is presented. For Zone 2A, no reinforcing is required for earthquake resistance in single-story residential buildings of standard clay brick or concrete block construction provided the ratio of shear wall length to roof load is similar to that included in the tests."

#### B. Criteria for Zone 2B

For Zone 2B, the maximum expected EPA of 0.2 g is provided by a shaking table peak acceleration of 0.24 g. For unreinforced walls this intensity was increased by 30 to 50 percent to account for the damaging effect of the second horizontal motion component.

Review of response observations revealed that the only unreinforced wall that withstood this intensity of shaking without damage was the in-plane wall of House 2 for which the mortar strength was measured to be 4,700 psi (32.4 MPa). The unreinforced in-plane walls of all other test structures, and the unreinforced out-of-plane walls of all other test structures exhibited damage after tests with peak accelerations less than 0.36 g. Also, the performance of cracked unreinforced walls was unsatisfactory during tests with less than 0.36 g peak accelerations. Based on these observations it was concluded that partial reinforcement is necessary in the walls of masonry houses built in Zone 2B.

When walls are partially reinforced little coupling is expected between in- and out-of-plane response mechanisms. Accordingly, the intensity of the single-component shaking table motions was increased by only 20 percent to account for the orthogonal motion effect. Thus, a shaking table motion with a peak of 0.29 g was taken as the basis for judgement of adequate performance. Test data reveals that no cracking damage developed in any of the partially reinforced walls during tests with peak accelerations of 0.29 g or less. In fact, no damage to the partially reinforced out-of-plane walls occurred in any test including peak accelerations greater than 0.6 g. Also, no requirement for dowels of such walls was indicated.

On the other hand, some cracking was observed in the partially reinforced in-plane walls of all test structures. Generally, this cracking was at the base of the piers and above the ends of the door and window lintels. It was associated with rigid-body rocking of the piers, and does not represent a serious damage condition.

The final step in formulating the design recommendations for Zone 2B is to generalize the essential factors of partial reinforcement included in the test structures. These recommendations are presented in the form of minimum standards which ensure adequate resistance to out-of-plane forces. These standards also pertain to the in-plane resistance, and it is believed that adequate in-plane resistance could be achieved by prescribing such minimum standards.

The principal recommendations concerning in-plane strength are presented in the form of a design procedure which involves first estimating the lateral force that would be developed in the structure due to the maximum expected Zone 2B earthquake. The acceleration inducing this force is given by the maximum EPA of Zone 2B increased by a factor of 2.5. Thus, the acceleration acting on the roof system is 0.5 g, and each in-plane wall resists half the total load.

The seismic force developed at the roof level must be resisted by shear stresses in the in-plane walls, and for the purpose of the following recommendations it is assumed that only panels that are at least 6 ft. (1.8 m) wide and without window penetrations will provide the required resistance. Maximum shear stresses calculated for wall panels which performed satisfactorily during the tests were 34, 38, 40, and 39 psi in Houses 1 to 4, respectively. Because these did not necessarily determine the limit of good performance, it is likely that the effective strength is higher than these values so the value of 40 psi ( $\text{kN/m}^2$ ) was selected as the allowed shear stress. It should be emphasized that the assumption of satisfactory performance with this magnitude of shear stress is based on the premise that the resisting panel has vertical reinforcement at each end capable of accomodating rocking rigid-body displacements. To account for the ductile response of the shear wall reinforced as recommended and for the forces resisted by the interior partitions of the house, it is recommended that the design load be 0.5 g times mass/1.5.

In conclusion, the following criteria are recommended for Zone 2B:

Single-story houses of clay brick or concrete block masonry built in Zone 2B must be partially reinforced. For the purpose of providing adequate seismic resistance, partial reinforcement must meet the following conditions:

- (1) Minimum reinforcing bar size is NO. 3.
- (2) Each exterior corner of the house must be reinforced by at least one doweled bar; dowels are not otherwise necessary.
- (3) For out-of-plane resistance:
  - (a) At least one bar is required in each pier extending from floor to lintel or ceiling height.
  - (b) Maximum bar spacing is 8 ft. (2.5 m) except that shear panels selected for in-plane resistance up to 12 ft. (3.5 m) long need not have more than two bars.
- (4) For in-plane resistance:
  - (a) The in-plane resistance is provided by shear panels which are defined as a wall or a portion of a wall extending from floor to lintel or ceiling height, at least 6 ft. (1.8 m) wide and without penetrations.
  - (b) A vertical bar is required at each edge of a shear panel.
  - (c) The total length of shear panels oriented along each axis must be sufficient to resist a horizontal force equal to half the weight of the roof system divided by 1.5 with the net shear stress not to exceed 40 psi ( $21 \text{ kN/m}^2$ ).

#### ACKNOWLEDGEMENTS

The investigation described in this paper has been funded by the U.S. Department of Housing and Urban Development. Planning of the research was done with the cooperation of an Applied Technology Council Advisory Panel.

REFERENCES

- [1] Güllkan, P., Mayes, R.L. and Clough, R.W., "Shaking Table Study of Single-Story Masonry Houses - Volume 1, Test Structures 1 and 2, Earthquake Engineering Research Center Report No. UCB/EERC-79/23, August 1979.
- [2] Gulkan, P., Mayes, R.L. and Clough, R.W., "Shaking Table Study of Single-Story Masonry Houses - Volume 2, Test Structure 3 and 4," Earthquake Engineering Research Center Report No. UCB/EERC-79/24, August 1979.
- [3] "Tentative Provisions for the Development of Seismic Regulations for Buildings," Applied Technology Council Publication ATC3-06, (NSF Publication 78-8, NBS Special Publication 510), U.S. Government Printing Office, June 1978.

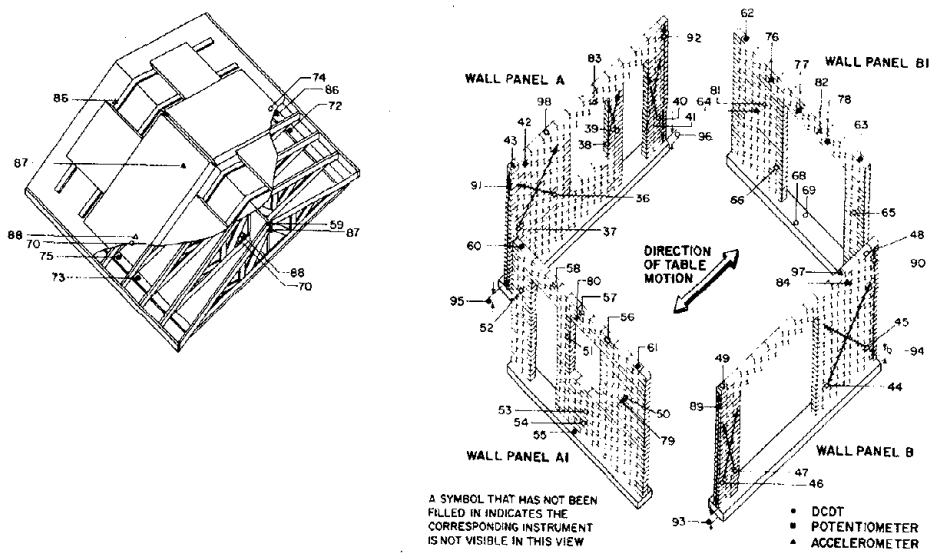


FIG. 1 TYPICAL TEST STRUCTURE

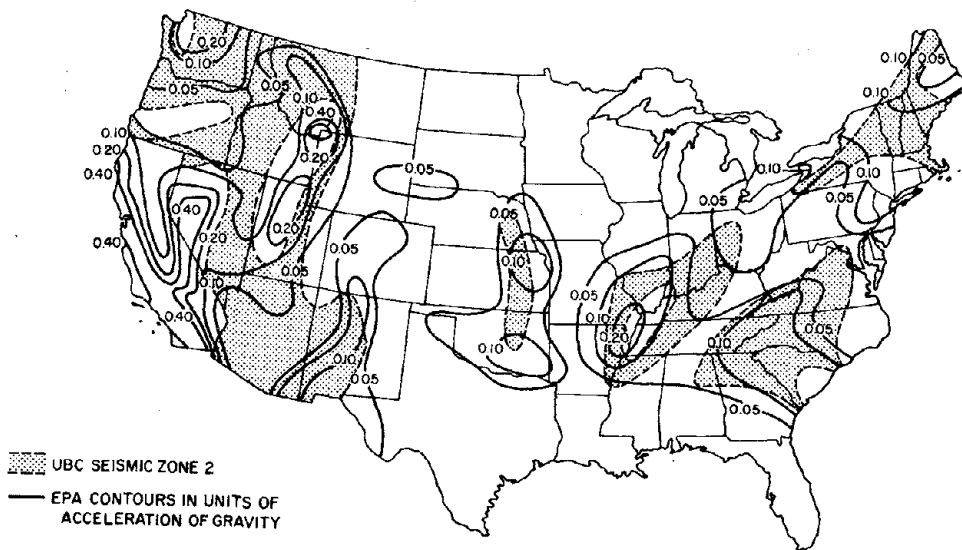


FIG. 2 ATC EFFECTIVE PEAK ACCELERATIONS FOR THE UNITED STATES

# ECCENTRIC SEISMIC BRACING OF STEEL FRAMES

Egor P. Popov<sup>I</sup>

## SUMMARY

Unlike conventional diagonal bracing, where the brace centerlines pass through the centers of beam-column joints, braces in eccentrically braced frames are deliberately off-set with respect to such joint centers. This provides short segments of floor beams between a column and a diagonal brace. Under severe cyclic loadings, the webs of the short beam segments adjacent to the columns yield cyclically in shear and serve as energy absorbing and dissipating devices. Some adoptions of this bracing scheme have been made in practice. In this paper the general concepts of the design of eccentrically braced steel frames are reviewed.

## INTRODUCTION

The use of eccentrically braced steel frames for resisting lateral loads is not entirely new. In his 1930 book on Wind Bracing Spurr [1] suggested their occasional use for architectural reasons, and it would appear that tall buildings using such bracing were designed and built in the New York area. More recently a very tall building was built in Texas using this scheme [2]. A more deliberate use of eccentric joints for seismic design may be attributed to Fujimoto [3], who performed a number of tests on eccentric K-braces. Some preliminary designs utilizing diagonal braces with eccentricities at the columns were made in 1972 by Degenkolb [4]. Experimental results on one-third scale models of eccentrically braced steel frames for the lower three stories of a 20-story building published by Roeder and Popov [5] renewed interest in this type of bracing, and some adoptions have been made in practice.

In this paper, first, the frames used in the Roeder-Popov experiments are described, followed by some selected experimental results. The extrapolation of the available information from small scale experiments to design follows. Areas of needed future research are then indicated.

## ECCENTRICALLY BRACED FRAMES

A 20-story, four-bay square office building served as the prototype. The bay widths were 24 ft (7.3 m), and the story heights were 12 ft (3.6 m) for all stories except the first, which was 15 ft (4.6 m). The structure was designed using the 1976 Uniform Building Code lateral load provisions [6], and the American Institute of Steel Construction (AISC) allowable stresses [7]. An elevation of the exterior braced frame is shown in Fig. 1.

A typical eccentric bracing arrangement is shown in Fig. 2. The short segments of the beams (shear links) providing the eccentricity  $e$  are so proportioned that during plastic deformation the webs yield before

---

<sup>I</sup>Professor of Civil Engineering, University of California, Berkeley, California, USA, 94720.

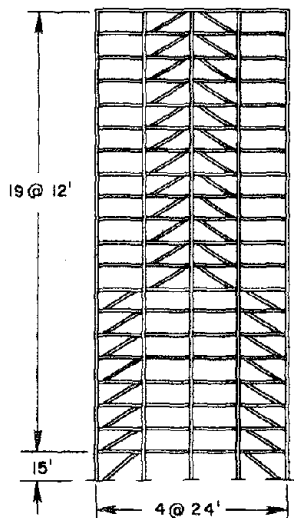


Fig. 1 Prototype Structure [5]

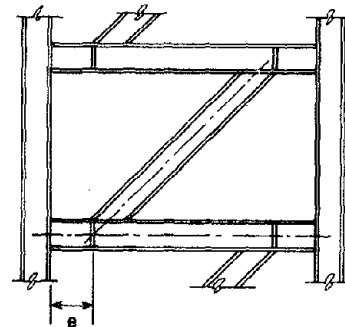


Fig. 2 Typical Eccentric Brace [10]

the plastic moment capacity of a beam is reached. Because of the cyclic yielding in the webs of the shear links during a severe earthquake, stiffeners along such links may be required. The braces are selected such that their capacity can cause yielding of the beam webs, thereby excluding the possibility of brace buckling. As is customary in the design of moment-resisting steel frames, the columns are selected using the strong column-weak beam approach.

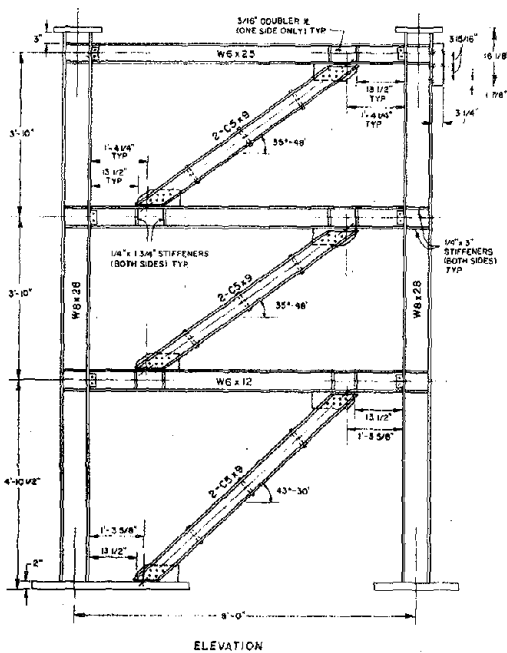


Fig. 3 Design of Test Frame 1 [5]

The details for one of two one-third scale models for a braced bay for the lower three floors of the prototype, based on the concepts outlined above, are shown in Fig. 3. The behavior of the shear links at the second and third floor levels was of particular interest. These links were parts of the W6 x 12 floor beams and were 13 in (330 mm) long. However, since 2 in (50 mm) wide shear tabs were welded both to the columns and to the beam webs, the effective unsupported web panels were approximately 11 in (280 mm) long and 6 in (150 mm) high. The webs of these beams were 0.23 in (5.8 mm) thick. The design called for no vertical stiffeners along the shear link.

### PRINCIPAL EXPERIMENTAL RESULTS

The two test frames behaved very well during experiments. The imposed lateral displacements at the third floor level attempted to simulate displacements equal to or exceeding those which might occur during an

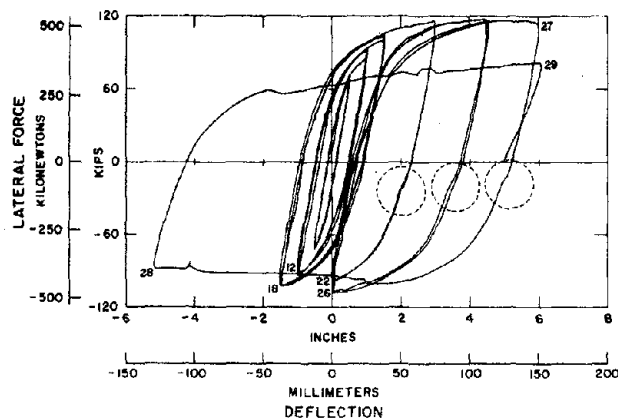


Fig. 4 Hysteretic Behavior of Test Frame 1 Lateral Force-Third Floor Deflection [5]

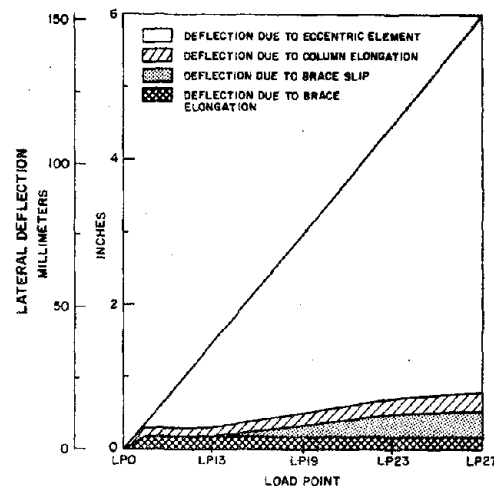


Fig. 5 Components of Lateral Deflection for Test Frame 1 [5]

El Centro and a Pacoima earthquake in tandem. Excellent hysteretic loops were observed well into the inelastic range. (See Fig. 4 for lateral force-third floor deflection loops for Test Frame 1.) The components for lateral deflection are shown in Fig. 5. After web yield begins in the shear links, the ductility of the frame is principally due to inelastic deformation in the shear links. The ultimate failure of the shear links, by tearing and buckling, occurred at very advanced stages of loading, having little practical meaning.

#### EXTRAPOLATIONS INTO DESIGN

The design of eccentrically braced steel frames must conform to the conventional elastic criteria stipulated in standard codes [6]. In conformity with good practice the story drift must be kept to a practical minimum. For example, the Structural Engineers Association of California recommends to limit [7] the elastic wind drift to 0.0025 times the story height, and for prescribed earthquake forces, to twice this amount. In calculating the story drift for eccentrically braced frames, it is appropriate to include the shear deformations of the links. A very useful bulletin for practical design of eccentrically braced frames has been prepared by Teal [8].

No special problems arise in applying the elastic methods of analysis, nor are there any particularly unusual problems in the design of columns and beams in the inelastic range of behavior except for the design of the shear links. The shear links themselves play a key role in maintaining the integrity of a frame, and their capacity in the inelastic range of behavior must be carefully determined and implemented in the design. Lateral torsional buckling of the links must be prevented, and buckling of the flanges and webs at extreme overloads must be minimized. The AISC lateral bracing provisions for plastic design [9] appear to be appropriate for preventing lateral torsional buckling. Usually this would require attaching the beam flanges to a column and providing a lateral brace at the other end of a link. (A less conservative bracing arrangement was found to be satisfactory in the frame tests referred to earlier [5].)

The buckling problem of the web and the flanges in the shear link is interrelated. If the suggestion [10] of setting the link length some 10

to 30% smaller than that which causes the development of plastic moments at the ends of a link is adhered to, the flanges are not likely to buckle until the web buckles. However, if the shear link length is set so that full plastic moments at the ends of a link could occur, a strong possibility of early flange buckling at extreme overloads can take place. Under such circumstances the flanges would force the thinner web to rotate and buckle. To avoid this highly undesirable situation, pairs of stiffeners spaced at approximately one-half of the buckling length of a flange should be provided at both ends of a link. Usually this would mean that stiffeners would be placed at both ends of a link at a spacing approximately equal to the flange width of a beam or less. The need for additional stiffeners along a link, if required, can be arrived at in a manner analogous to that discussed below.

If the development of plastic moment hinges at the ends of a link is prevented by reducing its length so as to cause no plastic moments, the basic problem becomes principally one of web buckling due to shear. In examining this problem it must be recognized that the AISC provisions [9] for determining shear capacities of rolled sections are directed toward monotonically applied loads. Moreover, the 1978 AISC Specifications relaxed requirements for the depth/web-thickness ratio for compact sections. Therefore, the problem of web buckling in the shear links needs to be carefully considered.

As stated earlier in the experiments on one-third scale models, the  $W6 \times 12$  shear links had an effective clear panel size of approximately  $11 \times 6$  in ( $280 \times 150$  mm). The webs were 0.23 in (5.8 mm) thick. In the prototype this translates into a non-standard  $W18 \times 108$  section with a 0.69 in (17.5 mm) web. No standard  $W18$  section can meet these requirements. The webs of the available sections are thinner, indicating a possibility of web buckling.

Some guidance on web buckling of beams under monotonic loads is available [11,12]. However, there is dearth of data as to the behavior of yielding webs under cyclic loading. Therefore, for the present it would seem reasonable to determine the required stiffeners along a link based on the satisfactory performance of the links in the test frames. This can be done by using direct geometric proportions. For example, consider a 36 in (900 mm) long shear link as part of a  $W18 \times 65$  floor beam with a 0.403 in (10.2 mm) thick web. The clear web panel size for the web of the given thickness could then be taken approximately as  $19 \times 10.5$  in ( $480 \times 270$  mm), i.e., in direct ratio to the web thicknesses; thereby requiring three pairs of double vertical stiffeners along a link. Instead of equal spacing of these stiffeners, a slightly closer spacing near the ends of a link than in the middle can be rationalized. In unusual cases some consideration of transferring an axial force through a shear link must also be given.

#### ADDITIONAL CONSIDERATIONS

The extent to which one should stiffen the webs of the shear links is tied-in with the required hinge rotation. If one designs for a maximum credible earthquake, and the extent of the permitted inelastic strain reversal is small, less stringent requirements on web stiffening may be justified.



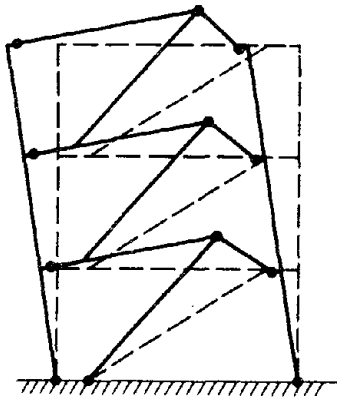


Fig. 6 Plastic Collapse Mechanism [10]

It is also of interest to note that a collapse mechanism for an eccentrically braced frame can be visualized as shown in Fig. 6. For the diagonal bracing scheme shown, large rotation demands are placed on the right links, whereas there is little of inelastic activity at the left links. For this reason, in some cases, it may be advantageous to significantly reduce the eccentricity of the left links as shown in Fig. 7(b).

Several other arrangements of eccentric connections are possible. An example is shown in Fig. 7(a) [3]. A different concept or using coupling beams between two conventionally designed braced frames is shown in

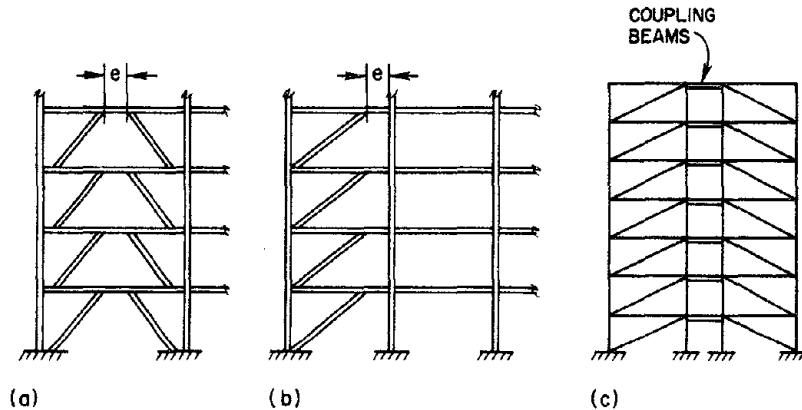


Fig. 7 Bracing Arrangement Schemes

Fig. 7(c). This approach is analogous to that of coupled reinforced concrete shear walls, and may have a particular advantage in reducing the axial forces in columns due to lateral loads.

#### CONCLUDING REMARKS

The great interest shown by designers is eccentrically braced steel frames is due to their apparent advantage in resisting lateral forces. This conclusion is reached mainly on the basis of elastic analyses. The beam sizes are smaller and the frames are stiffer than one would readily obtain in conventional moment-resistant designs. The simultaneous participation of the numerous shear links contributes to the efficiency of the system.

For code level seismic design [6] of eccentrically braced steel frames on elastic basis the same conclusions as above clearly apply. In the ductile range of frame behavior, however, some open questions remain. There is need for a better basis for determining the required web stiffeners along a link. Full-size experiments together with an appropriate theory on cyclic web buckling are needed. In some situations large shear hinge rotations can be anticipated. The extent of acceptable floor damage must be made more precise.

To place the highly promising eccentrically braced frame system on a firmer basis, further analytical studies are required. These must include elasto-plastic analyses for static and dynamic cases of different type buildings. To attain the status comparable to that of moment-resisting frames, experiments on a shaking table also appear to be very desirable.

#### ACKNOWLEDGEMENTS

The work reported was jointly sponsored by the National Science Foundation under Grant No. PFR-7908984 and the American Iron and Steel Institute as Project 193, for which the author is most grateful. The author is also indebted to Dr. Roeder who carried out the experimental work and developed the required computer programs. It is also a pleasure to acknowledge the useful discussions with Professor V. V. Bertero and with the AISC Project Advisory group, as well as with Daniel Manheim.

#### REFERENCES

- [1] Spurr, H. V., Wind Bracing, 1st edition, McGraw-Hill, New York, NY, 1930, p. 53.
- [2] Private communication by R. G. Troy.
- [3] Fujimoto, M., et al., "Structural Characteristics of Eccentric K-Braced Frames," Trans., Architectural Institute of Japan, No. 195, May 1972.
- [4] Private communication by H. J. Degenkolb.
- [5] Roeder, C. W., and E. P. Popov, "Eccentrically Braced Steel Frames for Earthquakes," J. Structural Division, ASCE, Vol. 104, No. ST3, March 1978.
- [6] Uniform Building Code, Intern. Conference of Building Officials, Pasadena, Calif., 1976.
- [7] Recommended Lateral Force Requirements and Commentary, Seismology Committee, Structural Engineers Association of California, 1973.
- [8] Teal, E. J., "Practical Design of Eccentric Braced Frames to Resist Seismic Forces," Structural Steel Educational Council, AISC, Los Angeles, Calif., 1980.
- [9] Manual of Steel Construction, AISC, 7th edition, New York, 1970.
- [10] Popov, E. P., and C. W. Roeder, "Design of an Eccentrically Braced Steel Frame," AISC Engineering Journal, 3rd Quarter, 1978, Vol. 15, No. 3.
- [11] Basler, K., "Strength of Plate Girders in Shear," J. Structural Division, ASCE, Vol. 87, No. ST7, Oct. 1961, and Trans. ASCE, Vol. 128, Part II, 1963.
- [12] Huang, J. S., et al. "Behavior and Design of Steel Beam-to-Column Moment Connections," Bulletin No. 188, Welding Research Council, October 1973.

## SEISMIC ISOLATION OF AN ELECTRON MICROSCOPE

W. G. Godden,<sup>I</sup> M. Aslam,<sup>II</sup> and D. Theodore Scalise<sup>III</sup>

## SUMMARY

A unique two-stage dynamic-isolation problem is presented by the conflicting design requirements for the foundations of an electron microscope in a seismic region. Under normal operational conditions the microscope must be isolated from ambient ground noise; this creates a system extremely vulnerable to seismic ground motions. Under earthquake loading the internal equipment forces must be limited to prevent damage or collapse. An analysis of the proposed design solution is presented. This study was motivated by the 1.5 MeV High Voltage Electron Microscope (HVEM) to be installed at the Lawrence Berkeley Laboratory (LBL) located near the Hayward Fault in California.

## INTRODUCTION

The design basis and principles for the Foundation Isolation System of a high-voltage electron microscope are described in this paper. The required resolving power of the microscope is such that a high degree of isolation from ambient noise is necessary, and a typical means of achieving this is to mount the microscope on a foundation consisting of a long-period resonator with minimum damping. Such a foundation typically consists of a massive concrete block mounted on linear springs, sometimes airbags, with resulting natural periods in the horizontal and vertical directions on the order of one second.

This system behaves as a low pass filter, and due to the absence of damping, would tend to have large amplitude sinusoidal-type displacements in the X, Y, or Z axes under seismic ground motions. These displacements would be large enough to create problems in the design of the equipment, the foundation, and particularly, in the design of the airbags that can be subjected to a limited amount of shear deformation without damage. Hence, some type of additional seismic restraint is called for -- a restraint that must be inoperative under normal conditions, that must restrict the maximum displacement of the microscope support block relative to the ground, and at the same time, reduce the internal forces in the microscope when compared with forces that would be caused by the original earthquake.

One possible solution is to install a coulomb friction device that engages only above a small prescribed level of block displacement. Such a device can be effective in limiting the maximum relative block motion, but at the same time it alters the frequency content of the ground motion transmitted to the equipment. Both of these factors are studied in this paper.

- 
- I Professor of Civil Engineering, University of California, Berkeley.  
II Senior Engineer, Bechtel Corporation, San Francisco.  
III Department Head, Engineering Sciences Department, Lawrence Berkeley Laboratory, University of California, Berkeley.

The results of computer analysis are presented in the form of time-history and spectral response graphs, and these show the conflicting requirements in the dual-isolation problem. Introducing friction damping to the ambient-vibration isolation system reduces maximum block displacements as would be expected. But depending on the friction coefficient selected and on the significant natural frequencies of the microscope, the resulting internal forces may either be reduced or in certain circumstances increased, compared with subjecting the equipment to the original earthquake. This suggests the domain of effective coulomb damping in such an application.

#### PHYSICAL DESCRIPTION OF FOUNDATION ISOLATION SYSTEM

The HVEM Foundation Isolation System includes four major components: (a) HVEM Support Block, (b) Vibration Isolation System, (c) Seismic Restraint System, and (d) Ground Foundation.

The HVEM Support Block (abbreviated herein as "Block") is designed to receive the HVEM microscope support legs and to satisfy the dynamic requirements of the ambient Vibration Isolation System. The Ground Foundation is designed to withstand all loads imposed by the Block and microscope and its own mass, due to gravitational or earthquake forces; its motion is herein referred to as motion of the Ground. The two isolation systems act between the Block and the Ground to modify the Ground motion.

The Vibration Isolation System is designed to isolate the Block and microscope from all ambient Ground vibrations, and requires the Block and microscope system to have natural frequencies in the one Hertz range. Such natural frequencies would pose extremely severe amplification problems (see Fig. 10) during an earthquake and call for the addition of damping. The Seismic Restraint System is designed to limit the peak accelerations of the Block during an earthquake using horizontal friction surfaces between the Block and the Ground.

Figures 1, 2, and 3 show components of the Foundation System including the air-bags which act as linear springs. The friction devices, which are not shown, are located between the air-bags and consist of friction washers under a constant normal compression. A small horizontal clearance ensures that these devices operate only during an earthquake.

#### BACKGROUND OF PRESENT ANALYSIS

##### Prior Developments

The earthquake sliding response [1] and the earthquake rocking response [2,3,4] of rigid bodies, unattached to the ground, have been previously investigated. These investigations derived mathematical models that were validated by experiments using the shaking table at the U.C. Earthquake Engineering Research Center [5].

In these studies, a computer program named BLOKSLD was written to solve the seismic sliding problem [1]. In the present study, BLOKSLD has been further developed to determine the response of the HVEM Seismic Restraint System.

The BLOKSLD program gives the instantaneous, maximum, and residual displacements (relative to the ground) and the accelerations of a rigid body responding in the sliding-mode to simultaneous vertical and horizontal earthquake accelerations as a function of the coefficient of friction between the rigid body and the ground. The forces on the Block are friction and the elastic spring force which is assumed to be proportional to the relative displacement between the rigid body and the ground.

### Equation of Motion

Figure 4 shows the horizontal forces acting on a sliding Block at (a) the threshold of sliding and (b) during sliding. The notation is as follows:  $g$  = acceleration of gravity;  $K$  = spring stiffness;  $M$  = mass of Block;  $s = u - x$  = relative horizontal displacement of Block;  $\dot{s} = ds/dt$ ;  $t$  = time;  $u$  = absolute horizontal ground displacement;  $\dot{u} = du/dt$ ;  $\ddot{u} = d^2u/dt^2$ ;  $W$  = weight of Block;  $x$  = absolute horizontal displacement of Block;  $\dot{x} = dx/dt$ ;  $\ddot{x} = d^2x/dt^2$ ;  $\mu$  = coefficient of friction. Subscript "0" on  $u$  and  $x$  denote their initial values.

At the threshold of sliding, the inertial force equals the frictional force:

$$M|\ddot{u}| = \mu W \quad (1)$$

Sliding commences when  $|\ddot{u}| > \mu g$ . During sliding the equation of motion derived from the relationship among the inertial, frictional, and linear spring forces is

$$\ddot{x} = \mu g (\text{sign of } \dot{s}) + \frac{Ks}{M} \quad (2)$$

$$\text{where } \dot{s} \equiv \dot{u} - \dot{x} = \text{velocity of block relative to ground} \quad (3)$$

The block reattaches to the ground when  $\dot{s} = 0$ . The BLOKSLD program is used to integrate the equation of motion subject to the above sliding and reattachment conditions for the given ground motion.

### ANALYSIS FOR HVEM ISOLATION FOUNDATION

The design-basis earthquake for this study was defined by Professor Bolt [6]. It has a peak acceleration in horizontal shaking of 0.7 g, a peak displacement of 1.77 ft and the bracketed duration of the sharp shaking is 25 seconds.

The motion of the HVEM foundation Block subjected to this earthquake depends on the natural period of the Block in horizontal motion, and the coefficient of friction which restrains this motion. The motion of the Block is the base motion as seen by the HVEM.

### HVEM Foundation Block Motion

In this study it is assumed that the total mass of the Block in horizontal motion includes the mass of the HVEM as a rigid body, and that the horizontal friction operates immediately following the horizontal

movement of the block (i.e., the very small clearance in the design to isolate the Block from ambient ground motions is neglected).

The following values related to the Block design have been used in this study:

Weight of Block + HVEM	$W = 260$ kips
Horizontal stiffness of 12 airbags	$K = 15.1$ k/in = $0.058 W/in$
Undamped natural period of horizontal motion of the Block	$T = 2\pi\sqrt{M/K} = 1.33$ seconds
Horizontal friction coefficient	$\mu = 0.20$ to $0.25$

As the peak acceleration of the earthquake is  $0.7 g$ , if  $\mu = 0.7$  the motion of Block and Ground are identical. For smaller values of  $\mu$  the Block motion is different from the base ground motion; in effect the response of the Block provides a modified earthquake to the HVEM.

#### Time-Histories of HVEM Support Block Motions

The results of the analysis are shown in Figures 5-8 which give the time-histories of the horizontal accelerations, velocities, and displacements for both the ground and the Block for different values of  $\mu$  and  $K$ . The air-bag spring constant  $K$  is expressed as a ratio of the Block weight per inch displacement.

Figure 5 shows that in the limiting case of very small friction ( $\mu = 0.01$ ), the harmonic Block accelerations and displacements are too large. Figure 6 shows that in the design friction range ( $\mu = 0.20$ ), the Block acceleration is reduced and relative displacements are small. Figure 7 is an enlargement of the first 12 seconds of Fig. 6. Figure 8 is for the limiting case of Block motion with friction but without linear spring ( $K = 0$ ).

These time-histories show clearly the significant reduction in Block accelerations achieved by the addition of friction restrainers.

#### Maximum Block Movement

The relative displacement between Block and ground is important in that a maximum clearance of 4 in. has been specified in the design. When  $\mu$  is reduced from 0.70 the relative displacement increases from zero and becomes very large at the resonant frequency of the block as  $\mu$  approaches zero. Computed values of Block displacement relative to ground for the design earthquake, for  $T = 1.33$  seconds, and for a wide range of  $\mu$  values are given in Fig. 9.

It will be noted that the minimum value of  $\mu$  which maintains the maximum relative block displacement within 4 in. is  $\mu = 0.175$ . It was recommended that a value slightly above this be used in the design.

## Response Spectra of Block Motion

The horizontal motion of the Block can be considered as a new earthquake, and its effect on the HVEM studied using response spectra is shown in Fig. 10. Comparing the response spectra for the Block motion with the original earthquake, the following can be noted:

1. Neglecting the case of very small values of friction coefficient ( $\mu = 0.01$ ), and except in the vicinity of  $T = 1.3$  (the undamped natural period of the block), the response spectrum due to Block motion is less than that for the original Ground motion.

2. In the vicinity of  $T = 0.13$  seconds (the undamped natural period of the HVEM in horizontal motion considering the HVEM as a lumped mass on its supporting frame), a reduction in  $\mu$  results in a reduction in seismic response of the HVEM. This is important in selecting an appropriate value of  $\mu$  as indicated above.

3. Using smoothed spectral values, Fig. 11 shows the spectral acceleration of the HVEM structure for discrete values at  $T$  and for a wide range of  $\mu$ . This indicates that at the suggested design value of  $\mu = 0.20$ , the peak acceleration of the HVEM as a SDOF system is in the order of 1.6g. All values shown are for 2% damping.

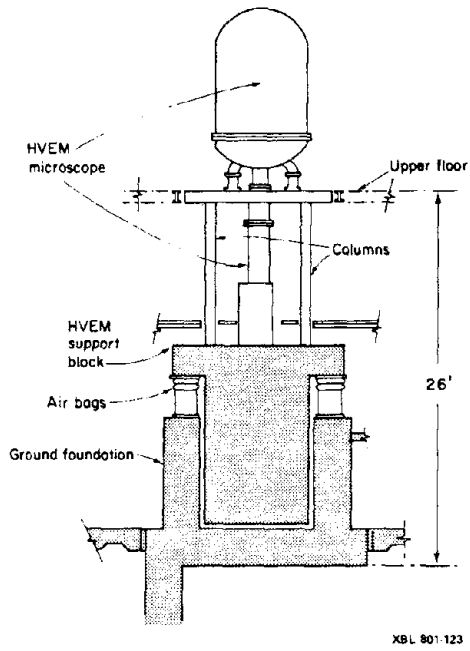
4. The isolation system using friction devices does provide a considerable reduction in spectral response, though possibly not as much as by more-costly continuously-yielding ductile devices.

## ACKNOWLEDGEMENTS

James G. Miller of LBL made all of the program modification and computer runs which provided the data in this report. Paul Hernandez and Walter Hartsough of LBL provided valuable support and guidance. This report was done with support from the U. S. Department of Energy under Contract No. W-7405-ENG-48.

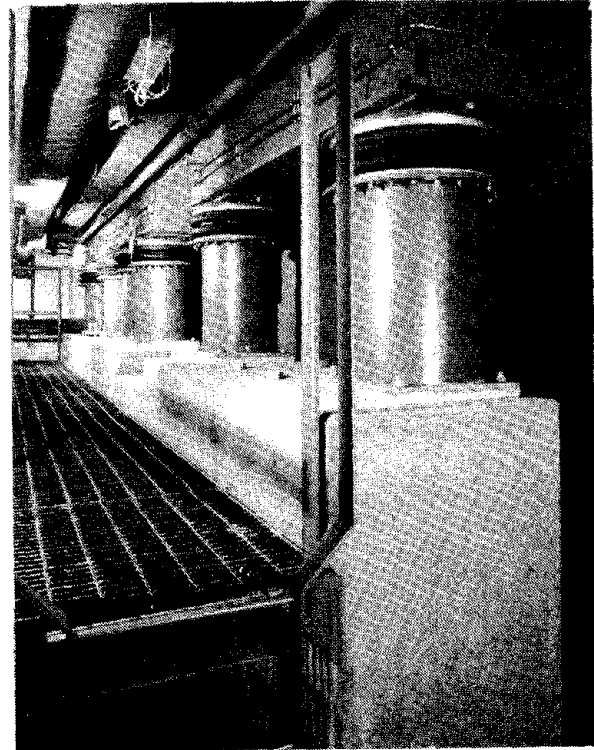
## REFERENCES

1. Aslam, M., Godden, W. G., and Scalise, D. T., "Sliding Response of Rigid Bodies to Earthquake Motions," LBL-3868, Lawrence Berkeley Laboratory, University of California, Berkeley, Calif., Sept., 1975.
2. Housner, G. W., "The Behavior of Inverted Pendulum Structures During Earthquakes," Bulletin of the Seismological Society of America, Vol. 53, No. 2, February 1963.
3. Aslam, M., Godden, W. G., and Scalise, D. T., "Earthquake Rocking Response of Rigid Bodies," Journal of the Engineering Mechanics Division, ASCE, February 1980.
4. Jennings, P. C., Housner, G. W., and Tsai, N. C., "Simulated Earthquake Motions," California Institute of Technology, Pasadena, Calif., April, 1968.
5. Rea, D., and Penzien, J., "Structural Research Using an Earthquake Simulator," Proceedings, Structural Engineering Association of California Conference, Monterey, Calif., 1972.
6. Bolt, Bruce; Private Communication, February 15, 1979.



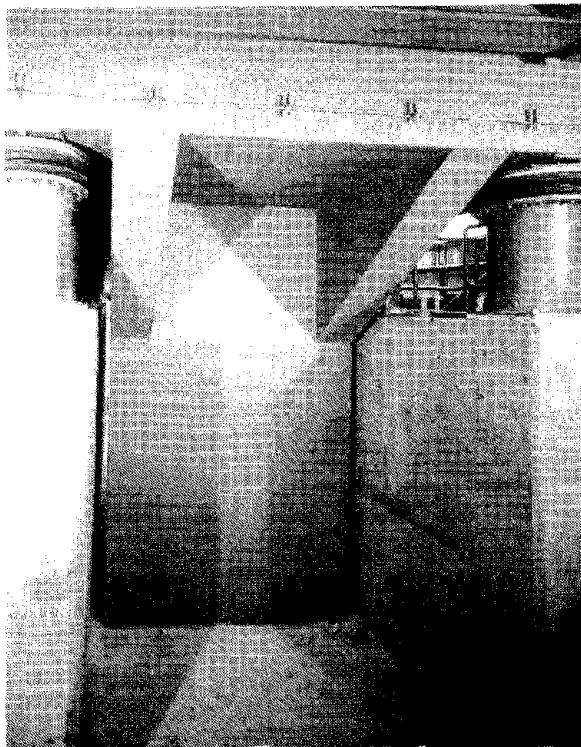
XBL 801-123

Fig. 1. HVEM physical layout diagram.



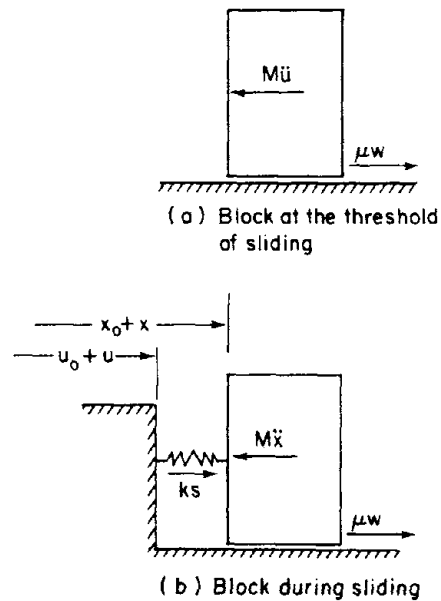
CBB 801-109

Fig. 2. Side-view photograph showing air bags.



CBB 801-107

Fig. 3. End-view photograph showing HVEM support block.



XBL 801-114

Fig. 4. Horizontal forces on unattached rigid block during an earthquake.



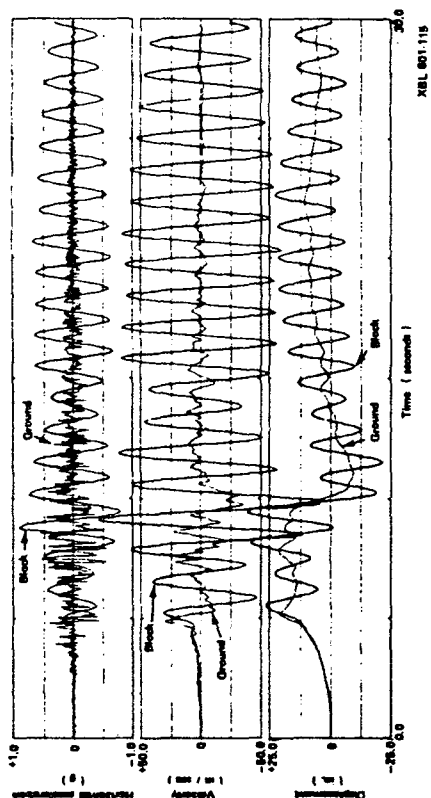


Fig. 5. Motion of microscope foundation block subjected to design earthquake [Bolt 2/15/79],  $\mu = 0.01$ ,  $K = 0.058$  W/in.,  $W = 260$  Kips

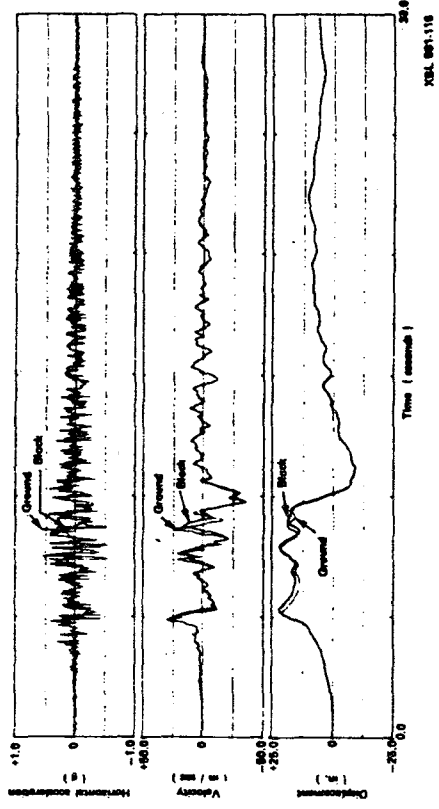


Fig. 6. Motion of microscope foundation block subjected to design earthquake [Bolt 2/15/79],  $\mu = 0.20$ ,  $K = 0.058$  W/in.,  $W = 260$  Kips.

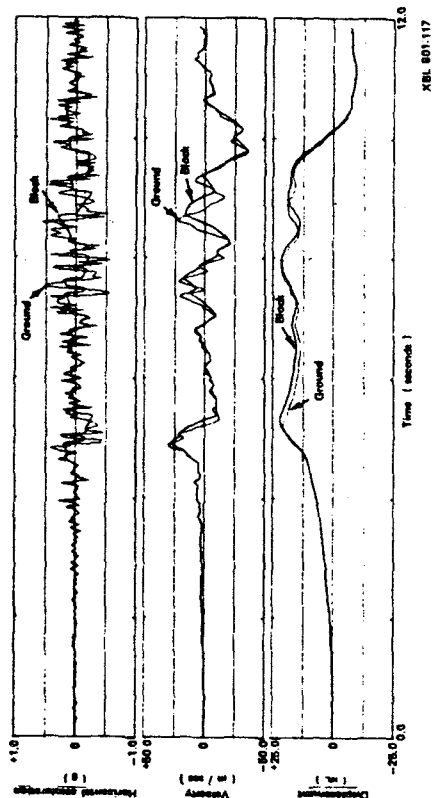


Fig. 7. Enlargement of first 12 seconds of Fig. 6,  $\mu = 0.20$ ,  $K = 0.058$  W/in.,  $W = 260$  Kips.

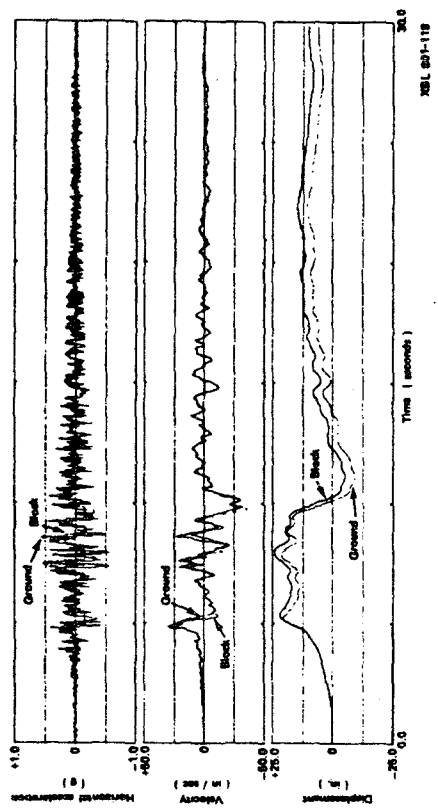


Fig. 8. Motion of microscope foundation block subjected to design earthquake [Bolt 2/15/79],  $\mu = 0.20$ ,  $K = 0.000$  W/in.,  $W = 260$  Kips.

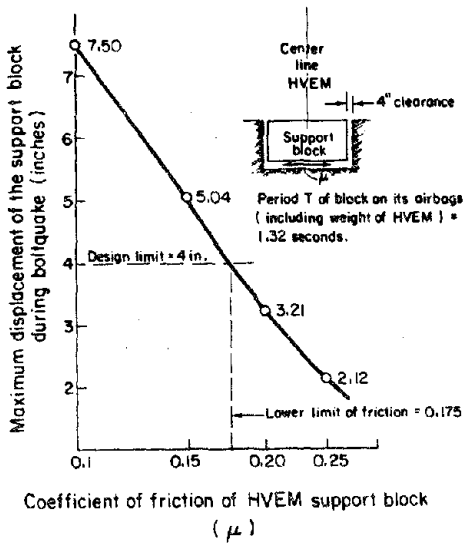


Fig. 9. Effect of friction on the maximum relative displacement of HVEM support block during design-basis earthquake.

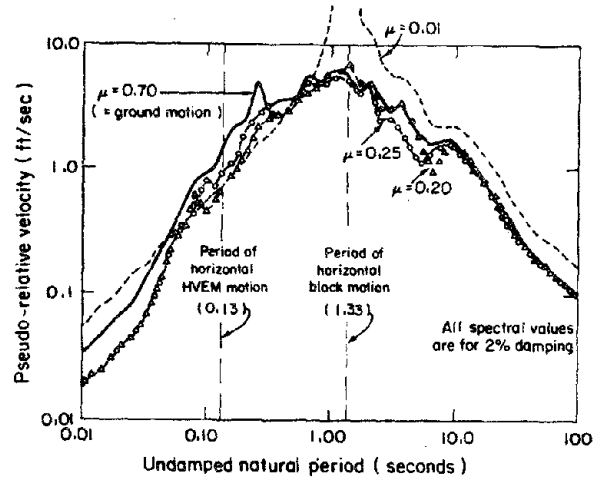


Fig. 10. Effect of block friction on spectral response of block motion.

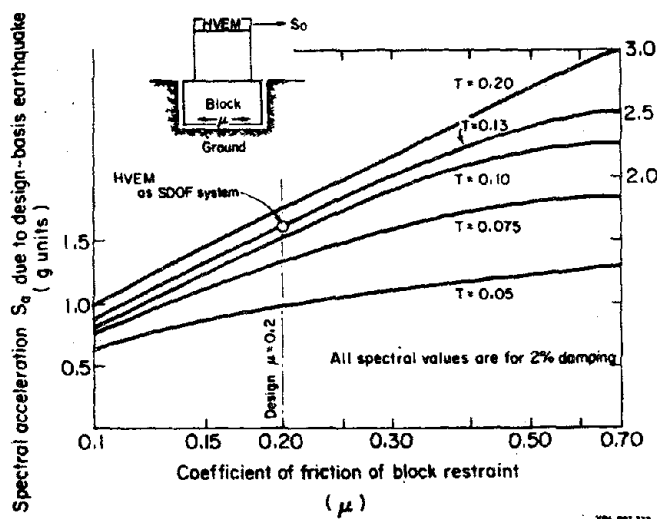


Fig. 11. Influence of block friction on spectral acceleration ( $S_a$ ) response due to design-basis earthquake.

EARTHQUAKE INSURANCE AND MICROZONED GEOLOGIC HAZARDS:  
UNITED STATES PRACTICE

by

Karl V. Steinbrugge<sup>I</sup>

Henry J. Lagorio<sup>II</sup>

S. T. Algermissen<sup>III</sup>

SUMMARY

Engineering and scientific microzonation applications to earthquake insurance are cost limited by the size of insurance premiums. High value buildings with high premiums allow a detailed examination of site specific geotechnical information. Generalized microzonation maps have best utility for low valued buildings. Experience indicates that the most effective usage comes from maps relating soil characteristics to monetary loss patterns by class of construction materials. Applying microzonation maps of active faults to dwellings is difficult for economic reasons while landsliding has difficult technical-economic problems. There are clear needs to improve microzonation techniques to suit insurance and other financial requirements.

INTRODUCTION

Earthquake engineers and scientists feel, with some justification, that their findings when applied by financial institutions should lead to savings to the public and also result in safer construction. Within this view, differential earthquake insurance premiums should acknowledge the degree of earthquake damage control which is included in the design as well as site related earthquake geologic hazards. In this paper, insurance practice in California, USA, will be used as an example of current practice and thinking, admitting that significant variants exist around the world. Emphasis is placed on single family dwellings and microzonation.

Earthquake insurance rates (and thereby premiums) are related to a combination of site conditions and to the earthquake damage potential of the structure itself. This paper, however, will be limited to a discussion of the first of these (site conditions) for which land-use and microzonation procedures are appropriate.

Microzonation with respect to geologic hazards has different meanings among members of the engineering and research communities and those

---

<sup>I</sup> Professor Emeritus, University of California, Berkeley, California.  
<sup>II</sup> Associate Dean for Research, College of Environmental Design, University of California, Berkeley, California.  
<sup>III</sup> Geophysicist, U. S. Geological Survey, Denver, Colorado.

who apply the results of their research. In this paper, the definition of microzonation is restricted to mean local maps which delineate varying degrees of each of three earthquake geologic hazards with respect to construction: (1) active fault traces, (2) potential landslide areas, and (3) structurally poor ground areas such as marshes. Resulting damage patterns are normally determined by others, doing so on an individual building analysis basis or on a building materials class basis. Seismicity (frequency of occurrence) is considered on a different map or set of maps. The two kinds of maps (geologic hazards and seismicity) complement each other and must be used together.

#### ENGINEERING/SCIENCE COMPONENTS OF EARTHQUAKE INSURANCE

Two fundamental components determine the basic rate for an individual building (or "risk" in insurance terminology). First, the building's probable maximum monetary loss must be determined for a maximum probable earthquake using a given recurrence interval (often 300 years). Second, the seismicity of the area must be factored into the insurance rate. The resulting basic rate may be modified by many factors, including geologic hazards, hazardous roof appendages, exposure hazards from adjoining structures, unrepaired previous earthquake damage, and the like.

The first rating component (probable maximum damage) may be based on a building classification system determined by either (1) materials of construction or by (2) the extent and adequacy of its damage control features. More often than not, economics dictate that the first of these two methods be applied to older non-earthquake resistive buildings of any value as well as to modern low-value earthquake resistive buildings. Moderate and high-value earthquake resistive buildings may warrant significant engineering attention, consistent with the economic caveat that these engineering expenses must be reasonable with respect to the premiums or justified by rate reductions based on this engineering attention. Table 1 is a summary of one major building classification and rating system showing its application to coastal California.

#### STATUS OF MICROZONATION PRACTICES IN INSURANCE

Earthquake premiums from a high-valued building (such as a high-rise) normally warrant an engineering review of construction drawings and geotechnical reports which, for modern buildings, should consider the factors included on microzonation maps. On the other end of the building value scale, site specific geotechnical reports rarely exist on individual single family wood frame dwellings, although they do exist for many modern housing subdivisions in California. Thus, microzonation maps of cities and other jurisdictions are important for the evaluation of low-valued structures and emphasis will henceforth be given to these.

From an equity standpoint, it is imperative that insurance rating methods be fair and be uniformly applied. This means that criteria for the preparation of microzonation maps must be such that all independent investigators can develop essentially the same results from the same source data. This is not the usual case when examining many current microzonation maps. One should also bear in mind that the insurance user of these maps normally does not have a professional background.

TABLE 1

**SIMPLIFIED EARTHQUAKE BUILDING CLASSIFICATIONS AND RATES  
SAN FRANCISCO AND LOS ANGELES**

(After Insurance Services Office)

Building Class	Summary Description	Story Height Limit	Major Special Conditions	Building Rate Cents/\$100	Deductible (in %)	Evaluation Required by Professional Engineer
11 (1)	Wood frame -- habitational	2	-	12.9	** 5	
11 (2)	Wood frame -- small	3	Non-dwellings up to 3,000 sq. ft.	21.4	** 5	
12	Wood frame -- other	-	-	21.4	** 5	
21	All-metal -- small	1	Up to 20,000 sq. ft. area	12.9	5	
22	All-metal -- large	-	-	21.4	5	
31	Steel frame -- superior	-	Superior earthquake resistive	21.4	5	Yes
32	Steel frame -- ordinary	-	Monolithic concrete floors	30.0	5	
33	Steel frame -- intermediate	-	Intermediate earthquake resistive	25.7	5	Yes
34	Steel frame -- other	-	Wood, metal, precast concrete floors	42.8	5	
41	Reinf. concrete -- superior	-	Superior earthquake resistive	25.7	5	Yes
42	Reinf. concrete -- ordinary	-	Monolithic concrete floors	42.8	5	
43	Reinf. concrete -- intermediate	-	Intermediate earthquake resistive	34.2	5	Yes
44	Reinf. concrete -- precast	-	Structural precast concrete	42.8	10	
45	Reinf. concrete -- other	-	Wood, metal floors; mixed concrete & steel frame	42.8	10	
52	Mixed constr. -- superior	1	Superior earthquake resistive	34.2	5	Yes
53	Mixed constr.	1	Ordinary earthquake resistive	42.8	10	*Yes
54	Mixed constr. -- intermediate	-	Intermediate earthquake resistive	51.3	10	*Yes
54	Mixed constr.	-	**Ordinary non-earthquake resistive	90.0	10	
55	Mixed constr.	-	Hollow masonry, adobe	135.0	10	
61 thru 65	Special earthquake resistive	-	Special design for damage control	12.9 to 30.0	5	Yes

\*Unless exempted (in certain specified jurisdiction).

\*\*Masonry veneered structures may take variable penalty.

\*\*\*Excluding hollow tile, hollow masonry, adobe, and cavity walls when used as part of a structural system.

### Structurally Poor Ground

Usable insurance oriented microzonation maps of metropolitan areas in California and a few areas elsewhere exist where property values are high and substantial amounts of earthquake insurance are written. The further application of various kinds of insurance microzonation maps showing structurally poor ground awaits the development and general acceptance of consistent mapping criteria. Additionally, it may be some time before certain special microzonation problems have generally accepted solutions. Significant unresolved problem areas have been identified in Santa Rosa, California from damage patterns observed after the 1906 and 1969 earthquakes, in Caracas after the 1967 earthquake, and in San Fernando after the 1971 earthquake.

### Geologically Active Faults

In California, microzonation maps show certain active faults within well-defined "special studies zones" as required by the Alquist-Priolo Act. However, the amount of potential destruction to dwellings from surface faulting is comparatively small as may be seen in Table 2 (Algermissen, 1972). This table shows that the probability of a dwelling being in the 50 meter fault zone is about 1:1000 along the Hayward fault and about 1:5000 along the San Andreas fault. However, based on experience from previous strike-slip fault movements, the damage probabilities would appear to be even more remote than the ratios suggest.

TABLE 2

DWELLINGS SUBJECTED TO VIBRATION AND TO FAULTING  
METROPOLITAN SAN FRANCISCO BAY AREA

	<u>*Dwellings at Risk</u>	<u>**Dwellings on or Near Fault Trace</u>
San Andreas Fault:		
Recurrence of 1906 earthquake	1,203,121	237
Hayward Fault:		
Magnitude = 7.0	1,203,121	1,138

\*Limited to a study area consisting of the 10 San Francisco Bay Area Counties.

\*\*Dwellings within 50 meters of the fault. Hayward fault figure proportionally adjusted from 300 meter zone to 50 meter zone.

As a result, most insurance companies do not find it economically feasible to determine dwelling location with respect to active faults, and fault proximity is not a component of the rate making process. Therefore, the excellent Alquist-Priolo maps have negligible insurance impact on low-valued structures. The economic aspects will be discussed in more detail in a following paragraph.

### Landsliding (Earthquake Induced)

Landslide microzonation maps have been difficult to interpret and apply on an equitable and consistent basis by non-professional personnel. Consider, for example, a map showing existing landslides in an area before development begins. Is one to assume that all new construction will include provisions which will correct existing landslide conditions according to best practice as required by law (building code)? If not, then how can an insurance rate be made without evaluating a soil report, and how can this be economically done? Does an old landslide now represent a stable condition, or is it a most likely candidate for further movement? Or will the next movement take place at a location between two recent landslides? What about hillside construction which is 10, 20, or 30 years old? It would seem that substantial amounts of study are needed, including clarification of criteria, before landslide hazard maps will have their rightful place in microzonation use by financial institutions.

### EARTHQUAKE INSURANCE IN CALIFORNIA

Earthquake insurance has been marketed by American insurance companies since at least 1916. However, it has never been widely purchased, being an estimated 7% of dwellings carrying fire insurance in metropolitan San Francisco and Los Angeles. In spite of the availability of the coverage, aggregate premiums in California in 1978 were only \$23,158,724 for all coverages identifiable as earthquake on all classifications of property including habitational. The 5 percent deductible is often held as a deterrent to the purchase of dwelling earthquake insurance. On the other hand, Kumreuther, et al (1978) concluded: "It seems likely that, unless the hazard appears probable, it will not be viewed as a problem and the individual will not consider protective measures such as insurance" (p. 243).

### ECONOMIC CONSIDERATIONS

#### Homeowner Viewpoint

Apart from psychological reasons (Kumreuther, 1978), economic considerations should influence an individual's decision on purchasing earthquake insurance. A uniform 25% rate penalty for structurally poor ground is applied to all non-dwelling properties in mapped areas; let us examine its comparative economic impact if it is also applied to dwellings.

In Table 3, a 25% rate penalty for structurally poor ground has been separately listed and brings the total earthquake premium to \$12.50 monthly. Fire insurance premiums and property taxes have not been included. While the mortgage in the example is \$60,000, the sale price of the land and improvements would be \$75,000 (with a 20% down payment). Experience has shown that a home buyer or developer is not greatly swayed by a \$10 monthly increase in payments. (The change of 0.25% in the mortgage interest rate from 1976 to 1977 was of a greater dollar amount than the earthquake insurance premium. Housing sales were not significantly affected by this change in interest rates.) The 1979 data have not been included due to instability in mortgage interest rates and marketing conditions resulting from inflation and governmental efforts to combat inflation.

TABLE 3

MORTGAGE AND EARTHQUAKE INSURANCE PAYMENTS  
METROPOLITAN SAN FRANCISCO BAY AREA

	Year		
	1976	1977	1978
<u>Mortgage:</u>			
30 year, \$60,000 mortgage, 20% down payment*			
Mortgage interest rate	8 3/4%	9%	10%
Monthly payment (interest plus principal)	\$472.03	\$482.78	\$526.55
<u>Earthquake Insurance:</u>			
Monthly "Homeowners Policy" earthquake premium**	\$ 10.00	\$ 10.00	\$ 10.00
Increased monthly earthquake premium for structurally poor ground	\$ 2.50	\$ 2.50	\$ 2.50

\*Land at 30% of land plus improvement (Bay Area average in 1978)

\*\*Based on amount of mortgage at its inception. 5% deductible applies. Rate is \$2.00 per \$1,000.

One recent private study conducted by the author on the geographic distribution of almost \$1,000 million in earthquake dwelling insurance showed:

<u>Area</u>	<u>Homeowner Earthquake Policies to Total Homeowner Policies</u>
San Francisco Bay Area	7:100
Waterfront housing in San Mateo County	21 to 32:100

It appears that homeowners may be aware of their geologic hazards on the San Mateo waterfront and be willing to pay for added insurance in their highly publicized hazard area. But they are not discouraged from living there. Quadrupling this geologic hazard penalty to \$10 per month probably would not discourage a sailing enthusiast from wanting to anchor his boat at his home.

One may conclude from the foregoing that economic incentives through present rate penalties are not an effective means to influence most homeowners or builders.

Insurance Company Viewpoint

An insurance company must pragmatically examine the cost of a micro-zonation program in the processing of dwelling policies which include earthquake coverage against the available additional premiums generated by the program. If a microzonation program were introduced into a company's procedure, it would be necessary to apply it nationwide to all



dwelling property on which earthquake is written to avoid the charge of unfair discrimination.

Experience data do not exist on premium income vs. costs for microzonation, but a hypothetical case will give indicative answers. It is reasonable to estimate that perhaps 1 in 50 dwellings in California are in areas for which a 25% rate surcharge could be made for insurance microzoned structurally poor ground. Further, assume a statewide average value for insured dwellings at \$60,000. The annual premium increase for the 25% rate penalty on a \$2.00/\$1,000.00 homeowners/dwelling policy would be \$30.00. Since every policy would have to be reviewed to see if the rate penalty should be applied, then the \$30.00 premium must be spread over 50 policies, or \$0.60 for each policy.

In company operations, premiums for homeowner policies are allocated on percentages such as the following (after "Bests Aggregates and Averages, Property-Casualty, 1977," Stock Companies, p. 113):

Losses and adjustment expense	65.2%
Production and outside costs	18.5%
Internal expense and inspection costs	10.1%
Federal and state taxes	2.9%
Profit and contingency reserves	3.3%
	<u>100.0%</u>

On this basis, 10.1% of the surcharge premium of \$30.00, or \$3.03, would be available to pay the cost of the microzonation program for 50 policies, or 6 cents per policy. This 6 cents can be multiplied by the number of years that the policy may be renewed without re-examination -- possibly ten years. Business judgment has indicated that the final result is not economically feasible.

#### ACKNOWLEDGMENTS

Information and advice were kindly furnished by many persons. Mr. Robert L. Odman (State Farm Fire and Casualty), Mr. Charles R. Ford, (Fireman's Fund Insurance Companies), and Mr. David R. Simmons (Insurance Information Institute) provided specific insurance data and background therefor. While the assistance and resources of insurance organizations and governmental agencies were available to the author, all opinions and conclusions are the sole responsibility of the author.

#### REFERENCES

- Algermissen, S. T., W. A. Rinehart, and J. C. Stepp (1972). "A Technique for Seismic Zoning: Economic Considerations," Vol. II, pp. 943/956 in Proceedings of the International Conference on Microzonation, Seattle, Washington.
- Insurance Services Office (1976). "Commercial Earthquake Insurance Manual." New York, New York.
- Kunreuther, Howard, et al (1978). Disaster Insurance Protection: Public Policy Lessons. New York: John Wiley & Sons.

- Rinehart, W., S. T. Algermissen, and Mary Gibbons (1976). "Estimation of Earthquake Losses to Single Family Dwellings." USGS Open File Report 76-156.
- Steinbrugge, Karl V. (1969). "Seismic Risk to Buildings and Structures on Filled Land in San Francisco Bay," pp. 103/115, in Geologic and Engineering Aspects of San Francisco Bay Fill, California Division of Mines and Geology, Special Report 97.
- Steinbrugge, Karl V. (1978). "Earthquake Insurance and Microzonation," Vol. I, pp. 203/213, in Proceedings of the Second International Conference on Microzonation, Seattle, Washington.

## EARTHQUAKE ENGINEERING RESEARCH CENTER REPORTS

NOTE: Numbers in parenthesis are Accession Numbers assigned by the National Technical Information Service; these are followed by a price code. Copies of the reports may be ordered from the National Technical Information Service, 5285 Port Royal Road, Springfield, Virginia, 22161. Accession Numbers should be quoted on orders for reports (PB --- ---) and remittance must accompany each order. Reports without this information were not available at time of printing. Upon request, EERC will mail inquirers this information when it becomes available.

- EERC 67-1 "Feasibility Study Large-Scale Earthquake Simulator Facility," by J. Penzien, J.G. Bouwkamp, R.W. Clough and D. Rea - 1967 (PB 187 905)A07
- EERC 68-1 Unassigned
- EERC 68-2 "Inelastic Behavior of Beam-to-Column Subassemblages Under Repeated Loading," by V.V. Bertero - 1968 (PB 184 888)A05
- EERC 68-3 "A Graphical Method for Solving the Wave Reflection-Refraction Problem," by H.D. McNiven and Y. Mengi - 1968 (PB 187 943)A03
- EERC 68-4 "Dynamic Properties of McKinley School Buildings," by D. Rea, J.G. Bouwkamp and R.W. Clough - 1968 (PB 187 902)A07
- EERC 68-5 "Characteristics of Rock Motions During Earthquakes," by H.B. Seed, I.M. Idriss and F.W. Kiefer - 1968 (PB 188 338)A03
- EERC 69-1 "Earthquake Engineering Research at Berkeley," - 1969 (PB 187 906)A11
- EERC 69-2 "Nonlinear Seismic Response of Earth Structures," by M. Dibaj and J. Penzien - 1969 (PB 187 904)A08
- EERC 69-3 "Probabilistic Study of the Behavior of Structures During Earthquakes," by R. Ruiz and J. Penzien - 1969 (PB 187 886)A06
- EERC 69-4 "Numerical Solution of Boundary Value Problems in Structural Mechanics by Reduction to an Initial Value Formulation," by N. Distefano and J. Schujman - 1969 (PB 187 942)A02
- EERC 69-5 "Dynamic Programming and the Solution of the Biharmonic Equation," by N. Distefano - 1969 (PB 187 941)A03
- EERC 69-6 "Stochastic Analysis of Offshore Tower Structures," by A.K. Malhotra and J. Penzien - 1969 (PB 187 903)A09
- EERC 69-7 "Rock Motion Accelerograms for High Magnitude Earthquakes," by H.B. Seed and I.M. Idriss - 1969 (PB 187 940)A02
- EERC 69-8 "Structural Dynamics Testing Facilities at the University of California, Berkeley," by R.M. Stephen, J.G. Bouwkamp, R.W. Clough and J. Penzien - 1969 (PB 189 111)A04
- EERC 69-9 "Seismic Response of Soil Deposits Underlain by Sloping Rock Boundaries," by H. Dezfulian and H.B. Seed - 1969 (PB 189 114)A03
- EERC 69-10 "Dynamic Stress Analysis of Axisymmetric Structures Under Arbitrary Loading," by S. Ghosh and E.L. Wilson - 1969 (PB 189 026)A10
- EERC 69-11 "Seismic Behavior of Multistory Frames Designed by Different Philosophies," by J.C. Anderson and V. V. Bertero - 1969 (PB 190 662)A10
- EERC 69-12 "Stiffness Degradation of Reinforcing Concrete Members Subjected to Cyclic Flexural Moments," by V.V. Bertero, B. Bresler and H. Ming Liao - 1969 (PB 202 942)A07
- EERC 69-13 "Response of Non-Uniform Soil Deposits to Travelling Seismic Waves," by H. Dezfulian and H.B. Seed - 1969 (PB 191 023)A03
- EERC 69-14 "Damping Capacity of a Model Steel Structure," by D. Rea, R.W. Clough and J.G. Bouwkamp - 1969 (PB 190 663)A06
- EERC 69-15 "Influence of Local Soil Conditions on Building Damage Potential during Earthquakes," by H.B. Seed and I.M. Idriss - 1969 (PB 191 036)A03
- EERC 69-16 "The Behavior of Sands Under Seismic Loading Conditions," by M.L. Silver and H.B. Seed - 1969 (AD 714 982)A07
- EERC 70-1 "Earthquake Response of Gravity Dams," by A.K. Chopra - 1970 (AD 709 640)A03
- EERC 70-2 "Relationships between Soil Conditions and Building Damage in the Caracas Earthquake of July 29, 1967," by H.B. Seed, I.M. Idriss and H. Dezfulian - 1970 (PB 195 762)A05
- EERC 70-3 "Cyclic Loading of Full Size Steel Connections," by E.P. Popov and R.M. Stephen - 1970 (PB 213 545)A04
- EERC 70-4 "Seismic Analysis of the Charaima Building, Caraballeda, Venezuela," by Subcommittee of the SEAONC Research Committee: V.V. Bertero, P.F. Fratessa, S.A. Mahin, J.H. Sexton, A.C. Scordelis, E.L. Wilson, L.A. Wyllie, H.B. Seed and J. Penzien, Chairman - 1970 (PB 201 455)A06

- EERC 70-5 "A Computer Program for Earthquake Analysis of Dams," by A.K. Chopra and P. Chakrabarti - 1970 (AD 723 994)A05
- EERC 70-6 "The Propagation of Love Waves Across Non-Horizontally Layered Structures," by J. Lysmer and L.A. Drake 1970 (PB 197 896)A03
- EERC 70-7 "Influence of Base Rock Characteristics on Ground Response," by J. Lysmer, H.B. Seed and P.B. Schnabel 1970 (PB 197 897)A03
- EERC 70-8 "Applicability of Laboratory Test Procedures for Measuring Soil Liquefaction Characteristics under Cyclic Loading," by H.B. Seed and W.H. Peacock - 1970 (PB 198 016)A03
- EERC 70-9 "A Simplified Procedure for Evaluating Soil Liquefaction Potential," by H.B. Seed and I.M. Idriss - 1970 (PB 198 009)A03
- EERC 70-10 "Soil Moduli and Damping Factors for Dynamic Response Analysis," by H.B. Seed and I.M. Idriss - 1970 (PB 197 869)A03
- EERC 71-1 "Koyna Earthquake of December 11, 1967 and the Performance of Koyna Dam," by A.K. Chopra and P. Chakrabarti 1971 (AD 731 496)A06
- EERC 71-2 "Preliminary In-Situ Measurements of Anelastic Absorption in Soils Using a Prototype Earthquake Simulator," by R.D. Borcherdt and P.W. Rodgers - 1971 (PB 201 454)A03
- EERC 71-3 "Static and Dynamic Analysis of Inelastic Frame Structures," by F.L. Porter and G.H. Powell - 1971 (PB 210 135)A06
- EERC 71-4 "Research Needs in Limit Design of Reinforced Concrete Structures," by V.V. Bertero - 1971 (PB 202 943)A04
- EERC 71-5 "Dynamic Behavior of a High-Rise Diagonally Braced Steel Building," by D. Rea, A.A. Shah and J.G. Bouwkamp 1971 (PB 203 584)A06
- EERC 71-6 "Dynamic Stress Analysis of Porous Elastic Solids Saturated with Compressible Fluids," by J. Ghaboussi and E. L. Wilson - 1971 (PB 211 396)A06
- EERC 71-7 "Inelastic Behavior of Steel Beam-to-Column Subassemblages," by H. Krawinkler, V.V. Bertero and E.P. Popov 1971 (PB 211 335)A14
- EERC 71-8 "Modification of Seismograph Records for Effects of Local Soil Conditions," by P. Schnabel, H.B. Seed and J. Lysmer - 1971 (PB 214 450)A03
- EERC 72-1 "Static and Earthquake Analysis of Three Dimensional Frame and Shear Wall Buildings," by E.L. Wilson and H.H. Dovey - 1972 (PB 212 904)A05
- EERC 72-2 "Accelerations in Rock for Earthquakes in the Western United States," by P.B. Schnabel and H.B. Seed - 1972 (PB 213 100)A03
- EERC 72-3 "Elastic-Plastic Earthquake Response of Soil-Building Systems," by T. Minami - 1972 (PB 214 868)A08
- EERC 72-4 "Stochastic Inelastic Response of Offshore Towers to Strong Motion Earthquakes," by M.K. Kaul - 1972 (PB 215 713)A05
- EERC 72-5 "Cyclic Behavior of Three Reinforced Concrete Flexural Members with High Shear," by E.P. Popov, V.V. Bertero and H. Krawinkler - 1972 (PB 214 555)A05
- EERC 72-6 "Earthquake Response of Gravity Dams Including Reservoir Interaction Effects," by P. Chakrabarti and A.K. Chopra - 1972 (AD 762 330)A08
- EERC 72-7 "Dynamic Properties of Pine Flat Dam," by D. Rea, C.Y. Liaw and A.K. Chopra - 1972 (AD 763 928)A05
- EERC 72-8 "Three Dimensional Analysis of Building Systems," by E.L. Wilson and H.H. Dovey - 1972 (PB 222 438)A06
- EERC 72-9 "Rate of Loading Effects on Uncracked and Repaired Reinforced Concrete Members," by S. Mahin, V.V. Bertero, D. Rea and M. Atalay - 1972 (PB 224 520)A08
- EERC 72-10 "Computer Program for Static and Dynamic Analysis of Linear Structural Systems," by E.L. Wilson, K.-J. Bathe, J.E. Peterson and H.H. Dovey - 1972 (PB 220 437)A04
- EERC 72-11 "Literature Survey - Seismic Effects on Highway Bridges," by T. Iwasaki, J. Penzien and R.W. Clough - 1972 (PB 215 613)A19
- EERC 72-12 "SHAKE-A Computer Program for Earthquake Response Analysis of Horizontally Layered Sites," by P.B. Schnabel and J. Lysmer - 1972 (PB 220 207)A06
- EERC 73-1 "Optimal Seismic Design of Multistory Frames," by V.V. Bertero and H. Kamil - 1973
- EERC 73-2 "Analysis of the Slides in the San Fernando Dams During the Earthquake of February 9, 1971," by H.B. Seed, K.L. Lee, I.M. Idriss and F. Makdissi - 1973 (PB 223 402)A14

- EERC 73-3 "Computer Aided Ultimate Load Design of Unbraced Multistory Steel Frames," by M.B. El-Hafez and G.H. Powell 1973 (PB 248 315)A09
- EERC 73-4 "Experimental Investigation into the Seismic Behavior of Critical Regions of Reinforced Concrete Components as Influenced by Moment and Shear," by M. Celebi and J. Penzien - 1973 (PB 215 884)A09
- EERC 73-5 "Hysteretic Behavior of Epoxy-Repaired Reinforced Concrete Beams," by M. Celebi and J. Penzien - 1973 (PB 239 568)A03
- EERC 73-6 "General Purpose Computer Program for Inelastic Dynamic Response of Plane Structures," by A. Kanaan and G.H. Powell - 1973 (PB 221 260)A08
- EERC 73-7 "A Computer Program for Earthquake Analysis of Gravity Dams Including Reservoir Interaction," by P. Chakrabarti and A.K. Chopra - 1973 (AD 766 271)A04
- EERC 73-8 "Behavior of Reinforced Concrete Deep Beam-Column Subassemblages Under Cyclic Loads," by O. Küstü and J.G. Bouwkamp - 1973 (PB 246 117)A12
- EERC 73-9 "Earthquake Analysis of Structure-Foundation Systems," by A.K. Vaish and A.K. Chopra - 1973 (AD 766 272)A07
- EERC 73-10 "Deconvolution of Seismic Response for Linear Systems," by R.B. Reimer - 1973 (PB 227 179)A08
- EERC 73-11 "SAP IV: A Structural Analysis Program for Static and Dynamic Response of Linear Systems," by K.-J. Bathe, E.L. Wilson and F.E. Peterson - 1973 (PB 221 967)A09
- EERC 73-12 "Analytical Investigations of the Seismic Response of Long, Multiple Span Highway Bridges," by W.S. Tseng and J. Penzien - 1973 (PB 227 816)A10
- EERC 73-13 "Earthquake Analysis of Multi-Story Buildings Including Foundation Interaction," by A.K. Chopra and J.A. Gutierrez - 1973 (PB 222 970)A03
- EERC 73-14 "ADAP: A Computer Program for Static and Dynamic Analysis of Arch Dams," by R.W. Clough, J.M. Raphael and S. Mojtahedi - 1973 (PB 223 763)A09
- EERC 73-15 "Cyclic Plastic Analysis of Structural Steel Joints," by R.B. Finkney and R.W. Clough - 1973 (PB 226 843)A08
- EERC 73-16 "QUAD-4: A Computer Program for Evaluating the Seismic Response of Soil Structures by Variable Damping Finite Element Procedures," by I.M. Idriss, J. Lysmer, R. Hwang and H.B. Seed - 1973 (PB 229 424)A05
- EERC 73-17 "Dynamic Behavior of a Multi-Story Pyramid Shaped Building," by R.M. Stephen, J.P. Hollings and J.G. Bouwkamp - 1973 (PB 240 718)A06
- EERC 73-18 "Effect of Different Types of Reinforcing on Seismic Behavior of Short Concrete Columns," by V.V. Bertero, J. Hollings, O. Küstü, R.M. Stephen and J.G. Bouwkamp - 1973
- EERC 73-19 "Olive View Medical Center Materials Studies, Phase I," by B. Bresler and V.V. Bertero - 1973 (PB 235 986)A06
- EERC 73-20 "Linear and Nonlinear Seismic Analysis Computer Programs for Long Multiple-Span Highway Bridges," by W.S. Tseng and J. Penzien - 1973
- EERC 73-21 "Constitutive Models for Cyclic Plastic Deformation of Engineering Materials," by J.M. Kelly and P.P. Gillis 1973 (PB 226 024)A03
- EERC 73-22 "DRAIN - 2D User's Guide," by G.H. Powell - 1973 (PB 227 016)A05
- EERC 73-23 "Earthquake Engineering at Berkeley - 1973," (PB 226 033)A11
- EERC 73-24 Unassigned
- EERC 73-25 "Earthquake Response of Axisymmetric Tower Structures Surrounded by Water," by C.Y. Liaw and A.K. Chopra 1973 (AD 773 052)A09
- EERC 73-26 "Investigation of the Failures of the Olive View Stairtowers During the San Fernando Earthquake and Their Implications on Seismic Design," by V.V. Bertero and R.G. Collins - 1973 (PB 235 106)A13
- EERC 73-27 "Further Studies on Seismic Behavior of Steel Beam-Column Subassemblages," by V.V. Bertero, H. Krawinkler and E.P. Popov - 1973 (PB 234 172)A06
- EERC 74-1 "Seismic Risk Analysis," by C.S. Oliveira - 1974 (PB 235 920)A06
- EERC 74-2 "Settlement and Liquefaction of Sands Under Multi-Directional Shaking," by R. Pyke, C.K. Chan and H.B. Seed 1974
- EERC 74-3 "Optimum Design of Earthquake Resistant Shear Buildings," by D. Ray, K.S. Pister and A.K. Chopra - 1974 (PB 231 172)A06
- EERC 74-4 "LUSH - A Computer Program for Complex Response Analysis of Soil-Structure Systems," by J. Lysmer, T. Udaka, H.B. Seed and R. Hwang - 1974 (PB 236 796)A05

- EERC 74-5 "Sensitivity Analysis for Hysteretic Dynamic Systems: Applications to Earthquake Engineering," by D. Ray  
1974 (PB 233 213)A06
- EERC 74-6 "Soil Structure Interaction Analyses for Evaluating Seismic Response," by H.B. Seed, J. Lysmer and R. Hwang  
1974 (PB 236 519)A04
- EERC 74-7 Unassigned
- EERC 74-8 "Shaking Table Tests of a Steel Frame - A Progress Report," by R.W. Clough and D. Tang - 1974 (PB 240 869)A03
- EERC 74-9 "Hysteretic Behavior of Reinforced Concrete Flexural Members with Special Web Reinforcement," by  
V.V. Bertero, E.P. Popov and T.Y. Wang - 1974 (PB 236 797)A07
- EERC 74-10 "Applications of Reliability-Based, Global Cost Optimization to Design of Earthquake Resistant Structures,"  
by E. Vitiello and K.S. Pister - 1974 (PB 237 231)A06
- EERC 74-11 "Liquefaction of Gravelly Soils Under Cyclic Loading Conditions," by R.T. Wong, H.B. Seed and C.K. Chan  
1974 (PB 242 042)A03
- EERC 74-12 "Site-Dependent Spectra for Earthquake-Resistant Design," by H.B. Seed, C. Ugas and J. Lysmer - 1974  
(PB 240 953)A03
- EERC 74-13 "Earthquake Simulator Study of a Reinforced Concrete Frame," by P. Hidalgo and R.W. Clough - 1974  
(PB 241 944)A13
- EERC 74-14 "Nonlinear Earthquake Response of Concrete Gravity Dams," by N. Pal - 1974 (AD/A 006 583)A06
- EERC 74-15 "Modeling and Identification in Nonlinear Structural Dynamics - I. One Degree of Freedom Models," by  
N. Distefano and A. Rath - 1974 (PB 241 548)A06
- EERC 75-1 "Determination of Seismic Design Criteria for the Dumbarton Bridge Replacement Structure, Vol. I: Description,  
Theory and Analytical Modeling of Bridge and Parameters," by F. Baron and S.-H. Pang - 1975 (PB 259 407)A15
- EERC 75-2 "Determination of Seismic Design Criteria for the Dumbarton Bridge Replacement Structure, Vol. II: Numerical  
Studies and Establishment of Seismic Design Criteria," by F. Baron and S.-H. Pang - 1975 (PB 259 408)A11  
(For set of EERC 75-1 and 75-2 (PB 259 406))
- EERC 75-3 "Seismic Risk Analysis for a Site and a Metropolitan Area," by C.S. Oliveira - 1975 (PB 248 134)A09
- EERC 75-4 "Analytical Investigations of Seismic Response of Short, Single or Multiple-Span Highway Bridges," by  
M.-C. Chen and J. Penzien - 1975 (PB 241 454)A09
- EERC 75-5 "An Evaluation of Some Methods for Predicting Seismic Behavior of Reinforced Concrete Buildings," by S.A.  
Mahin and V.V. Bertero - 1975 (PB 246 306)A16
- EERC 75-6 "Earthquake Simulator Study of a Steel Frame Structure, Vol. I: Experimental Results," by R.W. Clough and  
D.T. Tang - 1975 (PB 243 981)A13
- EERC 75-7 "Dynamic Properties of San Bernardino Intake Tower," by D. Rea, C.-Y. Liaw and A.K. Chopra - 1975 (AD/A008 406)  
A05
- EERC 75-8 "Seismic Studies of the Articulation for the Dumbarton Bridge Replacement Structure, Vol. I: Description,  
Theory and Analytical Modeling of Bridge Components," by F. Baron and R.E. Hamati - 1975 (PB 251 539)A07
- EERC 75-9 "Seismic Studies of the Articulation for the Dumbarton Bridge Replacement Structure, Vol. 2: Numerical  
Studies of Steel and Concrete Girder Alternates," by F. Baron and R.E. Hamati - 1975 (PB 251 540)A10
- EERC 75-10 "Static and Dynamic Analysis of Nonlinear Structures," by D.P. Mondkar and G.H. Powell - 1975 (PB 242 434)A08
- EERC 75-11 "Hysteretic Behavior of Steel Columns," by E.P. Popov, V.V. Bertero and S. Chandramouli - 1975 (PB 252 365)A11
- EERC 75-12 "Earthquake Engineering Research Center Library Printed Catalog," - 1975 (PB 243 711)A26
- EERC 75-13 "Three Dimensional Analysis of Building Systems (Extended Version)," by E.L. Wilson, J.P. Hollings and  
H.H. Dovey - 1975 (PB 243 989)A07
- EERC 75-14 "Determination of Soil Liquefaction Characteristics by Large-Scale Laboratory Tests," by P. De Alba,  
C.K. Chan and H.B. Seed - 1975 (NUREG 0027)A08
- EERC 75-15 "A Literature Survey - Compressive, Tensile, Bond and Shear Strength of Masonry," by R.L. Mayes and R.W.  
Clough - 1975 (PB 246 292)A10
- EERC 75-16 "Hysteretic Behavior of Ductile Moment Resisting Reinforced Concrete Frame Components," by V.V. Bertero and  
E.P. Popov - 1975 (PB 246 388)A05
- EERC 75-17 "Relationships Between Maximum Acceleration, Maximum Velocity, Distance from Source, Local Site Conditions  
for Moderately Strong Earthquakes," by H.B. Seed, R. Murarka, J. Lysmer and I.M. Idriss - 1975 (PB 248 172)A03
- EERC 75-18 "The Effects of Method of Sample Preparation on the Cyclic Stress-Strain Behavior of Sands," by J. Mullis,  
C.K. Chan and H.B. Seed - 1975 (Summarized in EERC 75-28)

- EERC 75-19 "The Seismic Behavior of Critical Regions of Reinforced Concrete Components as Influenced by Moment, Shear and Axial Force," by M.B. Atalay and J. Penzien - 1975 (PB 258 842)A11
- EERC 75-20 "Dynamic Properties of an Eleven Story Masonry Building," by R.M. Stephen, J.P. Hollings, J.G. Bouwkamp and D. Jurukovski - 1975 (PB 246 945)A04
- EERC 75-21 "State-of-the-Art in Seismic Strength of Masonry - An Evaluation and Review," by R.L. Mayes and R.W. Clough 1975 (PB 249 040)A07
- EERC 75-22 "Frequency Dependent Stiffness Matrices for Viscoelastic Half-Plane Foundations," by A.K. Chopra, P. Chakrabarti and G. Dasgupta - 1975 (PB 248 121)A07
- EERC 75-23 "Hysteretic Behavior of Reinforced Concrete Framed Walls," by T.Y. Wong, V.V. Bertero and E.P. Popov - 1975
- EERC 75-24 "Testing Facility for Subassemblages of Frame-Wall Structural Systems," by V.V. Bertero, E.P. Popov and T. Endo - 1975
- EERC 75-25 "Influence of Seismic History on the Liquefaction Characteristics of Sands," by H.B. Seed, K. Mori and C.K. Chan - 1975 (Summarized in EERC 75-28)
- EERC 75-26 "The Generation and Dissipation of Pore Water Pressures during Soil Liquefaction," by H.B. Seed, P.P. Martin and J. Lysmer - 1975 (PB 252 648)A03
- EERC 75-27 "Identification of Research Needs for Improving Aseismic Design of Building Structures," by V.V. Bertero 1975 (PB 248 136)A05
- EERC 75-28 "Evaluation of Soil Liquefaction Potential during Earthquakes," by H.B. Seed, I. Arango and C.K. Chan - 1975 (NUREG 0026)A13
- EERC 75-29 "Representation of Irregular Stress Time Histories by Equivalent Uniform Stress Series in Liquefaction Analyses," by H.B. Seed, I.M. Idriss, F. Makdisi and N. Banerjee - 1975 (PB 252 635)A03
- EERC 75-30 "FLUSH - A Computer Program for Approximate 3-D Analysis of Soil-Structure Interaction Problems," by J. Lysmer, T. Udaka, C.-F. Tsai and H.B. Seed - 1975 (PB 259 332)A07
- EERC 75-31 "ALUSH - A Computer Program for Seismic Response Analysis of Axisymmetric Soil-Structure Systems," by E. Berger, J. Lysmer and H.B. Seed - 1975
- EERC 75-32 "TRIP and TRAVEL - Computer Programs for Soil-Structure Interaction Analysis with Horizontally Travelling Waves," by T. Udaka, J. Lysmer and H.B. Seed - 1975
- EERC 75-33 "Predicting the Performance of Structures in Regions of High Seismicity," by J. Penzien - 1975 (PB 248 130)A03
- EERC 75-34 "Efficient Finite Element Analysis of Seismic Structure - Soil - Direction," by J. Lysmer, H.B. Seed, T. Udaka, R.N. Hwang and C.-F. Tsai - 1975 (PB 253 570)A03
- EERC 75-35 "The Dynamic Behavior of a First Story Girder of a Three-Story Steel Frame Subjected to Earthquake Loading," by R.W. Clough and L.-Y. Li - 1975 (PB 248 841)A05
- EERC 75-36 "Earthquake Simulator Study of a Steel Frame Structure, Volume II - Analytical Results," by D.T. Tang - 1975 (PB 252 926)A10
- EERC 75-37 "ANSR-I General Purpose Computer Program for Analysis of Non-Linear Structural Response," by D.P. Mondkar and G.H. Powell - 1975 (PB 252 386)A08
- EERC 75-38 "Nonlinear Response Spectra for Probabilistic Seismic Design and Damage Assessment of Reinforced Concrete Structures," by M. Murakami and J. Penzien - 1975 (PB 259 530)A05
- EERC 75-39 "Study of a Method of Feasible Directions for Optimal Elastic Design of Frame Structures Subjected to Earthquake Loading," by N.D. Walker and K.S. Pister - 1975 (PB 257 781)A06
- EERC 75-40 "An Alternative Representation of the Elastic-Viscoelastic Analogy," by G. Dasgupta and J.L. Sackman - 1975 (PB 252 173)A03
- EERC 75-41 "Effect of Multi-Directional Shaking on Liquefaction of Sands," by H.B. Seed, R. Pyke and G.R. Martin - 1975 (PB 258 781)A03
- EERC 76-1 "Strength and Ductility Evaluation of Existing Low-Rise Reinforced Concrete Buildings - Screening Method," by T. Okada and B. Bresler - 1976 (PB 257 906)A11
- EERC 76-2 "Experimental and Analytical Studies on the Hysteretic Behavior of Reinforced Concrete Rectangular and T-Beams," by S.-Y.M. Ma, E.P. Popov and V.V. Bertero - 1976 (PB 260 843)A12
- EERC 76-3 "Dynamic Behavior of a Multistory Triangular-Shaped Building," by J. Petrovski, R.M. Stephen, E. Gartenbaum and J.G. Bouwkamp - 1976 (PB 273 279)A07
- EERC 76-4 "Earthquake Induced Deformations of Earth Dams," by N. Serff, H.B. Seed, F.I. Makdisi & C.-Y. Chang - 1976 (PB 292 065)A08

- EERC 76-5 "Analysis and Design of Tube-Type Tall Building Structures," by H. de Clercq and G.H. Powell - 1976 (PB 252 220) A10
- EERC 76-6 "Time and Frequency Domain Analysis of Three-Dimensional Ground Motions, San Fernando Earthquake," by T. Kubo and J. Penzien (PB 260 556)A11
- EERC 76-7 "Expected Performance of Uniform Building Code Design Masonry Structures," by R.L. Mayes, Y. Omote, S.W. Chen and R.W. Clough - 1976 (PB 270 098)A05
- EERC 76-8 "Cyclic Shear Tests of Masonry Piers, Volume 1 - Test Results," by R.L. Mayes, Y. Omote, R.W. Clough - 1976 (PB 264 424)A06
- EERC 76-9 "A Substructure Method for Earthquake Analysis of Structure - Soil Interaction," by J.A. Gutierrez and A.K. Chopra - 1976 (PB 257 783)A08
- EERC 76-10 "Stabilization of Potentially Liquefiable Sand Deposits using Gravel Drain Systems," by H.B. Seed and J.R. Booker - 1976 (PB 258 820)A04
- EERC 76-11 "Influence of Design and Analysis Assumptions on Computed Inelastic Response of Moderately Tall Frames," by G.H. Powell and D.G. Row - 1976 (PB 271 409)A06
- EERC 76-12 "Sensitivity Analysis for Hysteretic Dynamic Systems: Theory and Applications," by D. Ray, K.S. Pister and E. Polak - 1976 (PB 262 859)A04
- EERC 76-13 "Coupled Lateral Torsional Response of Buildings to Ground Shaking," by C.L. Kan and A.K. Chopra - 1976 (PB 257 907)A09
- EERC 76-14 "Seismic Analyses of the Banco de America," by V.V. Bertero, S.A. Mahin and J.A. Hollings - 1976
- EERC 76-15 "Reinforced Concrete Frame 2: Seismic Testing and Analytical Correlation," by R.W. Clough and J. Gidwani - 1976 (PB 261 323)A08
- EERC 76-16 "Cyclic Shear Tests of Masonry Piers, Volume 2 - Analysis of Test Results," by R.L. Mayes, Y. Omote and R.W. Clough - 1976
- EERC 76-17 "Structural Steel Bracing Systems: Behavior Under Cyclic Loading," by E.P. Popov, K. Takanashi and C.W. Roeder - 1976 (PB 260 715)A05
- EERC 76-18 "Experimental Model Studies on Seismic Response of High Curved Overcrossings," by D. Williams and W.G. Godden - 1976 (PB 269 548)A08
- EERC 76-19 "Effects of Non-Uniform Seismic Disturbances on the Dumbarton Bridge Replacement Structure," by F. Baron and R.E. Hamati - 1976 (PB 282 981)A16
- EERC 76-20 "Investigation of the Inelastic Characteristics of a Single Story Steel Structure Using System Identification and Shaking Table Experiments," by V.C. Matzen and H.D. McNiven - 1976 (PB 258 453)A07
- EERC 76-21 "Capacity of Columns with Splice Imperfections," by E.P. Popov, R.M. Stephen and R. Philbrick - 1976 (PB 260 378)A04
- EERC 76-22 "Response of the Olive View Hospital Main Building during the San Fernando Earthquake," by S. A. Mahin, V.V. Bertero, A.K. Chopra and R. Collins - 1976 (PB 271 425)A14
- EERC 76-23 "A Study on the Major Factors Influencing the Strength of Masonry Prisms," by N.M. Mostaghel, R.L. Mayes, R. W. Clough and S.W. Chen - 1976 (Not published)
- EERC 76-24 "GADFLEA - A Computer Program for the Analysis of Pore Pressure Generation and Dissipation during Cyclic or Earthquake Loading," by J.R. Booker, M.S. Rahman and H.B. Seed - 1976 (PB 263 947)A04
- EERC 76-25 "Seismic Safety Evaluation of a R/C School Building," by B. Bresler and J. Axley - 1976
- EERC 76-26 "Correlative Investigations on Theoretical and Experimental Dynamic Behavior of a Model Bridge Structure," by K. Kawashima and J. Penzien - 1976 (PB 263 388)A11
- EERC 76-27 "Earthquake Response of Coupled Shear Wall Buildings," by T. Srichatrapimuk - 1976 (PB 265 157)A07
- EERC 76-28 "Tensile Capacity of Partial Penetration Welds," by E.P. Popov and R.M. Stephen - 1976 (PB 262 899)A03
- EERC 76-29 "Analysis and Design of Numerical Integration Methods in Structural Dynamics," by H.M. Hilber - 1976 (PB 264 410)A06
- EERC 76-30 "Contribution of a Floor System to the Dynamic Characteristics of Reinforced Concrete Buildings," by L.E. Malik and V.V. Bertero - 1976 (PB 272 247)A13
- EERC 76-31 "The Effects of Seismic Disturbances on the Golden Gate Bridge," by F. Baron, M. Arikan and R.E. Hamati - 1976 (PB 272 279)A09
- EERC 76-32 "Infilled Frames in Earthquake Resistant Construction," by R.E. Klingner and V.V. Bertero - 1976 (PB 265 892)A13



- UCB/EERC-77/01 "PLUSH - A Computer Program for Probabilistic Finite Element Analysis of Seismic Soil-Structure Interaction," by M.P. Romo Organista, J. Lysmer and H.B. Seed - 1977
- UCB/EERC-77/02 "Soil-Structure Interaction Effects at the Humboldt Bay Power Plant in the Ferndale Earthquake of June 7, 1975," by J.E. Valera, H.B. Seed, C.F. Tsai and J. Lysmer - 1977 (PB 265 795)A04
- UCB/EERC-77/03 "Influence of Sample Disturbance on Sand Response to Cyclic Loading," by K. Mori, H.B. Seed and C.K. Chan - 1977 (PB 267 352)A04
- UCB/EERC-77/04 "Seismological Studies of Strong Motion Records," by J. Shoja-Taheri - 1977 (PB 269 655)A10
- UCB/EERC-77/05 "Testing Facility for Coupled-Shear Walls," by L. Li-Hyung, V.V. Bertero and E.P. Popov - 1977
- UCB/EERC-77/06 "Developing Methodologies for Evaluating the Earthquake Safety of Existing Buildings," by No. 1 - B. Bresler; No. 2 - B. Bresler, T. Okada and D. Zisling; No. 3 - T. Okada and B. Bresler; No. 4 - V.V. Bertero and B. Bresler - 1977 (PB 267 354)A08
- UCB/EERC-77/07 "A Literature Survey - Transverse Strength of Masonry Walls," by Y. Omote, R.L. Mayes, S.W. Chen and R.W. Clough - 1977 (PB 277 933)A07
- UCB/EERC-77/08 "DRAIN-TABS: A Computer Program for Inelastic Earthquake Response of Three Dimensional Buildings," by R. Guendelman-Israel and G.H. Powell - 1977 (PB 270 693)A07
- UCB/EERC-77/09 "SUBWALL: A Special Purpose Finite Element Computer Program for Practical Elastic Analysis and Design of Structural Walls with Substructure Option," by D.Q. Le, H. Peterson and E.P. Popov - 1977 (PB 270 567)A05
- UCB/EERC-77/10 "Experimental Evaluation of Seismic Design Methods for Broad Cylindrical Tanks," by D.P. Clough (PB 272 280)A13
- UCB/EERC-77/11 "Earthquake Engineering Research at Berkeley - 1976," - 1977 (PB 273 507)A09
- UCB/EERC-77/12 "Automated Design of Earthquake Resistant Multistory Steel Building Frames," by N.D. Walker, Jr. - 1977 (PB 276 526)A09
- UCB/EERC-77/13 "Concrete Confined by Rectangular Hoops Subjected to Axial Loads," by J. Vallenias, V.V. Bertero and E.P. Popov - 1977 (PB 275 165)A06
- UCB/EERC-77/14 "Seismic Strain Induced in the Ground During Earthquakes," by Y. Sugimura - 1977 (PB 284 201)A04
- UCB/EERC-77/15 "Bond Deterioration under Generalized Loading," by V.V. Bertero, E.P. Popov and S. Viwathanatepa - 1977
- UCB/EERC-77/16 "Computer Aided Optimum Design of Ductile Reinforced Concrete Moment Resisting Frames," by S.W. Zagajski and V.V. Bertero - 1977 (PB 280 137)A07
- UCB/EERC-77/17 "Earthquake Simulation Testing of a Stepping Frame with Energy-Absorbing Devices," by J.M. Kelly and D.F. Tsztoo - 1977 (PB 273 506)A04
- UCB/EERC-77/18 "Inelastic Behavior of Eccentrically Braced Steel Frames under Cyclic Loadings," by C.W. Roeder and E.P. Popov - 1977 (PB 275 526)A15
- UCB/EERC-77/19 "A Simplified Procedure for Estimating Earthquake-Induced Deformations in Dams and Embankments," by F.I. Makdisi and H.B. Seed - 1977 (PB 276 820)A04
- UCB/EERC-77/20 "The Performance of Earth Dams during Earthquakes," by H.B. Seed, F.I. Makdisi and P. de Alba - 1977 (PB 276 821)A04
- UCB/EERC-77/21 "Dynamic Plastic Analysis Using Stress Resultant Finite Element Formulation," by P. Lukkunapvasit and J.M. Kelly - 1977 (PB 275 453)A04
- UCB/EERC-77/22 "Preliminary Experimental Study of Seismic Uplift of a Steel Frame," by R.W. Clough and A.A. Huckelbridge 1977 (PB 278 769)A08
- UCB/EERC-77/23 "Earthquake Simulator Tests of a Nine-Story Steel Frame with Columns Allowed to Uplift," by A.A. Huckelbridge - 1977 (PB 277 944)A09
- UCB/EERC-77/24 "Nonlinear Soil-Structure Interaction of Skew Highway Bridges," by M.-C. Chen and J. Penzien - 1977 (PB 276 176)A07
- UCB/EERC-77/25 "Seismic Analysis of an Offshore Structure Supported on Pile Foundations," by D.D.-N. Liou and J. Penzien 1977 (PB 283 180)A06
- UCB/EERC-77/26 "Dynamic Stiffness Matrices for Homogeneous Viscoelastic Half-Planes," by G. Dasgupta and A.K. Chopra - 1977 (PB 279 654)A06
- UCB/EERC-77/27 "A Practical Soft Story Earthquake Isolation System," by J.M. Kelly, J.M. Eiding and C.J. Derham - 1977 (PB 276 814)A07
- UCB/EERC-77/28 "Seismic Safety of Existing Buildings and Incentives for Hazard Mitigation in San Francisco: An Exploratory Study," by A.J. Meltsner - 1977 (PB 281 970)A05
- UCB/EERC-77/29 "Dynamic Analysis of Electrohydraulic Shaking Tables," by D. Rea, S. Abedi-Hayati and Y. Takahashi 1977 (PB 282 569)A04
- UCB/EERC-77/30 "An Approach for Improving Seismic - Resistant Behavior of Reinforced Concrete Interior Joints," by B. Galunic, V.V. Bertero and E.P. Popov - 1977 (PB 290 870)A06

- UCB/EERC-78/01 "The Development of Energy-Absorbing Devices for Aseismic Base Isolation Systems," by J.M. Kelly and D.F. Tsztoo - 1978 (PB 284 978)A04
- UCB/EERC-78/02 "Effect of Tensile Prestrain on the Cyclic Response of Structural Steel Connections, by J.G. Bouwkamp and A. Mukhopadhyay - 1978
- UCB/EERC-78/03 "Experimental Results of an Earthquake Isolation System using Natural Rubber Bearings," by J.M. Eidinger and J.M. Kelly - 1978 (PB 281 686)A04
- UCB/EERC-78/04 "Seismic Behavior of Tall Liquid Storage Tanks," by A. Niwa - 1978 (PB 284 017)A14
- UCB/EERC-78/05 "Hysteretic Behavior of Reinforced Concrete Columns Subjected to High Axial and Cyclic Shear Forces," by S.W. Zagajeski, V.V. Bertero and J.G. Bouwkamp - 1978 (PB 283 858)A13
- UCB/EERC-78/06 "Inelastic Beam-Column Elements for the ANSR-I Program," by A. Riahi, D.G. Row and G.H. Powell - 1978
- UCB/EERC-78/07 "Studies of Structural Response to Earthquake Ground Motion," by O.A. Lopez and A.K. Chopra - 1978 (PB 282 790)A05
- UCB/EERC-78/08 "A Laboratory Study of the Fluid-Structure Interaction of Submerged Tanks and Caissons in Earthquakes," by R.C. Byrd - 1978 (PB 284 957)A08
- UCB/EERC-78/09 "Model for Evaluating Damageability of Structures," by I. Sakamoto and B. Bresler - 1978
- UCB/EERC-78/10 "Seismic Performance of Nonstructural and Secondary Structural Elements," by I. Sakamoto - 1978
- UCB/EERC-78/11 "Mathematical Modelling of Hysteresis Loops for Reinforced Concrete Columns," by S. Nakata, T. Sproul and J. Penzien - 1978
- UCB/EERC-78/12 "Damageability in Existing Buildings," by T. Blejwas and B. Bresler - 1978
- UCB/EERC-78/13 "Dynamic Behavior of a Pedestal Base Multistory Building," by R.M. Stephen, E.L. Wilson, J.G. Bouwkamp and M. Button - 1978 (PB 286 650)A08
- UCB/EERC-78/14 "Seismic Response of Bridges - Case Studies," by R.A. Imbsen, V. Nutt and J. Penzien - 1978 (PB 286 503)A10
- UCB/EERC-78/15 "A Substructure Technique for Nonlinear Static and Dynamic Analysis," by D.G. Row and G.H. Powell - 1978 (PB 288 077)A10
- UCB/EERC-78/16 "Seismic Risk Studies for San Francisco and for the Greater San Francisco Bay Area," by C.S. Oliveira - 1978
- UCB/EERC-78/17 "Strength of Timber Roof Connections Subjected to Cyclic Loads," by P. Gülkan, R.L. Mayes and R.W. Clough - 1978
- UCB/EERC-78/18 "Response of K-Braced Steel Frame Models to Lateral Loads," by J.G. Bouwkamp, R.M. Stephen and E.P. Popov - 1978
- UCB/EERC-78/19 "Rational Design Methods for Light Equipment in Structures Subjected to Ground Motion," by J.L. Sackman and J.M. Kelly - 1978 (PB 292 357)A04
- UCB/EERC-78/20 "Testing of a Wind Restraint for Aseismic Base Isolation," by J.M. Kelly and D.E. Chitty - 1978 (PB 292 833)A03
- UCB/EERC-78/21 "APOLLO - A Computer Program for the Analysis of Pore Pressure Generation and Dissipation in Horizontal Sand Layers During Cyclic or Earthquake Loading," by P.P. Martin and H.B. Seed - 1978 (PB 292 835)A04
- UCB/EERC-78/22 "Optimal Design of an Earthquake Isolation System," by M.A. Bhatti, K.S. Pister and E. Polak - 1978 (PB 294 735)A06
- UCB/EERC-78/23 "MASH - A Computer Program for the Non-Linear Analysis of Vertically Propagating Shear Waves in Horizontally Layered Deposits," by P.P. Martin and H.B. Seed - 1978 (PB 293 101)A05
- UCB/EERC-78/24 "Investigation of the Elastic Characteristics of a Three Story Steel Frame Using System Identification," by I. Kaya and H.D. McNiven - 1978
- UCB/EERC-78/25 "Investigation of the Nonlinear Characteristics of a Three-Story Steel Frame Using System Identification," by I. Kaya and H.D. McNiven - 1978
- UCB/EERC-78/26 "Studies of Strong Ground Motion in Taiwan," by Y.M. Hsiung, B.A. Bolt and J. Penzien - 1978
- UCB/EERC-78/27 "Cyclic Loading Tests of Masonry Single Piers: Volume 1 - Height to Width Ratio of 2," by P.A. Hidalgo, R.L. Mayes, H.D. McNiven and R.W. Clough - 1978
- UCB/EERC-78/28 "Cyclic Loading Tests of Masonry Single Piers: Volume 2 - Height to Width Ratio of 1," by S.-W.J. Chen, P.A. Hidalgo, R.L. Mayes, R.W. Clough and H.D. McNiven - 1978
- UCB/EERC-78/29 "Analytical Procedures in Soil Dynamics," by J. Lysmer - 1978

- UCB/EERC-79/01 "Hysteretic Behavior of Lightweight Reinforced Concrete Beam-Column Subassemblages," by B. Forzani, E.P. Popov, and V.V. Bertero - 1979
- UCB/EERC-79/02 "The Development of a Mathematical Model to Predict the Flexural Response of Reinforced Concrete Beams to Cyclic Loads, Using System Identification," by J.F. Stanton and H.D. McNiven - 1979
- UCB/EERC-79/03 "Linear and Nonlinear Earthquake Response of Simple Torsionally Coupled Systems," by C.L. Kan and A.K. Chopra - 1979
- UCB/EERC-79/04 "A Mathematical Model of Masonry for Predicting Its Linear Seismic Response Characteristics," by Y. Mengi and H.D. McNiven - 1979
- UCB/EERC-79/05 "Mechanical Behavior of Lightweight Concrete Confined by Different Types of Lateral Reinforcement," by M.A. Manrique, V.V. Bertero and E.P. Popov - 1979
- UCB/EERC-79/06 "Static Tilt Tests of a Tall Cylindrical Liquid Storage Tank," by R.W. Clough and A. Niwa - 1979
- UCB/EERC-79/07 "The Design of Steel Energy Absorbing Restrainers and Their Incorporation Into Nuclear Power Plants for Enhanced Safety: Volume 1 - Summary Report," by P.N. Spencer, V.F. Zackay, and E.R. Parker - 1979
- UCB/EERC-79/08 "The Design of Steel Energy Absorbing Restrainers and Their Incorporation Into Nuclear Power Plants for Enhanced Safety: Volume 2 - The Development of Analyses for Reactor System Piping," "Simple Systems" by M.C. Lee, J. Penzien, A.K. Chopra, and K. Suzuki "Complex Systems" by G.H. Powell, E.L. Wilson, R.W. Clough and D.G. Row - 1979
- UCB/EERC-79/09 "The Design of Steel Energy Absorbing Restrainers and Their Incorporation Into Nuclear Power Plants for Enhanced Safety: Volume 3 - Evaluation of Commercial Steels," by W.S. Owen, R.M.N. Pelloux, R.O. Ritchie, M. Faral, T. Ohhashi, J. Toplosky, S.J. Hartman, V.F. Zackay, and E.R. Parker - 1979
- UCB/EERC-79/10 "The Design of Steel Energy Absorbing Restrainers and Their Incorporation Into Nuclear Power Plants for Enhanced Safety: Volume 4 - A Review of Energy-Absorbing Devices," by J.M. Kelly and M.S. Skinner - 1979
- UCB/EERC-79/11 "Conservatism In Summation Rules for Closely Spaced Modes," by J.M. Kelly and J.L. Sackman - 1979

- UCB/EERC-79/12 "Cyclic Loading Tests of Masonry Single Piers Volume 3 - Height to Width Ratio of 0.5," by P.A. Hidalgo, R.L. Mayes, H.D. McNiven and R.W. Clough - 1979
- UCB/EERC-79/13 "Cyclic Behavior of Dense Coarse-Grained Materials in Relation to the Seismic Stability of Dams," by N.G. Banerjee, H.B. Seed and C.K. Chan - 1979
- UCB/EERC-79/14 "Seismic Behavior of Reinforced Concrete Interior Beam-Column Subassemblages," by S. Viwathanatepa, E.P. Popov and V.V. Bertero - 1979
- UCB/EERC-79/15 "Optimal Design of Localized Nonlinear Systems with Dual Performance Criteria Under Earthquake Excitations," by M.A. Bhatti - 1979
- UCB/EERC-79/16 "OPTDYN - A General Purpose Optimization Program for Problems with or without Dynamic Constraints," by M.A. Bhatti, E. Polak and K.S. Pister - 1979
- UCB/EERC-79/17 "ANSR-II, Analysis of Nonlinear Structural Response, Users Manual," by D.P. Mondkar and G.H. Powell - 1979
- UCB/EERC-79/18 "Soil Structure Interaction in Different Seismic Environments," A. Gomez-Masso, J. Lysmer, J.-C. Chen and H.B. Seed - 1979
- UCB/EERC-79/19 "ARMA Models for Earthquake Ground Motions," by M.K. Chang, J.W. Kwiatkowski, R.F. Nau, R.M. Oliver and K.S. Pister - 1979
- UCB/EERC-79/20 "Hysteretic Behavior of Reinforced Concrete Structural Walls," by J.M. Vallenias, V.V. Bertero and E.P. Popov - 1979
- UCB/EERC-79/21 "Studies on High-Frequency Vibrations of Buildings I: The Column Effects," by J. Lubliner - 1979
- UCB/EERC-79/22 "Effects of Generalized Loadings on Bond Reinforcing Bars Embedded in Confined Concrete Blocks," by S. Viwathanatepa, E.P. Popov and V.V. Bertero - 1979
- UCB/EERC-79/23 "Shaking Table Study of Single-Story Masonry Houses, Volume 1: Test Structures 1 and 2," by P. Gülkan, R.L. Mayes and R.W. Clough - 1979
- UCB/EERC-79/24 "Shaking Table Study of Single-Story Masonry Houses, Volume 2: Test Structures 3 and 4," by P. Gülkan, R.L. Mayes and R.W. Clough - 1979
- UCB/EERC-79/25 "Shaking Table Study of Single-Story Masonry Houses, Volume 3: Summary, Conclusions and Recommendations," by R.W. Clough, R.L. Mayes and P. Gülkan - 1979

- UCB/EERC-79/26 "Recommendations for a U.S.-Japan Cooperative Research Program Utilizing Large-Scale Testing Facilities," by U.S.-Japan Planning Group - 1979
- UCB/EERC-79/27 "Earthquake-Induced Liquefaction Near Lake Amatitlan, Guatemala," by H.B. Seed, I. Arango, C.K. Chan, A. Gomez-Masso and R. Grant de Ascoli - 1979
- UCB/EERC-79/28 "Infill Panels: Their Influence on Seismic Response of Buildings," by J.W. Axley and V.V. Bertero - 1979
- UCB/EERC-79/29 "3D Truss Bar Element (Type 1) for the ANSR-II Program," by D.P. Mondkar and G.H. Powell - 1979
- UCB/EERC-79/30 "2D Beam-Column Element (Type 5 - Parallel Element Theory) for the ANSR-II Program," by D.G. Row, G.H. Powell and D.P. Mondkar
- UCB/EERC-79/31 "3D Beam-Column Element (Type 2 - Parallel Element Theory) for the ANSR-II Program," by A. Riahi, G.H. Powell and D.P. Mondkar - 1979
- UCB/EERC-79/32 "On Response of Structures to Stationary Excitation," by A. Der Kiureghian - 1979
- UCB/EERC-79/33 "Undisturbed Sampling and Cyclic Load Testing of Sands," by S. Singh, H.B. Seed and C.K. Chan - 1979
- UCB/EERC-79/34 "Interaction Effects of Simultaneous Torsional and Compressional Cyclic Loading of Sand," by P.M. Griffin and W.N. Houston - 1979
- UCB/EERC-80/01 "Earthquake Response of Concrete Gravity Dams Including Hydrodynamic and Foundation Interaction Effects," by A.K. Chopra, P. Chakrabarti and S. Gupta - 1980
- UCB/EERC-80/02 "Rocking Response of Rigid Blocks to Earthquakes," by C.S. Yim, A.K. Chopra and J. Penzien - 1980
- UCB/EERC-80/03 "Optimum Inelastic Design of Seismic-Resistant Reinforced Concrete Frame Structures," by S.W. Zagajeski and V.V. Bertero - 1980
- UCB/EERC-80/04 "Effects of Amount and Arrangement of Wall-Panel Reinforcement on Hysteretic Behavior of Reinforced Concrete Walls," by R. Iliya and V.V. Bertero - 1980
- UCB/EERC-80/05 "Shaking Table Research on Concrete Dam Models," by A. Niwa and R.W. Clough - 1980
- UCB/EERC-80/06 "Piping With Energy Absorbing Restrainers: Parameter Study on Small Systems," by G.H. Powell, C. Oughourlian and J. Simons - 1980

- UCB/EERC-80/07 "Inelastic Torsional Response of Structures Subjected to Earthquake Ground Motions," by Y. Yamazaki - 1980
- UCB/EERC-80/08 "Study of X-Braced Steel Frame Structures Under Earthquake Simulation," by Y. Ghanaat - 1980
- UCB/EERC-80/09 "Hybrid Modelling of Soil-Structure Interaction," by S. Gupta, T.W. Lin, J. Penzien and C.S. Yeh - 1980
- UCB/EERC-80/10 "General Applicability of a Nonlinear Model of a One Story Steel Frame," by B.I. Sveinsson and H. McNiven - 1980
- UCB/EERC-80/11 "A Green-Function Method for Wave Interaction with a Submerged Body," by W. Kioka - 1980
- UCB/EERC-80/12 "Hydrodynamic Pressure and Added Mass for Axisymmetric Bodies," by F. Nilrat - 1980
- UCB/EERC-80/13 "Treatment of Non-Linear Drag Forces Acting on Offshore Platforms," by B.V. Dao and J. Penzien - 1980
- UCB/EERC-80/14 "2D Plane/Axisymmetric Solid Element (Type 3 - Elastic or Elastic-Perfectly Plastic) for the ANSR-II Program," by D.P. Mondkar and G.H. Powell - 1980
- UCB/EERC-80/15 "A Response Spectrum Method for Random Vibrations," by A. Der Kiureghian - 1980
- UCB/EERC-80/16 "Cyclic Inelastic Buckling of Tubular Steel Braces," by V.A. Zayas, E.P. Popov and S.A. Mahin - June 1980
- UCB/EERC-80/17 "Dynamic Response of Simple Arch Dams Including Hydrodynamic Interaction," by C.S. Porter and A.K. Chopra - July 1980
- UCB/EERC-80/18 "Experimental Testing of a Friction Damped Aseismic Base Isolation System with Fail-Safe Characteristics," by J.M. Kelly, K.E. Beucke and M.S. Skinner - July 1980
- UCB/EERC-80/19 "The Design of Steel Energy-Absorbing Restrainers and their Incorporation into Nuclear Power Plants for Enhanced Safety (Vol 1B): Stochastic Seismic Analyses of Nuclear Power Plant Structures and Piping Systems Subjected to Multiple Support Excitations," by M.C. Lee and J. Penzien - 1980
- UCB/EERC-80/20 "The Design of Steel Energy-Absorbing Restrainers and their Incorporation into Nuclear Power Plants for Enhanced Safety (Vol 1C): Numerical Method for Dynamic Substructure Analysis," by J.M. Dickens and E.L. Wilson - 1980
- UCB/EERC-80/21 "The Design of Steel Energy-Absorbing Restrainers and their Incorporation into Nuclear Power Plants for Enhanced Safety (Vol 2): Development and Testing of Restraints for Nuclear Piping Systems," by J.M. Kelly and M.S. Skinner - 1980

- UCB/EERC-80/22 "3D Solid Element (Type 4-Elastic or Elastic-Perfectly-Plastic) for the ANSR-II Program," by D.P. Mondkar and G.H. Powell - 1980
- UCB/EERC-80/23 "Gap-Friction Element (Type 5) for the ANSR-II Program," by D.P. Mondkar and G.H. Powell - 1980
- UCB/EERC-80/24 "U-Bar Restraint Element (Type 11) for the ANSR-II Program," C. Oughourlian and G.H. Powell - 1980
- UCB/EERC-80/25 "Testing of a Natural Rubber Base Isolation System by an Explosively Simulated Earthquake," by J.M. Kelly 1980
- UCB/EERC-80/26 "Input Identification from Structural Vibrational Response," by Y. Hu - 1980
- UCB/EERC-80/27 "Cyclic Inelastic Behavior of Steel Offshore Structures," by V.A. Zayas, S.A. Mahin and E.P. Popov - 1980
- UCB/EERC-80/28 "Shaking Table Testing of a Reinforced Concrete Frame with Biaxial Response," M.G. Oliva and R.W. Clough 1980
- UCB/EERC-80/29 "Dynamic Properties of a Twelve-Story Prefabricated Panel Building," by J.G. Bouwkamp, J.P. Kollegger and R.M. Stephen - 1980
- UCB/EERC-80/30 "Dynamic Properties of a Eight-Story Prefabricated Panel Building," by J.G. Bouwkamp, J.P. Kollegger and R.M. Stephen - 1980
- UCB/EERC-80/31 "Predictive Dynamic Response of Panel Type Structures Under Earthquakes," by J.P. Kollegger and J.G. Bouwkamp 1980
- UCB/EERC-80/32 "The Design of Steel Energy-Absorbing Restrainers and their Incorporation into Nuclear Power Plants for Enhanced Safety: Vol 3, Testing of Commercial Steels in Low-Cycle Torsional Fatigue," by P. Spencer, E.R. Parker, E. Jongewaard and M. Drory - 1980
- UCB/EERC-80/33 "The Design of Steel Energy-Absorbing Restrainers and their Incorporation into Nuclear Power Plants for Enhanced Safety: Vol 4, Shaking Table Tests of Piping Systems with Energy-Absorbing Restrainers," by S.F. Stiemer and W.G. Godden - 1980
- UCB/EERC-80/34 "The Design of Steel Energy-Absorbing Restrainers and their Incorporation into Nuclear Power Plants for Enhanced Safety: Vol 5, Summary Report," by P. Spencer 1980

- UCB/EERC-80/35 "Experimental Testing of an Energy Absorbing Base Isolation System," by J. Kelly, M.S. Skinner and K.E. Beucke - 1980
- UCB/EERC-80/36 "Simulating and Analyzing Artificial Non-Stationary Earthquake Ground Motions," by R.F. Nau, R.M. Oliver and K.S. Pister - 1980
- UCB/EERC-80/37 "Earthquake Engineering at Berkeley," - 1980